



UNIVERSITEIT•STELLENBOSCH•UNIVERSITY
jou kennisvennoot • your knowledge partner

Modular approach to the development of a two- way radio receiver system



By Valpré Kellerman

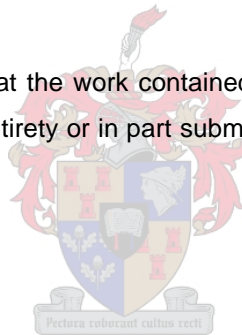
**Thesis presented in partial fulfillment of the requirements for the degree
Master of Science in Engineering at the University of Stellenbosch**

**Supervisor:
Prof JB de Swardt**

December 2004

Declaration

I, the undersigned, hereby declare that the work contained in this thesis is my own original work and that I have not previously in its entirety or in part submitted it at any university for a degree.



.....
Signed by VC Kellerman

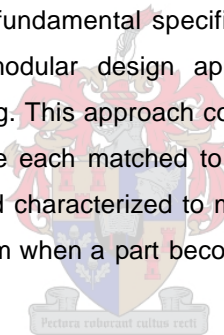
.....
Date

Abstract

The preliminary development of a FM radio receiver module is discussed. An existing narrowband system operating between 48MHz and 50MHz will be replaced. Digital components were investigated, compared and used with analogue techniques to build a more flexible two-way radio receiver system. A direct digital synthesizer was considered as a replacement for the current synthesized phased lock loop local oscillator and much attention was given to the local oscillator and mixer design, characteristics and measurement procedures.

A detailed study of receiver systems was undertaken to determine the specifications needed for every receiver component to achieve satisfactory receiver performance in the end. Receiver characteristics as well as receiver measurement procedures are defined. A software tool was developed to aid the design process, establishing computationally whether the receiver specifications are met prior to the final design.

The complete design process, from fundamental specifications through to the developed final receiver module is discussed. A modular design approach was used to guarantee easy manufacturing, substitution and testing. This approach comprises the break-down of the receiver into well defined components that are each matched to 50Ω. The separate components of the system were designed, measured and characterized to make it possible to replace only a single component instead of the entire system when a part becomes redundant.



Opsomming

Die grondslag vir die ontwikkeling van 'n FM radio ontvanger module word in hierdie dokument gelê. 'n Bestaande noubandstelsel wat tussen 48MHz and 50MHz ontvang word vervang deur hierdie nuwe stelsel wat aangewend sal kan word in die bestaande tweerigtingradio se omhulsel. Digitale komponente is ondersoek, vergelyk en gebruik saam met analoogtegnieke om 'n meer buigsame radiostelsel te bewerkstellig. 'n Direkte digitale sintitiseerder is oorweeg as 'n vervanging vir die huidige fasesluitlus ossillator met heelwat klem op die oscillator-en mengerontwerp, komponent spesifikasies en metingsprosedures.

'n Diepgaande studie van ontvangerstelsels is gedoen om te bepaal wat die tipiese spesifikasies vir elke ontvangerstadium is, sodat die finale ontvanger se spesifikasies behaal kan word. Ontvanger eienskappe en meetprosedures word volledig gedefinieer. 'n Sagtewareprogram is ontwikkel om die ontvanger-ontwerpsproses te vergemaklik deur vooraf te kan vasstel watter ontvangerspesifikasies bereik sal kan word al dan nie.

Die volledige ontwerpsproses, vanaf fundamentele spesifikasies tot by die finale ontvanger word omskryf. 'n Modulere-ontwerp prosedure is gebruik ter versekering van die maklike vervaardiging, vervanging en toetsing van elke komponent. Die radio is tydens ontwerp opgebreek in boublokkies wat elkeen aangepas word na 500. Elke aparte boublokkie van die ontvangerstelsel is afsonderlik ontwerp, gemeet en volledig gespesifiseer om dit moontlik te maak om slegs een komponent te vervang in plaas van die hele stelsel wanneer 'n enkele komponent nie meer beskikbaar is nie.

Table of contents

DECLARATION	- 1 -
ABSTRACT	- 2 -
OPSOMMING	- 3 -
TABLE OF CONTENTS	- 4 -
LIST OF ABBREVIATIONS AND SYMBOLS	- 7 -
LIST OF TABLES	- 10 -
LIST OF FIGURES	- 11 -
1 INTRODUCTION	1
1.1 THESIS STRUCTURE	2
2 BACKGROUND PRINCIPLES	4
2.1 RECEIVER CHARACTERISTICS AND OVERVIEW.....	4
2.1.1. <i>Receiver characteristics</i>	5
2.1.1. a Sensitivity	5
2.1.1. b Spurious responses.....	5
2.1.1. c Audio frequency response.....	8
2.1.1. d Audio frequency output power	9
2.1.1. e Dynamic range	9
2.1.1. f Receiver distortion.....	9
2.1.1. g Conclusion	10
2.1.2. <i>The receiver</i>	12
2.2 NOISE THEORY.....	14
2.2.1. <i>Noise figure calculations</i>	15
2.2.1. a Cascaded noise factor	16
2.2.1. b Noise factor contribution from image noise	16
2.2.1. c The noise contribution as a result of wideband LO noise	17
2.2.2. <i>Sensitivity calculation</i>	18
3 RECEIVER CALC 1.1	20
3.1 THE USER INTERFACE.....	20
3.2 CALCULATION OF RECEIVER PERFORMANCE.....	24
3.2.1. <i>Receiver sensitivity</i>	24
3.2.2. <i>Receiver selectivity/adjacent channel rejection</i>	26
3.2.3. <i>Dynamic range and power diagrams to predict distortion</i>	26
3.2.4. <i>Spurious responses</i>	28
3.3 CONCLUSION	29
4 DEVELOPMENT OF THE RECEIVER COMPONENTS	31
4.1 THE MIXER.....	31
4.1.1. <i>Theory of mixers</i>	32
4.1.1. a Active and passive mixers	32
4.1.1. b Mixer characteristics	33
4.1.1. c Types of mixers	39
4.1.2. <i>Designing, building and measuring different mixers</i>	40
4.1.2. a Balanced mixer (Singly balanced mixers).....	40
4.1.2. b Doubly balanced mixer	44
4.1.2. c Single device mixer	55
4.1.3. <i>Conclusion concerning mixers</i>	59

4.2 THE FRONT-END AMPLIFIER.....	62
4.2.1. Theory.....	62
4.2.1. a Stability.....	62
4.2.1. b Noise figure and gain.....	62
4.2.1. c 1dB compression point and intercept point	63
4.2.1. d Return loss.....	64
4.2.2. <i>Designing, measuring and building different front-end amplifiers</i>	64
4.2.2. a Design of a low noise amplifier.....	64
4.2.2. b Designing, building and measuring the GALI-S66	67
4.2.3. <i>Conclusion</i>	71
4.3 LOCAL OSCILLATOR.....	72
4.3.1. Theory.....	72
4.3.1. a Types.....	73
4.3.1. b Amplitude and phase noise of the local oscillator.....	78
4.3.2. <i>Designing, building and measuring different frequency generators</i>	80
4.3.2. a Designing, building and measuring the DDS	81
4.3.2. b Design of a crystal oscillator	85
4.3.3. <i>Comparison and conclusion</i>	88
4.4 RECEIVER FILTERS.....	89
4.4.1. <i>Front-end filters</i>	89
4.4.1. a Designing, building and measuring the front-end filters	89
4.4.1. b Conclusion	92
4.4.2. <i>The IF filter</i>	93
4.4.2. a Crystal filter.....	93
4.4.2. b Ceramic filter	94
4.4.2. c Conclusion	95
4.4.3. <i>Injection filter</i>	95
4.4.3. a Filter design and measurements.....	96
4.4.3. b Conclusion	98
4.4.4. <i>Conclusion</i>	98
4.5 THE AUDIO COMPONENTS.....	99
4.5.1. <i>The audio filter</i>	99
4.5.1. a Design and measurements	99
4.5.1. b Conclusion	101
4.5.2. <i>Audio amplifier</i>	101
4.5.2. a Building and measuring the audio amplifier IC	101
4.5.2. b Conclusion	103
4.6 IF RECEIVER SYSTEM DESIGN	104
4.6.1. <i>Design considerations</i>	104
4.6.2. <i>Measurements</i>	106
4.6.3. <i>Conclusion</i>	109
4.7 CONCLUSION	109
5 MEASUREMENTS OF RECEIVER SYSTEMS	110
5.1 INTRODUCTION.....	110
5.2 MEASUREMENT OF RADIO SPECIFICATIONS.....	111
5.2.1. <i>Sensitivity</i>	112
5.2.1. a Measurement procedure.....	112
5.2.1. b Measurements.....	113
5.2.1. c Conclusion	116
5.2.2. <i>Adjacent channel rejection / Selectivity</i>	117
5.2.2. a Measurement procedure.....	117
5.2.2. b Measurements.....	118
5.2.2. c Conclusion	120
5.2.3. <i>Spurious response rejection</i>	121
5.2.3. a Measurement procedure.....	121
5.2.3. b Measurements.....	122
5.2.3. c Conclusion	128
5.2.4. <i>Desensitization</i>	128

5.2.4. a	Measurement procedure.....	128
5.2.4. b	Measurements.....	129
5.2.5.	<i>Spurious radiation</i>	130
5.2.5. a	Measurement procedure.....	130
5.2.5. b	Measurements.....	131
5.2.5. c	Conclusion	133
5.2.6.	<i>Co-channel rejection</i>	134
5.2.6. a	Measurement procedure.....	134
5.2.6. b	Measurements.....	134
5.2.7.	<i>Conclusion</i>	135
5.3	INFLUENCE OF THE RECEIVER COMPONENTS ON RECEIVER CHARACTERISTICS	136
5.3.1.	<i>Influence of the front-end amplifier on receiver performance</i>	136
5.3.2.	<i>Influence of the front-end filters on receiver performance</i>	136
5.3.3.	<i>Influence of the mixer on receiver performance</i>	138
5.3.4.	<i>Influence of the injection filter on receiver performance</i>	140
5.3.5.	<i>Influence of the local oscillator on receiver performance</i>	141
5.3.6.	<i>Influence of the IF filter on receiver performance</i>	141
5.3.7.	<i>Influence of the audio filter on receiver performance</i>	142
5.4	DISCUSSION AND COMPARISON OF RESULTS.....	143
5.5	CONCLUSION	145
6	CONCLUSION AND RECOMMENDATIONS	147
6.1	CONCLUSION	147
6.2	RECOMMENDATIONS FOR FUTURE RESEARCH.....	148
	ACKNOWLEDGEMENTS	150
	BIBLIOGRAPHY	151
	APPENDIX A – LNA AMPLIFIER DESIGN	II
	APPENDIX B – DDS DESIGN	IX
	APPENDIX C – IF RECEIVER DESIGN	XII



List of abbreviations and symbols

AC	Alternating current
AF	Audio frequency
AM	Amplitude modulation
C_T	Total parallel capacitance
DAC	Digital to analog converter
dB	Decibel
dBc/Hz	Decibel with respect to the carrier frequency per hertz
dBm	Decibel with respect to milliwatt
DC	Direct current
DDS	Direct digital synthesizer
DSB	Double sideband
EMF	Electromagnetic field
EMI	Electromagnetic interference
ETSI	European Telecommunications Standards Institute
F	Noise factor – linear
F_{components}	Linear noise factor calculated from the cascaded component gains and noise factors
f_{IF}	Frequency of the intermediate frequency signal
F_{image}	Linear noise factor contributed by using the image frequency
f_{LO}	Frequency of the local oscillator
F_{LOWideband}	Linear noise factor contribution from the LO wideband noise
FM	Frequency modulation
f_{RF}	Frequency of the radio frequency signal
G_c	The conversion gain of the mixer
G_T	Transducer power gain
HTKA	Telecommunications authority Hong Kong
IC	Integrated circuit
IDA	Info-communications development authority of Singapore
IF	Intermediate frequency
IM	Intermodulation
IMD	Intermodulation distortion
IP1	1dB compression point
IP3	Intercept point
K	Kelvin

k	$k = 1.38 \times 10^{23} [J / K]$ - Boltzmann's constant
kHz	Kilohertz
L(f_m)	Single sideband phase noise at a frequency offset f _m from the carrier
LC filter	Inductor capacitor filter
LNA	Low noise amplifier
LO	Local oscillator
mA	milliampere
MDS	Minimum detectable signal
MHz	Megahertz
M_s	The mixer noise balance
mV_{pp}	millivolt peak to peak
NF	Noise figure
	$NF = 10 \log F [dB]$
PLL	Phase lock loop
P_{Lo}	Local oscillator power
P_s	Signal power
P_{SSB}	The phase noise power, in a 1 Hz bandwidth, at a frequency offset f _m from the carrier
Q	Quality factor
RF	Radio frequency
RL	Return loss
S	The specified adjacent channel rejection
SAW	Surface wave acoustic
S_{imin}	The minimum detectable signal power at the input of the receiver
SINAD	Signal plus noise and distortion-to-noise ratio and distortion ratio
SNR	Signal-to-noise ratio
SNR_{out}	Linear signal-to-noise ratio at the detector input
SSB	Single sideband
T₀	290K
THD	Total harmonic distortion
V	Voltage
VCO	Voltage controlled oscillator
VSWR	Voltage standing wave ratio
Z₀	Characteristic impedance of the system (usually 50Ω)
Ω	Ohm
f₀	Center frequency



- ? ₁ 3dB lower frequency limit
- ? ₂ 3dB upper frequency limit



List of tables

Table 1-1 Receiver specifications.	2
Table 2-1 Receiver properties and characteristics of the different components that influences them.	11
Table 2-2 Important functions and design restrictions of different radio components [8] [1] [9] [27].	14
Table 4-1 Mixer noise balance of the U2796B balanced mixer.	43
Table 4-2 Summary of the measured characteristics of the U2796B singly balanced mixer.	44
Table 4-3 Measured mixer noise balance of the SA602.	47
Table 4-4 Measured mixer noise balance of the SBL-1 doubly balanced mixer.	50
Table 4-5 Measured mixer noise balance of the AD831 doubly balanced mixer.	53
Table 4-6 Summary of the expected and measured characteristics of the doubly balanced mixers.	55
Table 4-7 Mixer noise balance of the dual-gate MOSFET mixer.	58
Table 4-8 Summary of the measured characteristics of the dual-gate MOSFET mixer.	59
Table 4-9 Comparisons between different mixers [1] [9] [35].	60
Table 4-10 Comparison between the measured characteristics of the mixers.	61
Table 4-11 Measured LNA properties summary.	66
Table 4-12 Comparison of some available amplifiers.	67
Table 4-13 Summary of the measured Gali-S66 amplifier properties.	71
Table 4-14 Comparison between the characteristics of the designed Gali-S66 and the AT-41533 single transistor amplifiers.	72
Table 4-15 Measured phase noise of the DDS output.	84
Table 4-16 Summary of the measured parameters of the designed front-end filters.	98
Table 4-17 Summary of the measured parameters of the IF filters.	98
Table 4-18 Summary of the measured characteristics of the two injection filters.	99
Table 4-19 Summary of some of the available audio amplifiers that was investigated.	102
Table 5-1 Summary of the different receiver component options.	111
Table 5-2 Receiver characteristics specifications limits.	112
Table 5-3 Sensitivity measurement results for different receiver component combinations.	115
Table 5-4 Adjacent channel rejection for different receiver component combinations.	120
Table 5-5 The image rejection of the receiver for different receiver component combinations.	124
Table 5-6 The IF rejection of the receiver for different receiver component combinations	127
Table 5-7 Receiver combination 1 for measuring the receiver desensitization.	129
Table 5-8 Receiver desensitization ratios for combination 1.	129
Table 5-9 Receiver combination 2 for measuring the receiver desensitization.	129
Table 5-10 Receiver desensitization for combination 2	129
Table 5-11 Receiver combination 3 for measuring the receiver desensitization	130
Table 5-12 Receiver desensitization ratios for combination 3	130
Table 5-13 Receiver combination 4 for measuring the receiver desensitization	130
Table 5-14 Receiver desensitization ratios for combination 4	130
Table 5-15 Receiver combination 1 for measuring the spurious radiations	131
Table 5-16 Receiver combination 2 for measuring the spurious radiations	132
Table 5-17 Receiver combination 3 for measuring the spurious radiations	133
Table 5-18 Receiver combination 4 for measuring the spurious radiations	133
Table 5-19 Receiver combination 1 for measuring the co-channel rejection	134
Table 5-20 The co-channel rejection ratios of receiver combination 1	134
Table 5-21 Receiver combination 2 for measuring the co-channel rejection	135
Table 5-22 The co-channel rejection ratios of receiver combination 2	135
Table 5-23 Receiver combination 3 for measuring the co-channel rejection	135
Table 5-24 The co-channel rejection ratios of receiver combination 3	135
Table 5-25 Comparison between expected and measured receiver performance	144
Table 5-26 Summary of the sensitivity, selectivity and spurious response rejection ratios of the measured combinations	146

List of figures

Figure 2-1 Block diagram of a double down-conversion super heterodyne receiver.	4
Figure 2-2 LO signal definitions for selectivity predictions [1].	7
Figure 2-3 Block diagram of the receiver system that was used.	12
Figure 2-4 Image noise.	16
Figure 2-5 Down-conversion of noise (Figure 2.5 p20 [10]).	17
Figure 3-1 The user interface and possible systems.	21
Figure 3-2 RF amplifier properties dialog box.	22
Figure 3-3 Opening a file.	23
Figure 3-4 The Options/System properties dialog box.	24
Figure 3-5 The calculation options dialog box.	25
Figure 3-6 Calculated power levels throughout the receiver, with an input power of -20dBm .	27
Figure 3-7 Calculated power levels, with an input power of 0dBm . Note warnings when the compression or intercept point of a component is exceeded.	28
Figure 3-8 Spurious response chart for a single frequency receiver with $f_{RF} = 50\text{MHz}$, $f_{IF} = 10.7\text{MHz}$ and $N = M = 3$.	29
Figure 4-1 Structure of chapter 4.	31
Figure 4-2 Set-up for measuring Conversion loss or gain and IP1.	33
Figure 4-3 Experimental set-ups for measuring isolation between ports (a) LO -RF isolation (b) LO-IF isolation (c) RF-LO isolation (d) RF-IF isolation [18] [19].	34
Figure 4-4 Mixer third order intermodulation products in the output signal [1] [9] [13] [57].	36
Figure 4-5 Illustrating Intercept and 1dB compression point - Figure 2-4 p18 [10].	37
Figure 4-6 Experimental arrangement for the measurement of IP3 [1] [18] [19].	37
Figure 4-7 Measurement set-up to measure the noise figure of a mixer.	38
Figure 4-8 Down-conversion of noise (Figure 2-5 p20 [10]).	38
Figure 4-9 Measurement set-up of the mixer noise balance [9].	39
Figure 4-10 The circuit diagram of the U2796B mixer.	40
Figure 4-11 Measured conversion gain of the U2796B balanced mixer.	41
Figure 4-12 The measured 1dB compression point of the U2796B balanced mixer.	42
Figure 4-13 Photo of the U2796B singly balanced mixer that was designed.	43
Figure 4-14 Circuit diagram of the SA602 mixer component that was designed.	45
Figure 4-15 A tapped capacitor impedance matching network [61] [63].	46
Figure 4-16 Measured conversion gain of the SA602.	46
Figure 4-17 1dB compression point of the SA602 doubly balanced mixer.	47
Figure 4-18 Photo of the SA602 active mixer that was built.	48
Figure 4-19 Photo of the SBL-1 passive mixer.	48
Figure 4-20 Measured conversion gain of the SBL-1 doubly balanced mixer.	49
Figure 4-21 1dB compression point of the SBL-1 doubly balanced mixer.	50
Figure 4-22 Circuit diagram of the AD831 mixer component.	51
Figure 4-23 Measure conversion gain of the AD831 doubly balanced mixer.	52
Figure 4-24 Measured 1dB compression point of the AD831 doubly balanced mixer.	52
Figure 4-25 LO-RF isolation.	53
Figure 4-26 LO-IF isolation.	53
Figure 4-27 Photo of the AD831 active mixer that was built.	54
Figure 4-28 The dual-gate MOSFET mixer circuit diagram [1] [35] [45].	56
Figure 4-29 Conversion gain of the dual-gate MOSFET mixer.	57
Figure 4-30 1dB compression point of the dual-gate MOSFET mixer.	57
Figure 4-31 The single device dual-gate MOSFET mixer component that was designed.	58
Figure 4-32 Structure of chapter 4: 4.2 Front-end amplifier.	61
Figure 4-33 Measurement set-up for measuring the IP1 of an amplifier.	63
Figure 4-34 Measurement set-up, for measuring the IP3 of an amplifier.	63
Figure 4-35 Photo of the designed AT-41533 single transistor low noise amplifier.	64
Figure 4-36 Measured 1dB compression point of the AT-41533 single transistor low noise amplifier.	65

Figure 4-37 Input return loss of the low noise amplifier.	66
Figure 4-38 Schematic of the Gali-S66 circuit.	68
Figure 4-39 Photo of the designed Gali-S66 amplifier component.	68
Figure 4-40 Measured s_{11} and s_{21} .	69
Figure 4-41 Gain of the amplifier over the frequency range.	69
Figure 4-42 1dB compression point of the Gali-S66 amplifier.	70
Figure 4-43 Return loss of the Gali-S66.	70
Figure 4-44 Structure of chapter 4: 4.3 Local oscillator.	72
Figure 4-45 Use of switched crystal oscillators to achieve frequency tuning in a super heterodyne receiver system.	73
Figure 4-46 Concept of oscillator resistance [9] [26].	74
Figure 4-47 Typical common emitter Colpitts oscillator divided into basic blocks.	75
Figure 4-48 Typical phase lock loop.	76
Figure 4-49 DDS circuit block diagram [43] [45] [46].	77
Figure 4-50 Phase noise definition [24] [33-34] [37] [39] [40] [42].	79
Figure 4-51 Circuit diagram of the AD9851 direct digital synthesizer component that was designed.	81
Figure 4-52 Photo of the designed direct digital synthesizer component.	82
Figure 4-53 The unfiltered DDS spectrum analyzer output.	82
Figure 4-54 The unfiltered DDS oscilloscope output.	82
Figure 4-55 The Chebyshev filtered DDS spectrum analyzer output.	83
Figure 4-56 The Chebyshev filtered DDS oscilloscope output.	83
Figure 4-57 The Butterworth filtered DDS spectrum analyzer output.	83
Figure 4-58 The Butterworth filtered DDS oscilloscope output.	83
Figure 4-59 Saved output spectrum of the DDS, with the Chebyshev filter at the output of the DDS, if the microcontroller tunes the DDS frequency to vary between 39.25MHz and 39.35MHz, in steps of 12.5kHz.	84
Figure 4-60 Common base Colpitts oscillator that was simulated.	85
Figure 4-61 FFT of the simulated emitter oscillator signal.	86
Figure 4-62 Circuit diagram of the crystal oscillator circuit component.	86
Figure 4-63 Photo of the crystal oscillator component.	87
Figure 4-64 The output spectrum of the crystal oscillator.	87
Figure 4-65 Structure of chapter 4: 4.4 Receiver filters.	88
Figure 4-66 Photo of the third order Butterworth filter. Center frequency at $f_0 = 50MHz$.	90
Figure 4-67 Third order Butterworth filter. Center frequency of $f_0 = 50MHz$.	90
Figure 4-68 Simulated s-parameters of the third order Butterworth filter. Center frequency at $f_0 = 50MHz$.	90
Figure 4-69 Measured s-parameters of the third order Butterworth filter. Center frequency at $f_0 = 50MHz$.	90
Figure 4-70 Photo of the fifth order Chebyshev filter. Center frequency at $f_0 = 50MHz$.	90
Figure 4-71 The fifth order Chebyshev filter. Center frequency at $f_0 = 50MHz$.	91
Figure 4-72 Simulated s-parameters of the fifth order Chebyshev filter. Center frequency at $f_0 = 50MHz$.	91
Figure 4-73 Measured s-parameters of the fifth order Chebyshev filter. Center frequency at $f_0 = 50MHz$.	91
Figure 4-74 Simple LC filter.	91
Figure 4-75 Simulated s-parameters of the simple bandpass filter.	92
Figure 4-76 Measured s-parameters of the simple bandpass filter.	92
Figure 4-77 Amplitude response comparison between the different designed front-end filters.	92
Figure 4-78 Photo of the crystal filter, 500 matched component.	93
Figure 4-79 Measured amplitude response of the crystal IF filter (spectrum analyzer).	94
Figure 4-80 Measured s-parameters of the crystal IF filter (network analyzer).	94
Figure 4-81 Photo of the ceramic filter, 50Ω matched component.	94
Figure 4-82 Measured s-parameters of the ceramic IF filter.	95
Figure 4-83 The third order Butterworth band pass filter. Center frequency of $f_0 = 39.3MHz$.	96

Figure 4-84 Photo of the third order Butterworth band pass filter component with a center frequency of $f_0 = 39.3MHz$.	96
Figure 4-85 Simulated s-parameters of the third order Butterworth band pass filter component with a center frequency of $f_0 = 39.3MHz$.	97
Figure 4-86 Measured s-parameters of the third order Butterworth band pass filter component with a center frequency of $f_0 = 39.3MHz$.	97
Figure 4-87 Circuit diagram of the third order Chebyshev band pass filter component with a center frequency of $f_0 = 39.3MHz$.	97
Figure 4-88 Photo of the third order Chebyshev band pass filter component with a center frequency of $f_0 = 39.3MHz$.	97
Figure 4-89 Simulated s-parameters of the third order Chebyshev band pass filter component with a center frequency of $f_0 = 39.3MHz$.	98
Figure 4-90 Measured s-parameters of the third order Chebyshev band pass filter component with a center frequency of $f_0 = 39.3MHz$.	98
Figure 4-91 Structure of chapter 4: 4.5 The audio components.	99
Figure 4-92 Circuit diagram: active audio filter circuit component.	100
Figure 4-93 Comparison between the simulated and measured power ratio of the active audio amplifier.	100
Figure 4-94 The designed audio filter component.	101
Figure 4-95 Circuit diagram of the NCP2890 audio amplifier component.	102
Figure 4-96 Photo of the NCP2890 audio amplifier component that was designed.	103
Figure 4-97 Structure of chapter 4: 4.6 IF receiver system design.	103
Figure 4-98 Circuit diagram of the SA605 IF receiver system that was designed.	105
Figure 4-99 SA605 IF receiver circuit that was designed and built.	105
Figure 4-100 The two measurement set-ups necessary to measure the capture ratio.	106
Figure 4-101 The noise floor at the output of the combiner with the noise source switched on and off	106
Figure 4-102 The minimum signal-to-noise ratio at the IF receiver input for a deviation of $\pm 1.5kHz$ and with 10kHz resolution bandwidth.	107
Figure 4-103 The minimum signal-to-noise ratio at the IF receiver input for a deviation of $\pm 2.5kHz$ and with 10kHz resolution bandwidth.	107
Figure 4-104 Quadrature tank measurement set-up.	108
Figure 4-105 Measured quad tank s-curve of the IF receiver.	109
Figure 5-1 Summary of the proposed receiver measurements and comparisons.	110
Figure 5-2 The HP8920A RF communication test set of Hewlett Packard.	113
Figure 5-3 Set-up for measuring the receiver sensitivity.	113
Figure 5-4 Sensitivity measurements summarized for every measured combination.	116
Figure 5-5 Measurement set-up for measuring the desensitization, adjacent channel, co-channel and spurious response - rejection ratio of the receiver.	117
Figure 5-6 Selectivity results summarized for the different combinations.	120
Figure 5-7 Image rejection ratio measurements in progress.	122
Figure 5-8 Image rejection ratio results summarized for the different combinations	125
Figure 5-9 IF rejection results summarized for the different combinations	128
Figure 5-10 Measurement set-up for measuring the spurious radiations of the receiver	131
Figure 5-11 Spurious radiations detected over the frequency span from 1kHz to 300MHz	131
Figure 5-12 Spurious radiations detected over the frequency span from 500kHz to 25MHz	131
Figure 5-13 Spurious radiations detected over the frequency span from 1kHz to 300MHz	132
Figure 5-14 Spurious radiations detected over the frequency span from 500kHz to 25MHz	132
Figure 5-15 Spurious radiations detected over the frequency span from 1kHz to 300MHz	133

1 Introduction

The incredible growth of portable wireless communication over the past decade has created a demand for portable wireless devices that are smaller, lighter, and cheaper and that still have high performance. Luckily, advances in radio frequency architecture are allowing this reduction of size and cost by replacing analogue components with their digital counterparts. Progress that was essential includes the development of improved integrated mixers and of higher performance analogue to digital converters. Conventional analogue techniques, however, are still used in two-way radios today because of their low power consumption. It has not been possible to replace these components with their digital counterparts, which tend to need more current. Replacement of analogue with digital components, if possible, would allow for much more flexibility in two-way radios. The effect that recently developed digital components would have in the system's performance and power consumption needs to be investigated [1] [2] [3].

Most portable equipment is optimized for either high performance or power-efficient operation, but increasingly modern applications require both. Thus, the challenge is to develop flexible, high performance receivers with low power consumption, low cost and small size. Energy consumption and receiver performance are inseparably linked in portable RF communications and, consequently, designers have to consider power constraints throughout the design process [1] [2] [4].

The aim of this work was to develop a preliminary radio module to improve an existing radio module for military use. The new system will replace the present narrowband system operating between 48MHz and 50MHz and provide a two-way radio that can be used in the existing radio housing with the specifications listed in *Table 1-1*. Digital components were investigated, compared and used with analogue techniques to build a more flexible two-way radio transceiver. A Direct Digital Synthesizer (DDS) has been considered as a replacement for the current synthesized phased lock loop (PLL) local oscillator and a lot of attention was given to the local oscillator and mixer designs.

The receiver was broken up into well-defined components that were matched to 50Ω. This modular design approach was used to guarantee easy manufacturing, substitution and testing. The flexibility also enables the designer to upgrade, increase capacity or bandwidth or reorganize the receiver easily in the future. The separate components of the system were designed, measured and characterized to make it possible to replace only a single component instead of the entire system when a part becomes obsolete.

A software tool was also developed to aid this replacement process by establishing whether a certain new characterized component would be useful in the system and how the system's performance would be affected. Amongst other things attention was given to the calculations of the signal-to-noise ratio, sensitivity, selectivity and spurious responses of the receiver. This will help to make intelligent and informed decisions concerning component replacement. This will also enable the designer to evaluate the receiver system in the preliminary design component and determine if the specifications are met.

Attention was given to minimizing the size and power consumption of the product throughout the design process while maximizing performance.

Maximum usable sensitivity	<0.5 μ V SINAD (20dB) \Rightarrow -113dBm in a 50 Ω system
Maximum AF output power	>200mW into 8 Ω .
AF response	300Hz to 2.7kHz (-6dB)
Image rejection	Better than 70dB
IF rejection	Better than 70dB
Adjacent channel rejection	Better than 70dB
Volume control	6 stepped volumes
Receiver distortion	6% max at audio output of 1.42Vrms

Table 1-1 Receiver specifications.

The channel spacing requirement is 12.5kHz for frequencies between 30MHz and 300MHz [5]. The maximum permissible frequency deviation for this 12.5kHz channel spacing is ± 2.5 kHz [5-7].

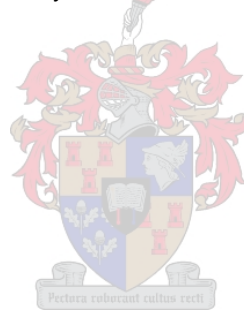
1.1 Thesis structure

This thesis is ordered as follows:

- Chapter 2 provides an overview of the necessary background principles. Receiver characteristics are defined and explained. The receiver components that influence every receiver characteristic are summarized. Receiver topology is discussed from a systems point of view and the main design restrictions and objectives of every receiver component are discussed. The chapter concludes with an essential discussion of noise theory, which will enable the designer to calculate the signal-to-noise ratio and the sensitivity of the receiver system, prior to the design.
- Chapter 3 introduces the computer software tool, **ReceiverCALC^{1.1}**, which was written to help the designer to determine if receiver specifications will be met. This helps to predict system performance and aids the theoretical replacement of redundant or costly parts.

Detailed descriptions are given to show how the program calculates the receiver characteristics.

- Chapter 4 provides a detailed description of the hardware design for every receiver component. Due to the modular design approach used, every component needs to be measured and characterized thoroughly. More than one unit is developed for every receiver component, each with different characteristics. This enables comparison of their influence on the receiver performance. This chapter also gives detailed descriptions of local oscillator and mixer terminology, characteristics and measurement methods. Phase noise is also investigated thoroughly.
- Chapter 5 describes the measurement procedures of the receiver characteristics. The receiver performance is measured while interchanging the different well-defined receiver components that were discussed in chapter 4. The influence of every component on the receiver characteristics can be confirmed with those anticipated in chapter 2. After this the measured receiver characteristics is compared to those calculated by using the software tool described in chapter 3. Conclusion are made concerning the utility **ReceiverCALC^{1.1}**.
- Chapter 6 concludes with a summary and recommendations for future work.



2 Background principles

2.1 Receiver characteristics and overview

A receiver is essentially a system that is used to recover information signals from high frequency radio signals. Many different topologies can be used to perform this function. Amongst these is the direct conversion receiver, which uses a mixer and an oscillator, at the radio frequency (RF), to down-convert the signal directly to base band. This receiver is constantly being investigated by the competitive cellular market, because of its small size, weight, simplicity, low external parts count, low cost and its potential to form a single radio receiver chip. The super heterodyne receiver, shown in *Figure 2-1*, is still the most popular receiver because of its superior performance. This receiver uses a mixer and an oscillator to perform frequency down-conversion to an intermediate frequency (IF) that is usually between the RF signal and the base band. This allows sharp cut-off filters to improve selectivity as well as higher gain due to the IF amplifier. Tuning is accomplished by varying the frequency of the local oscillator. It can also be a single or double conversion receiver in which the down-conversion to an IF frequency is done once or twice [1] [8] [9] [10].

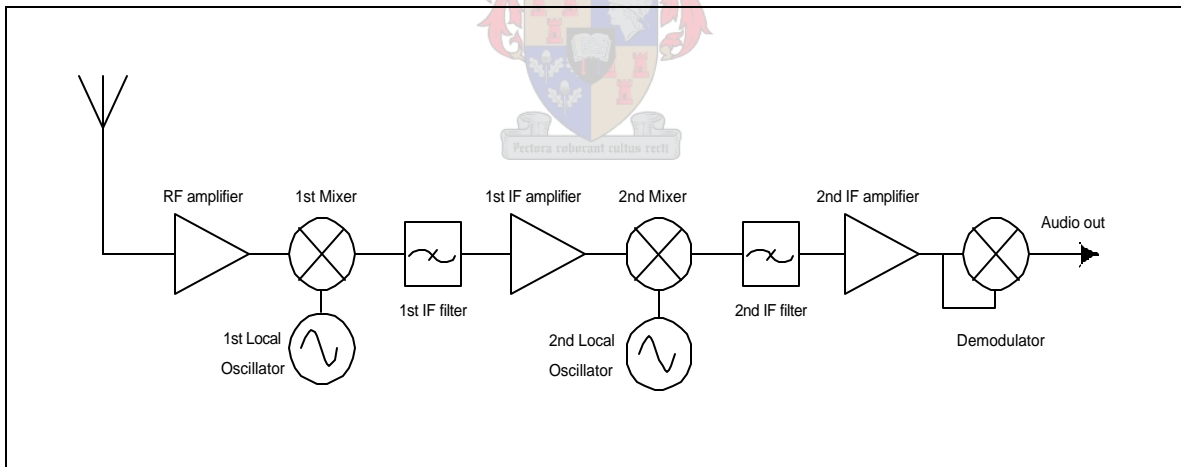


Figure 2-1 Block diagram of a double down-conversion super heterodyne receiver.

If a super heterodyne receiver utilizes a first IF frequency that is greater than the received RF frequency, it is said to be an up-conversion receiver, while a down-conversion receiver converts a high RF frequency to a lower first IF frequency.

A brief summary of the receiver characteristics follows. The different components and their most important functions and design restrictions are summarized in chapter 4.



2.1.1. Receiver characteristics

The most important receiver performance specifications are sensitivity, selectivity, distortion, audio frequency (AF) response, AF output power, IF and image rejection. Receiver characteristics are normally specified. The designer must be knowledgeable as to how to measure and attain them. These receiver properties are briefly defined in this section. Measuring techniques are described in chapter 5 [1] [8] [9].

2.1.1. a Sensitivity

Receiver sensitivity is, in essence, the quality that allows the reception of weak signals. This is not the ability of the receiver to amplify small signals, but rather the ability of the receiver to respond to weak signals, without the internal noise masking those signals. Sensitivity thus deals with the noise figure of the receiver [1] [8] [9] [11].

This minimum detectable signal power (or the voltage derived from the minimum detectable signal power), is specified for a specific required output signal-to-noise ratio (SNR) or signal plus noise and distortion-to-noise and distortion ratio (SINAD).

This important figure of merit does not depend on the gain of the receiver, because the signal and noise are amplified nearly equally. Therefore, careful consideration must be given to device choices in the front-end of the receiver to achieve a good noise figure. To optimize the noise figure and, consequently, the sensitivity, these devices should have a low noise figure. If the sensitivity of a receiver system is not as good as expected, more transmitter power might be necessary to achieve the same performance, which can be a concern, especially in portable equipment that have restrictions on their power consumption [1] [8] [9] [11] [32].

2.1.1. b Spurious responses

A spurious response is an unwanted frequency that produces a demodulated output in the receiver if it is encountered at a high power level. Spurious responses occur: [44]

- when a signal is received at a frequency where it is not transmitted.
- when a signal passes through to the IF stage due to insufficient RF selectivity (image and IF rejection).
- when signals appear to be received, but actually originate within the LO.
- when interfering signals cause cross modulation and desensitization .



The front-end of broadband receivers need to be broadband if they are not tuneable. Thus, undesired spurious responses are especially a problem in broadband receivers [1].

Most receiver responses result from the harmonics that is generated in the mixing process. These harmonics are called intermodulation products and can be calculated for a down-conversion receiver by using the equation [1] [9]

$$f_{IM} = |mf_{RF} - nf_{LO}| \quad (2.1)$$

where m and n are positive integers and the order of these products is $|m| + |n|$. f_{RF} and f_{LO} are the respective frequencies of the incoming RF signal and the local oscillator signal.

Most of these spurious responses fall outside the pass band of the IF, but some may fall inside the pass band. The amount of power contained in a specific intermodulation product decreases as the order increases. Therefore, they are usually negligible if their order is higher than approximately 6 [9].

The most important spurious responses include:

- Image – can be predicted by the image rejection.
- Half IF – rejection predicted by the mixer IP2.
- IF – Susceptibility for direct IF feed through predicted by IF rejection.
- Second image in dual conversion receivers – suppressed by the first IF filter.
- LO spurious responses.
- High order spurious responses close to the receiver frequency.

Three of the most important subcases of this broad definition of spurious responses is discussed next, namely the selectivity, IF rejection and image rejection.

i. Selectivity / Adjacent channel rejection

The receiver selectivity is the capability of the receiver to differentiate between the desired signal and interfering signals that appear at adjacent channel frequencies. This is determined by the selectivity of the IF filter, the oscillator phase noise, the synthesizer spurious responses, the IF bandwidth and the required SNR at the demodulator input. Selectivity is gradually becoming more important as regulations are moving towards narrower channel spacing. The narrowband requirements of a filter to achieve high selectivity is usually not achievable at the higher receive frequencies and, therefore, is applied at the IF frequency [1] [20] [40] [42].

Selectivity can be calculated by using the following formula [1]



$$Selectivity = -SNR_{output} - 10 \log \left[10^{(-IF_{sel}(f_{\Delta})/10)} + 10^{(-Spurs(f_{\Delta})/10)} + B \times 10^{(L(f_{\Delta})/10)} \right] \quad [dB] \quad (2.2)$$

where

- SNR_{output} is the signal-to-noise ratio at the detector input for a specified receiver output performance e.g. 12dB SINAD [dB].
- f_{Δ} is the frequency offset of the adjacent channel.
- $IF_{sel}(f_{\Delta})$ is the IF filter rejection at the adjacent channel [dB].
- $Spurs(f_{\Delta})$ is the LO spurious signals present in the IF bandwidth at $f_{IF} \pm f_{\Delta}$ as shown in Figure 2-2 [dBc].
- $L(f_{\Delta})$ is the single sideband (SSB) phase noise at a frequency offset equal to the channel spacing [dBc/Hz].
- B is the IF filter noise bandwidth (approximately IF bandwidth) [Hz].

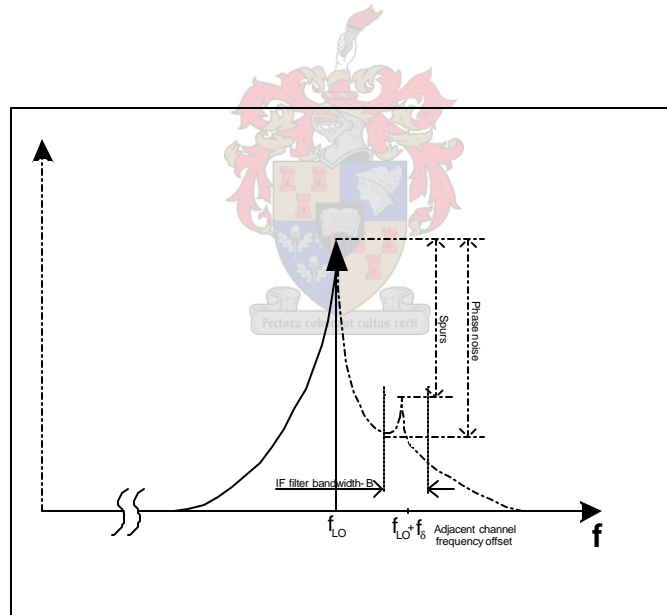


Figure 2-2 LO signal definitions for selectivity predictions [1].

ii. Image rejection

Mixers generate signals at the sum and difference frequencies of the input signals. If a down-conversion mixer is used, $f_{LO} < f_{RF}$ and

$$f_{RF} = f_{LO} + f_{IF} \quad (2.3)$$

An RF frequency at $f_{RF} = f_{image} = f_{LO} - f_{IF}$ if replaced into (2.3), will give an IF frequency of $-f_{IF}$ [9].

Mathematically this frequency is identical to the IF frequency because of the fact that the Fourier spectrum of a real signal is symmetric about zero frequency, and thus contains negative as well as positive frequencies. This RF frequency is defined as the image frequency and is defined as $f_{image} = f_{LO} - f_{IF}$ for high side injection, where $f_{LO} < f_{RF}$ and $f_{image} = f_{LO} + f_{IF}$ for low side injection, where $f_{LO} > f_{RF}$ [9] [22] [21] [44].

The desired and the image frequencies are separated by $2f_{IF}$. If the front-end filtering of the receiver is not sufficient the receiver will not be able to differentiate between the desired signal and the interfering image signal [9] [21].

The image rejection of the receiver is thus essentially the property that will determine how well an interfering signal at the image frequency will be rejected. The insertion loss of a filter with a sharp cut-off frequency is usually higher. Therefore, the image reject filter is usually placed after the RF amplifier, where it will have a smaller effect on the noise figure of the system, because the insertion loss before an amplifier will degrade the noise figure of the amplifier [56] [9] [21].

iii. IF rejection

A receiver's ability to reject signals at the receiver's first IF is its IF rejection property. Due to imperfect isolation between mixer ports, the signals present at the RF port of the mixer will pass through to the IF port. If a high interfering signal at the IF frequency is present at the RF port, it will pass through to the IF circuitry and cause desensitization and interference. IF rejection problems are serious because the receiver will receive the interfering signal at the IF frequency, no matter where the receiver is tuned. The IF rejection of the receiver is determined by both the mixer's RF-IF isolation as well as the frequency response of the front-end components [14] [20].

2.1.1. c Audio frequency response

Audio bandwidth should be limited by an audio filter to attenuate interference as well as the IF noise that originates in the receiver after the first IF filter. This will enhance the receiver signal-to-noise ratio. Audio frequencies should typically be between $\pm 300\text{Hz}$ and $\pm 2500\text{Hz}$ for voice communications [11].



2.1.1. d Audio frequency output power

This property specifies the available power [normally in W or mW] that should be available from the output of the audio amplifier, to drive the speaker or headphones. This property is usually defined for a load impedance of 8Ω [8].

2.1.1. e Dynamic range

The dynamic range of a receiver is set by the difference between the maximum allowable signal and the minimum detectable signal of the receiver. This quality expresses the ability of the receiver to deliver high performance in the presence of strong signals. The maximum allowable signal can be either the 1dB compression point or the third order intercept point. The dynamic range depends on the noise characteristics and the required SNR of the receiver, as well as on the compression and intercept points of the different components [9] [11] [24].

2.1.1. f Receiver distortion

Distortion is any difference between the original signal and the demodulated signal. Harmonic distortion occurs when the input signal power level of a component exceeds the 1dB compression point of that component and spurious responses are added to the signal at integral multiples of the original frequency [8] [9] [20] [23] [31].

Intermodulation distortion occurs when spurious responses, at the sums and differences of two input frequencies, are added to the original signal. Input signals exceeding the 3rd order intercept point will cause intermodulation distortion [8] [9] [23] [31].

Filters are not ideal and will therefore cause *linear* amplitude or frequency distortion by altering the existing frequency component amplitudes. Filters also cause phase or delay distortion, by delaying the different frequency components of a signal by various amounts, depending on their frequency. Excellent phase response and a sharp amplitude cut-off response tend to be incompatible goals in a filter. Phase and delay distortion is not so important where speech signals are received, because the human ear is not sensitive to small changes in phase [8] [9] [31].

Care must be taken to minimize the distortion in a receiver, by designing for a high dynamic range, reducing the signal levels into devices, minimizing the number of gain components, increasing selectivity and taking distortion that is added to the signal due to certain filter topologies, into account [8] [24].



2.1.1. g Conclusion

The different receiver characteristics that were defined and discussed in this section are influenced by certain characteristics of the different components of the receiver. A summary of the receiver characteristics and the different components that influences them are given in *Table 2-1*.



	Sensitivity	Selectivity	AF response	Distortion	Image rejection	Dynamic range	IF rejection	AF output power	Suppression of LO energy	Half IF rejection	Attenuation of 2nd image	Active device power
PRE-SELECT FILTER:												
Bandwidth				x	x		x		x	x		
Insertion loss	x					x						
Insertion loss at Image	x				x	x						
Noise figure	x					x						
Noise figure at Image	x					x						
RF AMPLIFIER (LNA):												
Noise figure	x					x						x
Noise figure at image	x					x						
Gain	x			x		x	x					
Gain at image	x				x	x						
1dB compression point				x		x						
IP3				x		x						
Bandwidth					x		x					
Reverse isolation		x							x			
IMAGE FILTER:												
Selectivity -bandwidth				x	x		x		x	x		
Insertion loss	x					x						
Insertion loss at image	x				x	x						
Noise figure	x					x						
Noise figure at image	x					x						
1st MIXER:												
Conversion gain/loss	x			x		x						x
Noise figure	x					x						
1dB compression point				x		x						
IP3				x		x						
IP2				x		x				x		
Noise balance	x					x						
LO-RF isolation									x			
RF-IF isolation							x					
LO-IF isolation												
INJECTION FILTER:												
Selectivity -bandwidth	x					x						
FIRST OSCILLATOR:												
LO power	x					x						x
Phase noise	x	x				x						
Wideband AM noise	x	x				x						
Spurious signals		x		x								
IF FILTER:												
Selectivity -Bandwidth	x	x	x			x						
Insertion loss	x			x		x					x	
Noise figure	x					x						
IF AMPLIFIER:												
Gain	x			x		x						x
Noise figure	x					x						
DETECTOR PROPERTIES:												
Required SNR at input	x	x				x						x
AUDIO FILTER:												
Bandwidth	x		x	x		x						
AUDIO AMPLIFIER:												
Gain			x	x		x		x				x

Table 2-1 Receiver properties and characteristics of the different components that influences them.



2.1.2. The receiver

The receiver system topology that was implemented is shown in *Figure 2-3*. This system is a double down-conversion super heterodyne receiver, which uses low side injection. The second IF circuitry, including the modulator, is implemented using a single IC. The system had to be designed for low power consumption to make it practical for portable equipment. This adds constraints to the receiver performance, and intermodulation distortion (IMD) occurs more easily [11].

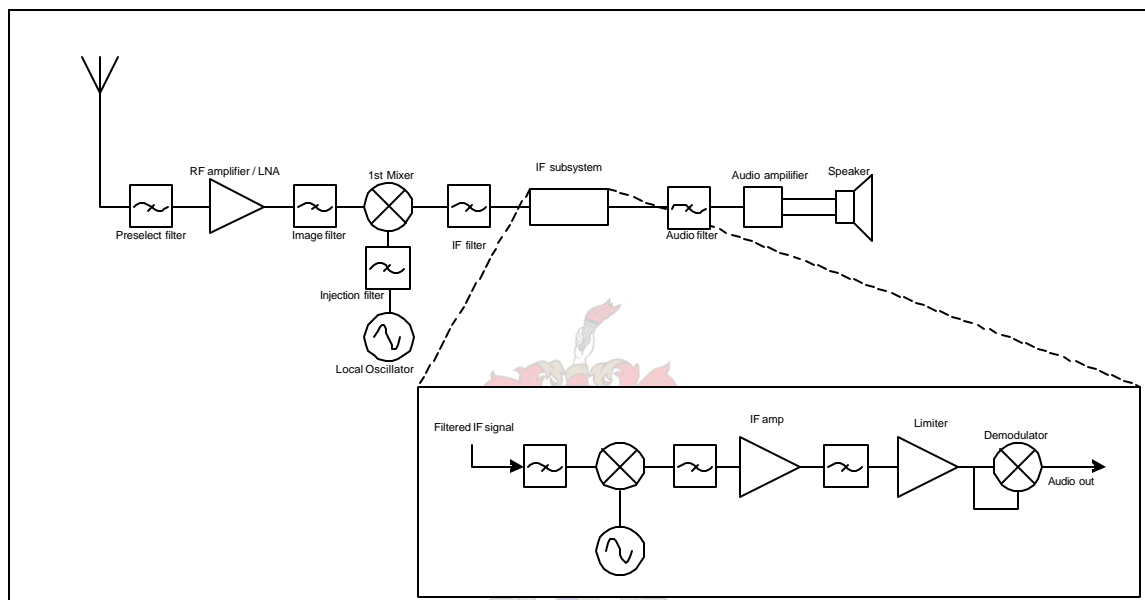


Figure 2-3 Block diagram of the receiver system that was used.

The main functions and most important design considerations of the different receiver components are given in the table below.

Device	Main objectives	Other functions	Design restrictions
Pre-select filter	<ul style="list-style-type: none"> Prevents strong interfering signals to saturate RF amplifier or mixer. Minimize IM distortion. 	<ul style="list-style-type: none"> Attenuate f_F to improve IF rejection. Suppress LO energy. Low attenuation of receiver spurious responses e.g. image. 	<ul style="list-style-type: none"> Placed before RF amplifier, thus insertion loss should be minimized to optimize overall noise figure. Filter will not have a sharp cut-off (high insertion loss associated with sharp cut-off).



Image reject filter	<ul style="list-style-type: none"> Reject image frequency. 	<ul style="list-style-type: none"> Attenuate f_F increase IF rejection. Reduce harmonic distortion. Suppress LO energy. Suppress 2nd harmonic of RF amplifier. 	<ul style="list-style-type: none"> Placed after RF amplifier, thus insertion loss will have less effect on noise figure of system, but should still be minimized.
RF amplifier	<ul style="list-style-type: none"> Important for good sensitivity. Provides amplification of small RF signal. 	<ul style="list-style-type: none"> Isolate pre-select and image filter : Improve selectivity. Attenuate LO signal power with high reverse isolation. 	<ul style="list-style-type: none"> Low noise figure critical for overall low system noise figure. High compression point to limit distortion & improve dynamic range. Gain >20dB is not desirable: -can cause instability -require high mixer compression point.
Mixer	<ul style="list-style-type: none"> Translate signal from one frequency to another. 	<ul style="list-style-type: none"> Suppress LO signal power : LO-IF isolation. Attenuate signals at f_{IF} to improve IF rejection : RF-IF isolation. 	<ul style="list-style-type: none"> Noise balance will affect AM noise rejection from LO – influence sensitivity. Conversion gain/ loss will affect sensitivity. High IP3 and compression point will limit intermodulation distortion (IMD): Have the highest input power levels in the receiver.
Oscillator	<ul style="list-style-type: none"> Generate signals at f_{LO} for mixer - used to process receiver signals. 		<ul style="list-style-type: none"> Phase noise influences adjacent channel selectivity performance. Wideband noise will influence sensitivity. Will cause receiver spurious responses if high spurious responses



			<p>present.</p> <ul style="list-style-type: none"> ▪ Should oscillate despite temperature and power supply variations. ▪ LO power needed depends on mixer.
Injection filter	<ul style="list-style-type: none"> ▪ Placed between LO and mixer to attenuate wideband AM noise around LO frequency and harmonics. 	<ul style="list-style-type: none"> ▪ Attenuate 2nd order intercept point. 	<ul style="list-style-type: none"> ▪ The need for this filter is determined by the LO output power and spurious responses, as well as by the input power needed for the LO mixer port.
IF filters	<ul style="list-style-type: none"> ▪ Provides adjacent channel rejection. ▪ Sets overall noise bandwidth of the system. 	<ul style="list-style-type: none"> ▪ Remove unwanted mixer products. ▪ Attenuation of 2nd image. 	<ul style="list-style-type: none"> ▪ Bandwidth determines modulation bandwidth. ▪ Can obtain selectivity from previous filters, but bandwidth and cut-off requirements are impractical to realize at RF frequencies, and insertion loss will have a more significant effect on the overall noise figure in the front-end.
IF amp	<ul style="list-style-type: none"> ▪ High gain component. 		<ul style="list-style-type: none"> ▪ IP3 must be high, especially if no IF filter is used.

Table 2-2 Important functions and design restrictions of different radio components [8] [1] [9] [27].

2.2 Noise theory

The designer of a new receiver should be able to evaluate his/her system concerning signal and noise to be sure that his/her system's output SNR is sufficient to meet specifications. Accurate prediction of the noise figure of a system is extremely important to avoid unnecessary re-design of the system to achieve a better sensitivity, especially for high performance receivers. This section will explain how these important calculations can be done [32] [56].



Thermal noise can be defined as the small random currents in a conductor, due to thermal agitation, which competes with the desired signal current. Noise that competes with the desired signal causes degradation in the desired signal-to-noise ratio between the input and output of a certain component. This is called the linear noise factor (F) of the component. The noise figure (NF) of a component is defined as

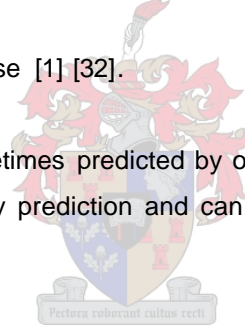
$$NF = 10 \log F \text{ [dB]} \quad (2.4)$$

The sensitivity of the receiver is closely related to the overall noise figure of the receiver (as stated in the previous section). A single number is, as a rule, not adequate to describe how well a receiver will function in all circumstances. These sensitivity calculations remain simply an estimation of the noise performance and, therefore, of the sensitivity of the system [8] [25] [26] [27] [56].

The noise figure of a system depends on the

- different component gains and noise figures.
- the image noise.
- local oscillator wideband noise [1] [32].

The noise figure of a system is sometimes predicted by only using the cascaded noise factor as discussed in 2.2.1. a This is a risky prediction and can result in sensitivity specifications not being met [32].



Descriptions of these different noise contributions and their role in the bigger picture will be given in this section, as well as a description of how to calculate the receiver sensitivity from this predicted noise figure. The local oscillator phase noise will be discussed in detail in chapter 4.

2.2.1. Noise figure calculations

The total linear noise factor of the system that is used to calculate the receiver sensitivity is given by

$$F_{tot} = F_{stages} + F_{image} + F_{LOnoise} \quad (2.5)$$

where

- F_{stages} is the linear noise factor calculated from the cascaded component gains and noise factors.
- F_{image} is the linear noise factor contributed by using the image frequency.
- $F_{LOWideband}$ is the linear noise factor contribution from the LO wideband noise [1].



Local oscillator (LO) wideband noise contributes significantly to the sensitivity degradation of the receiver. The image noise contribution is usually very small, but can still be of paramount importance, especially in very sensitive receivers [1] [32].

2.2.1. a Cascaded noise factor

The desired signal in a receiver system travels through a cascade of many stages, each degrading the signal-to-noise ratio in a way. The linear cascaded system noise factor can be calculated if every component gain and noise figure is known from

$$F_{stages} = F_1 + \frac{F_2 - 1}{G_1} + \frac{F_3 - 1}{G_1 G_2} + \dots + \frac{F_K - 1}{G_1 G_2 G_3 \dots G_{K-1}} \quad (2.6)$$

F_k is the linear noise factor and G_k is the gain of every component where $k = 1, 2, 3 \dots K$ and K is the number of components up to but excluding the demodulator [1] [26] [56].

It can be seen from (2.6) that the first component should have a low noise figure and at least moderate gain for a good overall system noise figure. Thus, the noise factor is dominated by the first component because the effect of the following components is minimized by the gains of the previous components. If the first component of the receiver system is a low noise amplifier, as shown in *Figure 2-3*, the noise performance of the system will be improved. On the other hand, an attenuator directly before an amplifier will degrade the noise figure. Therefore, the filter prior to the low noise amplifier in the super heterodyne receiver shown in *Figure 2-3* will degrade the noise performance of the receiver system significantly [26] [56].

2.2.1. b Noise factor contribution from image noise

The noise at the image frequency, that is present at the first mixer's input port, will down-convert to the IF band as demonstrated in *Figure 2-4* [1] [56].

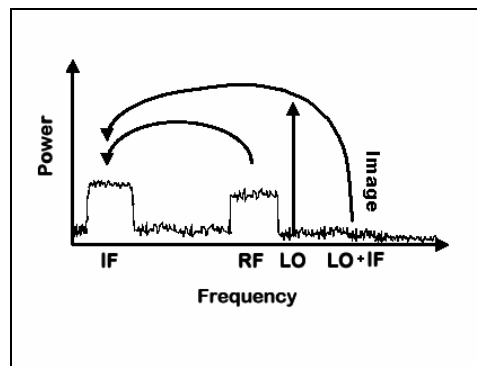


Figure 2-4 Image noise.



The noise factor contribution due to the image noise can be predicted as follows

$$F_{image} = \frac{\prod_{i=1}^N G_i}{\prod_{i=1}^N G_i} \left[F_{i_1} + \frac{F_{i_2} - 1}{G_{i_1}} + \frac{F_{i_3} - 1}{G_{i_1} G_{i_2}} + \dots + \frac{F_{i_N} - 1}{G_{i_1} G_{i_2} \dots G_{i_{N-1}}} \right] \quad (2.7)$$

where F_n is the noise factor and G_n is the gain of every component at the desired frequency, F_{i_n} is the noise factor and G_{i_n} is the gain of the components at the image frequency. $n = 1, 2, 3, \dots, N$ where N is the number of components up to but excluding the detector [1].

The image filter attenuates the image by reflection. Thus, this filter is not matched at the image frequency. Conventional cascaded noise figure analysis, assumes that all the components are matched and that the noise figure of a passive component is equal to its loss. This assumption is not true in the mismatched case. If the mixer input port termination is reactive it will produce no thermal noise and a zero noise figure can be assigned to the image filter - $F_{i_n} = 1$ ($NF = 0dB$) [56] [1].

For well designed multiple conversion receivers with a high gain front-end, the thermal noise amplified by the components that follow is negligible. Therefore, the analysis can only be carried out up to the first mixer [1].

2.2.1. c The noise contribution as a result of wideband LO noise

Local oscillator wideband noise separated from the LO frequency and its harmonics by $\pm f_{IF}$ will mix with a higher conversion loss than the desired signal. This will produce noise at the IF output as demonstrated in *Figure 2-5* [1] [10].

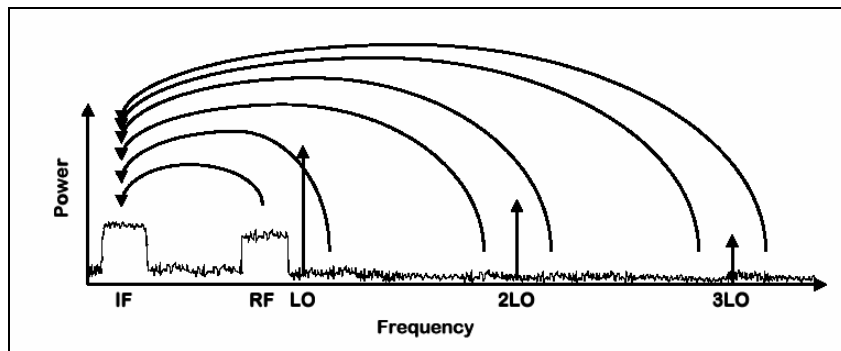


Figure 2-5 Down-conversion of noise (Figure 2.5 p20 [10]).



The noise figure contribution as a result of the LO AM wideband noise is calculated from [1]

$$F_{LOwideband} = \sum_{s=1}^M \frac{10^{[(P_{LO} W_s - L_s - M_s)/10]}}{1000kT_0 \prod_{j=1}^N G_j} \quad (2.8)$$

where P_{LO} is the local oscillator power [dBm].

W_s is the wideband noise level of sideband s [dBc/Hz].

L_s is the loss of the injection filter at sideband s [dB] - $L_s = 0dB$ for no injection filter.

M_s is the mixer noise balance for sideband s .

$k = 1.38 \times 10^{-23}$ [J /K] - Boltzmann's constant.

$T_0 = 290K$.

G_j is the gain of the components at the desired frequency.

$j = 1,2,3...N$ and N is the number of components up to and including the mixer.

$s = 1,2,3,...M$ where M is the number of sidebands taken into account.

This will degrade the sensitivity of the receiver significantly and has to be taken into account when the overall noise figure is predicted [1] [10].

2.2.2. Sensitivity calculation

As stated previously, sensitivity is the minimum detectable signal power (in dBm) or voltage (usually in μV) which will give a specified SNR or SINAD. The minimum detectable signal power or receiver sensitivity can be calculated by using the overall predicted noise figure from [1] [9]

$$S_{i_{min}} = kBT_0 F \left(\frac{S_o}{N_o} \right)_{min} \quad (2.9)$$

where F is calculated using (2.5).

$k = 1.38 \times 10^{-23}$ [J /K] - Boltzmann's constant.

$T_0 = 290K$.

SNR_{out} is the required linear signal-to-noise ratio at the detector input.

B is the equivalent noise bandwidth of the system [Hz].

$S_{i_{min}}$ is the minimum detectable signal power at the input of the receiver in watt. Thus, the sensitivity is $10 \log(S_{i_{min}} / 10^{-3})$ [dBm].

The minimum detectable signal voltage can be calculated by using

$$V_i = \sqrt{2Z_0 S_i} \quad [V_{rms}] \quad (2.10)$$

where Z_0 is the characteristic impedance of the system (normally 50 Ω) [9].

The IF filter, usually the narrowest filter in the system, sets the overall noise bandwidth of the system. As the cut-off of a filter becomes sharper, its noise equivalent bandwidth approaches its



3dB bandwidth. Thus, the noise bandwidth of the system is usually approximated by using the bandwidth of the IF filter [1] [9] [31].

The sensitivity of a practical receiver system will be improved to represent the sensitivity predicted if the different components are well matched to each other and if the different components are perfectly tuned to the desired frequency. Appropriate matching filters in a system tend to optimize the SNR by narrowing the bandwidth and by removing LO AM wideband noise as well as image noise. Filters can increase the noise figure of the system by introducing loss and attenuating the signal while the noise stays the same [56].



3 ReceiverCALC^{1.1}

Prior to the design of a new receiver system, the designer should be able to evaluate his/her system to predict performance. This will enable him to determine if specifications are met, and to use different components to improve performance.

Existing systems that need to use new components due to part replacement because of redundancy, cost or improvement can also be evaluated to determine if the characteristics of the new component are comparable with the original.

The computer program, **ReceiverCALC^{1.1}**, was written in *Delphi* [53] to predict the specifications of a receiver system. This program is easy to use and enables the system designer to compare different components and their effects on the overall receiver performance easily.

In this chapter **ReceiverCALC^{1.1}** and all its functions and advantages will be discussed. A copy of this program is given as an appendix CD in the folder 'ReceiverCALC'. The *Delphi*[53] code is also provided on this CD in the folder 'Delphi programming code', and can be viewed in *Delphi* [53].

3.1 The user interface

ReceiverCALC^{1.1} predicts the performance specifications of dual down-conversion receivers. The designer first has a choice between a dual conversion receiver with discreet components and a dual conversion receiver with the second IF circuitry integrated on a single chip (as shown in *Figure 3-1*). Each of these options opens a new window (with corresponding flexible system) that will be able to predict the most important specifications of the system.

Both of these receiver systems can be changed to fit the chosen receiver topology by selecting or deselecting the checkboxes in the system properties box at the bottom of the screen. This will activate or eliminate chosen components in the given topology. Warnings are given to show which system specifications will be influenced if a certain receiver component is eliminated. System properties are automatically calculated and updated each time a component is eliminated or inserted.



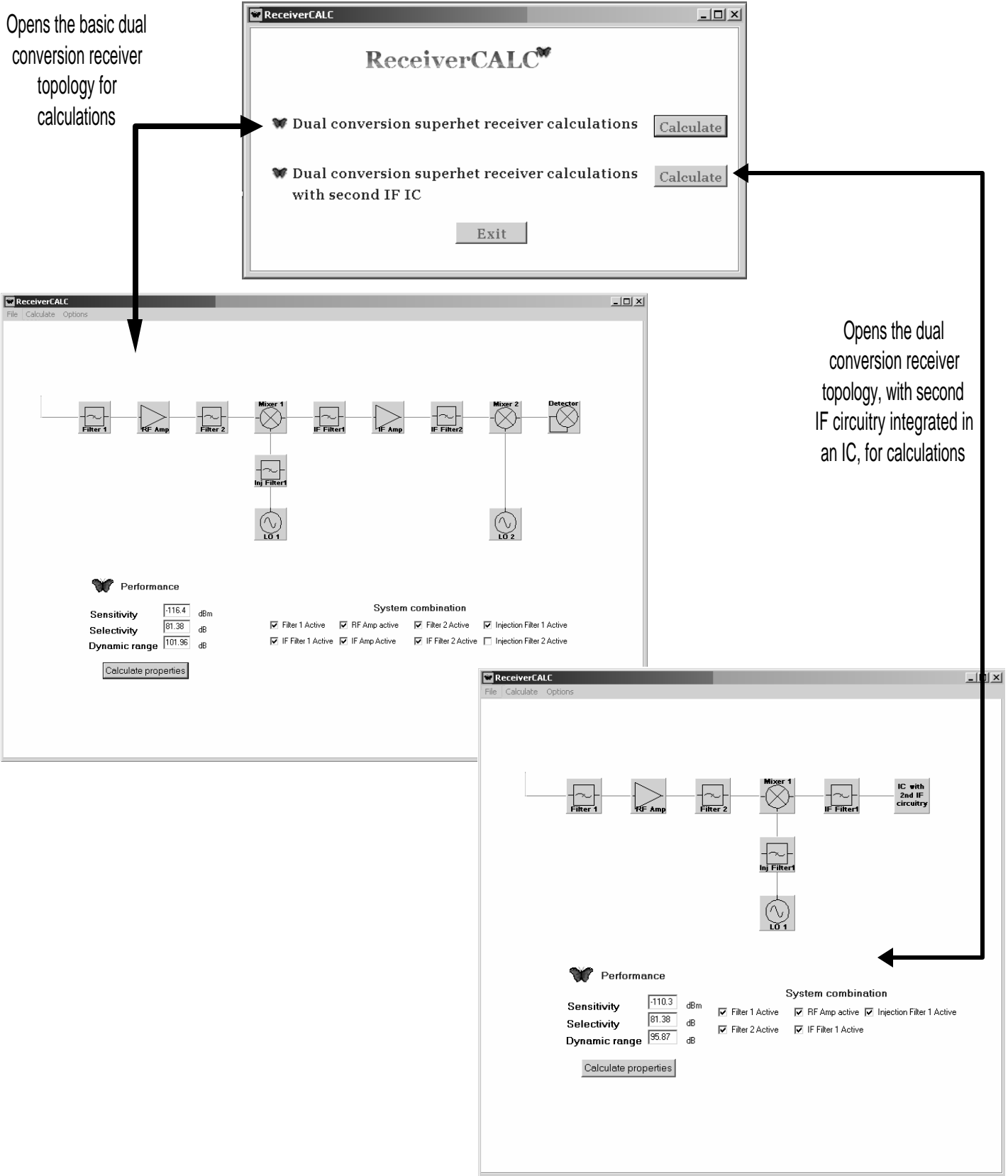


Figure 3-1 The user interface and possible systems.



Component properties can be seen and changed by clicking on the corresponding component. For example, a click on the RF amplifier opens up the dialog box given below in *Figure 3-2*. The properties of the RF amplifier can now be changed. If any property value is left empty or an unrealistic value is given, an error will be given when the OK button is pressed. If the exit icon in the right top corner is used, a warning is shown and the value is restored to its default. All the other component properties can be changed likewise.

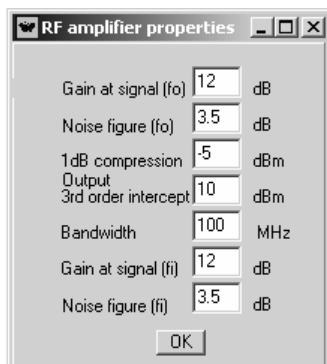


Figure 3-2 RF amplifier properties dialog box.

The active form and all its properties and settings in all the dialog boxes can be saved by selecting File/Save, typing a file name into the save dialog box and the clicking OK. If the file already exists, an option will be given to replace the file or not. The format of the files that is saved is text files. To open a file just click on File/Open and select the desired file as shown in *Figure 3-3*. The file is tested, to see if it was written by **ReceiverCALC^{1.1}**. If the file is the correct format, it will be opened and all the corresponding settings will be loaded. To start a new file, select File/New, and all the properties will be restored to their default values. To close the program, click on the exit icon in the top right corner or select File/Close.



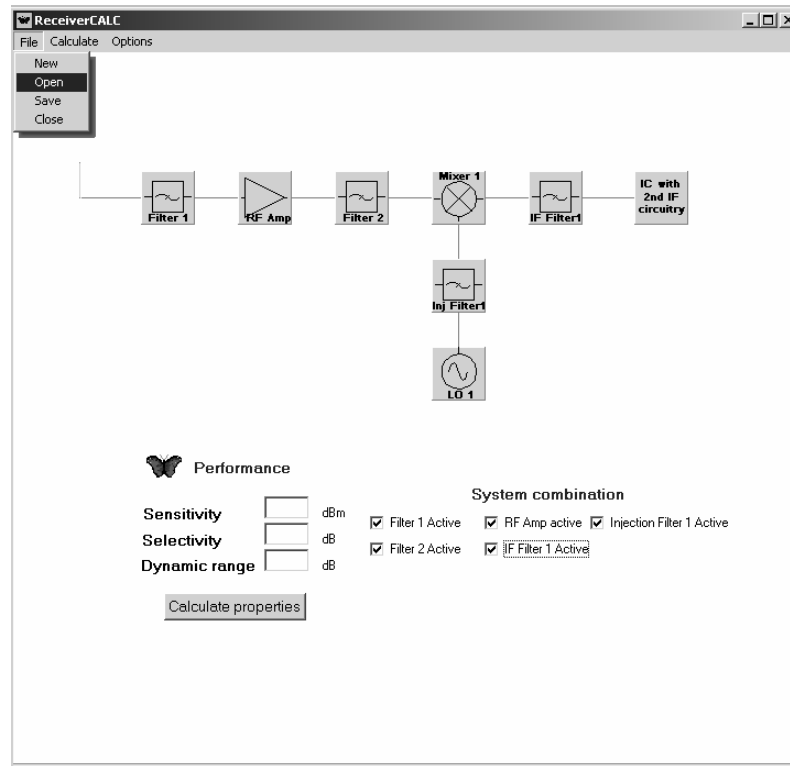


Figure 3-3 Opening a file.

ReceiverCALC^{1.1} can be used to calculate the receiver selectivity (adjacent channel rejection), sensitivity, spurious responses and dynamic range. A power diagram, to determine the power levels throughout the receiver, can also be drawn. Each of these calculations can be done by clicking on the corresponding calculation under the Calculate menu button and are discussed in the next section. The sensitivity, selectivity and dynamic range can also be calculated by clicking on the calculate properties button.

When calculating spurious responses, it is important to know what the receiver frequency range and channel spacing is and whether a doubly balanced mixer is used or not (certain spurious responses are rejected if a doubly balanced mixer is used). This can be selected in the dialog boxes under Calculate/Spurs or Calculate/Selectivity or under Options/System Properties as shown in Figure 3-4. The properties in these dialog boxes are similar and, if they are changed in one dialog box, they automatically change in the other, and in all the component properties dialog boxes where applicable.



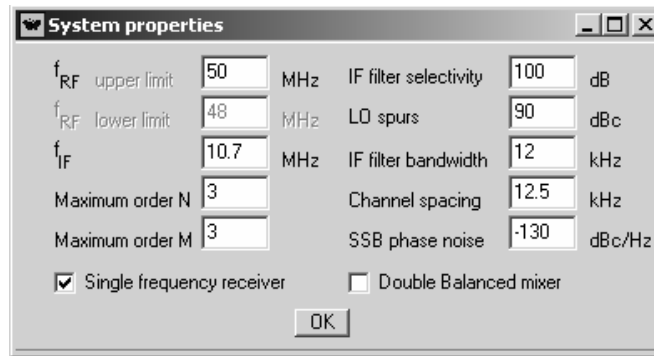
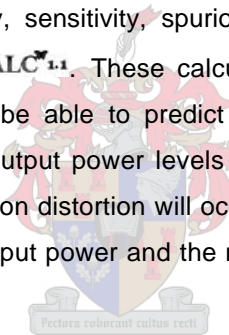


Figure 3-4 The Options/System properties dialog box.

The calculations that can be done with **ReceiverCALC^{1.1}** are discussed in the section.

3.2 Calculation of receiver performance

Calculation of the receiver selectivity, sensitivity, spurious responses, distortion and dynamic range are possible with **ReceiverCALC^{1.1}**. These calculated receiver specifications are only predictions because they will never be able to predict a system's performance accurately in reality. Calculation of the input and output power levels throughout the receiver is important to determine if harmonic or intermodulation distortion will occur. The dynamic range is predicted by calculating the minimum detectable input power and the maximum input power without harmonic or intermodulation distortion occurring.



3.2.1. Receiver sensitivity

The receiver sensitivity is predicted or calculated with equations as described in section 2.2.2. The calculations done by **ReceiverCALC^{1.1}** will, by default, take the noise contributions of the component gains and the noise figures into account as well as the noise contribution because of the image and wideband LO-noise. This will give a more accurate prediction of the sensitivity than the one that is normally predicted by only considering the cascaded component gain and noise figure contributions.

If this is not preferred, or if not all the required component properties are known, the noise figure contributions that must be taken into account by the calculator can be selected under Calculate/Calculation options. The checkboxes in this dialog box can be checked or unchecked to specify your specific need as shown *Figure 3-5*. If these checkboxes are enabled or disabled, the corresponding properties in the component properties dialog boxes will be disabled.



The antenna noise temperature is by default room temperature but can also be changed here. The noise bandwidth of the system can also be changed in this dialog box, and will automatically be updated in all relevant dialog boxes.

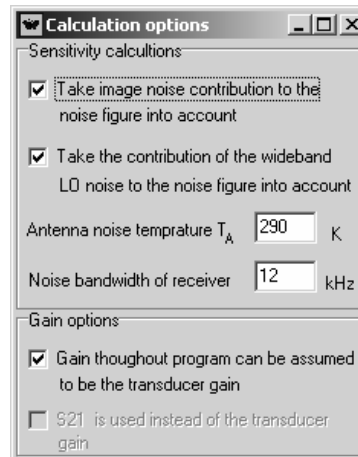


Figure 3-5 The calculation options dialog box.

The disabling of these noise figure contributions is not encouraged, because it will result in less accurate results. Accurate prediction of sensitivity is essential to prevent

- re-design of the expensive receiver front-end.
- requirement of more transmitter power to achieve the same performance, especially in portable equipment that requires low power consumption.
- over-design of the receiver to achieve a low noise figure at the expense of other receiver specifications.
- the use of unnecessary expensive low noise front-end components or unnecessary complex time consuming design of amplifiers with a low noise figure [1] [8] [32].

It should be remembered that the noise figure of a passive component would be approximately equal to the loss of the component. Thus, the noise figures of passive mixers and filters should be easy to specify. Noise figures and gains of the relevant active components should be specified on the datasheets of the components. Different receiver components will require certain noise figures, which will achieve the overall system sensitivity specification. Therefore, the noise figure requirement of a certain receiver component can be predicted with **ReceiverCALC^{1.1}**, before designing the component [25] [26].

The selectivity of a system is reliant on the bandwidth and cut-off characteristic of the IF filter, which implies that these filters should have sharp cut-off characteristics. As the cut-off of a filter



becomes sharper, its noise equivalent bandwidth approaches its bandwidth. Thus the noise equivalent bandwidth of the system is predicted by **ReceiverCALC^{1.1}** according to the bandwidth of the IF filter. If the IF filter is not present the designer should enter the noise equivalent bandwidth in the Calculate/Calculation options dialog box [9] [31].

3.2.2. Receiver selectivity/adjacent channel rejection

Receiver selectivity is fast becoming one of the most important design considerations (and restrictions), as regulations are getting more stringent. As previously stated in 2.1.1. b) this property depends on the selectivity of the IF filter, the oscillator phase noise, synthesizer spurious responses, IF bandwidth and required SNR at the detector input. Selectivity of the system is predicted by **ReceiverCALC^{1.1}** by using equation (2.2). If more than one filter is present, the first one's bandwidth and selectivity will be used and if no IF filters are activated this property will only be given as poor.

Prediction of the selectivity of the receiver is important to determine

- What is an acceptable oscillator phase noise.
- What the restrictions should be on the IF filter.
- How significant oscillator spurious responses are.

3.2.3. Dynamic range and power diagrams to predict distortion

The dynamic range of the receiver system is one of its most important design considerations because it will determine how the receiver will operate in the presence of strong and very weak input signals. Poor dynamic range will cause desensitization and distortion [9] [11].

The dynamic range of a receiver can be calculated by using [9] [11]

$$\text{Dynamic range [dB]} = \text{Maximum allowable signal power [dBm]} - \text{Minimum detectable signal power [dBm]} \quad (3.1)$$

The minimum detectable input signal power (sensitivity) is calculated by using the noise figure as described in section 3.2.1. The maximum allowable signal power can be calculated by calculating the signal levels throughout the receiver for a specific input power, to determine if the compression point or the intercept point of any device is exceeded. The input signal is chosen as the highest intercept point in the receiver and decreased repeatedly until the signals throughout the receiver do not exceed component 1dB compression or intercept points. This is the maximum allowable input signal power [9].



ReceiverCALC[™] also enables the designer to calculate the receiver power levels throughout the receiver by plotting a diagram of power levels. A typical diagram is shown in *Figure 3-6*.

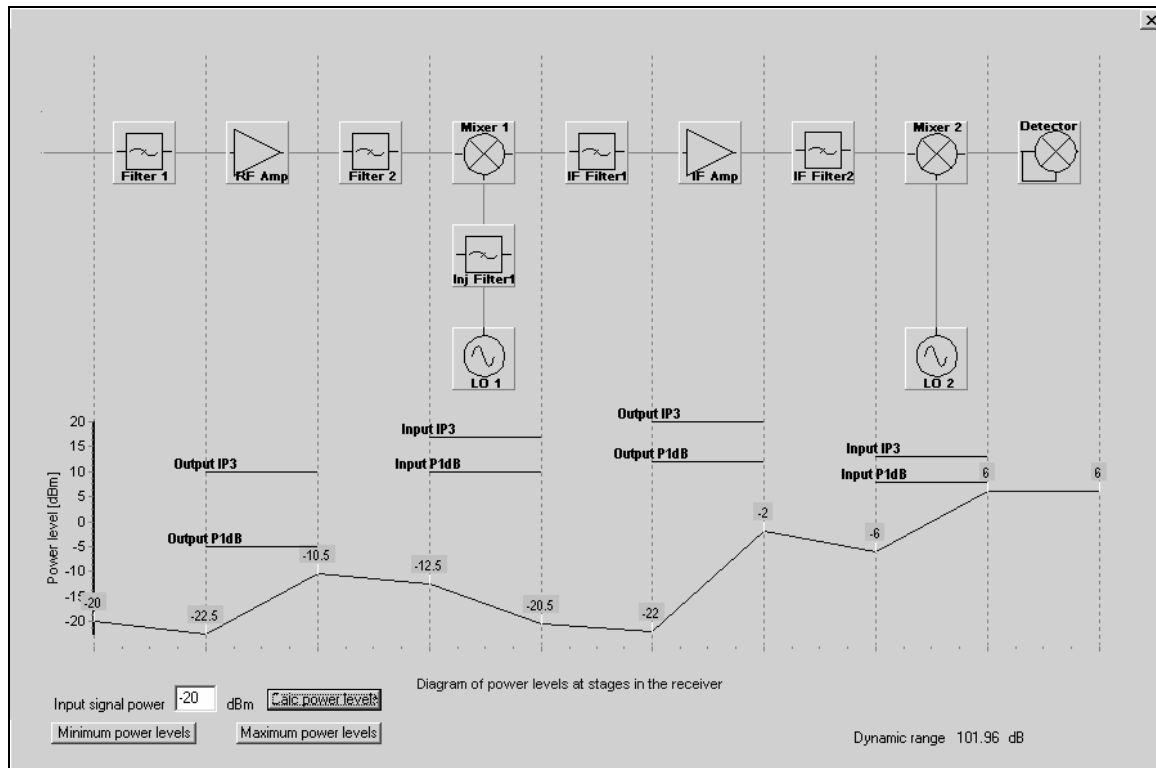


Figure 3-6 Calculated power levels throughout the receiver, with an input power of -20dBm .

This very powerful tool enables the designer to determine the effect of changing component specifications and makes it easy to see if 1dB compression points or intercept points are exceeded. Messages will warn the designer if these points are exceeded as shown in *Figure 3-7* [9]. The maximum allowable and minimum detectable signal levels throughout the receiver can also be plotted on similar diagrams.

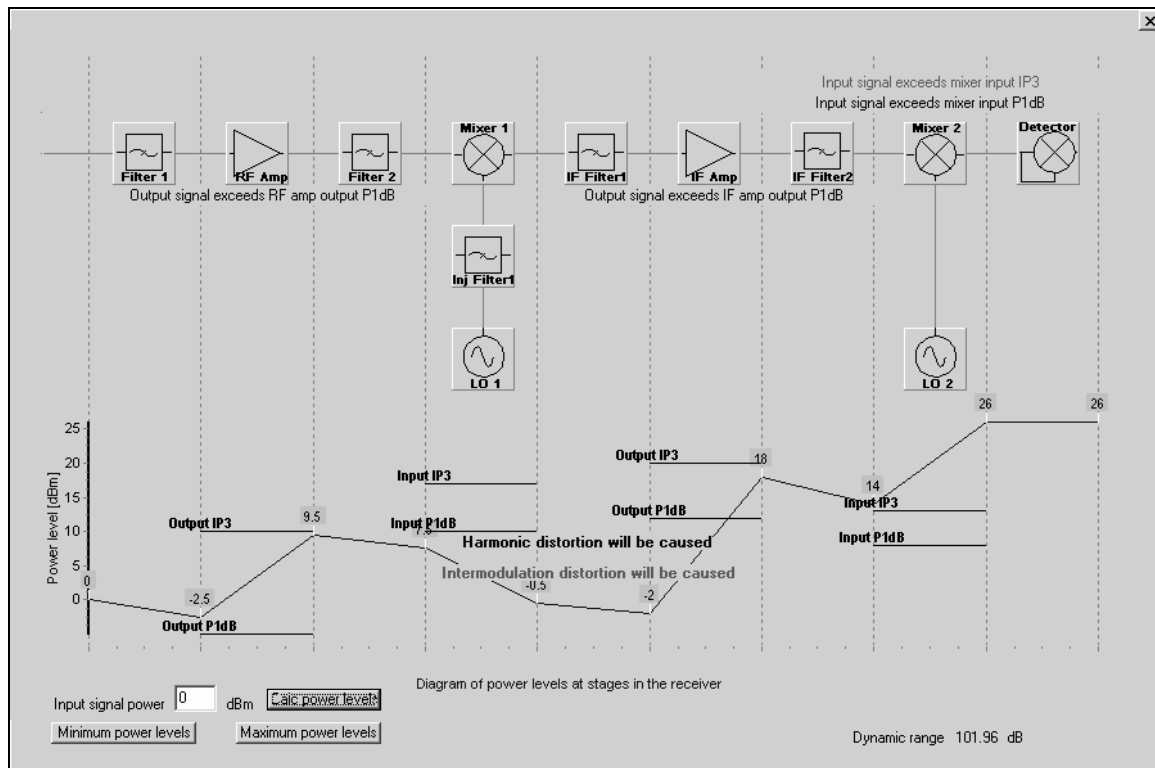


Figure 3-7 Calculated power levels, with an input power of 0dBm. Note warnings when the compression or intercept point of a component is exceeded.

3.2.4. Spurious responses

The calculation of receiver spurious responses, as defined in the previous chapter, is essential to determine if some of them will fall in the IF pass band. There is a large combination of responses to check. Therefore, it is helpful to have a computer program determine the responses [9].

For a single frequency receiver, there is only a single known f_{RF} and f_{LO} . Therefore, the intermodulation products can simply be calculated by using $f_{IM} = |mf_{RF} - nf_{LO}|$ where $m=1,2,3...M$ and $n=1,2,3...N$.

A multi channel receiver is built to receive a specified RF frequency range and demodulate it to a certain known IF. This receiver will have a certain known channel spacing, f_{Δ} . Intermodulation products can be calculated by firstly calculating the specific RF frequencies that are spaced by the known channel spacing f_{Δ} . The LO frequency for each individual RF frequency is calculated next, with $f_{LO} = f_{RF} - f_{IF}$. Intermodulation product frequencies can now be calculated for every f_{RF} and f_{LO} with $f_{IM} = |mf_{RF} - nf_{LO}|$ where $m=1,2,3...M$ and $n=1,2,3...N$. The order of these products is $|m| + |n|$. M and N are the upper limits of the maximum orders to be searched and are

usually sufficient if greater than 6. This is because the magnitude of the intermodulation products decreases with increasing order and usually products greater than 6 are negligibly small [1] [9].

A graph is drawn with these calculated spurious responses. Another graph with only the IF pass band is also drawn to determine if any spurious responses falls inside the IF pass band. A typical graph is shown below in *Figure 3-8*.

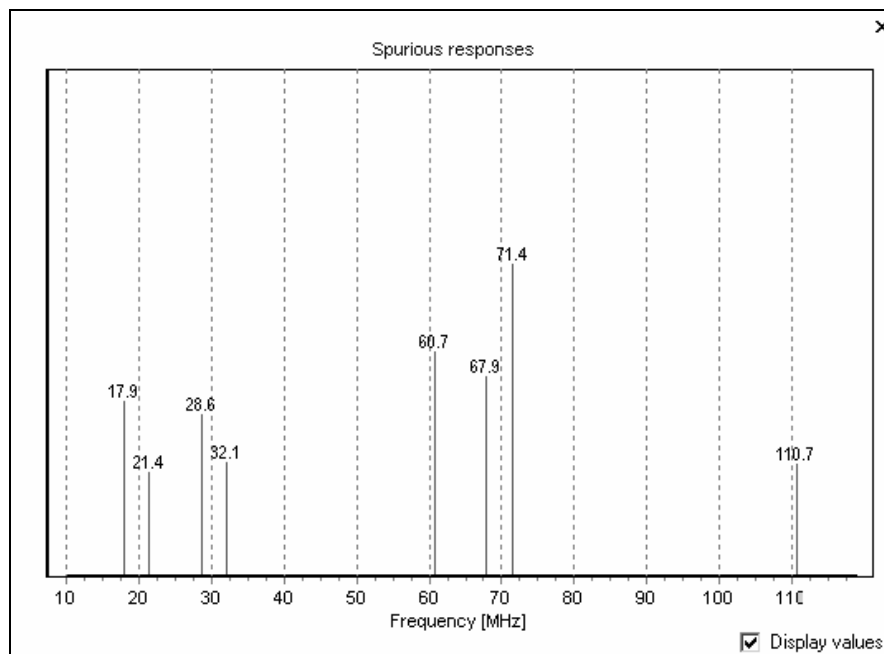


Figure 3-8 Spurious response chart for a single frequency receiver with $f_{RF} = 50\text{MHz}$, $f_{IF} = 10.7\text{MHz}$ and $N = M = 3$.

3.3 Conclusion

The equations used to predict the system performance assume that the component properties are linear and that all components are perfectly matched to each other. This will definitely not be the case in an actual system. Therefore, it is very important to remember that the receiver specifications that will be calculated with **ReceiverCALC^{1.1}** are only predictions. In reality, one value will never be sufficient to predict a receiver system's performance in all conditions.

Every component as shown in the previous chapter has its own unique functions. Insertion of every new component in the system will always involve a trade-off between different system specifications. This can be potentially dangerous because, while one property might seem to improve significantly and the system seems simpler and less expensive, it can be so easily forgotten that this will be at the expense of another important receiver specification. This can be



illustrated by removing the image reject filter, before the first mixer. Even though the receiver sensitivity will be improved, the image rejection specification might not be achieved as a result. The designer will, however, be warned to consider this when removing components of the system.

Predictions of the receiver performance, on the other hand, are essential to aid the designer in evaluating the receiver system prior to the design of the receiver. This is very important to prevent over-designing for certain specifications, thus compromising others, as well as to prevent trying to improve performance afterwards by using different components, resulting in extra cost, complexity and time consumption.



4 Development of the receiver components

A modular design approach was used to design the receiver. The receiver is divided into components that are each designed, built and matched to 50Ω and then measured and characterized separately. This modular design approach enables the designer to upgrade easily to increase bandwidth or replace parts when components become obsolete in the future. Impedance matching in high frequency networks is necessary to ensure maximum power transfer. Power at high frequencies is expensive and should not be wasted. Impedance matching in high frequency networks is also important to improve the signal-to-noise ratio [26].

This chapter discusses the theory of the individual receiver components and then provides a hardware design description for every receiver component. An overview of the chapter is shown in *Figure 4-1*.

Due to the modular design approach used, every component needs to be measured and characterized thoroughly. More than one unit was developed for every receiver component, some with better characteristics than others. This information is critical to enable the comparison of their influence on receiver performance in the next chapter.

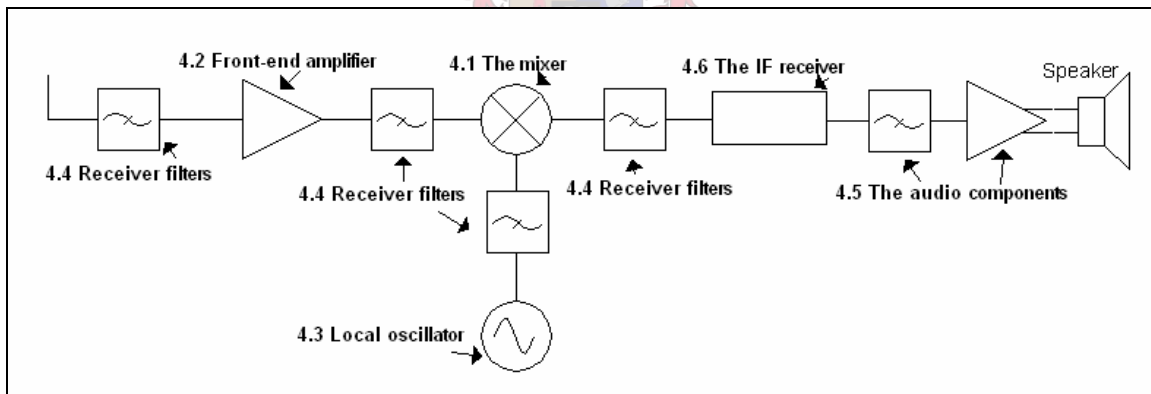


Figure 4-1 Structure of chapter 4.

4.1 The mixer

Mixers are the primary devices that are used in communication systems to achieve frequency conversion without affecting the modulation properties of the signal at the RF input port. Operation of mixers is typically based on the non-linearity of a diode or a transistor. Important properties include dynamic range, conversion loss (or gain), image response, bandwidth,



intercept point, port isolation, noise figure, voltage standing wave ratio (VSWR) and LO noise rejection [35] [1] [9] [13] [24].

Mixer types and characteristics will be discussed in this section, followed by a description of the mixers that were designed and their measured performance. The section will conclude with a comparison of the various mixers.

4.1.1. Theory of mixers

4.1.1. a Active and passive mixers

A *passive mixer* is a mixer where the energy for the frequency-translated output signal comes from the input signal and the LO supply. These mixers are usually implemented by using the non-linear properties of diodes. These types of mixers have an inherent conversion loss due to the frequency translation process and the impedance matching at the three ports, which leads to resistive mixer losses [1] [9] [12] [16] [35].

The output power of an *active mixer* comes from a DC power supply, rather than from the LO and is generally implemented by using the non-linear properties of transistors. As a result, lower LO levels can be used and active mixers offer gain [1] [9] [12] [35].

Passive diode mixers and active transistor mixers are different and thus it is difficult to compare their performance. Active mixers may have a conversion gain, but also typically have a poorer noise figure than passive mixers. Comparisons of active and passive mixers should incorporate the cascade result of the subsequent components [1] [9] [35].

The greatest benefit of passive mixers is that they do the majority of tasks at least adequately, although not exceptionally well. Passive mixers generally require more LO power, have a better noise figure and a smaller dynamic range while they are broadband devices, with moderate distortion, conversion loss, port isolation, spurious response rejection, LO noise rejection and low phase noise [1] [9] [35].

Active mixers on the other hand, may have a conversion gain, typically require less LO power, have a wider dynamic range and may present superior performance for some of these characteristics but not for all. Active mixers are also compatible with monolithic processes even though they are rather complex circuits with a typically poor noise figure [1] [9] [35].



4.1.1. b Mixer characteristics

As noted above the most important properties of mixers include conversion loss (or gain), image response, 1dB compression point, intercept point, port isolation, noise figure and LO noise rejection. A short description of the most important mixer properties, that will be measured, will be given in this section, as well as a description of why they are significant and how to measure them [9] [13] [57].

i. Conversion gain or loss

The amount of attenuation or amplification of the signal from the RF input port to the IF output port of a mixer is referred to as the mixer's conversion gain. This gain can be positive or negative (in which case it is referred to as conversion loss). This loss is inherent due to the frequency translation process and the impedance matching at the three ports, which lead to resistive mixer losses. Active mixers may amplify the input power. This important figure of merit for mixers is defined as follows:

$$G_c [dB] = RFpower_{in} [dBm] - IFpower_{out} [dBm] \quad (4.1)$$

The conversion gain of a mixer is extremely important, because the noise figure of a receiver may be minimized through minimizing the losses in the first RF components. This in return will influence the sensitivity of the receiver [9] [13] [57].

The instrumental set-up for measuring conversion gain is shown in *Figure 4-2*. The gain or loss is usually specified at a specific frequency and input LO power level.

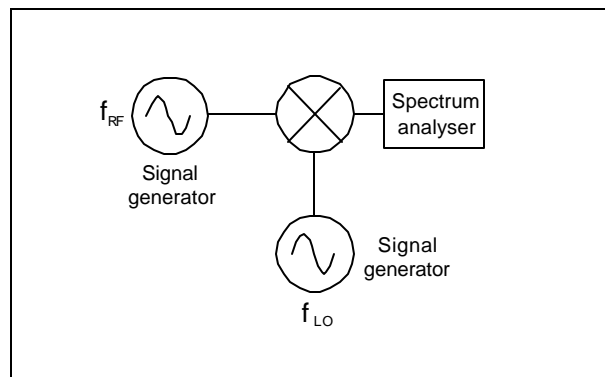


Figure 4-2 Set-up for measuring Conversion loss or gain and IP1.

ii. Isolation

Isolation refers to the ability of a mixer to attenuate the coupling of RF power input at one port to another port of the mixer. High isolation between ports is preferred because unnecessary signal feed through in mixers will waste RF power, disguise the IF signal output and cause electromagnetic interference [9] [13] [22] [24].

LO-to-RF and LO-to-IF isolation are the most important and are generally the only characteristics specified. The LO-to-RF port isolation is extremely important, because LO power coupled to the RF port of the mixer will be radiated by the antenna, causing interference with other services or users. LO-to-IF isolation is essential, because high leakage of LO power through the mixer will mask the IF, especially when it falls in the IF band. In addition RF-to-IF isolation is specified, especially when high RF input power signals are used or if a broadband IF is used, thus allowing the RF feed through to fall in the IF band [9] [13] [22].

For measuring isolation, 50Ω impedances are required at the unused ports, while the mixer is still DC biased and driven at the LO input as normal. Measurement set-ups shown in *Figure 4-3* are used to measure different port-to-port isolations. The reduction of signal input power level between one port of the mixer and any other port is measured [18] [19] [22].

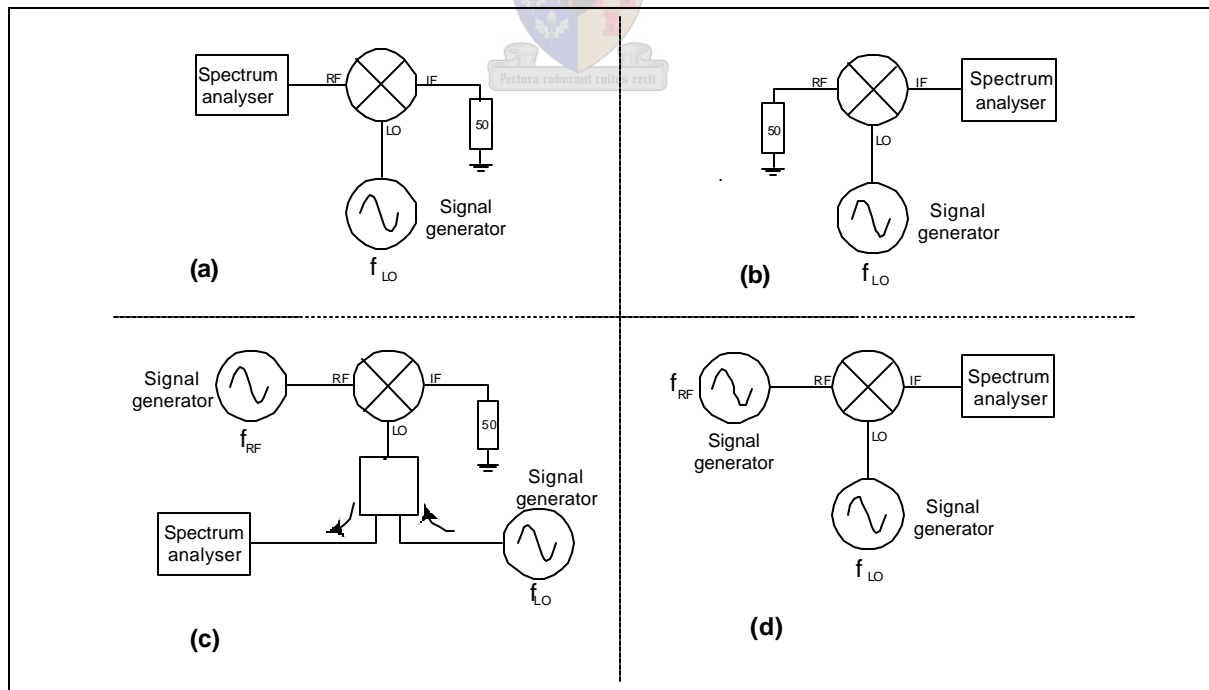


Figure 4-3 Experimental set-ups for measuring isolation between ports (a) LO-RF isolation (b) LO-IF isolation (c) RF-LO isolation (d) RF-IF isolation [18] [19].

iii. 1dB compression point

Above a certain input power level, the output power level of a mixer will fail to follow input level changes linearly (illustrated in *Figure 4-5*). This happens because of device saturation and the fact that the losses in the mixer will now start to increase with increasing signal power. The 1 dB compression point of a mixer is the point where the output level of the mixer has fallen 1dB below the anticipated output level of the mixer if an ideal linear transfer function is assumed. This value is usually taken as the upper limit of the dynamic range and input power levels that exceed this value will cause harmonic distortion. The experimental set-up for measuring the 1dB compression point is the same as for conversion loss, as shown in *Figure 4-2*. The 1dB compression point is specified for a specific LO input power level [1] [9] [22] [24] [26] [57].

iv. Intercept point

An input signal consisting of two narrowly spaced frequencies (ω_1 and ω_2) into a non-linear circuit will generate intermodulation products at its output of the form: [9] [19]

$$IMproduct = \pm mF_1 \pm nF_2 \quad (4.2)$$

The order of these products is $|m| + |n|$. Thus $3\omega_1; 3\omega_2; 2\omega_1 + \omega_2; 2\omega_2 + \omega_1; 2\omega_1 - \omega_2$ and $2\omega_2 - \omega_1$ are the six third order intermodulation products that will be generated as shown in *Figure 4-4*. The most critical of these products is $2\omega_2 - \omega_1$ and $2\omega_1 - \omega_2$ which fall very close to f_{RF} , and will be down-converted into the IF pass band. This output is derived by first defining the two input signals of the mixer as [1] [9] [17]

$$v_i = V_o (\cos \omega_1 t + \cos \omega_2 t) \quad (4.3)$$

The output of a non-linear circuit can be modeled as a Taylor series. Therefore, the output signal can be expressed as: [9]

$$v_{out} = a_0 + a_1 V_o (\cos \omega_1 t + \cos \omega_2 t) + a_2 V_o^2 (\cos \omega_1 t + \cos \omega_2 t)^2 + a_3 V_o^3 (\cos \omega_1 t + \cos \omega_2 t)^3 + \dots \quad (4.4)$$

The $(\cos(\omega_1 t) + \cos(\omega_2 t))^3$ term in equation 4.4 will lead to the six third order intermodulation products derived earlier. It can be seen from this equation that an increase in the input voltage amplitude, V_o , leads to a V_o^3 increase in the amplitude of the third order intermodulation products [1][9][17].

Third order intercept point (IP3) is defined as the input or output power level where the desired signals and third order intermodulation products are equal in amplitude. When this is represented on a graph, with input power on the X-axis and output power on the Y-axis, the third order intermodulation products' power will fall on a straight line with a slope of 3 and a desired output signal power on a straight line with a slope 1. The two



lines will intercept if the linear portions of these lines are extended. The XY coordinate of the point where they intercept are the respective input and output intercept point [1] [9] [13] [17] [24] [57].

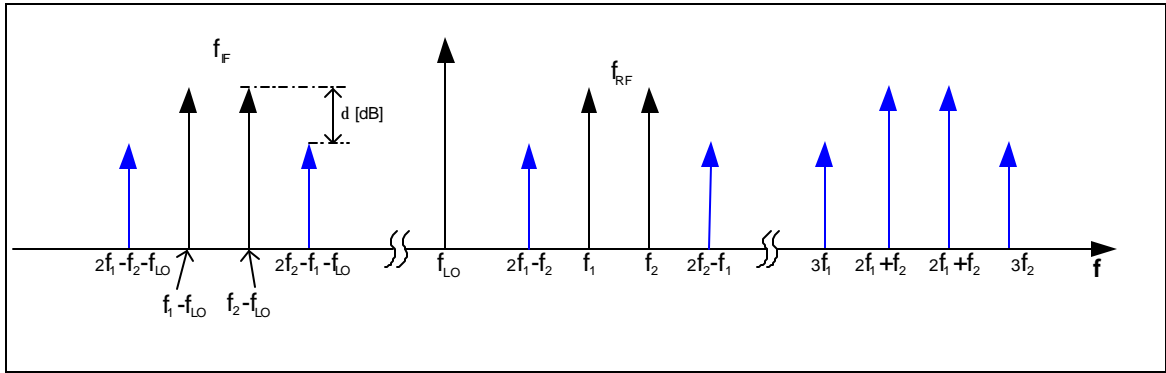


Figure 4-4 Mixer third order intermodulation products in the output signal [1] [9] [13] [57].

This point is extremely important, because input power levels in excess of the third order intercept point will cause intermodulation distortion. This intercept point is reliant on the LO and RF frequency and it is specified for a given LO power level. A device's IP3 also depends very strongly on its terminating impedances at all ports. For this reason attenuators are included at each port during high performance mixer measurements [1] [9] [13] [17] [57].

When measuring IP3 of a mixer, the experimental set-up shown in *Figure 4-6* is used. Two equivalent low amplitude RF input signals that are narrowly spaced are combined and fed into the mixer. The IF output spectrum of the mixer on the spectrum analyzer will include down-converted third order intermodulation products as well as the desired signals, as shown in *Figure 4-4*. The output intercept point (in dBm) can now be calculated by using the formula

$$IP3_{out} = P_{out} + \frac{d}{2} \quad (4.5)$$

Where P_{out} is the output power in dBm and d is the difference between the desired output signal and the third order intermodulation products as shown in *Figure 4-4* [1] [17] [24] [57].

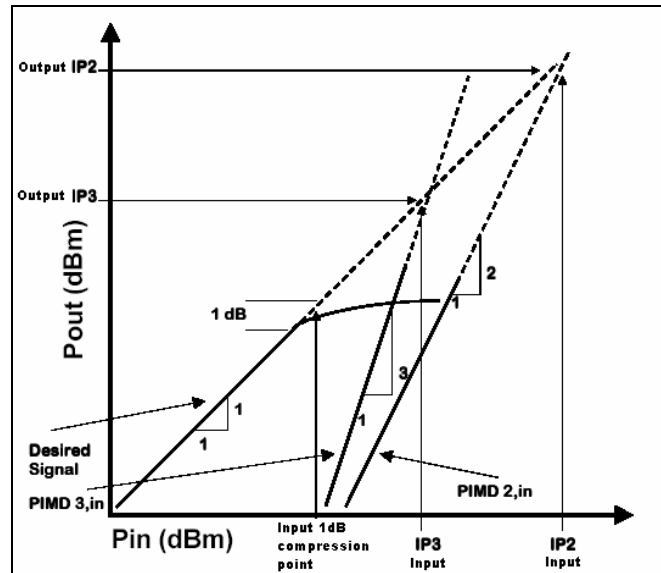


Figure 4-5 Illustrating Intercept and 1dB compression point - Figure 2-4 p18 [10].

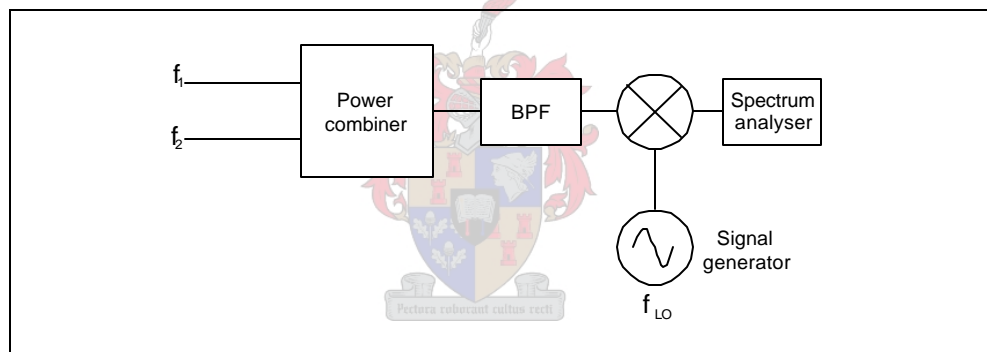


Figure 4-6 Experimental arrangement for the measurement of IP3 [1] [18] [19].

The input intercept point of the mixer can be calculated from the output intercept point by adding or subtracting the mixer conversion gain or loss. Mixer intercept point is usually specified with respect to input, while amplifier intercept point is generally specified as an output intercept point [1] [9] [17] [24] [57].

v. Noise figure

The noise figure of a mixer is the difference between the RF input signal-to-noise ratio and the IF output signal-to-noise ratio in dB. The double sideband (DSB) noise figure includes signal and noise powers at the RF and image signal, while the single sideband (SSB) noise figure includes the noise power at image signal, but neglects the image signal power [9] [13] [57].



In general, SSB noise figure is specified because only one of the signals that are produced in the mixing process is normally desired. If the mixer performance is the same at the image and wanted frequencies, SSB noise figure is twice (or 3dB more) that of the DSB noise figure, because half of the signal is discarded. This assumption is routinely used to specify the SSB noise figure, because DSB noise figure is frequently easier to measure. The measurement set-up to measure the noise figure of the receiver is shown in *Figure 4-7* [9] [13] [57].

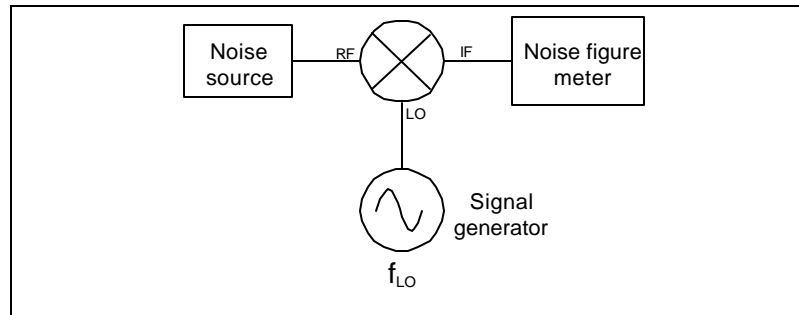


Figure 4-7 Measurement set-up to measure the noise figure of a mixer.

vi. LO wideband AM noise rejection

Local oscillator wideband noise separated from the LO frequency and its harmonics by $\pm f_{IF}$ will mix, with a higher conversion loss than the desired signal, to produce noise at the IF output as demonstrated in *Figure 4-8*. This will degrade the SNR and consequently the sensitivity of the receiver, and has to be measured separately at $nf_{LO} \pm f_{IF}$ for each n .

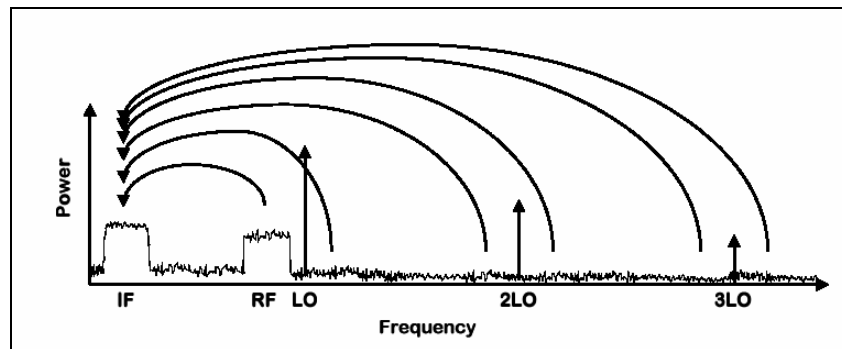


Figure 4-8 Down-conversion of noise (Figure 2-5 p20 [10]).

This conversion loss for the relevant sideband from the LO port to the IF port is called mixer noise balance [9].

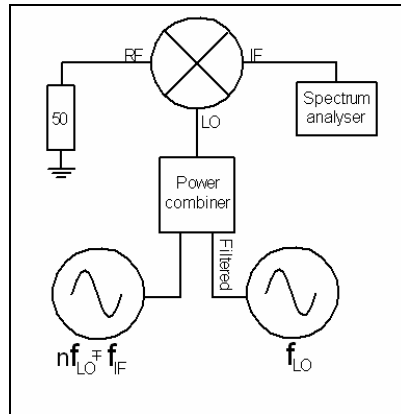


Figure 4-9 Measurement set-up of the mixer noise balance [9].

The measurement set-up for measuring the mixer noise balance is shown in *Figure 4-9*. Any signal or noise at $nf_{LO} \pm f_{IF}$ will be transferred to the mixers IF port. Thus, when measuring the mixer's noise balance, a small signal is used, instead of noise. f_{LO} stays fixed, while different signals, with a much lower power level than f_{LO} , are applied at $nf_{LO} \pm f_{IF}$ to the LO port of the mixer. The mixer noise balance at every nth LO harmonic is calculated using

$$M_s = A_{IF} - A_s \quad (4.6)$$

where A_{IF} is the power level in dBm on the spectrum analyzer at f_{IF} and A_s is the input level in dBm of the $nf_{LO} \pm f_{IF}$ signal, after the combiner [9].

vii. Image response

The noise at the signal's image frequency will down-convert to the IF. This is usually with a similar conversion loss to the desired signal. This noise will increase the noise figure and degrade the sensitivity of the receiver. This can be dealt with by either using an image reject filter at the input of the mixer or by implementing an image reject mixer, which is a combination of balanced mixers and hybrids [1] [35].

4.1.1. c Types of mixers

There are three general categories of mixers: single-ended or single device mixers, balanced mixers and doubly balanced mixers. Other mixer topologies e.g. triple balanced mixers are also available. Every category of mixers has advantages and disadvantages which will be discussed and compared in the following sections:

i. U2796B

a Design

The U2796B is a single-balanced mixer from ATMEL, specifically designed for down-conversion of signals and works for frequency inputs of up to 2GHz. This mixer has a very low current consumption, which makes it attractive for portable equipment. The circuit diagram of the mixer component is shown in *Figure 4-10*. L_2 , C_5 and C_7 are part of a tapped capacitor impedance matched output network that was designed. The measured characteristics of this designed component are discussed next.

b Measurements◆ **Conversion gain**

The conversion gain of the component is measured as 7dB, which is good, although 2dB less than the expected gain. This is shown in *Figure 4-11*. According to the datasheets, some gain may be lost if a center tapped capacitor impedance matched output network is used.

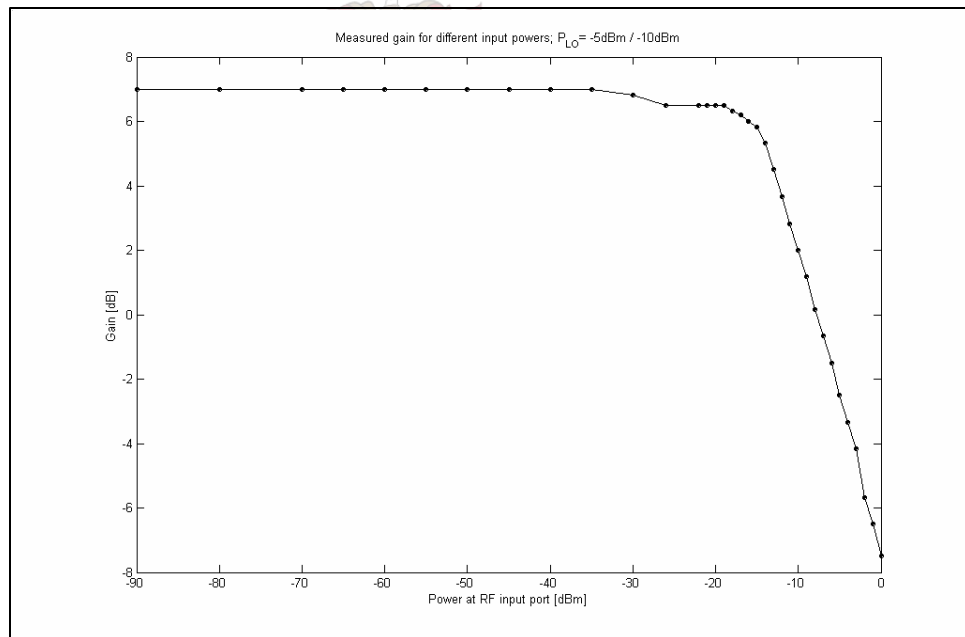


Figure 4-11 Measured conversion gain of the U2796B balanced mixer.

◆ **1 dB compression point and third order intercept point**

The input 1dB compression point is measured as -16dBm. This is close to the expected -15dBm. The 1dB compression point measurement is shown in *Figure 4-12*.



The measured output third order intercept point is 2dBm. Thus, the input third order intercept point is -5dBm, which is close to the expected input intercept point of -4dBm.

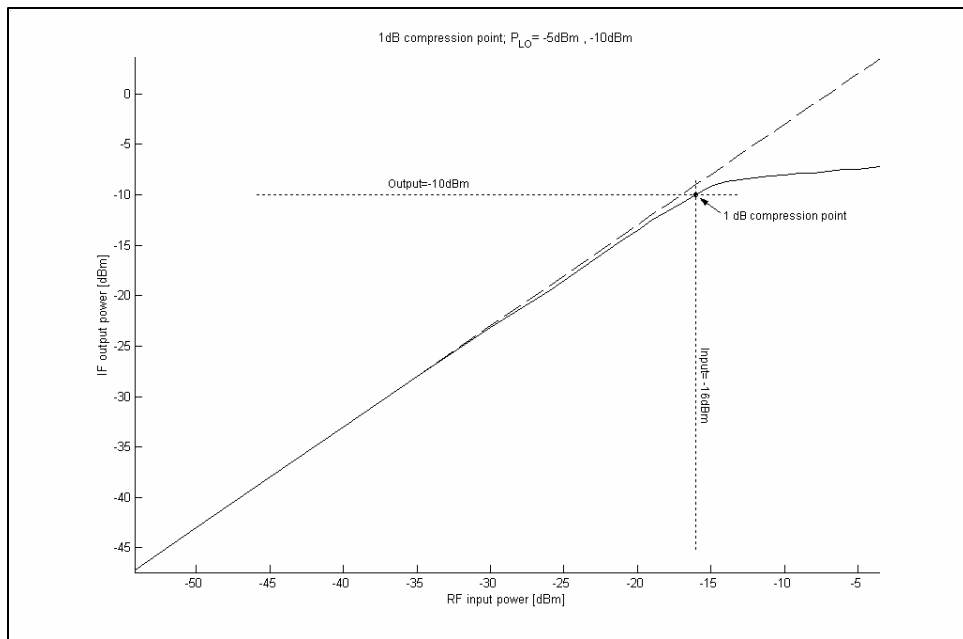


Figure 4-12 The measured 1dB compression point of the U2796B balanced mixer.

◆ Isolation

The LO-RF isolation is measured as greater than 41dB for $P_{LO} > -30\text{dBm}$, which is close to the expected 40dB. The measured RF-LO isolation is always more than 61dB for an LO input power of -10dBm.

The LO-IF isolation is 25dB as expected when $P_{LO} > -10\text{dBm}$, while the RF-IF isolation is measured to be more than 22dB for an LO power of -10dBm

◆ Noise figure

The noise figure was measured as 9dB with the noise figure meter, which is exactly what was expected.

◆ Power requirements

The U2796B requires $5V_{DC}$ to operate and draws 2.3mA current, which is less than the already low expected 3.2mA. This is very practical for a portable receiver.

◆ Mixer noise balance

A summary of the measured mixer noise balance is given in *Table 4-1*.



	Frequency $f_{LO} = 39.3\text{MHz}$ $f_{IF} = 10.7\text{MHz}$	$M_s = A_F - A_s$
$f_{LO} - f_{IF}$	28.6 MHz	31 dB
$2f_{LO} + f_{IF}$	89.3 MHz	41 dB
$2f_{LO} - f_{IF}$	67.9 MHz	38 dB
$3f_{LO} + f_{IF}$	128.6 MHz	51 dB
$3f_{LO} - f_{IF}$	107.2 MHz	46 dB

Table 4-1 Mixer noise balance of the U2796B balanced mixer.

◆ **Image response**

The gain at the image (28.6MHz) was measured to be 7dB. This is the same as at the desired frequency.

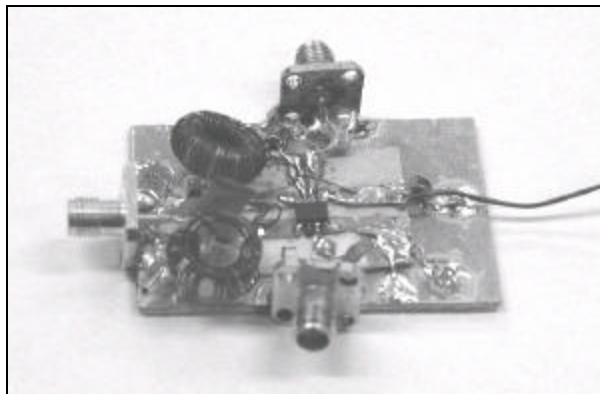


Figure 4-13 Photo of the U2796B singly balanced mixer that was designed.

c Conclusion

This mixer component, shown in *Figure 4-13*, draws very little current, which makes it very attractive to use for portable receivers. It also has a moderate gain and good isolation characteristics. The characteristics of this mixer are summarized in *Table 4-2*.



Characteristics			U2796B
Type			Active Singly balanced
Conversion gain [dB]		Expected	9
		Measured	7
Isolation [dB]	LO-RF	Expected	40
		Measured	>41
	LO-IF	Expected	25
		Measured	>25
	RF-LO	Expected	NS
		Measured	>61
1 dB compression point [dBm]		Expected	-15 (in)
		Measured	-16(in)
Intercept point [dBm]		Expected	-4 (in)
		Measured	-5(in)
Noise figure [dB]		Expected	9
		Measured	9
Average mixer noise balance [dB]			41
Gain at image dB]			7
DC power supply	Current [mA]	Expected	3.2
		Measured	2.3
	Voltage [V]	2.2 - 5.5	
Maximum RF power [dBm]			23 (5V DC)
Maximum LO power [dBm]			0
Minimum required LO power [dBm]			-10

Table 4-2 Summary of the measured characteristics of the U2796B singly balanced mixer.



4.1.2. b Doubly balanced mixer

If high port-to-port isolation, excellent LO, wideband AM noise rejection and suppression of all even harmonics of the RF and LO signal are required, a doubly balanced mixer is the answer.

Doubly balanced mixers consist of two singly balanced mixers and thus, use twice as many diodes or transistors which means that doubly balanced mixers generally requires 3dB higher LO power than singly balanced mixers. Higher LO power in return causes a greater 1dB compression point, which is usually taken as the top of the dynamic range, and greater third order intercepts. Thus, doubly balanced mixers generally have a better dynamic range than singly balanced mixers [1] [9] [58] [16].

A high LO power also means high current consumption. This characteristic makes doubly balanced diode mixers less desirable for portable equipment than active balanced mixers that have good performance at lower LO input power [35] [1] [9] [52] [58].



Balanced diode mixers have a significant conversion loss, which will increase the noise figure of the receiver and will influence the sensitivity of the receiver [52].

i. SA602

a Design

The SA602 is an active doubly balanced Gilbert cell mixer from Philips semiconductors. The mixer has low current consumption, operates for RF frequencies up to 500MHz and has an on board oscillator. Alternatively, an external LO signal between 200mV_{pp} and 300mV_{pp} can be applied to the chip via a DC blocking capacitor. The RF input and IF output ports can be single or double-ended [8] [65].

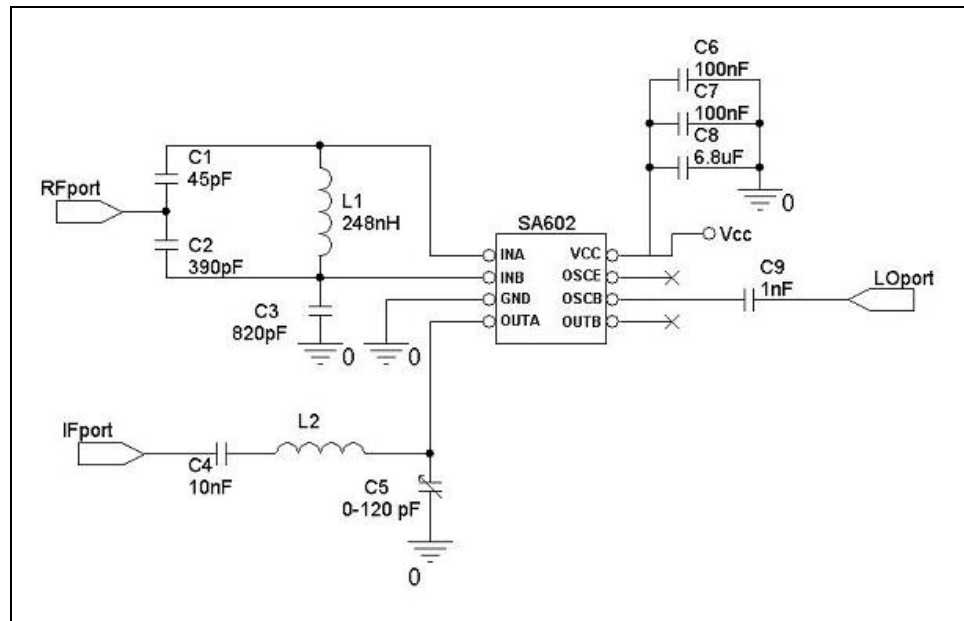


Figure 4-14 Circuit diagram of the SA602 mixer component that was designed.

The application circuit diagram is shown in *Figure 4-14*. C_1 , C_2 and L_1 are part of the tapped capacitor impedance matched network. This type of impedance match network is shown in *Figure 4-15* [61] [63].

The measured characteristics of this component are discussed next.



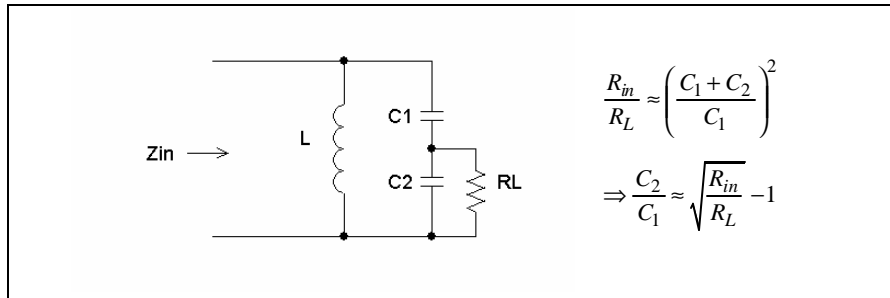


Figure 4-15 A tapped capacitor impedance matching network [61] [63].

b Measurements

◆ Conversion gain

A conversion gain of 7dB was measured and is shown in Figure 4-16.

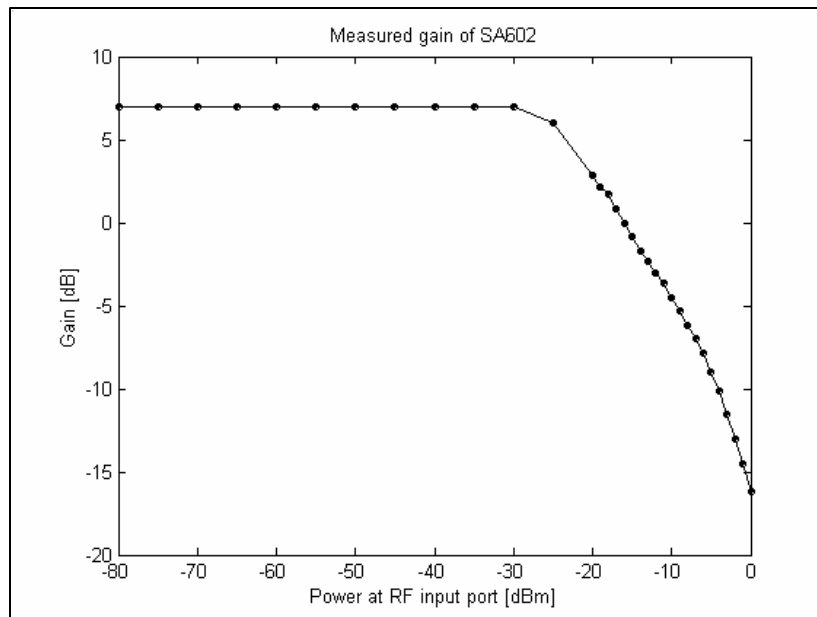


Figure 4-16 Measured conversion gain of the SA602.

◆ 1 dB compression point and third order intercept point

A 1dB compression point of -25dBm was measured. This is approximately 15dB less than the third order intercept point, which is a rough estimation of what can be expected. The 1dB compression point is shown in Figure 4-17.

The output third order intercept point that was measured is -9.5dBm (-16.5dBm input intercept point). The expected input intercept point is -13dBm.



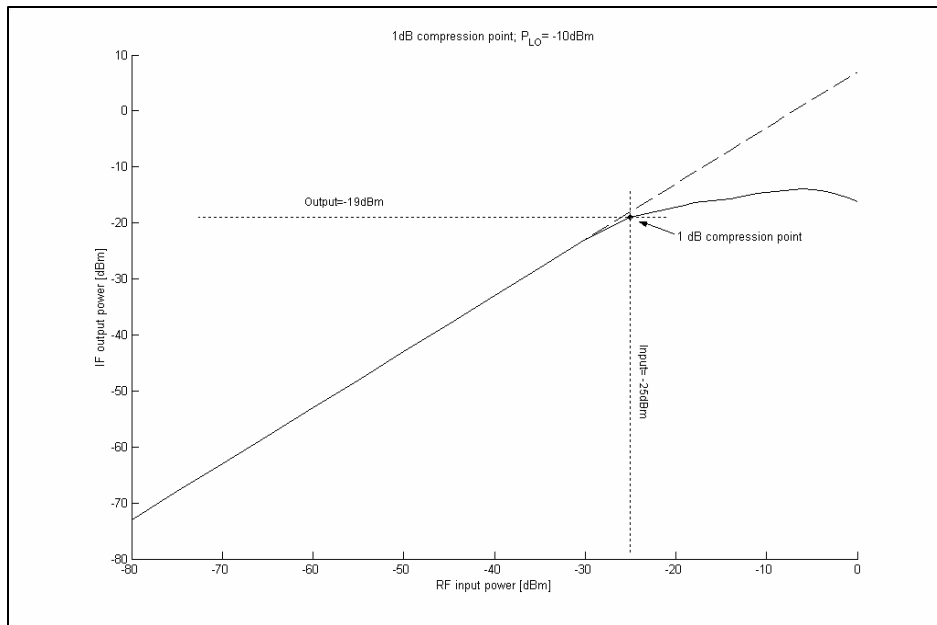


Figure 4-17 1dB compression point of the SA602 doubly balanced mixer.

◆ **Isolation**

The LO-RF isolation always measured greater than 103dB, which is excellent. The RF-LO isolation is not specified on the datasheets, and measures greater than 32dB for an LO input power of -10dBm. The LO-IF isolation is also very good and was measured greater than 72dB. The RF-IF isolation was measured to be more than 47dB for an LO power of -10dBm.

◆ **Noise figure**

A noise figure of 9.5dB was measured on the noise figure meter, while a noise figure of 5dB was expected.

◆ **Mixer noise balance**

The mixer noise balance measurement results are given below in *Table 4-3*.

	Frequency $f_{LO} = 39.3\text{MHz}$ $f_{IF} = 10.7\text{MHz}$	$M_s = A_F - A_s$
$f_{LO} - f_{IF}$	28.6 MHz	69 dB
$2f_{LO} + f_{IF}$	89.3 MHz	82 dB
$2f_{LO} - f_{IF}$	67.9 MHz	80 dB
$3f_{LO} + f_{IF}$	128.6 MHz	82 dB
$3f_{LO} - f_{IF}$	107.2 MHz	82 dB

Table 4-3 Measured mixer noise balance of the SA602.



◆ **Power requirements**

The SA602 mixer component requires $5V_{DC}$ and draws 1.2mA current when active, which is very little.

◆ **Image response**

A -20dB gain was measured at the image frequency (28.6MHz). A photo of this designed component is shown in *Figure 4-18*.

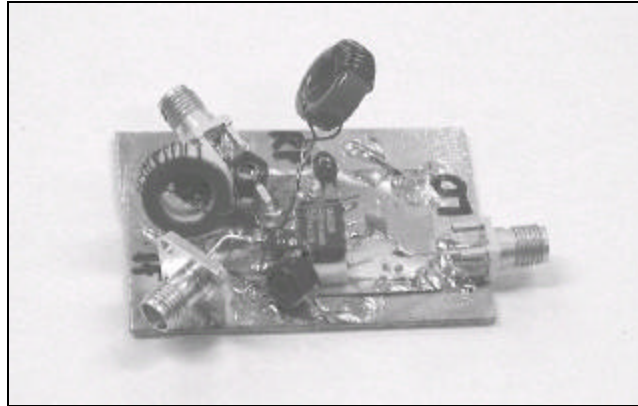


Figure 4-18 Photo of the SA602 active mixer that was built.

ii. SBL-1

a Design

The SBL-1 from Mini-Circuits is a passive doubly balanced mixer, which has little loss, relatively good isolation and can operate at frequencies of up to 1500MHz. This mixer is very easy to use, and only three DC blocking capacitors are needed at each port, to ensure that no DC enters the mixer.

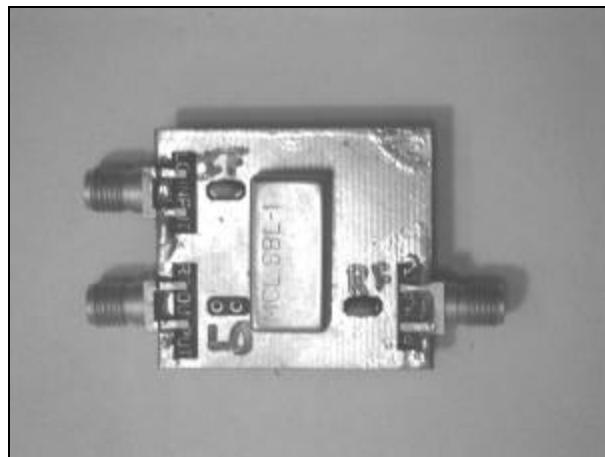


Figure 4-19 Photo of the SBL-1 passive mixer.



The measured characteristics of the SBL-1 passive mixer component are discussed next.

b Measurements

◆ Conversion gain

As shown in *Figure 4-20* a conversion gain of -5dB was measured, which is what can be expected, according to the datasheets.

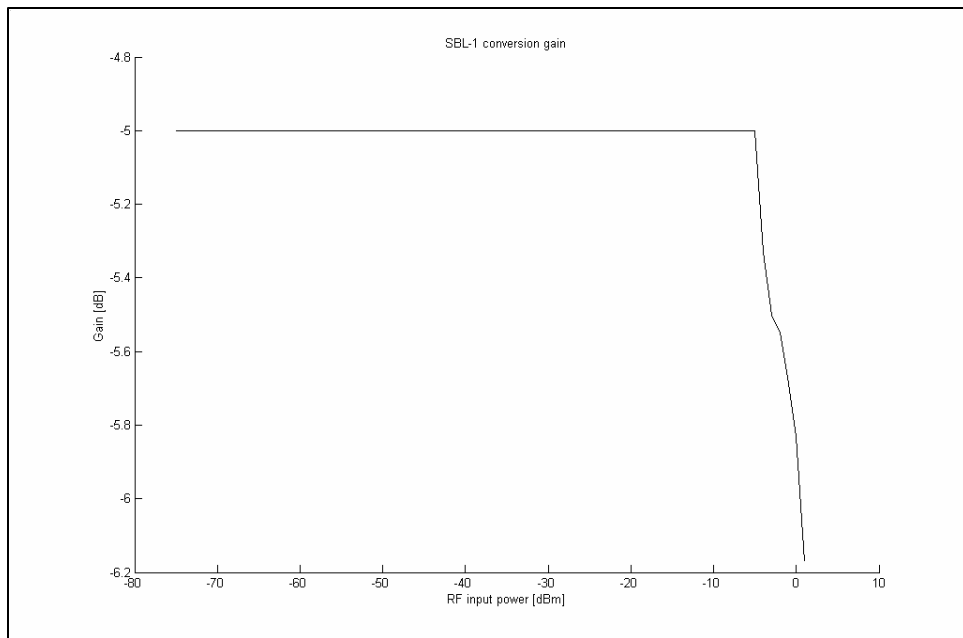


Figure 4-20 Measured conversion gain of the SBL-1 doubly balanced mixer.

◆ 1 dB compression point and third order intercept point

An input 1dB compression point of 0.5dBm was measured, as shown in *Figure 4-21*. The measured output third order intercept point is 10.5dBm, thus the input third order intercept point is 5.5dBm.

◆ Isolation

A minimum LO-RF isolation of 35dB was expected (typical 45dB), but a better isolation of 52dB was measured. The RF-LO isolation, which is not specified on datasheets, was measured as 52dB.

The LO-IF isolation was expected to be a minimum of 25dB. This isolation should typically be 40dB. An isolation >40dB was measured. The RF-IF isolation is not



specified on datasheets, and 40dB isolation was measured with an LO power of 7dBm.

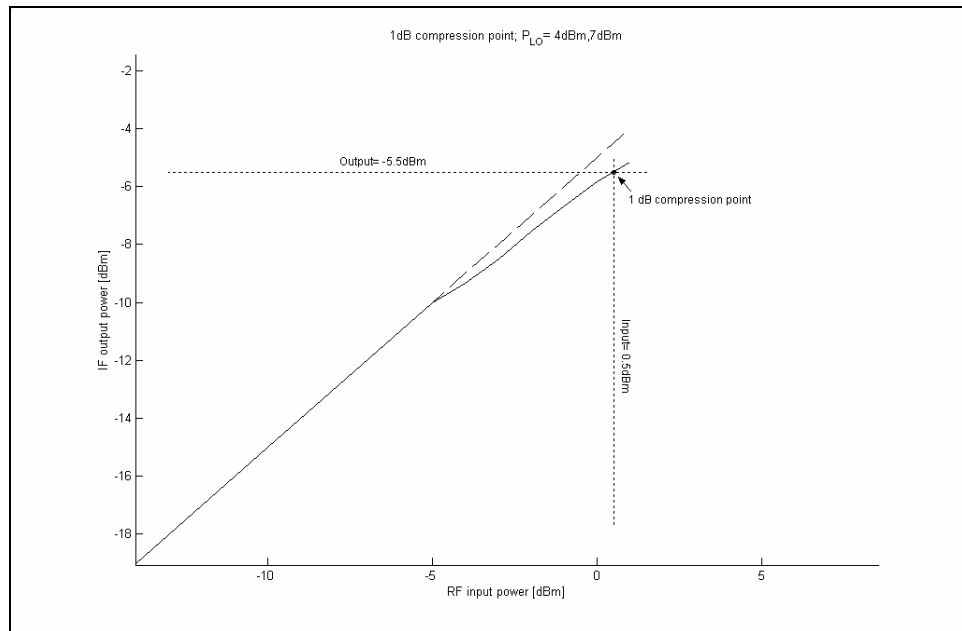


Figure 4-21 1dB compression point of the SBL-1 doubly balanced mixer.

◆ Mixer noise balance

The mixer noise balance results are given in the table below.

	Frequency $f_{LO} = 39.3\text{MHz}$ $f_{IF} = 10.7\text{MHz}$	$M_s = A_F - A_s$
$f_{LO} - f_{IF}$	28.6 MHz	43 dB
$2f_{LO} + f_{IF}$	89.3 MHz	35 dB
$2f_{LO} - f_{IF}$	67.9 MHz	36 dB
$3f_{LO} + f_{IF}$	128.6 MHz	32 dB
$3f_{LO} - f_{IF}$	107.2 MHz	33 dB

Table 4-4 Measured mixer noise balance of the SBL-1 doubly balanced mixer.

◆ Image response

A -5dB gain was measured at the image frequency, which is the same as the gain at the desired frequency.



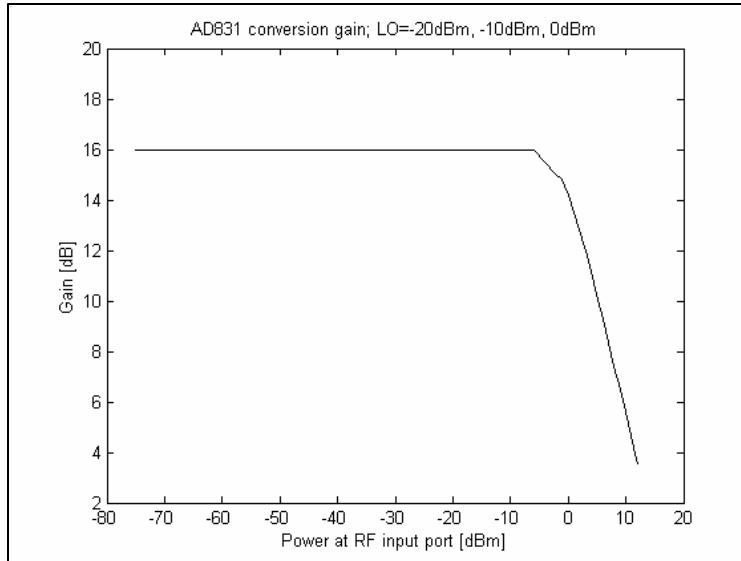


Figure 4-23 Measure conversion gain of the AD831 doubly balanced mixer.

◆ **1 dB compression point and third order intercept point**

An output 1dB compression point of 10dBm was expected, while an output 1dB compression point of 13dBm was measured. This is shown in *Figure 4-24*.

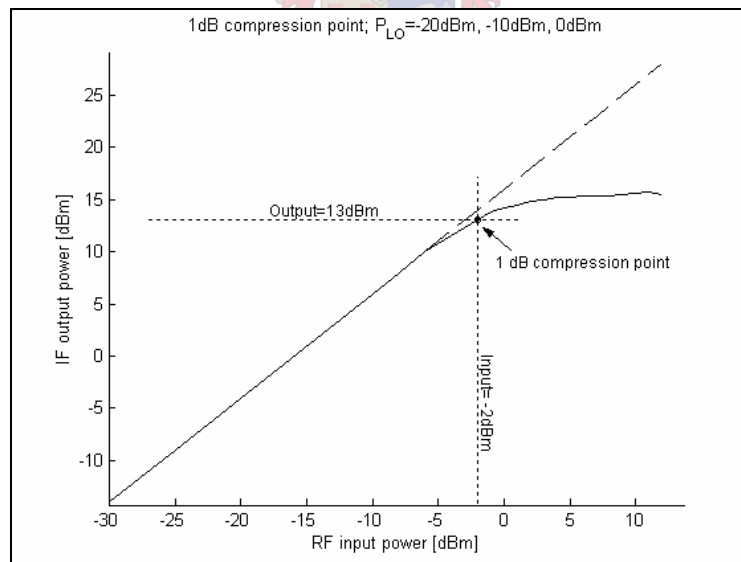


Figure 4-24 Measured 1dB compression point of the AD831 doubly balanced mixer.

An output intercept point of 12.5dBm was measured.



◆ **Isolation**

70dB LO-RF isolation was expected, according to datasheets. The LO-RF isolation was always measured to be greater than 70dB as shown in *Figure 4-25*. The RF-LO isolation is not specified on the datasheets. Isolation more than 70dB for an LO input power of -20dBm was measured

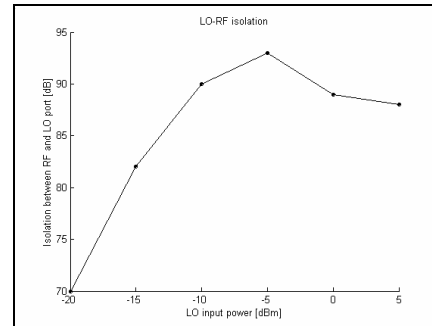


Figure 4-25 LO-RF isolation.

30dB LO-IF isolation is expected, according to datasheets. The measured isolation is more than 30dB for an LO input power of more than -6dB. For smaller LO input power the isolation decreases until zero for LO input power less than -32dBm as shown in *Figure 4-26*

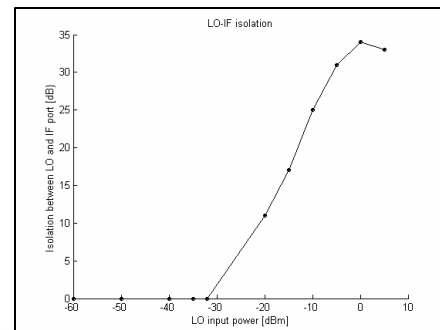


Figure 4-26 LO-IF isolation.

An RF-IF isolation of 45dB is expected, while an isolation of more than 31dB was measured.

◆ **Noise figure**

A noise figure of 8.6dB was measured on the noise figure meter. According to the datasheets, a 10.5dB noise figure can be expected at 70MHz, thus an 8.6dB noise figure at 50MHz is feasible.

◆ **Mixer noise balance**

The mixer noise balance results are summarized in *Table 4-5*.

	Frequency $f_{LO} = 39.3\text{MHz}$ $f_{IF} = 10.7\text{MHz}$	$M_s = A_F - A_s$
$f_{LO} - f_{IF}$	28.6 MHz	37 dB
$2f_{LO} + f_{IF}$	89.3 MHz	33 dB
$2f_{LO} - f_{IF}$	67.9 MHz	35 dB
$3f_{LO} + f_{IF}$	128.6 MHz	36 dB
$3f_{LO} - f_{IF}$	107.2 MHz	34 dB

Table 4-5 Measured mixer noise balance of the AD831 doubly balanced mixer.



◆ **Power requirements**

The AD831 requires $5V_{DC}$ and $9V_{DC}$ and consumes 96mA current when active, which is a lot and unpractical for portable equipment.

A photo of the designed mixer component is shown in *Figure 4-27*.

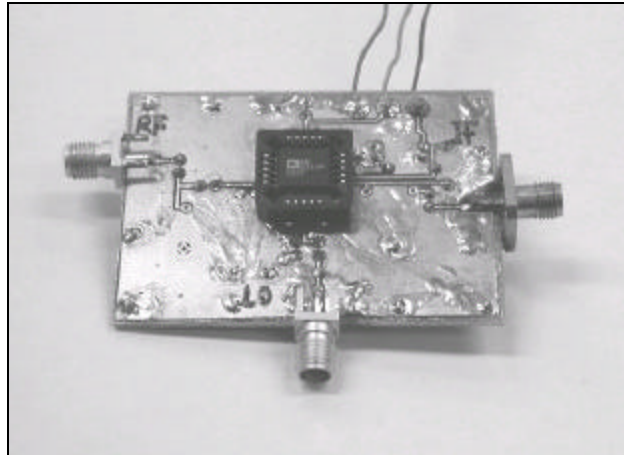


Figure 4-27 Photo of the AD831 active mixer that was built.

iv. Conclusion and a comparison between the doubly balanced mixers

All three the doubly balanced mixers built work well and have different strengths and weaknesses, which will influence the receiver performance.

The SA602 has the best isolation and average mixer noise balance, the worst noise figure and uses very little power, which makes it ideal for a portable receiver. The AD831 on the other hand, unexpectedly has the highest conversion gain, requires the least LO input power and uses a lot of current, which makes it unpractical for portable equipment. The SBL-1 has the lowest noise figure, the lowest gain, uses no DC power and requires the most LO power.

The influence of every mixers' characteristics on the system's performance will be evaluated in the next chapter.

A summary of the expected and measured component characteristics is given in *Table 4-6*. (All the 1dB compression points and intercept points are referred to as the input, unless otherwise specified.)



Characteristics			AD831	SA602	SBL-1
Type			Active Doubly balanced	Active Doubly balanced	Passive Doubly balanced
Conversion gain [dB]		Expected	11	17	-5.6
		Measured	16	7	-5
Isolation [dB]	LO-RF	Expected	70	*NS	35-45
		Measured	>70	>103	>52
	LO-IF	Expected	30	*NS	25-40
		Measured	0-30	>72	>40
	RF-LO	Expected	45	*NS	*NS
		Measured	>70	>32	52
1 dB compression point [dBm]		Expected	-16	≈ -28	*NS
		Measured	-3	-25	0.5
Intercept point [dBm]		Expected	8	-13	*NS
		Measured	-3.5	-16.5	5.5
Noise figure [dB]		Expected	± 10.5	5	*NS
		Measured	8.6	9.5	5
Average mixer noise balance [dB]			35	79	36
Gain at image dB]			16	-20	-5
DC power supply	Current [mA]	Expected	100	2.4	Passive device
		Measured	96	1.2	
	Voltage [V]	5 & 9	5		
Maximum RF power [dBm]			19.5	*NS	1
Maximum LO power [dBm]			10	-6.5	*NS
Minimum required LO power [dBm]			-20	-10	4 Typical: 7

*NS - Not specified

Table 4-6 Summary of the expected and measured characteristics of the doubly balanced mixers.

4.1.2. c Single device mixer

Single device mixers are devices that are used to translate frequency by using only a single non-linear device. This group includes i.e. single diode mixers, single FET mixers and dual-gate MOSFET mixers [1] [35].

Advantages of single device mixers are typically

- High conversion efficiency.
- Low noise.
- They are inexpensive [1] [35].

Disadvantages of single device mixers include:

- The need for special structures to combine the LO and RF signals.
- The need for a filter to achieve good LO-to-IF isolation.



- Local oscillator AM noise is not attenuated; therefore, an injection filter is required.
- The filters and drains, that are necessary at inputs and outputs of single device mixers, places impedance constraints on the input and output ports. This inherently requires that single-device mixers are narrowband [1] [35].

The dual-gate MOSFET mixer is one single device mixer that does not need special structures to combine the LO and RF signals. It has good LO-RF isolation, which avoids some of the impedance restrictions. These mixers are very sensitive to the drain impedance at their IF frequency. A dual-gate MOSFET mixer circuit was built and measured to demonstrate some of the characteristics of single device mixers. This mixer was deliberately designed to be poor, to make comparison with a very poor mixer possible [1] [35].

i. BF982 dual-gate MOSFET mixer

a Building and measuring the dual-gate MOSFET mixer

The BF982 dual-gate MOSFET was used for this single device mixer. This dual-gate MOSFET was first biased and then coupling capacitors were added at every input and output port, to ensure that no DC enters the mixer. The circuit used is given below in *Figure 4-28*.

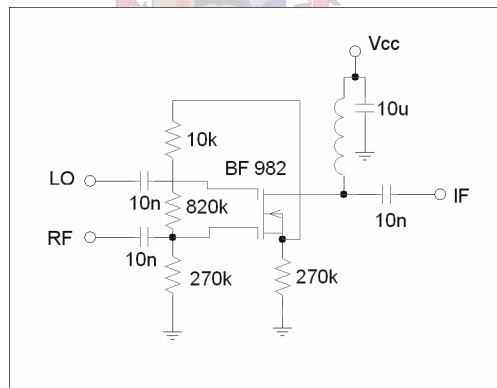


Figure 4-28 The dual-gate MOSFET mixer circuit diagram [1] [35] [45].

Next, this mixer component is measured, with the techniques described in 4.1.1. b. The results are:

◆ Conversion gain

The conversion gain of the dual-gate MOSFET mixer is measured to be -22dB, as shown in *Figure 4-29* which is very poor. This is because of the fact that there



is no resonant LC circuit at the drain. This mixer was deliberately designed to be poor, to make comparison with a very poor mixer possible.

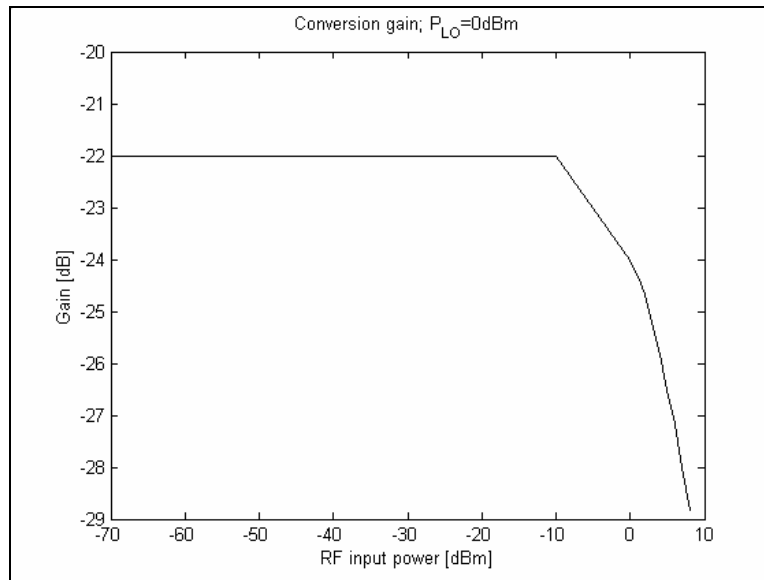


Figure 4-29 Conversion gain of the dual-gate MOSFET mixer.

◆ **1 dB compression point and third order intercept point**

The expected input 1dB compression point is -5dBm as shown in Figure 4-30. The measured output third order intercept point is -11dBm (11dBm input intercept point)

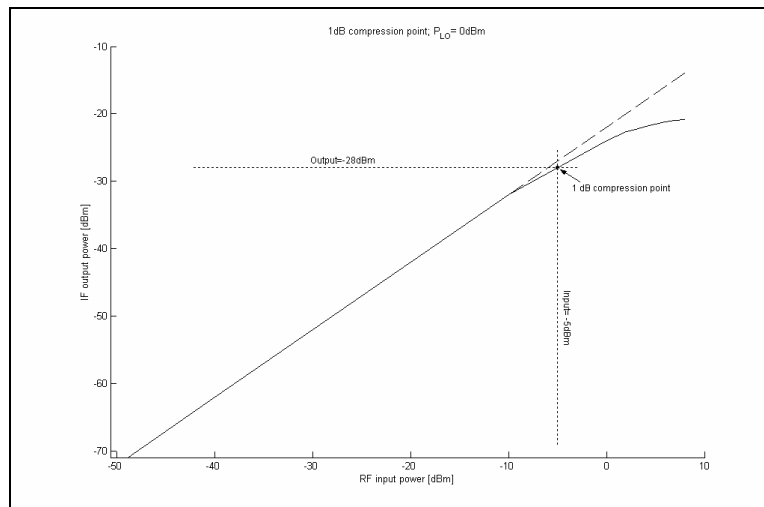


Figure 4-30 1dB compression point of the dual-gate MOSFET mixer.



◆ **Isolation**

The measured LO-RF isolation is always greater than 40dB for $P_{LO} > -20\text{dBm}$. The RF-LO isolation measures as more than 24dB for an LO input power of 0dBm. LO-IF isolation is $>19\text{dB}$ when $P_{LO} > -20\text{dBm}$. Lastly the RF-IF isolation is measured to be more than 15dB.

◆ **Noise figure**

A noise figure of 13dB was measured on the noise figure meter.

◆ **Mixer noise balance**

The results are shown in *Table 4-7* below.

	Frequency $f_{LO} = 39.3\text{MHz}$ $f_{IF} = 10.7\text{MHz}$	$M_s = A_F - A_s$
$f_{LO} - f_{IF}$	28.6 MHz	22 dB
$2f_{LO} + f_{IF}$	89.3 MHz	18 dB
$2f_{LO} - f_{IF}$	67.9 MHz	19 dB
$3f_{LO} + f_{IF}$	128.6 MHz	16 dB
$3f_{LO} - f_{IF}$	107.2 MHz	17 dB

Table 4-7 Mixer noise balance of the dual-gate MOSFET mixer.

◆ **Power requirements**

The dual-gate MOSFET mixer component was operated from $9V_{DC}$. A 1.4mA current is drawn when active.

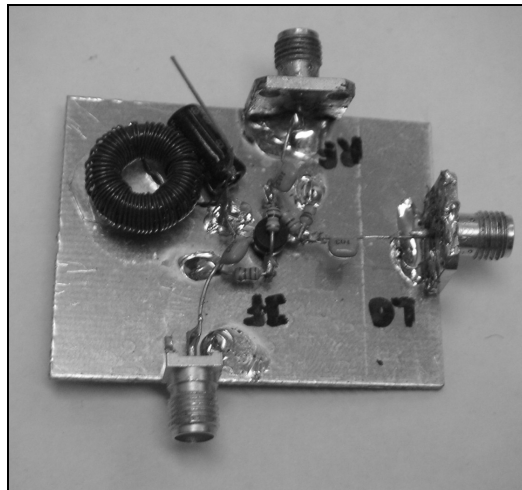


Figure 4-31 The single device dual-gate MOSFET mixer component that was designed.

◆ **Image response**

The gain at the image frequency (28.6MHz) was measured to be -22dB. This is the same gain as at the desired frequency.

ii. Conclusion

The mixer component that was designed is shown in *Figure 4-31*. Even though this mixer does not have excellent characteristics, the influence of its specific characteristics on the receiver system will be compared with mixers with better characteristics in the next chapter. A summary of its characteristics is given in *Table 4-8*.

Characteristics			Dual-gate MOSFET
Type			Active Single device
Conversion gain [dB]		Measured	-22
Isolation [dB]	LO-RF	Measured	41
	LO-IF	Measured	>19
	RF-LO	Measured	>24
1 dB compression point [dBm]		Measured	-5
Intercept point [dBm]		Measured	-11(out)
Noise figure [dB]		Measured	13
Average mixer noise balance [dB]			18
Gain at image dB]			-22
DC power supply	Current [mA]	Measured	1.4
	Voltage [V]		9
Maximum RF power [dBm]			8
Maximum LO power [dBm]			1
Minimum LO power [dBm]			

Table 4-8 Summary of the measured characteristics of the dual-gate MOSFET mixer.

4.1.3. Conclusion concerning mixers

The different mixer components built and characterized in this section, worked well and their influence on the receiver system's performance will be compared in the next chapter. Certain advantages and disadvantages of mixers were predicted in 4.1.1. A summary of these advantages is given in *Table 4-9*.



	Advantages	Disadvantages
Single device	<ul style="list-style-type: none"> ▪ Low distortion. ▪ Simple & inexpensive. ▪ LO-RF isolation of dual-gate MOSFET mixer good without the use of filters - avoids some of the impedance restrictions . ▪ Single diode mixers used at high microwave frequencies because other alternatives are not available or too costly. 	<ul style="list-style-type: none"> ▪ Port-to-port isolation depends on external filters . ▪ No inherent suppression of spurious responses . ▪ Local oscillator AM noise not attenuated - requires an injection filter . ▪ Need special structures to combine RF and LO and requires some type of IF filter for good LO-to-IF isolation: LO-RF diplexer and IF filters limits applications . ▪ Filters and drains at inputs and outputs necessary - impedance constraints inherently require that single-device mixers are narrowband . ▪ Decent noise figure and moderate bandwidth .
Balanced	<ul style="list-style-type: none"> ▪ Rejection of certain even order IMD products and spurious responses . ▪ AM noise rejection of LO. ▪ High LO-RF isolation. ▪ Avoids LO-IF leakage. ▪ Rejection of LO energy from IF. ▪ Active balanced mixers generally has 3dB better interception point than active single device mixers . 	<ul style="list-style-type: none"> ▪ Poor choice when broadband IF is needed. ▪ RF/LO bandwidth less than 20%. ▪ RF-IF isolation depends on filters . ▪ Active balanced mixers generally require 3dB higher LO power than single device mixers .
Doubly balanced	<ul style="list-style-type: none"> ▪ High port-to-port isolation. ▪ Excellent LO wideband AM noise rejection. ▪ Suppress all even harmonics of the RF and LO signal. ▪ Wide RF and LO bands ▪ Broadband IF can partially overlap with RF and LO bands . ▪ Avoids LO-IF leakage. ▪ Active doubly balanced mixers generally have a higher third order intercept point than other types of mixers. ▪ Active balanced mixers perform well at low LO power. 	<ul style="list-style-type: none"> ▪ Not ideal input matching at RF port. ▪ Active doubly balanced mixers generally require 6dB higher LO power than single device mixers . ▪ Passive doubly balanced mixers require a high LO power for linear performance. ▪ Circuit complexity of active doubly balanced mixers is higher than that of passive mixers , but they are compatible with monolithic processes .

Table 4-9 Comparisons between different mixers [1] [9] [35].



A summary of the measured mixer characteristics is given in *Table 4-10* below. This clearly shows that the passive mixer has the smallest noise figure and that the single device mixer has the worst characteristics.

Characteristics		AD831	SA602	Dual-gate MOSFET	SBL-1	U2796B
Type		Active Doubly balanced	Active Doubly balanced	Active Single device	Passive Doubly balanced	Active Singly balanced
Conversion gain [dB]		16	7	-22	-5	7
Isolation [dB]	LO-RF	>70	>103	41	>52	>41
	LO-IF	0-30	>72	>19	>40	>25
	RF-LO	>70	>32	>24	52	>61
1 dB compression point [dBm]		-3	-25	-5	0.5	-16
Intercept point [dBm]		-3.5	-16.5	11	5.5	-5
Noise figure [dB]		8.6	9.5	13	5	9
Average mixer noise balance [dB]		35	79	18	36	41
Gain at image dB]		16	-20	-22	-5	7
DC power supply	Current [mA]	96	1.2	1.4	Passive device	2.3
	Voltage [V]	5 & 9	5	9		2.2 - 5.5
Maximum RF power [dBm]		19.5	*NS	8	1	23 (5V DC)
Maximum LO power [dBm]		10	-6.5	1	*NS	0
Minimum required LO power [dBm]		-20	-10	*NS	4 Typical: 7	-10

*NS – Not specified

Table 4-10 Comparison between the measured characteristics of the mixers.

Mixer types and characteristics were discussed in this section. Five different mixer components were designed and their performance measured. This will enable a comparison of the influence of the mixer characteristics on receiver performance. A discussion of the front-end amplifiers follows in the next section as is shown in *Figure 4-32*.

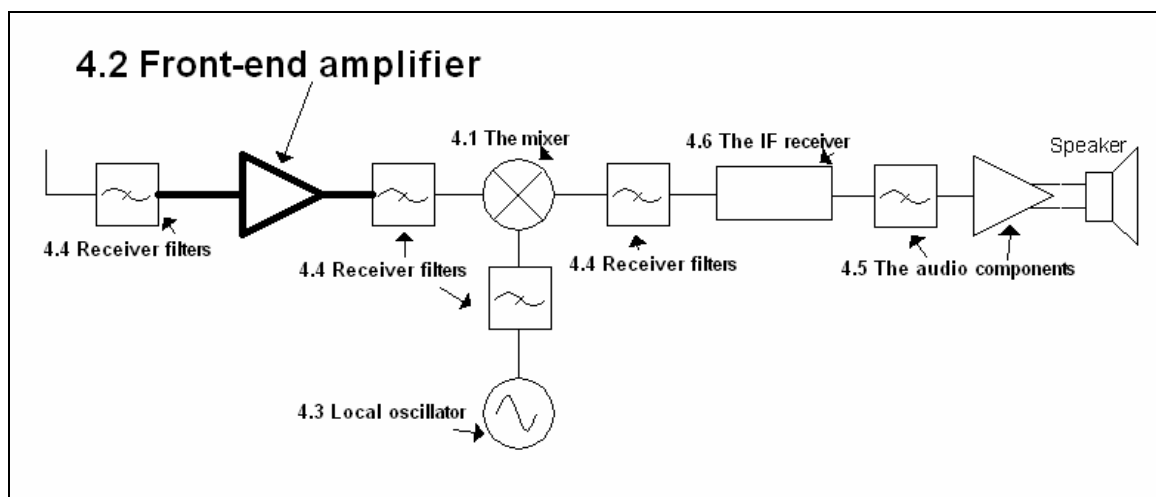


Figure 4-32 Structure of chapter 4: 4.2 Front-end amplifier.

4.2 The front-end amplifier

The front-end amplifier provides amplification of the incoming RF signal. This is important to improve the sensitivity of the receiver. Careful consideration must be given to the choice of the devices in the front-end of the receiver to achieve a good noise figure and consequently a practical sensitivity as discussed in section 2.1.1. a. To optimize the noise figure and consequently the sensitivity, these devices should have a low noise figure and a high dynamic range. The most critical part of the system, for an overall low system noise figure, is the front-end amplifier. Front-end amplifier characteristics will be discussed in this section. Different amplifier components were designed and their performance measured. This enables a comparison of the influence of the front-end amplifier characteristics on receiver performance.

4.2.1. Theory

Important characteristics of the RF amplifier include stability, noise figure, gain, 1dB compression point, intercept point and return loss. These are described briefly in this section.

4.2.1. a Stability

“Unconditionally stable” is a term applied to an amplifier that will not oscillate regardless of load or source impedance. One method to determine stability is by plotting stability circles on the Smith chart. If all the stability circles lie outside the Smith chart, the device is unconditionally stable. On the contrary, stability circles inside the Smith chart indicate that the device can be stable for certain load and source impedances, but not for all. These source and load impedances can be determined from the Smith chart [9] [17] [25].

Another method to determine unconditional stability is by using Rollet’s condition. This states that a device is unconditionally stable if the conditions

$$K = \frac{1 - |s_{11}|^2 - |s_{22}|^2 + |\Delta|^2}{2|s_{12}s_{21}|} > 1 \quad (4.8)$$

and

$$|\Delta| = |s_{11}s_{22} - s_{12}s_{21}| < 1 \quad (4.9)$$

are simultaneously satisfied [9].

4.2.1. b Noise figure and gain

As previously discussed, the noise figure of the front-end amplifier is the main contributor to the noise figure of the receiver system. Therefore, the noise figure of the front-end amplifier has a major influence on the sensitivity of the system. An amplifier that is optimized for noise will not have optimum gain and visa versa. There is always a trade-off between noise figure and gain. The optimum source impedance, for which an amplifier will have minimum noise figure, is usually



specified by the manufacturer. On the contrary, an amplifier, which is designed for maximum gain, will have input and output impedances that are matched simultaneously.

4.2.1. c 1dB compression point and intercept point

The 1dB compression point defines the output level at which the amplifier's gain is compressed by 1dB as illustrated in Figure 4-5. Input power levels that exceed this value will cause harmonic distortion. The experimental set-up for measuring the 1dB compression point of an amplifier is shown in Figure 4-33.

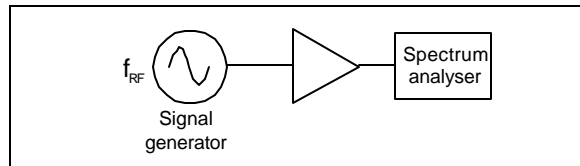


Figure 4-33 Measurement set-up for measuring the IP1 of an amplifier.

Third order intercept point ($IP3$) is a measure of third order products generated by a second signal arriving at a device such as an amplifier as discussed in section 4.1.1. The intercept point of an amplifier is extremely important because power levels in excess of the third order intercept point will cause intermodulation distortion.

When measuring $IP3$ of an amplifier the experimental set-up shown in Figure 4-34 is used. The $IP3$ of a device also depends very strongly on its terminating impedances at all ports. Therefore, attenuators are included at each port if high performance amplifier measurements are done. The intercept point can be calculated from

$$IP3_{out} = P_{out} + \frac{\delta}{2} \quad (4.10)$$

Where P_{out} is the output power in dBm and δ is the difference between the desired output signal and the third order intermodulation products as shown in Figure 4-4 [1] [17] [24] [57].

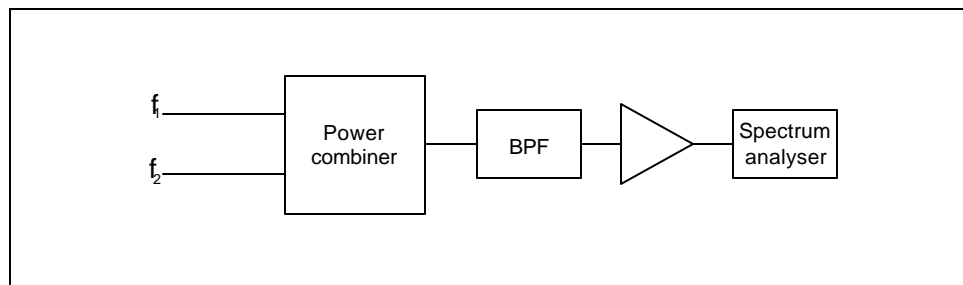


Figure 4-34 Measurement set-up, for measuring the IP3 of an amplifier.



The input intercept point can be calculated by subtracting the gain from the output intercept point. Amplifier intercept point is generally specified as an output intercept point [1] [9] [17] [24] [57].

4.2.1. d Return loss

The return loss is calculated with the equation

$$RL = -20 \log |\Gamma_{in}| \quad [dB] \quad (4.11)$$

For a perfectly matched load, no power will be reflected ($\Gamma_{in} = 0$), and the return loss is infinity.

4.2.2. Designing, measuring and building different front-end amplifiers

4.2.2. a Design of a low noise amplifier

The AT-41533, low noise NPN bipolar transistor from Hewlett Packard was used to design a low noise amplifier at 50MHz. This device has a good noise figure of less than 1dB and a reasonable gain at 50MHz.

The design was done in several steps, namely:

- Design of a biasing network
- Determine stability and design a stable amplifier
- Design input and output matching networks
- Measure scattering parameters and confirm that the final amplifier is unconditionally stable

The low noise amplifier design is discussed in detail in Appendix A. A photo of this component is shown in *Figure 4-35*.

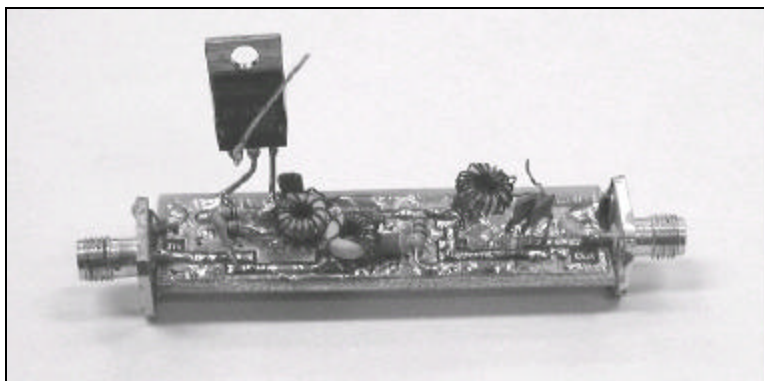


Figure 4-35 Photo of the designed AT-41533 single transistor low noise amplifier.

Final measurements of the amplifier characteristics follows.



i. Measurements

a Noise figure

The most important design consideration for this front-end RF amplifier was the noise figure, and some of the gain had to be sacrificed for this. The noise figure was measured with the HP noise figure meter to be 1.6dB, which is a relatively low noise figure.

b Gain

The measured gain at 50MHz, where the amplifier was designed and matched is 16dB, which is better than expected for a low noise amplifier.

c 1dB compression point and intercept point

The measured output compression point is -1dBm as shown in *Figure 4-36*.

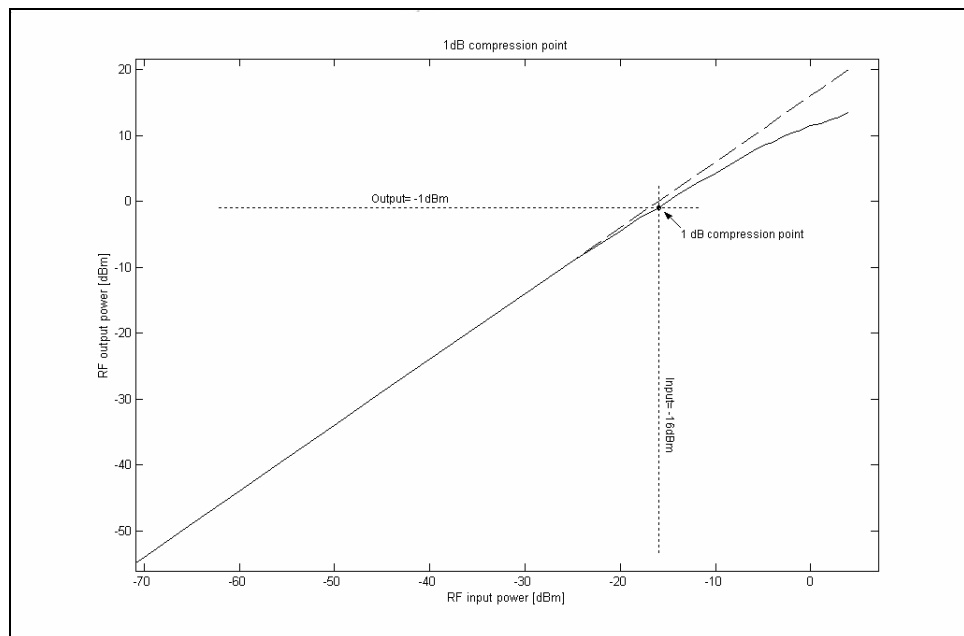


Figure 4-36 Measured 1dB compression point of the AT-41533 single transistor low noise amplifier.

The measured third order output intercept point is -1dBm.

d Return loss

A big return loss is desirable, but is not expected here, because the amplifier is not that well matched to improve the noise figure. The return loss over the frequency band is shown in *Figure 4-37*. The return loss at 50MHz is 3.9dB.



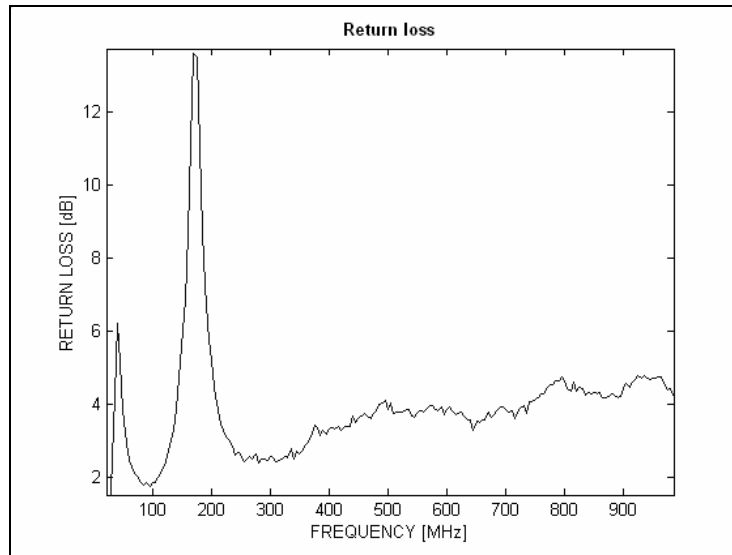


Figure 4-37 Input return loss of the low noise amplifier.

ii. Conclusion

Property	Measured value	Comment
Noise figure	1.6dB at 50MHz	Reasonably low noise figure
Stability	Unconditionally stable	The amplifier is unconditionally stable over the measured frequency band
Return loss	3.9dB at 50MHz	A lot of power is reflected, which is the sacrifice that has to be made to achieve a low noise figure
Gain	16dB at 50MHz	This is a good gain
Matching	$ s_{11} < -3dB$ and $ s_{22} = -15dB$ at 50MHz	The input impedance is not that well matched, to achieve a better noise figure. The output impedance is very well matched, which will improve the gain.
1dB compression point	-1dBm	
Intercept point	-1dBm	
Power supply	$V_{cc} = 5V$ and $I_{cc} = 45mA$. $I_c < 5mA$.	The amplifier draws very little current
3dB Bandwidth	49%	Reasonable bandwidth

Table 4-11 Measured LNA properties summary.



4.2.2. b Designing, building and measuring the GALI-S66

An amplifier with a better input impedance match and a poorer noise figure was designed and built to determine how this will influence the performance of the receiver system. Many available amplifiers were investigated to find ones with a low noise figure, operating current and at least moderate gain, as shown in *Table 4-12*. The Gali-S66 was chosen, because of its relatively low noise figure and low current consumption, high gain and high return loss compared to other available RF amplifiers.

Model	BW [MHz]	Gain [dB]	Impedance match	NF [dB]	DC current [mA]	DC voltage [V]	Comments
Philips							
SA5204	200	20	500	6	25	5	No external components
RF micro devices							
RF2046	DC-3000	22	500	3.8	35	3.5	
RF2336	DC-3000	20	500	3.8	35	3.5	
RF2360	5-1000	20	750	1.2	104	6-9	Low noise figure Large DC current
Analog Devices							
AD603	DC-90	31	1000	8.8	12.5	5	Voltage controlled amplifier Small DC current High gain and noise figure
AD8350	DC-1000	20	2000	6	28	5-10	
Mini-circuits							
MAR-6SM	DC-2000	20	VSWR: In 1.7:1 Out 1.7:1	3	16	3.5	Small DC current
MAR-8SM	DC-1000	32.5	Not matched	3.3	36	7.8	Conditionally stable High gain
RAM-6	DC-2000	20	VSWR: In 1.4 Out 1.3	2.8	16	3.5	Small DC current
RAM-8	DC-1000	32.5	Not matched	3	36	7.8	Conditionally stable High gain
Gali-S66	DC-3000	22	VSWR: In 1.25 Out 1.7	2.7	16	3.5	Small DC current
Gali-52	DC-2000	22.9	VSWR: In 1.35 Out 1.4	2.7	50	4.4	Large DC current
VAM-6	DC-2000	19.5	VSWR: In 1.6 Out 1.5	3	16	3.3	Small DC current

Table 4-12 Comparison of some available amplifiers.

i. Design of the GALI-S66 amplifier

The Gali-S66 amplifier of mini-circuits was chosen. A circuit was designed in *Protel* [55] and built. The schematic of the Gali-S66 circuit is shown in *Figure 4-38*.



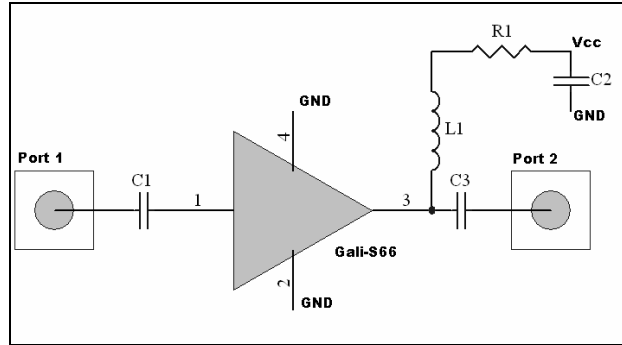


Figure 4-38 Schematic of the Gali-S66 circuit.

This circuit was built, measured, and worked well. A photo of the amplifier component is shown in *Figure 4-39*.



Figure 4-39 Photo of the designed Gali-S66 amplifier component.

ii. Measuring the Gali-S66 amplifier circuit

a Noise figure

The noise figure was measured with the HP noise figure meter as 2.2dB, which is lower than the 2.7dB specified on the datasheets.

b Gain

The transducer power gain can be calculated from the s -parameters and will reduce to $G_T = |s_{21}|^2$ if the input and output ports of the amplifier are perfectly matched and thus, no power is reflected. The magnitude of s_{11} at the input of the Gali-S66 amplifier is $-24dBm$ at $50MHz$ and is plotted in *Figure 4-40*. This is much better than the impedance match ($|s_{11}| < -3dB$) of the low noise amplifier in the previous section, which implies that the power that will be reflected from the Gali-



S66 amplifier is much smaller. Thus, the calculated gain will be much closer to $|s_{21}|^2$. The magnitude of s_{21} is plotted in *Figure 4-40* and is $s_{21} = 21.266\text{dB} \approx 21.3\text{dB}$ at 50MHz .

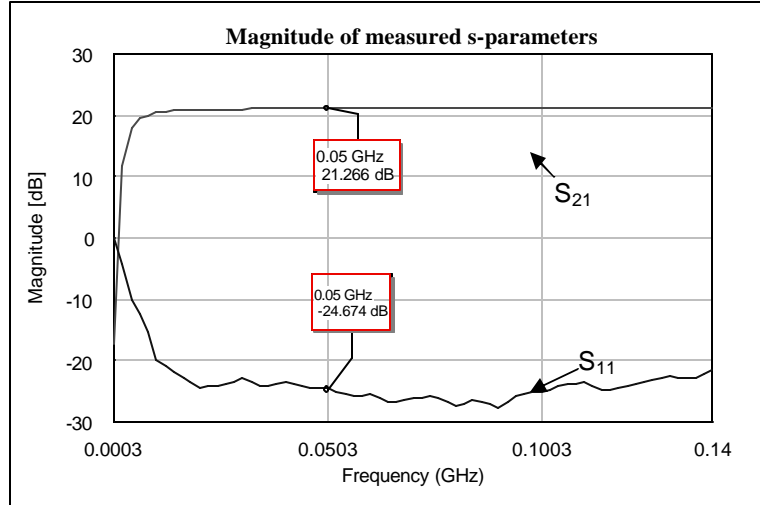


Figure 4-40 Measured s_{11} and s_{21} .

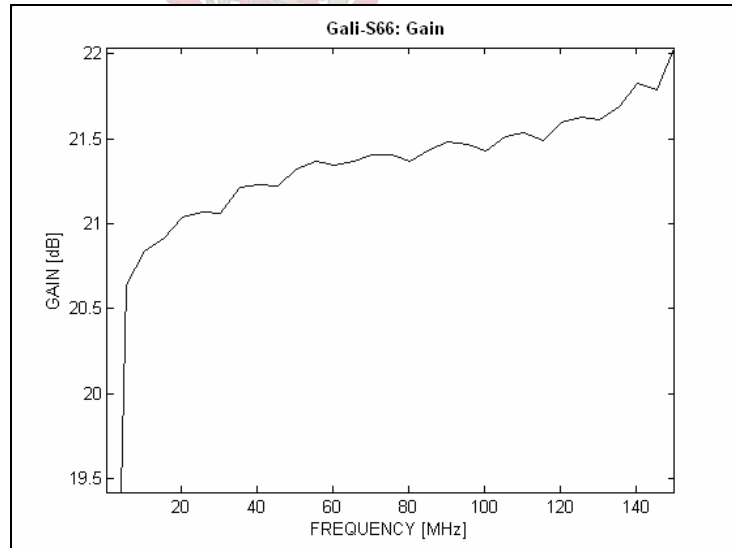


Figure 4-41 Gain of the amplifier over the frequency range.

The amplifier gain was calculated and plotted over the entire frequency range with *Matlab* [54] and is shown in *Figure 4-41*. The calculated transducer gain at 50MHz using the measured s-parameters, is 21.3dB as was predicted by $|s_{21}|^2$.

c 1dB compression point and intercept point

The output 1dB compression point was measured at -3dBm , while an output intercept point of 12.5dBm was measured.

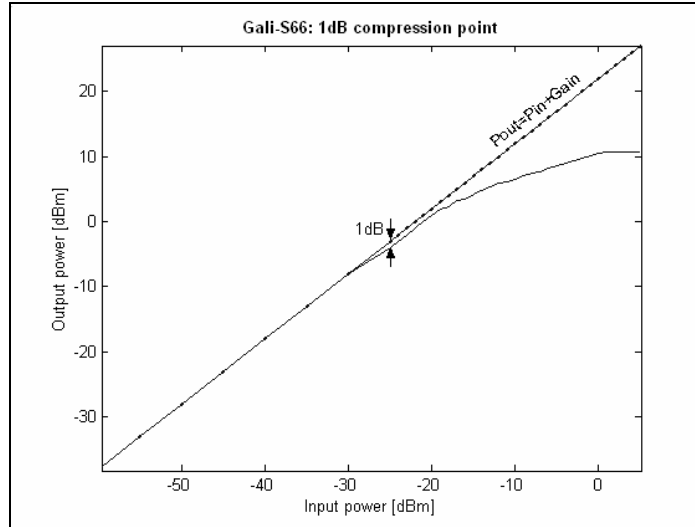


Figure 4-42 1dB compression point of the Gali-S66 amplifier.

d Return loss

The return loss of the Gali-S66 was expected to be 19dB. Thus, the input impedance match is expected to be good.

The return loss at 50MHz was measured as 16.5dB. The return loss over the frequency band is shown below.

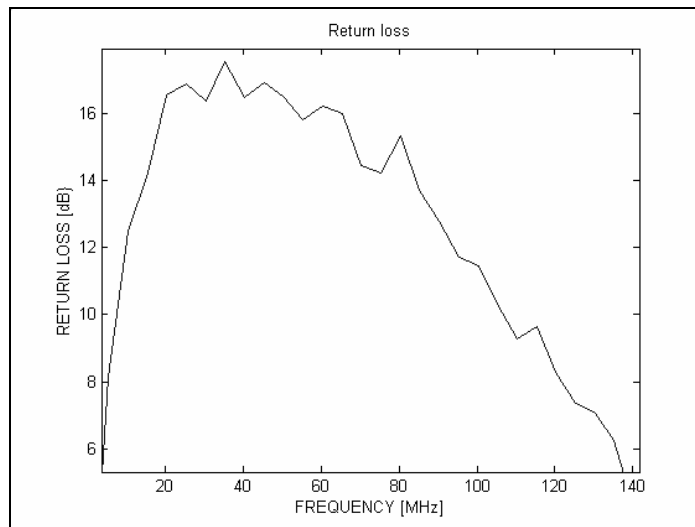


Figure 4-43 Return loss of the Gali-S66.



iii. Conclusion

Property	Measured value	Comment
Noise figure	2.2dB	Lower than the expected 2.8dB
Stability	Unconditionally stable	
Return loss	16.5dB	
Gain	21.3dB	High gain as expected
Matching	$ s_{11} = -24dBm$ and $ s_{22} = -28dB$ at 50MHz	Good impedance match at output and input ports
Output 1dB compression point at 50MHz	-3dBm	Lower than the expected 1dBm at 2GHz
Output intercept point at 50MHz	12.5dBm	
Power supply	$V_{cc} = 9V$, $I_{cc} = 14.5mA$	Less than the expected 16mA

Table 4-13 Summary of the measured Gali-S66 amplifier properties.

4.2.3. Conclusion

Both amplifiers work well at 50MHz and have different advantages and disadvantages. These are summarized in Table 4-14.

Property	AT-41533 transistor amplifier	Gali-S66 amplifier
Noise figure	1.6dB	2.2dB
Stability	Unconditionally stable	Unconditionally stable
Return loss	3.9dB	16.5dB
Gain	16dBm	21.3dB
Matching	$ s_{11} < -3dB$ and $ s_{22} = -15dB$ at	$ s_{11} = -24dBm$ and $ s_{22} = -28dB$ at

	50MHz	50MHz
Output 1dB compression point at 50MHz	-1dBm	-3dBm
Output intercept point at 50MHz	-1dBm	12.5dBm
Power supply	$V_{cc} = 5V$, $I_{cc} = 46mA$ $I_c = 5mA$	$V_{cc} = 9V$, $I_{cc} = 14.5mA$

Table 4-14 Comparison between the characteristics of the designed Gali-S66 and the AT-41533 single transistor amplifiers.

Front-end amplifier characteristics were discussed in this section, two amplifier components were designed, built and their performance measured. This will enable a comparison of the influence of these characteristics on receiver performance. A discussion of the local oscillator follows in the next section as shown in *Figure 4-44*.

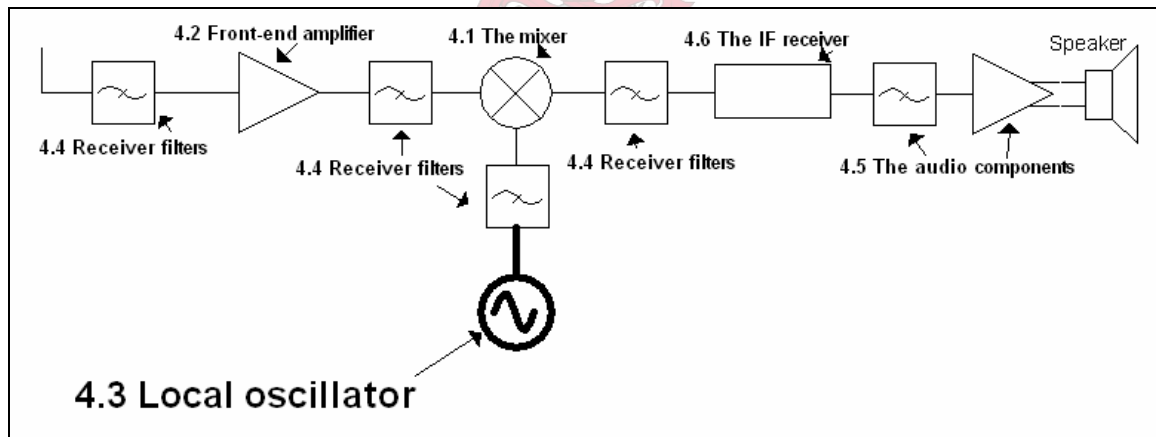


Figure 4-44 Structure of chapter 4: 4.3 Local oscillator.

4.3 Local oscillator

4.3.1. Theory

Oscillators and frequency synthesizers are of paramount importance in receiver systems. They provide the signals that are used to demodulate received signals in receivers as well as the signals that are transmitted in transmitters [1] [9].

In a super heterodyne receiver, frequency tuning is accomplished by varying the frequency of the local oscillator. This can be done with a voltage-controlled oscillator (VCO) for low frequencies and wideband modes. Narrowband tuning at high frequencies on the other hand is nearly impossible to achieve with a VCO. This is because VCO frequency stability and precise frequency-tuning accuracy decreases as the VCO frequency increases [8].

If a radio is only required to tune to a few channels, switched crystals can be used as shown in *Figure 4-45*. As the number of channels increase, the size and cost of the radio will increase rapidly. The number of crystals that are used can be decreased significantly by using a multi-conversion receiver and placing a crystal bank at each LO [8].

A different approach to achieve precise narrowband frequency tuning at high frequencies, involves frequency synthesis. Frequency synthesizers derives exact high frequency signals, by using accurate reference oscillators e.g. crystal oscillators. *Direct digital synthesizers* (DDS) and *phase lock loops* (PLL) are examples of frequency synthesizers.

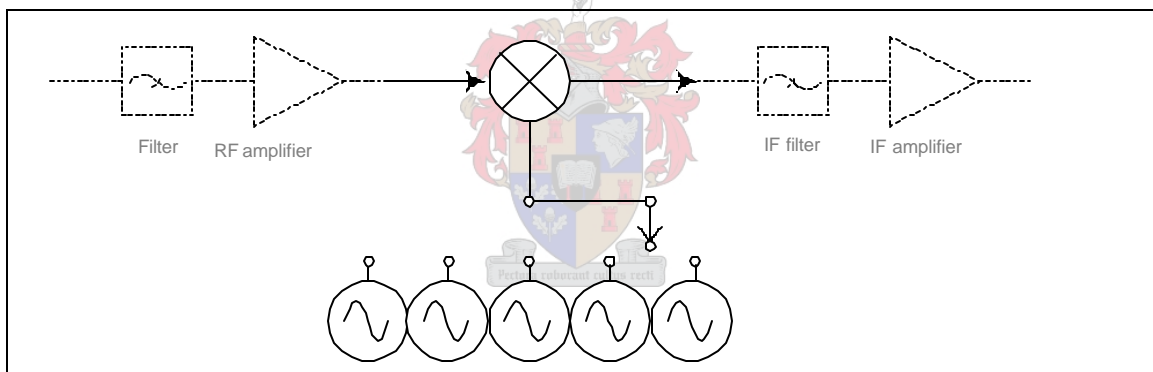


Figure 4-45 Use of switched crystal oscillators to achieve frequency tuning in a super heterodyne receiver system.

A short description of the different types of frequency generators, their most important characteristics and a comparison between the different options, that were built and measured, follows.

4.3.1. a Types

i. Oscillators

An oscillator is a circuit that generates AC waveforms from DC power. Basic building blocks of oscillators include: [9] [26]

- A resonator that determines the frequency e.g. a LC circuit or crystal.



- An active circuit with a negative resistance and a gain at the oscillator frequency e.g. an transistor or diode circuit.
- Components that limit the amplitude and stabilize the oscillation.

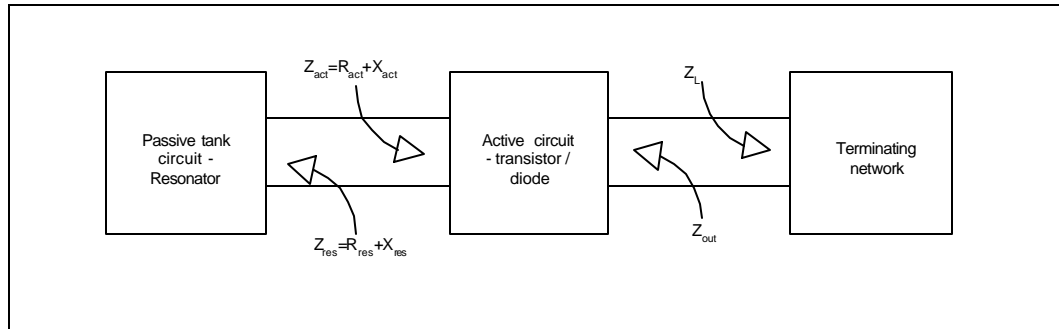


Figure 4-46 Concept of oscillator resistance [9] [26].

The two basic elements of an oscillator, namely the active circuit and the resonator, are shown in *Figure 4-46*. The input resistance of both of these blocks is of paramount importance, to enable oscillation and is defined in this figure. To enable oscillation the prerequisites that must be met, are:

- **Condition 1:** $R_{act} + R_{res} \leq 0$

Since the resonator circuit is passive ($R_{res} > 0$) the above condition will imply that $R_{act} < 0$. This condition will determine if the circuit oscillates [9] [26].

- **Condition 2:** $X_{act} + X_{res} = 0$
 $X_{act} = -X_{res}$

The point where X_{act} intercept $-X_{res}$, determines the frequency where the circuit will oscillate [9] [26].

Numerous oscillator topologies are available e.g. Hartley, Colpitts, Clapp, Pierce and Wien Bridge. A typical Colpitts oscillator circuit is shown in *Figure 4-47*. The oscillator is divided into the resonant and active circuit to illustrate the above conditions for oscillation.

The resonator chosen in *Figure 4-47* is a LC tank. The Q value of a resonator is a very important figure of merit, because it determines if the oscillator will have a steep resonating gradient and as a result, low phase noise. Therefore, a high Q factor is desirable in a resonator. A wide variety of resonator elements are available that can replace the LC tank in *Figure 4-47*.



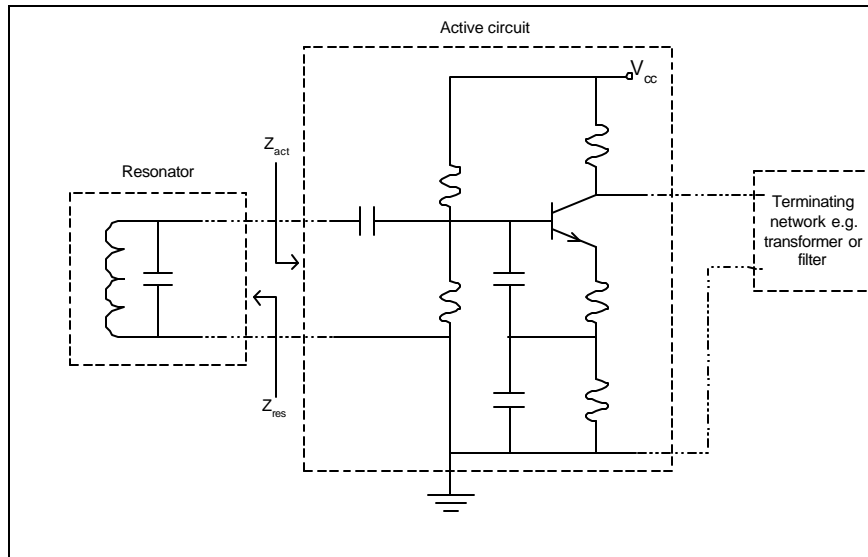


Figure 4-47 Typical common emitter Colpitts oscillator divided into basic blocks.

Resonators include: [1] [9] [26] [37]

- LC circuits are used up to 10GHz. Higher Q values are achievable at lower frequencies.
- Crystal resonators have very high Q values (typically 100 000). The highest frequency where crystals are available is approximately 200MHz
- Coaxial transmission line resonators are produced for high frequencies and have relatively high Q values.
- Dielectric resonators have high Q values (up to 5000) and are used at high frequencies. Applications are limited to products that would not be exposed to too much vibration, etc.
- Strip line resonators have low Q values (typically 100) and are used at high frequencies.
- Metal cavities work well at high frequencies but are not practical in applications where space is limited, because they are rather large (In the order of λ or $\lambda/2$).

ii. Phase lock loops (PLL)

Phase lock loops use feedback to control the output frequency of a VCO accurately. This closed frequency control system consist off a voltage controlled oscillator (VCO), a phase detector, a loop filter, stable frequency reference source and often an amplifier in addition, as shown in *Figure 4-48*.



When the loop is locked the high frequency output $f_{out} = Nf_{ref}$, where N is the number by which the frequency divider divides the output frequency and f_{ref} is the frequency of the stable reference source.

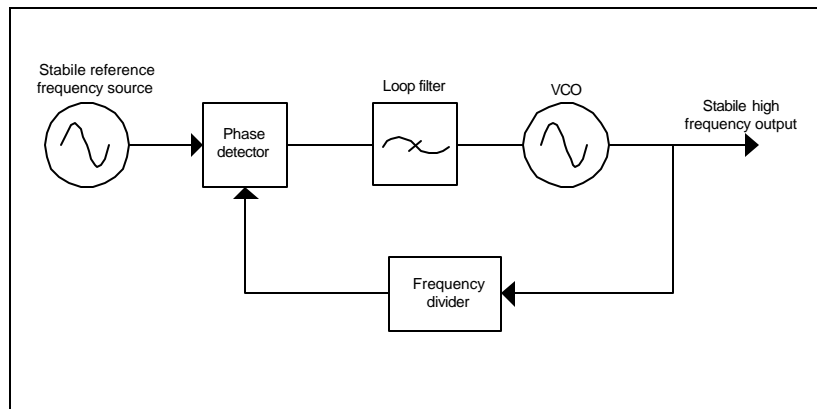


Figure 4-48 Typical phase lock loop.

Phase lock loops are typically implemented by combining a voltage-controlled oscillator (VCO), a phase lock loop IC, a stable reference frequency oscillator and a loop filter. The loop filter should set-up a trade-off between noise and settling time. PLL's have good frequency accuracy and phase noise characteristics, but settling loop times between changes in frequency can be long [8] [9] [47].

iii. Direct digital synthesizer (DDS)

Direct digital synthesizers generate precise frequency-tunable output waveforms, by dividing a high frequency reference clock by a factor set by a programmable tuning word. The output resolution is the smallest difference between the two frequencies at the output [43] [45] [46].

DDS operation can be explained with reference to *Figure 4-49*. It can be summarized as follows:

- A *frequency tuning word* is provided typically by a microprocessor or some form of a digital control unit and written into the frequency register.
- A frequency word from the *frequency register* is loaded into the *phase register*, at each clock pulse. This is used to calculate the phase of the waveform. The output of the phase accumulator is linear, as shown in *Figure 4-49* and cannot be used to generate a waveform.
- The *phase to amplitude converter* will use this phase input to determine a data value, representing the amplitude of the waveform at this phase, as stored in the waveform memory. This is read and delivered to a *digital to analog converter*.



- The *digital to analog converter* (DAC) will deliver an analog voltage, of the form stored in the waveform memory, and of the frequency, specified by the frequency control word.
- A *low pass filter*, which will remove the sampling effects on the signal, follows. The reference clock runs at a single fixed frequency, which will simplify the design of this filter.

The reference clock of the DDS should be at least twice as high as the highest frequency that will be generated. Some DDS ICs includes a reference clock multiplier that reduces the frequency requirement on the precision reference clock. This will also enable the DDS to use existing system clock sources, thereby reducing costs [43] [46].

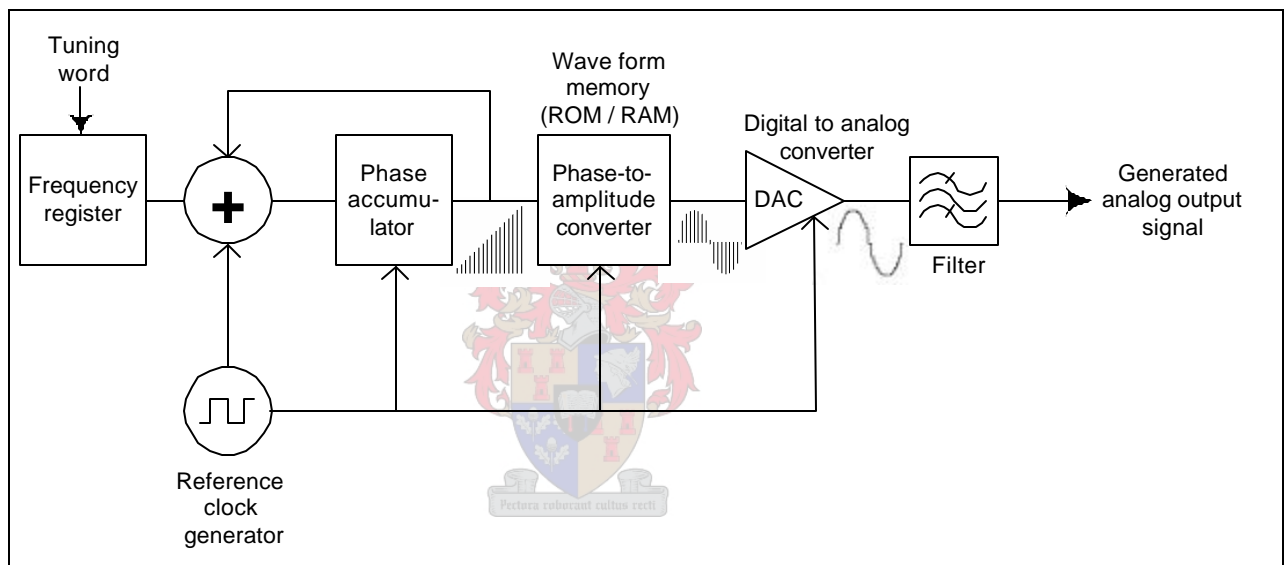


Figure 4-49 DDS circuit block diagram [43] [45] [46].

Advantages of DDS include [43] [46]:

- The frequency stability and accuracy of the DDS is dependent on its reference oscillator. Thus, it can be as accurate as a crystal-controlled oscillator or even a temperature compensated crystal oscillator for extreme cases.
- High resolution enables the DDS to generate specific desired output frequencies, and make very precise changes in frequency, with no over or undershoot loop settling time abnormalities.
- Phase and amplitude can be controlled and changed precisely.
- Phase lock loops may need tuning due to temperature drift and component aging after a while. This will not be necessary for digital synthesizers.
- The DDS is capable of generating any arbitrary waveform, because it functions by recalling a waveform stored in its memory. Some synthesizers use RAM memory



for waveform storage in which case any arbitrary waveform can be built into the memory to be recalled.

4.3.1. b Amplitude and phase noise of the local oscillator

Oscillators are susceptible to phase and amplitude noise. Amplitude noise includes any differences in the amplitude, and is usually negligible, because it is typically fed into a limiter or mixer that removes the effect of the amplitude noise. Phase noise or timing jitter is the random fluctuation of the frequency of an oscillator signal [8] [9] [37] [42].

The cause of phase noise is changes in device temperature and noise or interfering signals elsewhere in the circuitry (EMI), which couple to the oscillator via the power supply or substrate [9] [40] [42] [43].

Frequency stability is critical in oscillators. The short-term stability of an oscillator can be seen on a spectrum analyzer. The discrete spikes in the spectrum viewed are caused by spurious signals coming from the oscillator harmonics, while the phase noise will appear as a wide continuous distribution restricted around the output signal. Without phase noise, all the signal power would be focused at the desired signal frequency [9] [38] [40] [42].

Phase noise will limit the selectivity of the receiver and cause down-conversion of signals that are located nearby the desired signal (reciprocal mixing). Since restrictions on receiver selectivity are becoming more important; this phenomenon is of paramount importance and can limit the system performance. Phase noise will also have an influence on the sensitivity of the receiver. Any noises close to f_{LO} will produce noise products close to f_{IF} and degrade sensitivity. The sensitivity of the receiver can be degraded by the phase noise, if the phase noise leaks through the mixer or mixes with the RF or LO signal to produce noise at the IF port [8] [1] [9] [33] [37] [39] [40] [41].



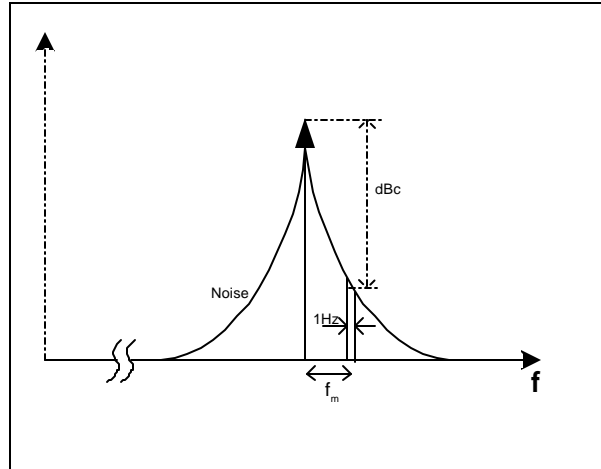


Figure 4-50 Phase noise definition [24] [33-34] [37] [39] [40] [42].

Phase noise ($L(f_m)$) is defined as the ratio of power, in a 1 Hz bandwidth, at a given offset f_m from the signal, to the total signal power. Phase noise is expressed in decibels relative to the carrier power per Hertz of bandwidth [dBc/Hz] [9] [24] [34] [39] [41] [42].

The phase noise of an oscillator can be measured using a spectrum analyzer, with a 1 Hz resolution bandwidth. The signal power is measured first and then the phase noise power at a particular offset f_m from the carrier is measured. The ratio of these two powers is the normalized power, referred to the signal, at a frequency offset, f_m . This ratio is the SSB phase noise and is calculated using [33] [40]

$$L(f_m) = 10 \log \frac{P_S}{P_{SSB}} \quad (4.12)$$

where P_S is the signal power, and P_{SSB} is the phase noise power, in a 1 Hz bandwidth, at a frequency offset f_m from the carrier.

The maximum phase noise, at a given offset, f_m , that is required to achieve a specified adjacent channel rejection can be predicted with [9] [42]

$$L(f_m) = SNR - S - 10 \log B \text{ [dBc / Hz]} \quad (4.13)$$

where

- SNR is the desired signal-to-noise ratio at the output of the receiver [dB]
- S is the specified adjacent channel rejection / selectivity [dB]
- B is the bandwidth of the IF filter in [Hz]

A high Q of the tank in a LC oscillator, will cause low phase noise and visa versa [37].



In phase lock loop systems phase noise can be caused by the leakage of the reference signal, harmonics of the VCO, spurious frequencies generated by the phase detector and noise within the pass band of the oscillator feedback circuit that will be amplified [9] [42].

The output signal quality of a DDS is dependent on the signal quality of the reference clock that is driving the DDS. The phase noise of the reference signal of the direct digital synthesizer is reduced in the output. Therefore, the 30MHz output signal of the DDS will have less phase noise than the 120MHz reference clock. There is however a limit to this reduction, called the residual phase noise. If the phase noise of the reference clock is better than the residual phase noise, the DDS output signal will not exceed this. Thus, one should not make too much of an effort to limit the phase noise of the reference clock just to have an overall DDS output phase noise that is still approximately the same [43].

Reference clock multipliers, that can be enabled, are included in some DDS ICs. The advantages of these reference clock multipliers are:

- The DDS can use another existing system clock, which will simplify the system and reduce costs.
- A low frequency reference clock can be used, which means a reduction in complexity and cost of the clock oscillator [43]

This frequency multiplication will however, degrade the phase noise of the reference clock. On the other hand, oscillators at lower frequencies typically have a lower phase noise than oscillators at high frequencies [42] [43].

The frequency stability of the local oscillator is extremely important, because it will determine whether the desired frequency will be received or not. The oscillator frequency should be insensitive to DC changes.

4.3.2. Designing, building and measuring different frequency generators

A DDS and a crystal oscillator was designed next. The phase lock loop was not designed here, but instead the Rohde & Schwarz SML03 signal generator was used. This signal source has a PLL on the inside that was used to do the comparisons with in the next chapter. The estimated phase noise of this signal generator measured with the spectrum analyser at 12.5kHz is -108dBc/1Hz.



4.3.2. a Designing, building and measuring the DDS

An AD9851 direct digital frequency synthesizer from Analog Devices was built. This is a DDS IC with a six-time reference clock enable function, a built in 10 bit digital to analog converter and a tuning resolution of approximately 0.04Hz. Reference clock rates of up to 180MHz can be accommodated. It produces a sine wave that can be used directly as a frequency source.

The AD9851 is essentially a digitally controlled oscillator, which will generate an output frequency dependent on the contents of its 40-bit register. The contents of this 40-bit register and thus, the output frequency of the AD9851 were chosen in this application to be controlled by the low-power ATmega8L microcontroller from the ATMEL AVR family of microcontrollers. The ATmega8L was chosen for its low power consumption, which is a major consideration in portable devices.

The hardware and software design of this possible digital replacement for the local oscillator is discussed in detail in Appendix B.

The circuit diagram of this frequency source component is shown in *Figure 4-51* and a photo of the component is shown in *Figure 4-52*.

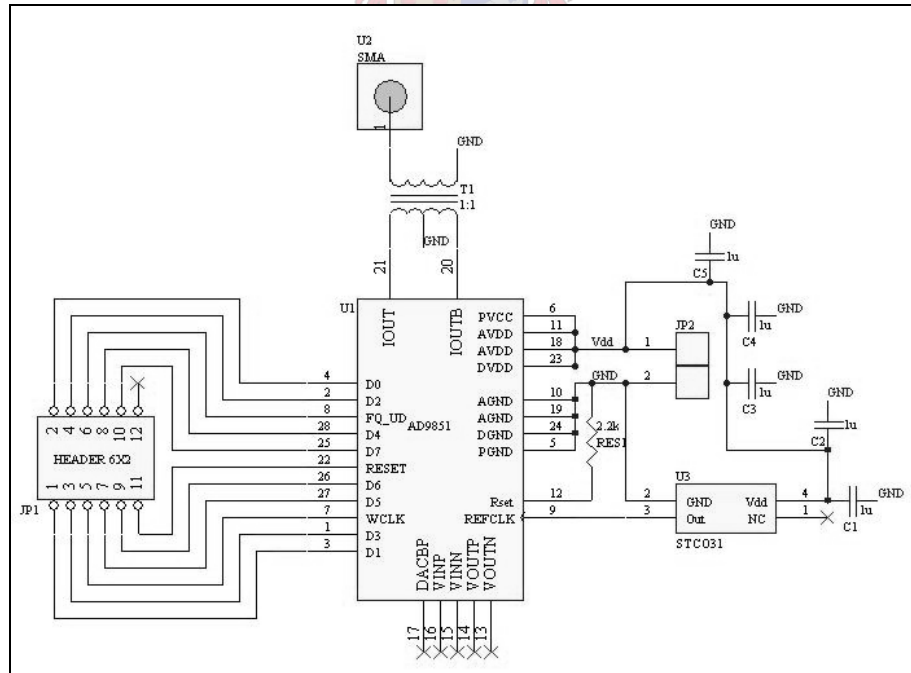


Figure 4-51 Circuit diagram of the AD9851 direct digital synthesizer component that was designed.

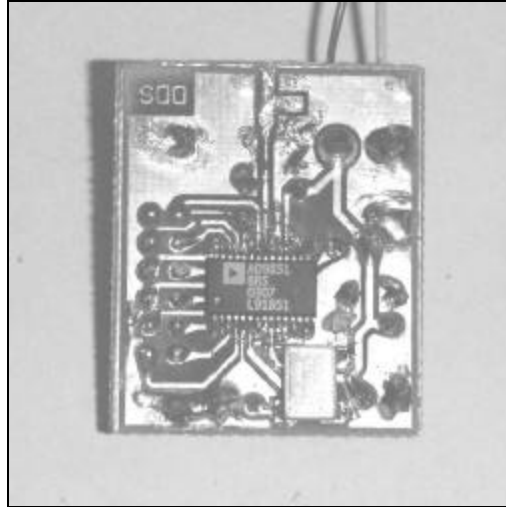


Figure 4-52 Photo of the designed direct digital synthesizer component.

i. Measurements

The output signal of the DDS was investigated next, using a spectrum analyzer and the Tektronix TDS 380 oscilloscope. The unfiltered DDS output spectrum is shown in *Figure 4-53*, when the DDS is programmed to generate an output signal at 39.3MHz . The unfiltered output amplitude of the DDS is 2dBm . The harmonics of the output signal can be seen clearly in the spectrum at 78.6MHz , 117.9MHz and at 157.2MHz . The reference signal that leaks through is also seen at 20MHz as well as its harmonics at $60, 100, 140$ & 180MHz . The unfiltered DDS Tektronix TDS 380 oscilloscope output is shown in *Figure 4-54*. This signal is modulated quite badly by these high frequency signals and is difficult to distinguish.

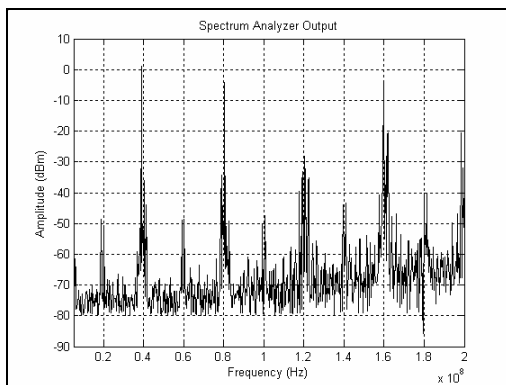


Figure 4-53 The unfiltered DDS spectrum analyzer output.

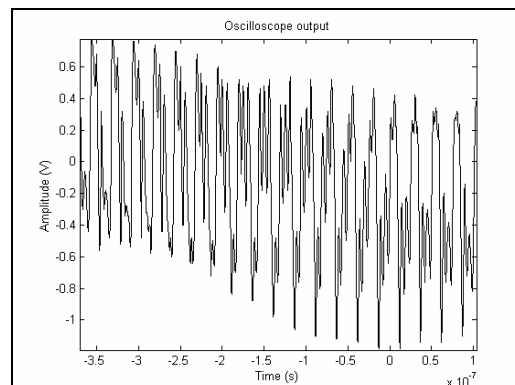


Figure 4-54 The unfiltered DDS oscilloscope output.



Next, the Chebyshev injection filter that will be discussed in section 4.4.3 was coupled to the DDS output. The filtered output spectrum is shown in *Figure 4-55*. The output amplitude of this filtered DDS output is $\pm 0dBm$. Thus, the filter filters out all the DDS harmonics but introduces a $2dBm$ insertion loss. The sinusoidal output of the DDS as seen on the Tektronix TDS 380 oscilloscope is shown in *Figure 4-56*. This signal is much more useful than the unfiltered signal.

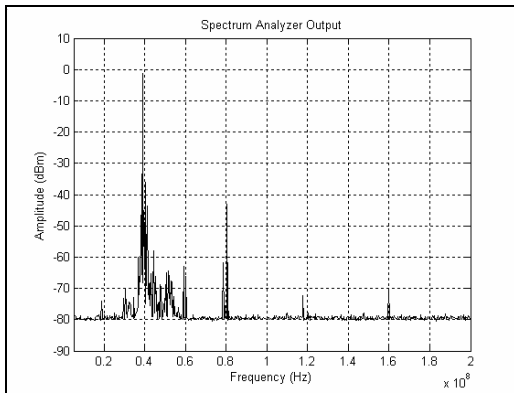


Figure 4-55 The Chebyshev filtered DDS spectrum analyzer output.

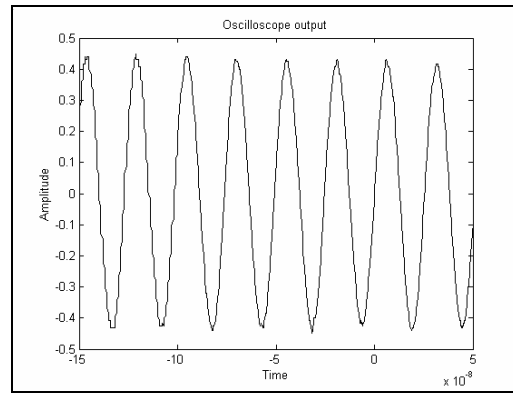


Figure 4-56 The Chebyshev filtered DDS oscilloscope output.

The Butterworth injection filter that will be discussed in section 4.4.3 was coupled to the output of the DDS. The filtered output spectrum is shown and output amplitude of this filtered DDS output is $1dBm$. Thus, the filter introduces a conversion loss and filters out the DDS harmonics, at the expense of a phase delay and as a result, the signal is slightly distorted. The output of the DDS as seen on the Tektronix TDS 380 oscilloscope is shown in *Figure 4-58*.

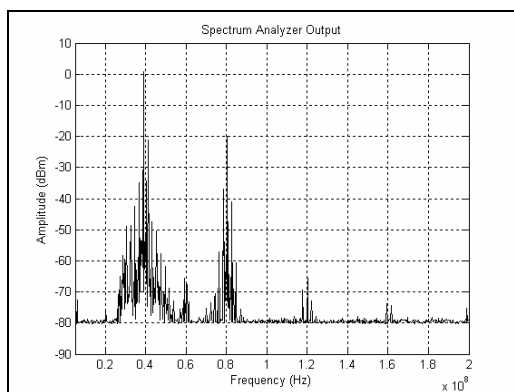


Figure 4-57 The Butterworth filtered DDS spectrum analyzer output.

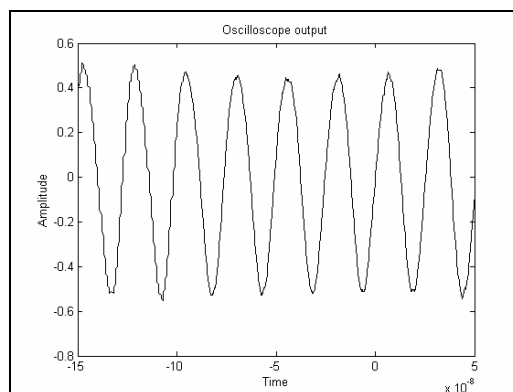


Figure 4-58 The Butterworth filtered DDS oscilloscope output.



The phase noise of the DDS was measured at offsets of $\pm 12.5\text{kHz}$ from the carrier frequency (thus at 39.3125MHz and 39.2875MHz), with a HP8562A spectrum analyzer. The smallest resolution bandwidth of this spectrum analyzer is 100Hz , so the phase noise was measured per 100Hz and then the phase noise per 1Hz was estimated by subtracting 20dB (divided by 100). The results are summarized in *Table 4-15*.

Unfiltered DDS output	$L(12.5\text{kHz}) = -110 \text{ dBc/Hz}$
Chebyshev filtered DDS output	$L(12.5\text{kHz}) = -110 \text{ dBc/Hz}$
Butterworth filtered DDS output	$L(12.5\text{kHz}) = -110 \text{ dBc/Hz}$

Table 4-15 Measured phase noise of the DDS output.

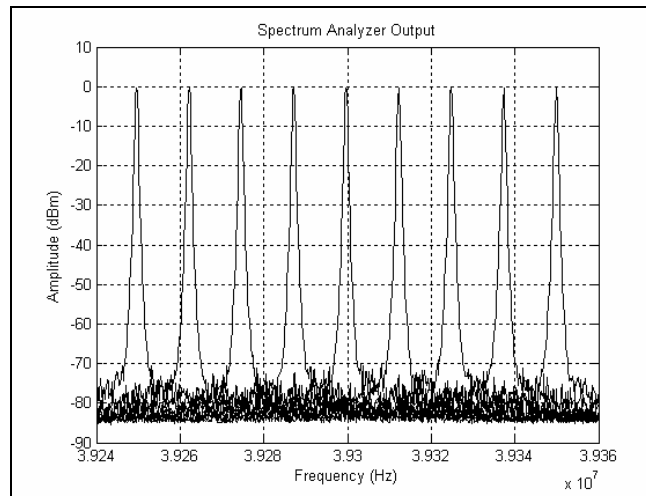


Figure 4-59 Saved output spectrum of the DDS, with the Chebyshev filter at the output of the DDS, if the microcontroller tunes the DDS frequency to vary between 39.25MHz and 39.35MHz , in steps of 12.5kHz .

The output spectrum of the DDS when the microcontroller that tunes the DDS output frequency, vary the frequency between 39.25MHz and 39.35MHz , in steps of 12.5kHz , is shown in *Figure 4-59*. The DDS and ATmega8L microcontroller, which tunes the frequency, collectively draw 90mA current when active.

ii. Conclusion

The designed DDS component works better than expected. It was easy to program but it draws a lot of current, which is a problem when used for portable devices. It should however function well in the receiver system. This will be tested in the following section.



4.3.2. b Design of a crystal oscillator

i. Designing and simulating

A crystal oscillator that oscillates at 38MHz was built, using the principles discussed in 4.3.1. ai, to make comparison with the other local oscillators possible. The common base Colpitts oscillator configuration was chosen and simulated in Microsim. The circuit diagram is shown in *Figure 4-60*.

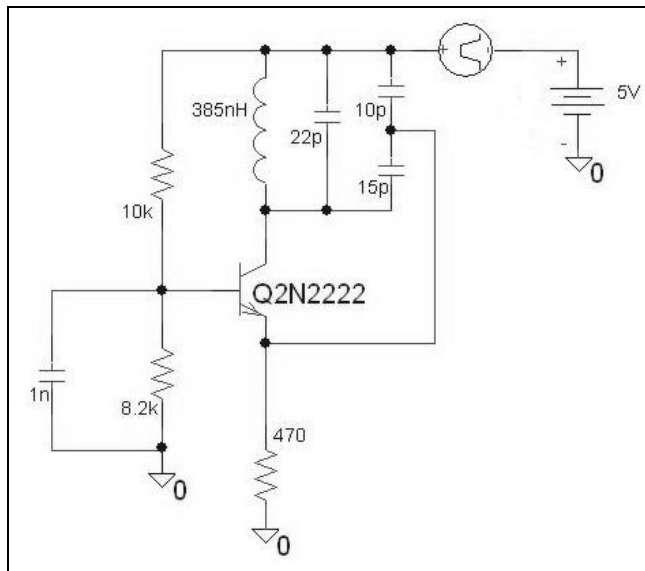


Figure 4-60 Common base Colpitts oscillator that was simulated.

The FFT of this simulated signal is shown in *Figure 4-61*. It can be seen that this circuit oscillates at 38MHz.



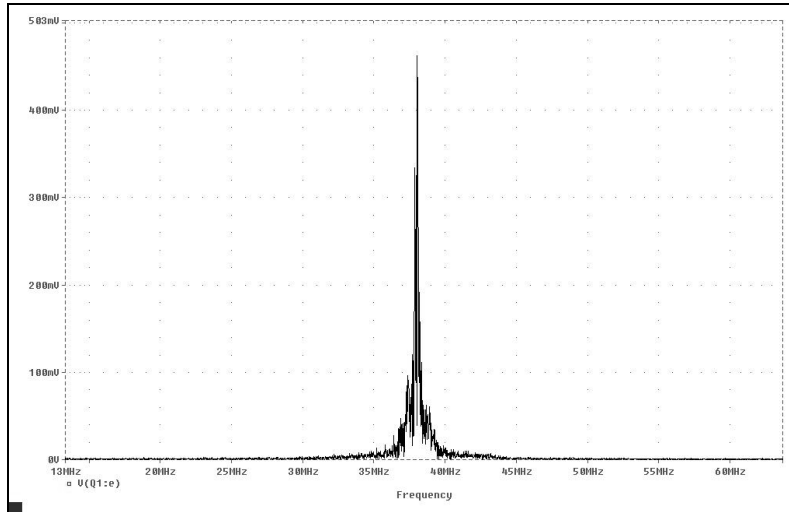


Figure 4-61 FFT of the simulated emitter oscillator signal.

To build a crystal oscillator, the LC resonator needs to be replaced with a crystal resonator at 38MHz. If one of the over tone modes of the crystal is used, it is better to put the crystal in the feedback path. That way, the circuit will only oscillate at the over tone, because the rest of the circuit is designed for this frequency.

A crystal can be seen as a high impedance at all frequencies except at the oscillating frequency. If a high impedance is placed in the feedback path, oscillation will stop and the oscillator will have no output signal. However, at the oscillating frequency, there will be feedback and the circuit will oscillate. The circuit that was built is shown in *Figure 4-62*.

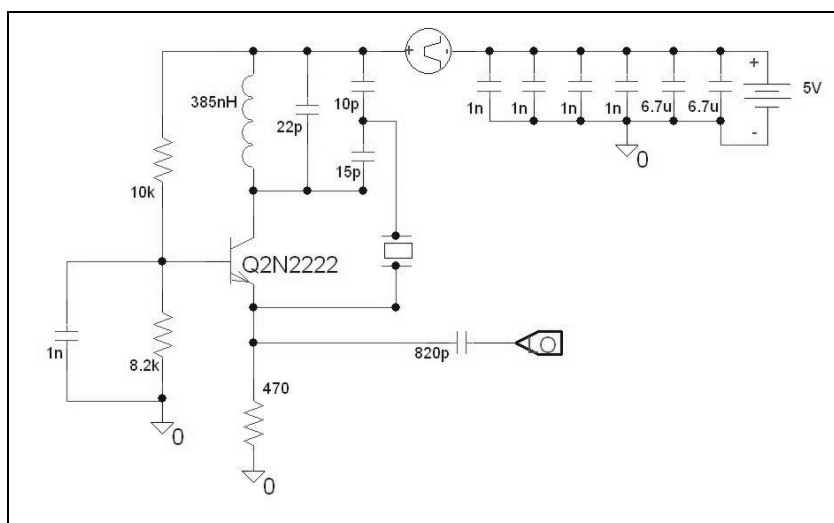


Figure 4-62 Circuit diagram of the crystal oscillator circuit component.

Next, the measurements of this circuit are discussed.

ii. Measurements

The crystal oscillator that was built is shown in *Figure 4-63*. This circuit oscillated the first time round.

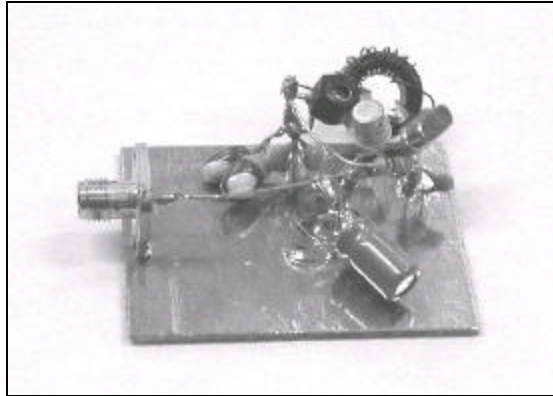


Figure 4-63 Photo of the crystal oscillator component.

The output frequency of this oscillator was measured on the HP8562A spectrum analyzer and is shown in *Figure 4-64*. The integer multiples of the output frequency can be seen clearly. The output signal has a frequency of 38MHz and an amplitude of 1dBm.

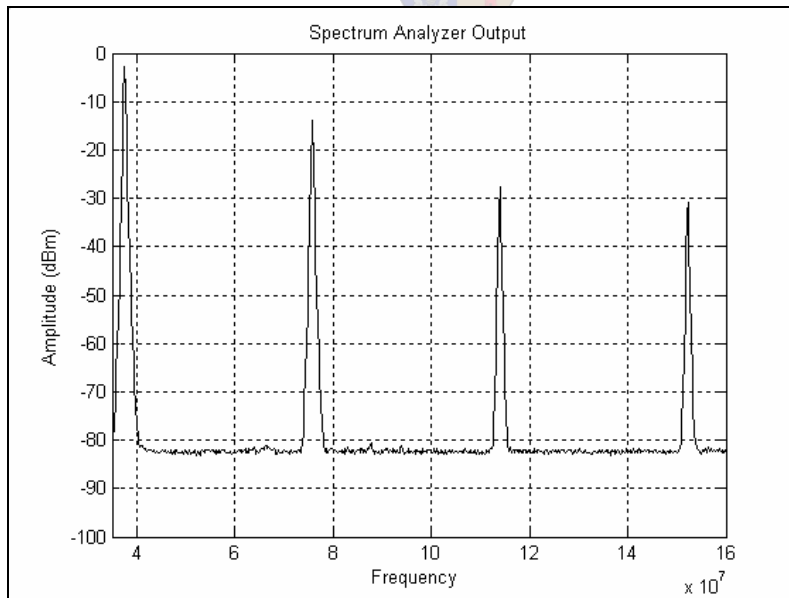


Figure 4-64 The output spectrum of the crystal oscillator.



The phase noise was measured per 100Hz on the HP8562A spectrum analyzer and estimated as -112dBc/1Hz.

This frequency source draws 20.8mA current when active.

iii. Conclusion

The crystal oscillator that was simulated and built works well. This oscillator will be used in the receiver system in the next chapter. The oscillator is not sensitive to the DC voltage and the frequency remains stable for slight changes in voltage.

4.3.3. Comparison and conclusion

The DDS draws much more current than the crystal oscillator, but can tune over a wide frequency range, while the crystal oscillator can only be used at one frequency but has less phase noise. Switched crystal oscillators can also be used to tune to different frequencies, but this approach can be more expensive and difficult to implement and will again draw more current.

Both a DDS and a crystal oscillator were designed. In the next chapter these two components as well as a Rohde & Schwarz SML03 signal generator instead of a PLL will be used to compare the influence of the local oscillator component on the receiver's measured performance.

Next, the design of the receiver filters will be discussed, as shown in *Figure 4-65*.

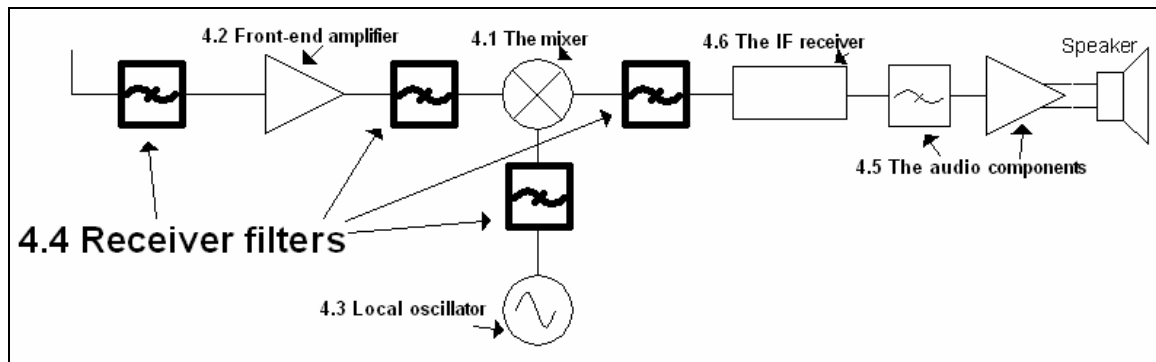


Figure 4-65 Structure of chapter 4: 4.4 Receiver filters.

4.4 Receiver filters

4.4.1. Front-end filters

The main functions of the two front-end filters, the pre-select filter and image filter, as discussed in section 2.1.2 are: [1] [8] [9]

- To prevent strong interfering signals from saturating the RF amplifier or mixer and thus, minimizing the IM distortion.
- To reject the image frequency.
- To attenuate receiver spurious responses e.g. IF rejection.
- To suppress the LO signal energy power.

It is of vital importance at this point in the receiver chain to minimize the insertion loss of these filters to optimize the overall noise figure of the receiver. Thus, these filters will typically not have a sharp cut-off, as high insertion loss is usually associated with a sharp cut-off characteristic. An inductor-capacitor (LC) filter is typically sufficient, and will reduce the cost and complexity of the system. Losses can further be reduced by choosing components with little losses e.g., an inductor with a high Q core. Parasitic components should be taken into account by reducing the length of component pins and by keeping the length of the transmission lines as short as possible [1] [8] [9].

Some wideband receivers use electronically tuned resonant circuits that use a varactor diode tuned by a control voltage as the receiver operating frequency is changed. Other receivers might provide one or more front-end components that are shifted for different frequency ranges [8].

4.4.1. a Designing, building and measuring the front-end filters

Three front-end filters were designed, namely a 3rd order Butterworth filter, a 5th order Chebyshev filter with 0.5dB ripple and a simple LC filter.

After these low pass filters were impedance scaled and transformed, they were simulated in *Microwave Office* [50], to determine their response. The simulated and measured results of these filters are discussed next.



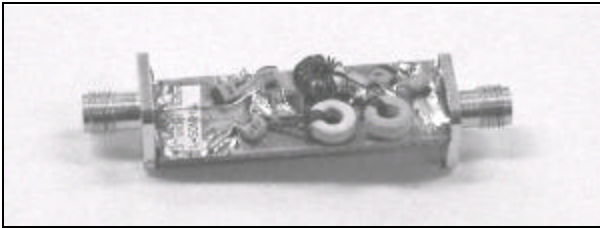


Figure 4-66 Photo of the third order Butterworth filter. Center frequency at $f_0 = 50\text{MHz}$.

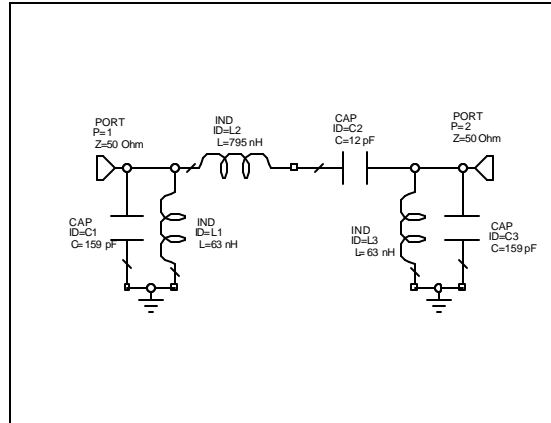


Figure 4-67 Third order Butterworth filter. Center frequency of $f_0 = 50\text{MHz}$.

The Butterworth filter component is shown in *Figure 4-66* and the circuit diagram can be seen in *Figure 4-67*. This filter was designed to be a third order filter with a 3dB pass band of almost 20MHz. The loss in the pass band is almost zero as can be seen in the simulated results in *Figure 4-68*, while the filter is matched well between 45MHz and 58MHz with $|s_{11}| \& |s_{22}| < -10\text{dB}$. In reality, the filter is not ideal, but still has almost no loss in the pass band and a good impedance match between 45MHz and 58MHz with $|s_{11}| \& |s_{22}| < -10\text{dB}$. This is shown in *Figure 4-69*.

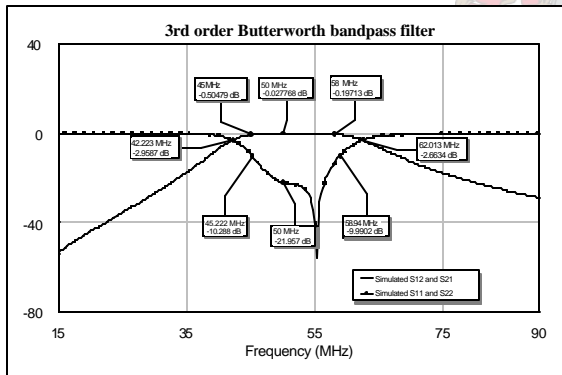


Figure 4-68 Simulated s-parameters of the third order Butterworth filter. Center frequency at $f_0 = 50\text{MHz}$.

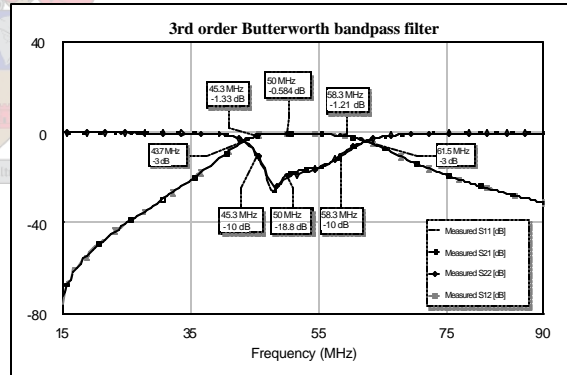


Figure 4-69 Measured s-parameters of the third order Butterworth filter. Center frequency at $f_0 = 50\text{MHz}$.

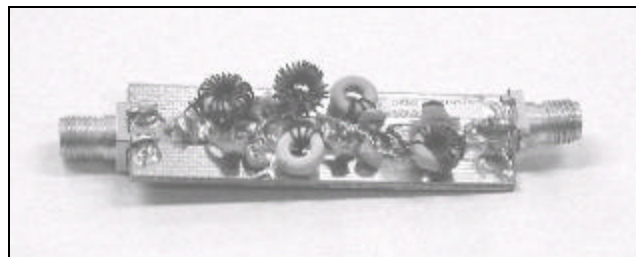


Figure 4-70 Photo of the fifth order Chebyshev filter. Center frequency at $f_0 = 50\text{MHz}$.

The Chebyshev filter component is shown in *Figure 4-70* and the simulated and built circuit diagram can be seen in *Figure 4-71* below.

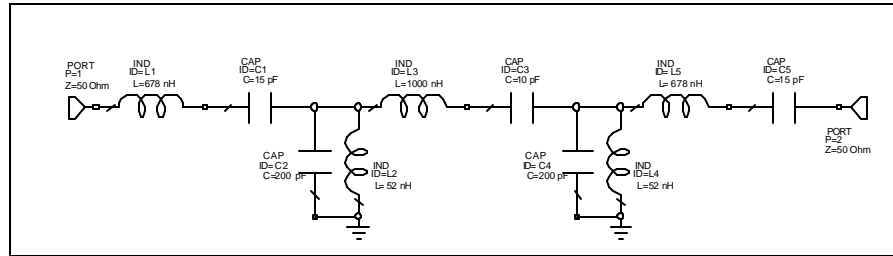


Figure 4-71 The fifth order Chebyshev filter. Center frequency at $f_0 = 50\text{MHz}$.

This filter was designed to be a fifth order filter with a maximum of 0.5dB ripple in the 3dB pass band (between 40MHz and 61MHz). It has a sharper cut-off response outside the pass band than the third order Butterworth filter, because of its higher order as can be seen in *Figure 4-72*. The measured filter is not ideal, with more loss in the pass band (42MHz and 60MHz). The filter has a good impedance match as is shown in the measured results in *Figure 4-73*.

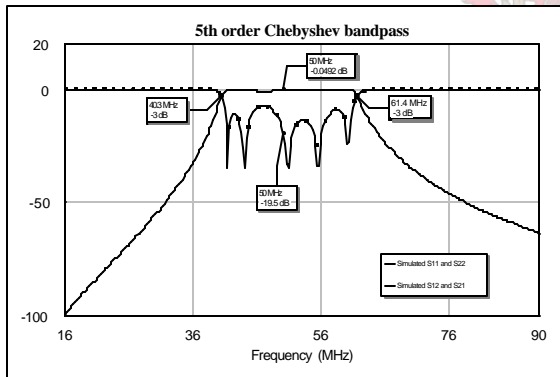


Figure 4-72 Simulated s-parameters of the fifth order Chebyshev filter. Center frequency at $f_0 = 50\text{MHz}$.

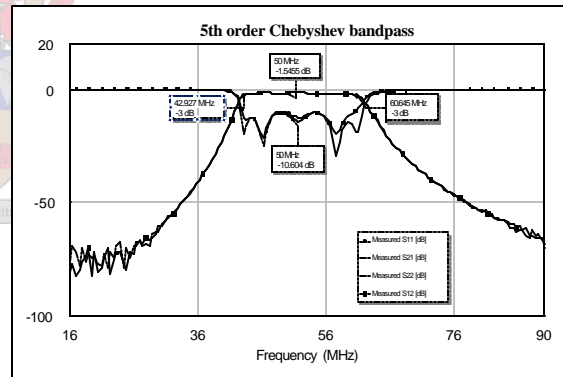


Figure 4-73 Measured s-parameters of the fifth order Chebyshev filter. Center frequency at $f_0 = 50\text{MHz}$.

The simple LC filter shown in *Figure 4-74*, was designed next.

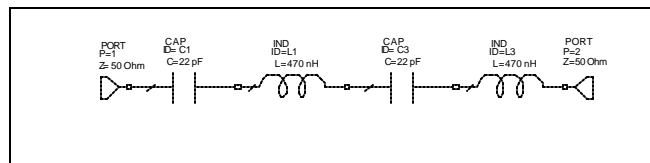


Figure 4-74 Simple LC filter.

According to simulated results of the filter, shown in *Figure 4-75*, the pass band of the filter is expected to be smaller than the previous two filters. The measured results, shown in *Figure 4-76*, illustrate a small loss in the 3dB pass band between 40MHz and 54MHz.

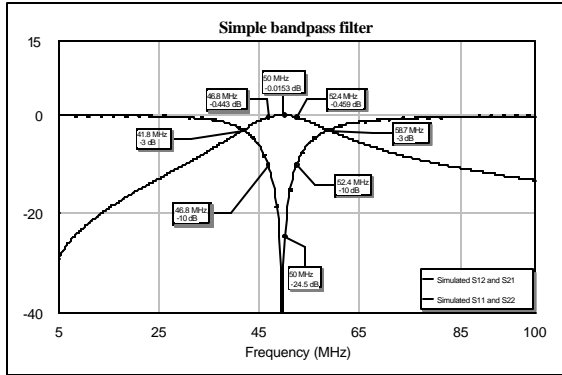


Figure 4-75 Simulated s-parameters of the simple bandpass filter.

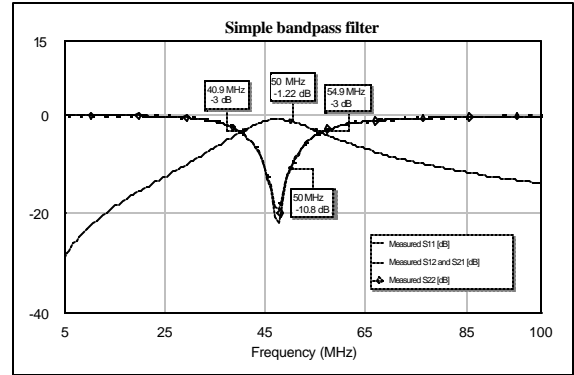


Figure 4-76 Measured s-parameters of the simple bandpass filter.

4.4.1. b Conclusion

The three filters that were designed will be used as image and pre-select filters in the receiver system and the effect of their characteristics on the system's performance will be compared. Their attenuation at the image frequency is compared in *Figure 4-77*.

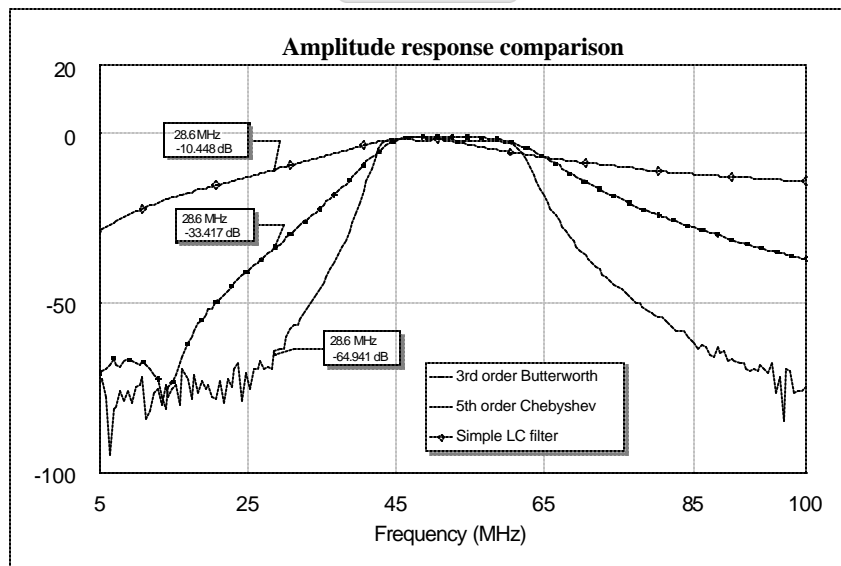


Figure 4-77 Amplitude response comparison between the different designed front-end filters.

4.4.2. The IF filter

The IF filter provides the adjacent channel rejection, sets overall noise bandwidth of the receiver system and removes unwanted mixer products from the spectrum. The bandwidth of this filter also determines the modulation bandwidth of the signal. Therefore, the bandwidth and selectivity of this filter are of critical importance and will directly influence the system's selectivity and sensitivity [8] [1] [9].

This application requires a channel spacing of 12.5kHz and therefore the maximum permissible frequency deviation is $\pm 2.5\text{kHz}$ (discussed in chapter 5). The adjacent channel rejection requirement is $>70\text{dB}$ as shown in *Table 1-1*. Thus, a filter with a very high selectivity and a small bandwidth (high Q value) is required. A ceramic filter and crystal filter with center frequencies of 10.7MHz are characterized in this section.

4.4.2. a Crystal filter

The realizable Q values for inductors set a limit on the bandwidth of band pass LC filters. Thus, higher Q elements need to be employed e.g. surface acoustic wave resonators, coaxial transmission line resonators, dielectric resonators, strip line resonators, metal cavities or crystal resonators. Of these, the Q of the quartz crystal resonators is the highest. Thus, crystal filters with a high selectivity and a small bandwidth are realizable but only for frequencies up to approximately 200MHz [1] [8] [9] [26] [37].

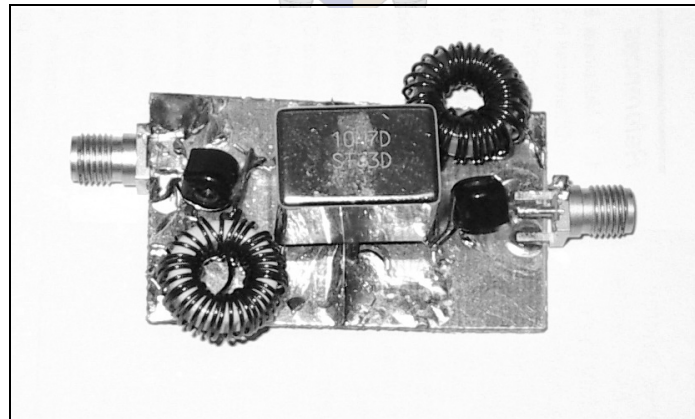


Figure 4-78 Photo of the crystal filter, 50Ω matched component.

The 10M7D-crystal filter from STC frequency technology was chosen. According to the datasheets, this filter has a center frequency of 10.7MHz , a small 3dB pass band of $\pm 3.75\text{kHz}$, an excellent selectivity at the adjacent channel ($\pm 12.5\text{kHz}$) of 90dB , a ripple of 2dB and a loss of 4dB . The filter was matched to 50Ω to complete the component and measured on the network

analyzer. The final crystal IF filter component was measured on the HP8562A spectrum analyzer and on the network analyzer. The results are shown below.

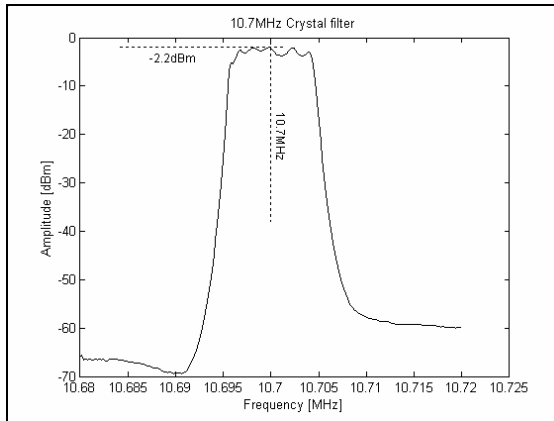


Figure 4-79 Measured amplitude response of the crystal IF filter (spectrum analyzer).

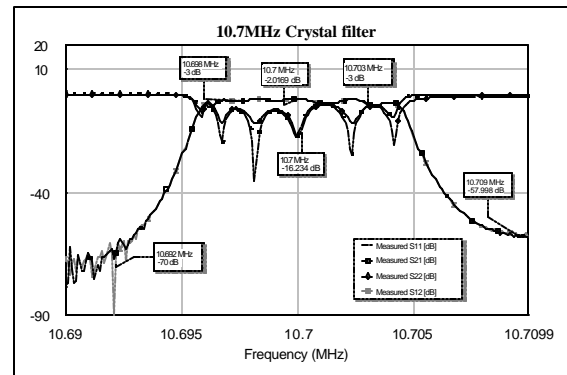


Figure 4-80 Measured s-parameters of the crystal IF filter (network analyzer).

The selectivity was not as good as expected. This will influence the adjacent channel rejection requirement directly. It is probably caused by the coupling between the input and output connector on the IF filter component and does not mean that the filter itself does not meet the specifications on the datasheets. The coupling problem will most probably be solved if strip line is used.

4.4.2. b Ceramic filter

Ceramic filters are made of high stability piezoelectric ceramics that function as resonators. The frequency is primarily adjusted by the size and thickness of the ceramic element. These filters typically have a lower Q than a crystal filter.

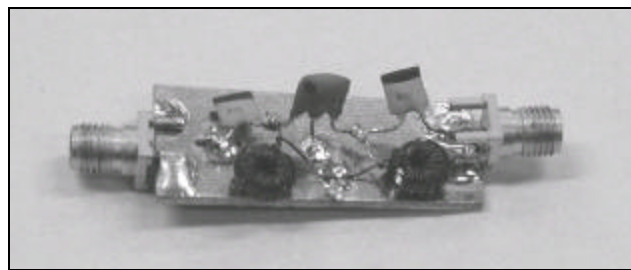


Figure 4-81 Photo of the ceramic filter, 50Ω matched component.

The SFELA10M7FALL-B0 from the Cerafil range for FM receivers from Murata Manufacturing Co., Ltd. was chosen. According to the datasheets the expected center frequency of this filter is $10.7\text{MHz} \pm 30\text{kHz}$, it has a 3dB pass band of $280\text{kHz} \pm 50\text{kHz}$, and a minimum attenuation of 25dB

can be expected as well as a loss of $7\text{dB} \pm 2\text{dB}$ in the pass band. The measured results are given in *Figure 4-82*.

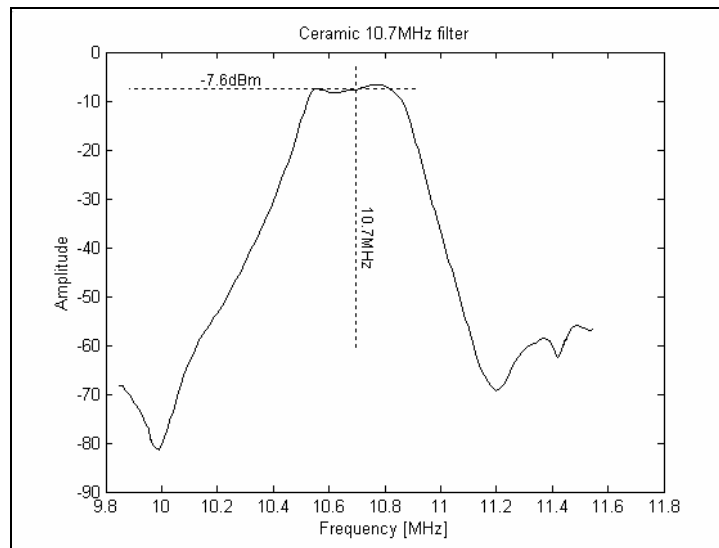


Figure 4-82 Measured *s*-parameters of the ceramic IF filter.

The filter performed very close to what was predicted by the datasheets, with a pass band of 300kHz , a loss in the pass band of 7.7dB and with a filter attenuation bigger as the expected 25dB . The pass band of this filter is much wider than that of the crystal filter. The selectivity will probably not be good enough to satisfy the requirement for the adjacent channel rejection.

4.4.2. c Conclusion

From the measured results the IF filter components built, proved to work reasonably well although they might not meet the specification for the adjacent channel rejection. Fortunately, the adjacent channel rejection depends on other parameters as was discussed in 2.1.1. bi. The influence of these two filters and their performance on the receiver system's characteristics will be evaluated in the next section.

4.4.3. Injection filter

The injection filter attenuates wideband AM noise around the LO frequency and its harmonics. This filter may improve the sensitivity of the system depending on the LO output power and spurious responses, as well as on the input power needed for the LO mixer port. Two injection filters were designed and the influence of their presence and their characteristics on the system's performance are tested in chapter 5 [1].

4.4.3. a Filter design and measurements

A third order Butterworth and a third order Chebyshev filter with maximum 0.5dB ripple in the pass band, both with a center frequency of 39.3MHz were designed.

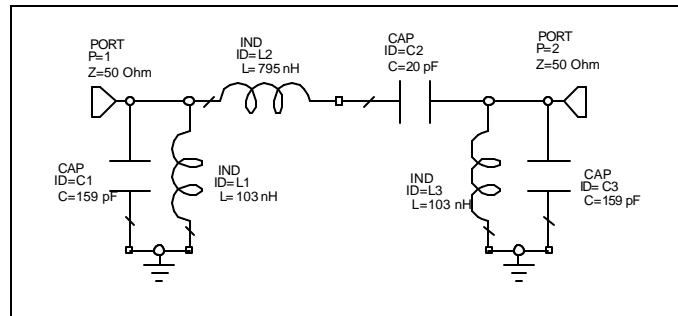


Figure 4-83 The third order Butterworth band pass filter. Center frequency of $f_0 = 39.3\text{MHz}$.

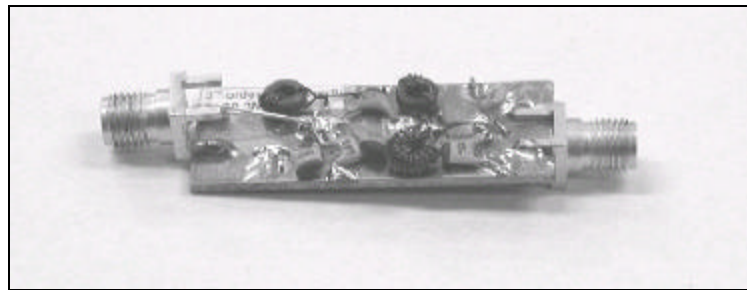


Figure 4-84 Photo of the third order Butterworth band pass filter component with a center frequency of $f_0 = 39.3\text{MHz}$.

The Butterworth filter was designed to be a third order filter with a 3dB pass band of approximately 20MHz. The loss in the pass band is expected to be practically zero as can be seen in the simulated results in *Figure 4-85*, while the filter is matched well between 33MHz and 47MHz with $|s_{11}| \& |s_{22}| < -10\text{dB}$. The measured filter results, shown in *Figure 4-86*, reveal that the filter in reality has practically no loss in the pass band and a good impedance match.



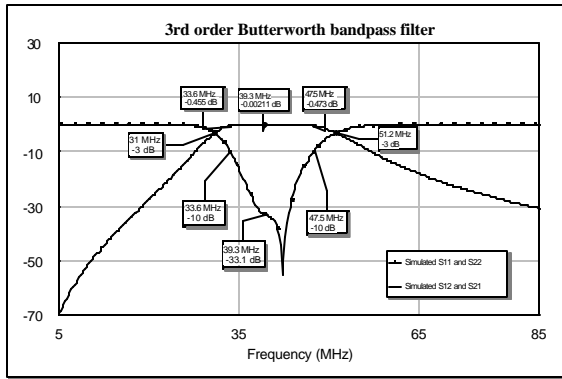


Figure 4-85 Simulated s-parameters of the third order Butterworth band pass filter component with a center frequency of $f_0 = 39.3\text{MHz}$.

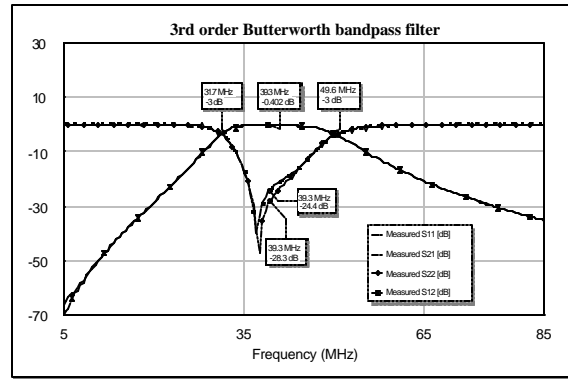


Figure 4-86 Measured s-parameters of the third order Butterworth band pass filter component with a center frequency of $f_0 = 39.3\text{MHz}$.

The fifth order Chebyshev filter was designed to have a maximum of 0.5dB ripple in the 3dB pass band (approximately 20MHz). The circuit diagram of the designed filter and the photo of the filter component are shown in *Figure 4-87* and *Figure 4-88* respectively.

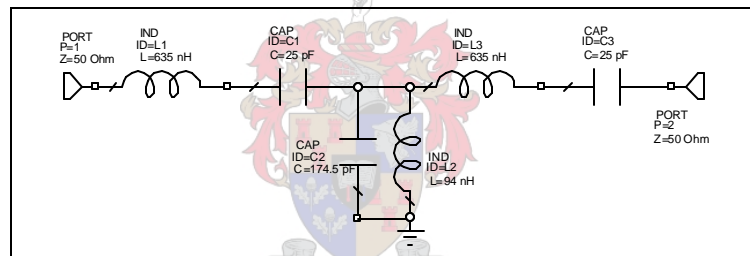


Figure 4-87 Circuit diagram of the third order Chebyshev band pass filter component with a center frequency of $f_0 = 39.3\text{MHz}$.

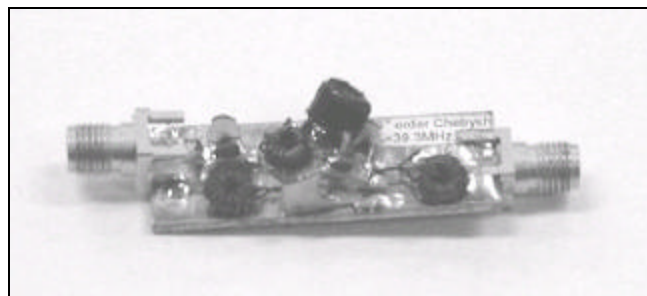


Figure 4-88 Photo of the third order Chebyshev band pass filter component with a center frequency of $f_0 = 39.3\text{MHz}$.

The simulated and measured results are shown in *Figure 4-89* and *Figure 4-90*. There is practically no loss in the pass band, the component is well matched and has a broad pass band.



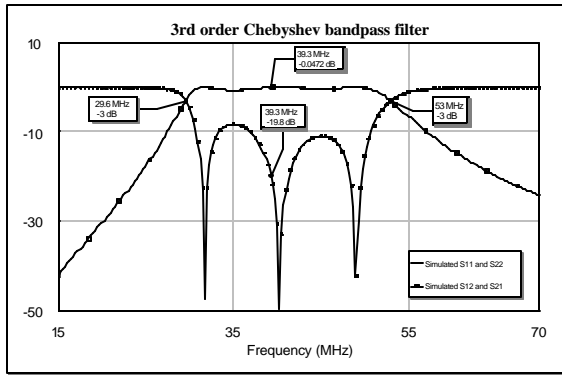


Figure 4-89 Simulated s-parameters of the third order Chebyshev band pass filter component with a center frequency of $f_0 = 39.3\text{MHz}$.

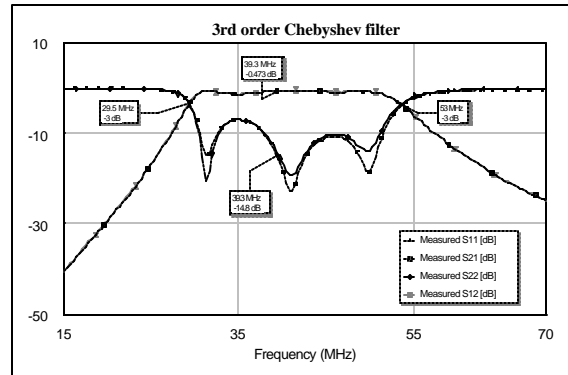


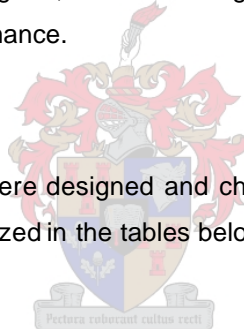
Figure 4-90 Measured s-parameters of the third order Chebyshev band pass filter component with a center frequency of $f_0 = 39.3\text{MHz}$.

4.4.3. b Conclusion

The two injection filters that were designed, meet the design specifications and are expected to improve the receiver system’s performance.

4.4.4. Conclusion

The most important receiver filters were designed and characterized in this section. Their most important characteristics are summarized in the tables below.



Front-end filter	Gain [dB]	Noise figure [dB]	Bandwidth [MHz]	Gain at image [dB]	Noise figure at image [dB]
3 rd order Butterworth filter	-0.5	0.5	13	-33	33
5 th order Chebyshev filter	-1.5	1.5	18	-65	65
Simple LC filter	-1.22	1.2	6	-10	10

Table 4-16 Summary of the measured parameters of the designed front-end filters.

IF filter	Gain [dB]	Noise figure [dB]	Selectivity at adjacent channel [dB]	Bandwidth [kHz]
Crystal filter	-2	2	65	7.5
Ceramic filter	-7.7	7.7	0.1	300

Table 4-17 Summary of the measured parameters of the IF filters.



Injection filter	Gain [dB]	Noise figure [dB]	Attenuation at $f_{LO} \pm f_{IF}$ [dB]	Attenuation at $2f_{LO} \pm f_{IF}$ [dB]	Attenuation at $3f_{LO} \pm f_{IF}$ [dB]
3 rd order Butterworth filter	-0.4	0.4	0.8 (+) 5.65 (-)	36 (+) 23 (-)	50
3 rd order Chebyshev filter	-0.5	0.5	3.4 (+) 9.9 (-)	23 (+) 37 (-)	45

Table 4-18 Summary of the measured characteristics of the two injection filters.

The audio modules will be discussed in the next section as shown in *Figure 4-91*.

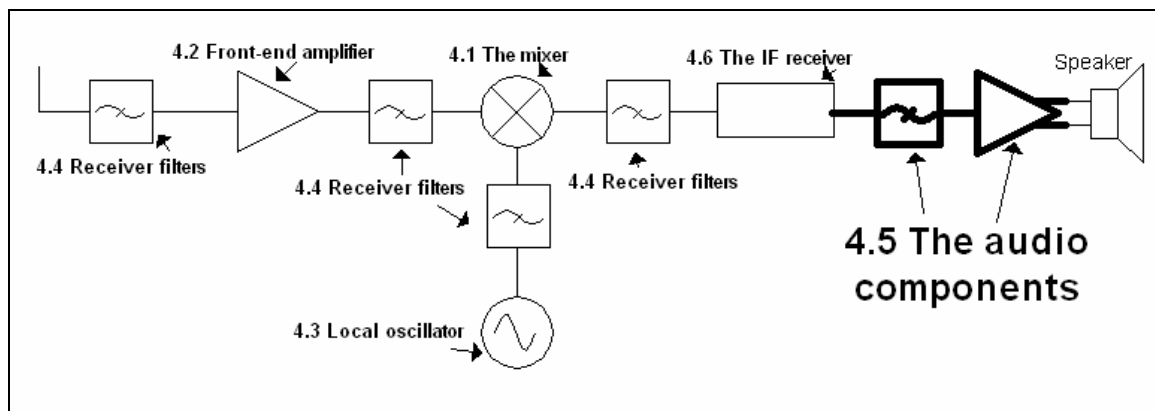


Figure 4-91 Structure of chapter 4: 4.5 The audio components.

4.5 The audio components

4.5.1. The audio filter

The audio filter is usually a 300Hz-3kHz band pass filter, implemented with active filter technology. The advantage of using active filters at low frequencies is that inductors are not required, which can be rather bulky and difficult to attain. Another advantage is that they can have a gain instead of a loss. The function of this filter is to limit the frequency band, to reject out of band audio signals e.g. power supply hum, interference and the IF noise that originates in the receiver after the first IF filter. It is expected that this filter will improve the sensitivity of the receiver [1] [8] [48].

4.5.1. a Design and measurements

A two-pole low pass Butterworth active filter as well as a two-pole high pass Butterworth active filter were designed and connected in series to form an audio filter as shown in *Figure 4-92* [48 p856-858] [66]. The simulated and measured response of this filter is compared in *Figure 4-93*.



The AF response specification is a 6dB bandwidth of 300Hz to 2.7kHz. This specification is clearly met by the designed filter.

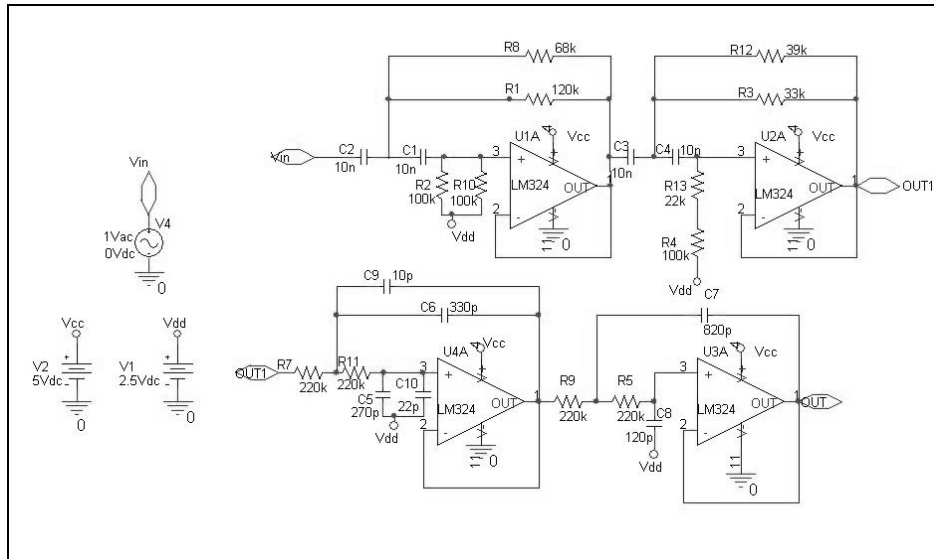


Figure 4-92 Circuit diagram: active audio filter circuit component.

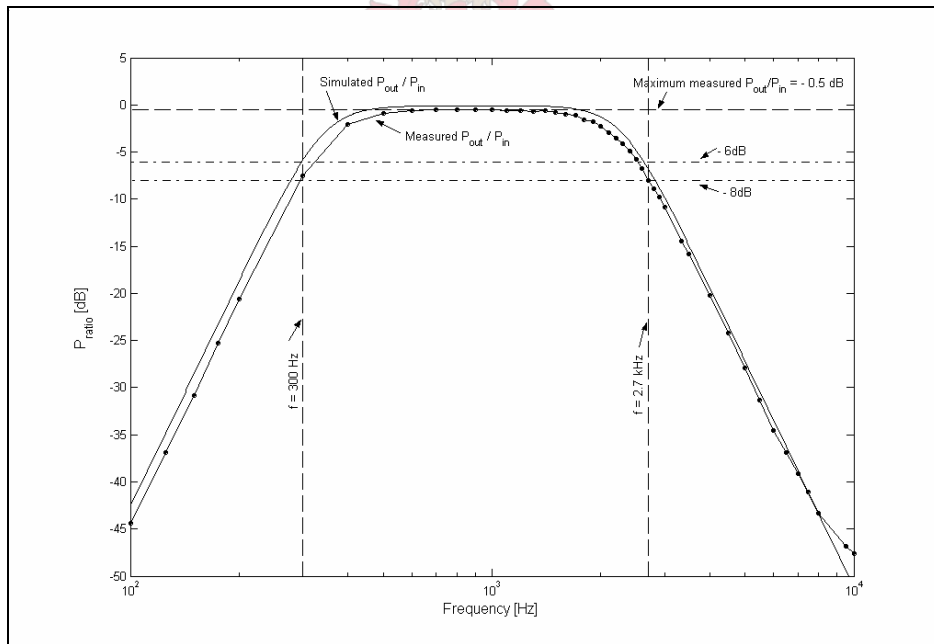


Figure 4-93 Comparison between the simulated and measured power ratio of the active audio amplifier.

If this filter is used at the output of the IF receiver, the sensitivity would be much improved. The filter draws little current and performs well.



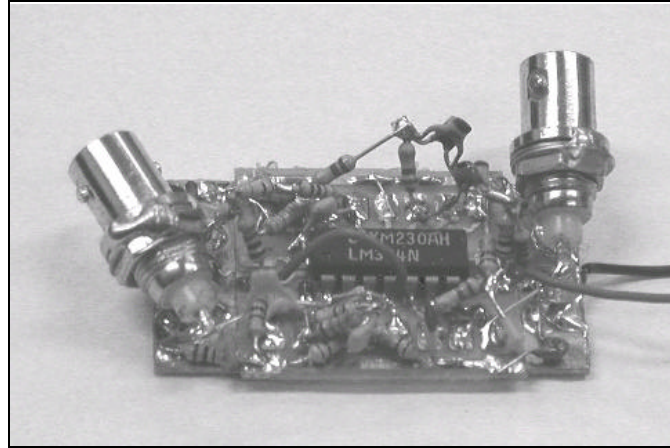


Figure 4-94 The designed audio filter component.

4.5.1. b Conclusion

The audio filter that was designed ought to improve the system's performance and meets the original design specifications given in *Table 1-1*.

4.5.2. Audio amplifier

Audio amplifiers are the building blocks that will amplify the small-demodulated received signal to a signal with practical amplitude. These building blocks should be able to deliver audio power into a load without generating significant distortion, overheating or using a lot of current. This section will focus on the designed audio amplifier that was built [66].

4.5.2. a Building and measuring the audio amplifier IC

A vast number of audio amplifier IC's are available on the market. Some of the IC's that were considered are summarized in *Table 4-19*.

Model	Manufacturer	P _{out} Max [W]	DC voltage [V]	Distortion 8Ω load	BW	DC current [mA]	Comments
NJM386	JRC	0.325	4-12	0.2% P _o =125mW V=6V	300kHz	3	• Ideal for battery operation
TDA7052	Philips	1.2	3-18	0.2% P _o =100mW V=6V	20Hz-20kHz	4	• No external components
LM388	National Semiconductor	1.5	4-12	0.1% P _o =0.5W V=12V	300kHz	16	
TBA820M	Unison Technologies	1.2	3-14	0.3% P _o =0.5W 9V	20Hz-20kHz	4	• Class B amplifier
LM380	National Semiconductor	2.5	8-22	0.2% P _o =2W	100kHz	7	• Output protected against short circuits
NJM2073	JRC	1.2	1.8-15	0.2%	130kHz	6	



				Po=0.5W 0.1% Po=0.5W			
TDA8552	Philips	1.4	5			14	<ul style="list-style-type: none"> • Digital volume control
MC34119	Motorola	0.150	2-16	0.5%	1.5MHz	2.7	<ul style="list-style-type: none"> • Chip disable input
SM2211	Analog Devices	1	2.7-5.5	0.2% TDH @ 1W	4MHz	9.5	<ul style="list-style-type: none"> • Shutdown mode
MAX4295	MAXIM	1.2	2.7-5.5		1.25MHz	2.8	<ul style="list-style-type: none"> • Class D amplifier • 87% efficient
MAX4297	MAXIM	1.2	2.7-5.5		1.25MHz	4.6	<ul style="list-style-type: none"> • Class D amplifier • 87% efficient
NCP2890	ON Semiconductor	1	2.2-5.5	0.02% TDH @ 1W	10Hz- 20kHz	1.90	<ul style="list-style-type: none"> • Small DC current • Few external components • Shutdown mode

Table 4-19 Summary of some of the available audio amplifiers that was investigated.

The NCP2890 audio amplifier IC from ON Semiconductor was chosen, because of its low DC current, low distortion and shutdown mode. This audio amplifier is specifically designed for portable applications and can deliver 1W of continuous average power into an 8Ω load. The gain of this amplifier can be controlled externally with resistors. The circuit diagram is shown in *Figure 4-95*.

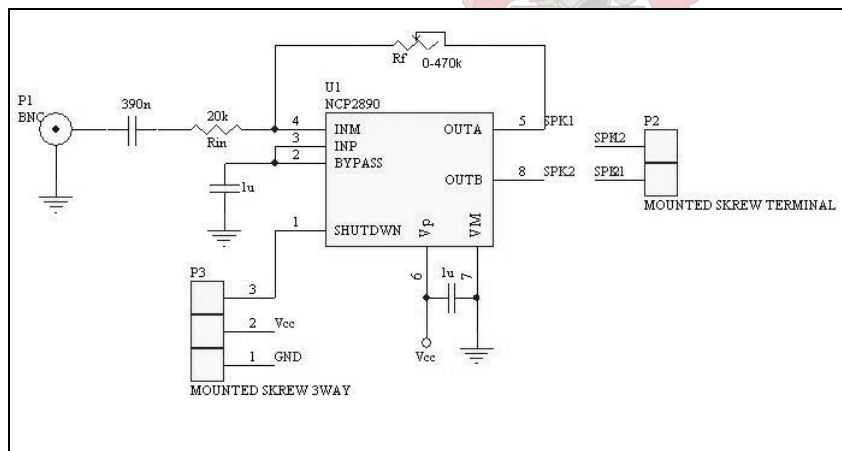


Figure 4-95 Circuit diagram of the NCP2890 audio amplifier component.

The differential gain of this amplifier circuit is given by

$$G = 2 \frac{R_f}{R_{in}} \quad (4.14)$$

Thus the maximum gain of this circuit, when the potentiometer is at its maximum, is 47. This is enough to amplify the 180mV_{pp} output of the SA605 IF receiver to 8V_{pp} over an 8Ω speaker load, which is 1W of average, output power. The gain of the amplifier was measured and delivered a

maximum of 1W of continuous output power to the speaker with ease. The volume can be controlled by varying the potentiometer. A photo of the audio amplifier component is shown in *Figure 4-96*.

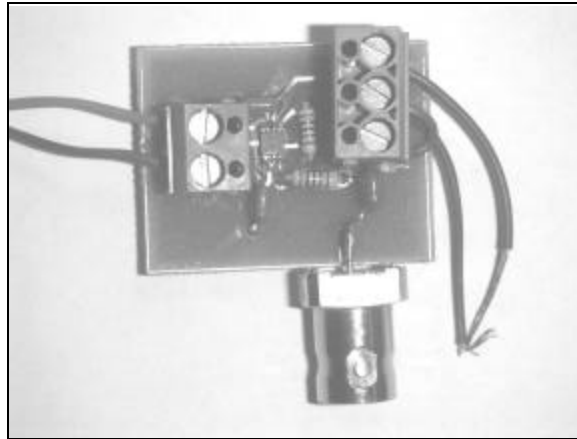


Figure 4-96 Photo of the NCP2890 audio amplifier component that was designed.

4.5.2. b Conclusion

The specifications given in *Table 1-1*, state that the receiver should be able to deliver an output power greater than 200mW into an 8Ω load. This specification is met by this audio amplifier, which can deliver up to 1W into an 8Ω load. The volume control is specified to be at least 6 stepped volumes. This specification is also met, because the audio amplifier's volume can be varied continuously. The audio amplifier component that was built performed well.



The IF receiver system will be discussed in the next section as shown in *Figure 4-97*.

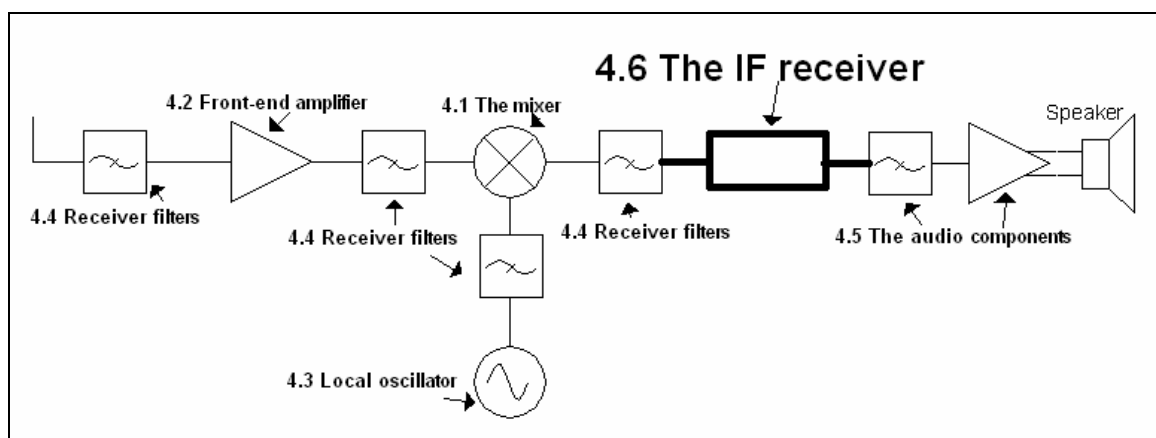


Figure 4-97 Structure of chapter 4: 4.6 IF receiver system design.



4.6 IF receiver system design

The IF receiver system, which consists of all the second IF circuitry and the demodulator is very likely to be contained in an integrated circuit (IC). Important characteristics of this IF receiver system IC includes: [1]

- Noise figure
- Intercept point
- Amplitude limiting properties
- Signal-to-noise ratio at the input required for a specific base band performance e.g. 20dB SINAD

This section discusses the design and measurements of this very important component in the receiver chain.

4.6.1. Design considerations

The SA605 from Philips semiconductors is a FM receiver system IC that combines the SA602 mixer and onboard oscillator and the IF amplifiers and quadrature detector of the SA604 into one chip. This FM receiver system can be used to receive and demodulate the second IF in a super heterodyne receiver, or it can be used as a single conversion receiver. It also has low current consumption, which makes it attractive for portable receiver systems. The system can handle input signals up to 500MHz, has $\pm 102\text{dB}$ IF limiter and amplifier gain and has a low mixer noise figure of 5dB. According to the datasheets, an excellent sensitivity of 0.22mV into a 50Ω matching network can be achieved (-120dBm) for a output signal with a SINAD of 12dB . Thus, it is estimated that this IF receiver system should be able to meet the overall receiver system's sensitivity specification, given in *Table 1-1* as -113dBm for an output signal with a SINAD of 20dB .

This IF receiver circuit receives the filtered down-converted 10.7MHz signal. It then mixes this signal down to the second IF frequency, which is 455kHz, and then filters, amplifies and demodulates the signal. The circuit diagram of the SA605 circuit is shown in *Figure 4-99*.

This filtering is done by the CFULA455KF4A-B0 ceramic filter, from the Murata's Cerafil range for communications equipment. According to the datasheets, this filter has a center frequency of $455\text{kHz} \pm 1.5\text{kHz}$, a 6dB pass band of $\pm 7.5\text{kHz}$, a minimum stop band attenuation of 27dB , a maximum loss of 6dB and a input and output impedance of $1.5\text{k}\Omega$. The output of the mixer is internally loaded with a $1.5\text{k}\Omega$ resistor, and the input resistance of the IF amplifier and limiter is $1.5\text{k}\Omega$. Thus matching to these filters is not necessary [63] [64].

The detailed design description of the SA605 is discussed in Appendix C.



The SA605 includes a received signal strength indicator (RSSI) pin, which will reveal if any instability is present. This reading should be less than $250mV$ if the device is biased and no signal is fed into it. A reading higher than $250mV$ on the RSSI output pin indicates a regeneration problem, due to poor lay out or too much gain in the IF component. Too much IF gain may cause instability.

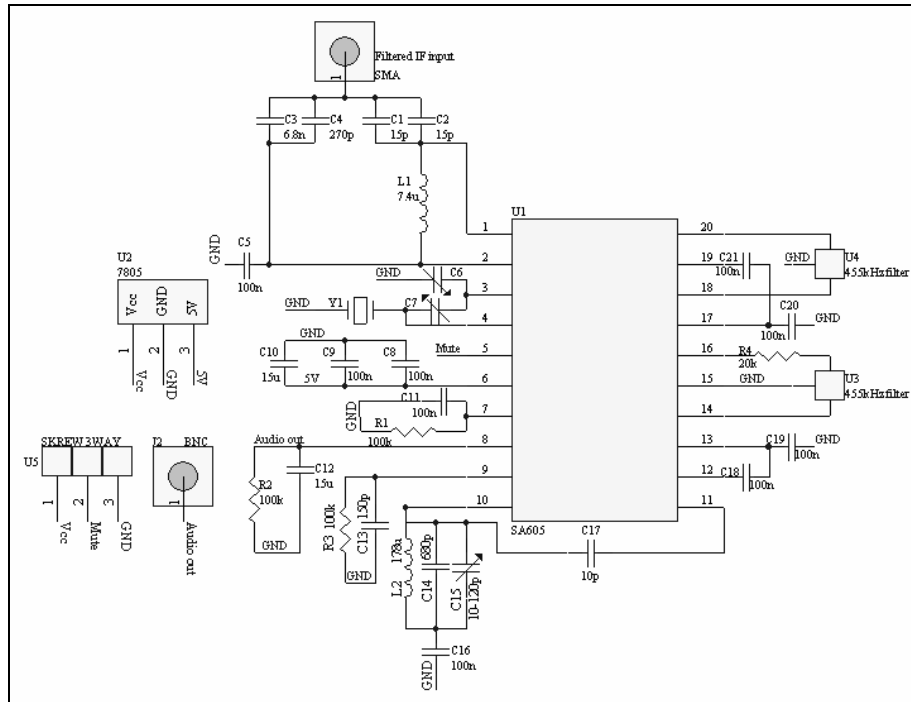


Figure 4-98 Circuit diagram of the SA605 IF receiver system that was designed.

A photo of the designed IF receiver component is shown in *Figure 4-99*. The measurements done on this designed IF receiver component are discussed next.

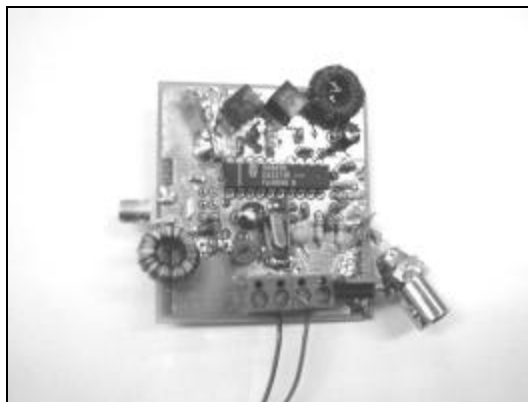


Figure 4-99 SA605 IF receiver circuit that was designed and built.

4.6.2. Measurements

◆ Capture ratio

The capture ratio is the IF signal-to-noise ratio at the detector input required to meet a certain base band specification. In this instance, the specification is a SINAD of $20dB$. The measurement set-up to measure the minimum signal-to-noise ratio at the IF receiver input is shown in *Figure 4-100*.

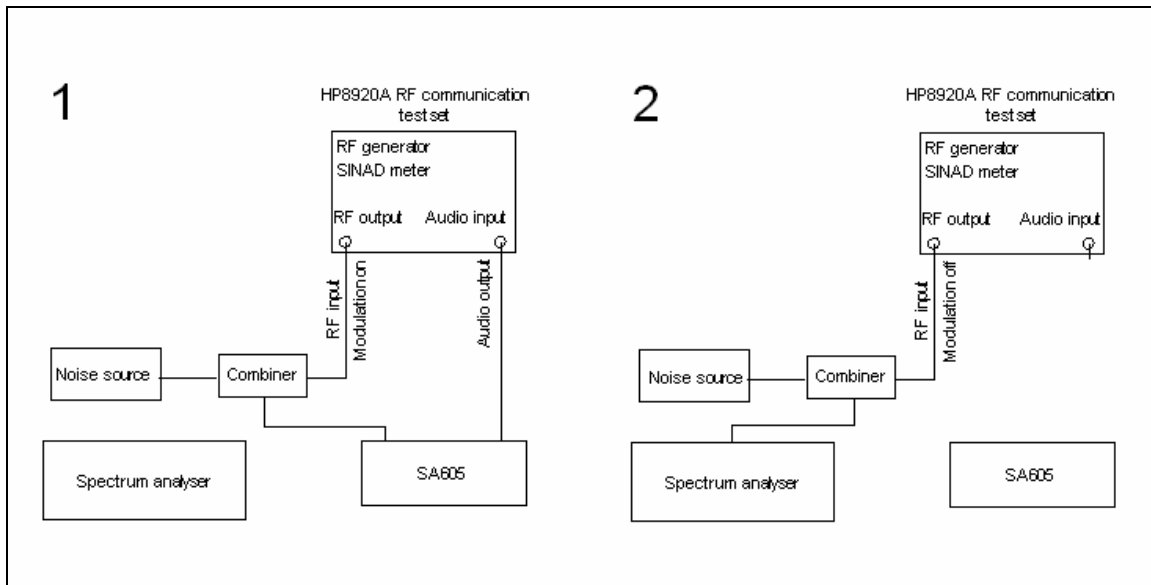


Figure 4-100 The two measurement set-ups necessary to measure the capture ratio.

To measure the minimum IF signal-to-noise ratio, a noise source was used to generate noise. The measured noise floor of the coming out of the combiner is $\pm -102dBm$. The noise source increased the noise floor to $-82dBm$. This is shown in *Figure 4-101*.

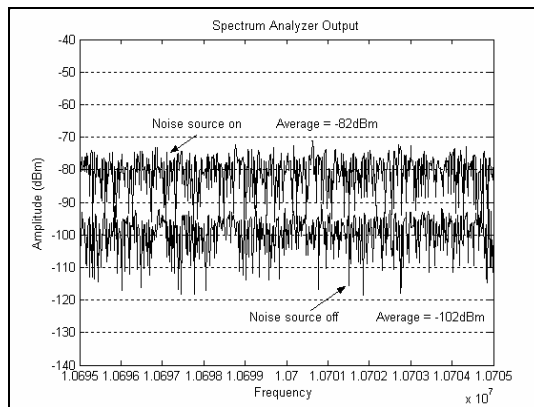


Figure 4-101 The noise floor at the output of the combiner with the noise source switched on and off

The noise signal together with the desired signal was inserted into a combiner and fed into the IF receiver. The SINAD of the receiver output signal was measured with the HP8920A RF communication test set from Hewlett Packard. The 10.7MHz input signal's power was decreased to the minimum point that could receive a 20dB SINAD signal.

Next the IF receiver was disconnected and the modulation on the IF signal was switched off. The output of the combiner was fed into the spectrum analyzer to determine the smallest signal-to-noise ratio that would still meet the 20dB SINAD specification. This is shown in *Figure 4-102* and *Figure 4-103*.

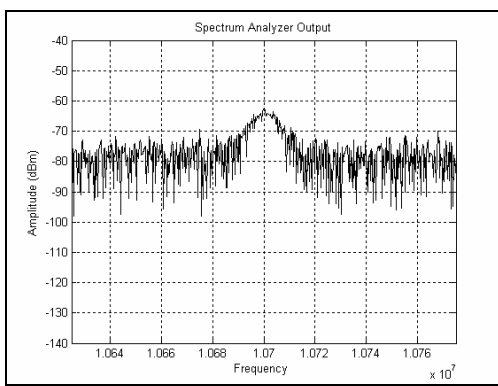


Figure 4-102 The minimum signal-to-noise ratio at the IF receiver input for a deviation of $\pm 1.5\text{kHz}$ and with 10kHz resolution bandwidth.

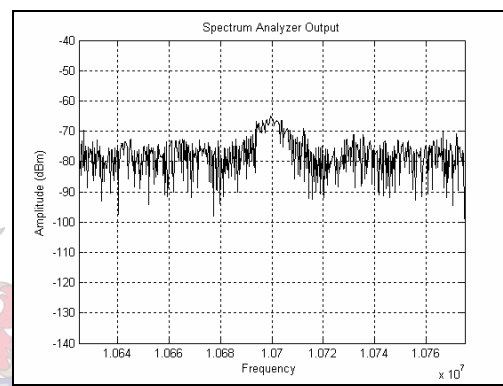


Figure 4-103 The minimum signal-to-noise ratio at the IF receiver input for a deviation of $\pm 2.5\text{kHz}$ and with 10kHz resolution bandwidth.

It is important to note that the resolution bandwidth of the spectrum analyzer must be set to 7.5kHz , which is the noise bandwidth of the system, to achieve correct results. The resolution bandwidth of the HP8562A spectrum analyzer can however only be set on 3kHz or 10kHz . Therefore, the signal-to-noise ratio was measured per 10kHz and then the signal-to-noise ratio per 7.5kHz was estimated by adding 1.25dB (multiplying with 1.33 because $7.5\text{kHz} \times 1.33 = 10\text{kHz}$)

If the IF signal has a deviation of 60% of the maximum permissible frequency deviation ($\pm 1.5\text{kHz}$), the minimum signal-to-noise ratio is $17\text{dB} + 1.25\text{dB} = 18.25\text{dB}$ for a noise bandwidth of 7.5kHz . For an IF signal with 100% frequency deviation ($\pm 2.5\text{kHz}$) the minimum signal-to-noise ratio is $14\text{dB} + 1.25\text{dB} = 15.25\text{dB}$ for a noise bandwidth of 7.5kHz .



◆ **S-Curve**

If the Q of the quad tank is too high for the deviation, distortion will be caused. A too low Q will cause low audio levels.

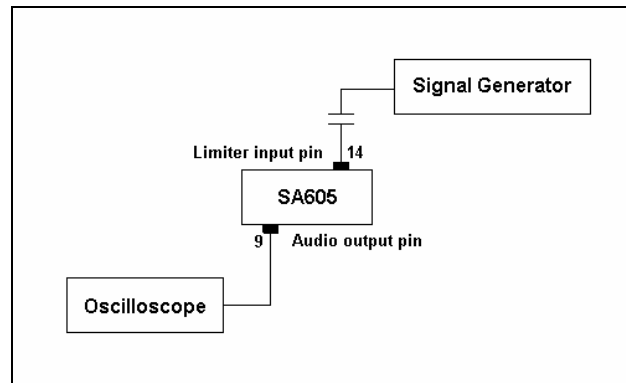


Figure 4-104 Quadrature tank measurement set-up.

The set-up to measure the quad tank of the IF receiver system is shown in *Figure 4-104*. A signal generator is connected to the input of the limiter through a DC blocking capacitor. While the modulation is turned off, the output DC voltage at the audio pin is measured, for increasing frequency. The s-curve is plotted and shown in *Figure 4-105*. The s-curve is centered around 455kHz and has a linear range of $\pm 15\text{kHz}$. The overall linearity determines how much deviation is possible before distortion will occur. Thus, the demodulator will be able to demodulate a signal with a deviation of $\pm 15\text{kHz}$ before distortion will occur.

The application requires a deviation of $\pm 3\text{kHz}$, therefore, the s-curve is satisfactory, because its linearity exceeds $452 - 458\text{kHz}$.



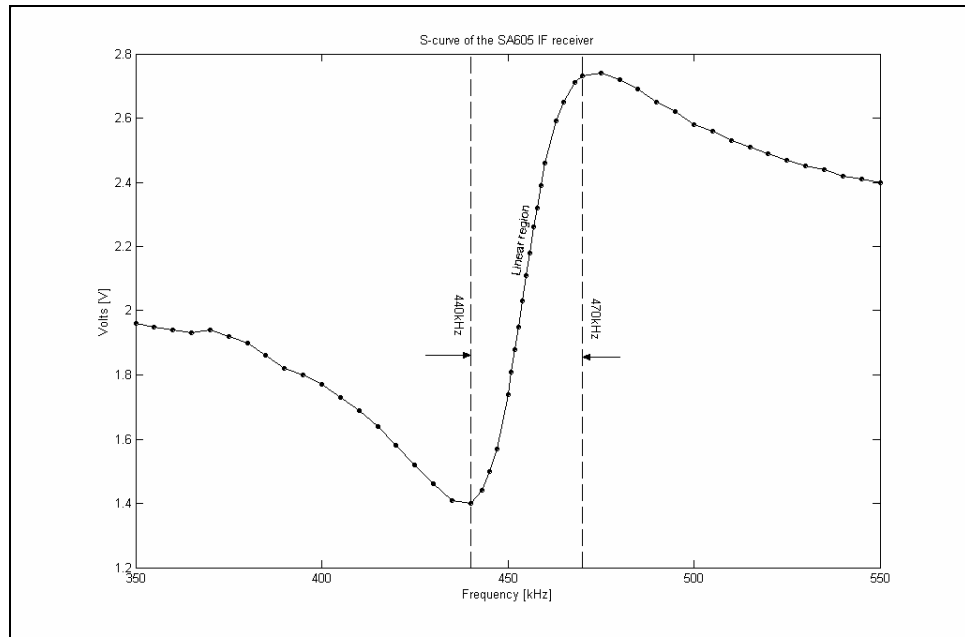


Figure 4-105 Measured quad tank s-curve of the IF receiver.

◆ **RSSI indicator**

The reading on the RSSI pin was $95mV$ if the device is biased and no signal is fed into the device. This reading should be less than $250mV$. Thus, no instability is present.

A $180mV_{pp}$ output signal was measured at the output of the SA605, until the RF input power, drops below the maximum sensitivity level.

4.6.3. Conclusion

This IF receiver system works performed well and will be used in the receiver system to receive the first IF, mix it down to the second IF, amplify and demodulate the signal.

4.7 Conclusion

The individual components were investigated, chosen, designed and built. Theory was used to select appropriate measurement methods, and each separate component was measured, characterized and compared to others. These developed components will be used in receiver measurements in the next chapter. They will be substituted with each other to enable system performance comparison.



5 Measurements of receiver systems

5.1 Introduction

In this chapter, the correct methods to measure the receiver characteristics as described in chapter 2 are discussed. The receiver performance was measured while interchanging the different well-defined receiver components that were discussed in the chapter 4. The influence of every component on the receiver characteristics is confirmed in section 5.3 and is similar to the theory summarized in *Table 2-1* and *Table 2-2*. These proposed measurements and comparisons are summarized in *Figure 5-1*.

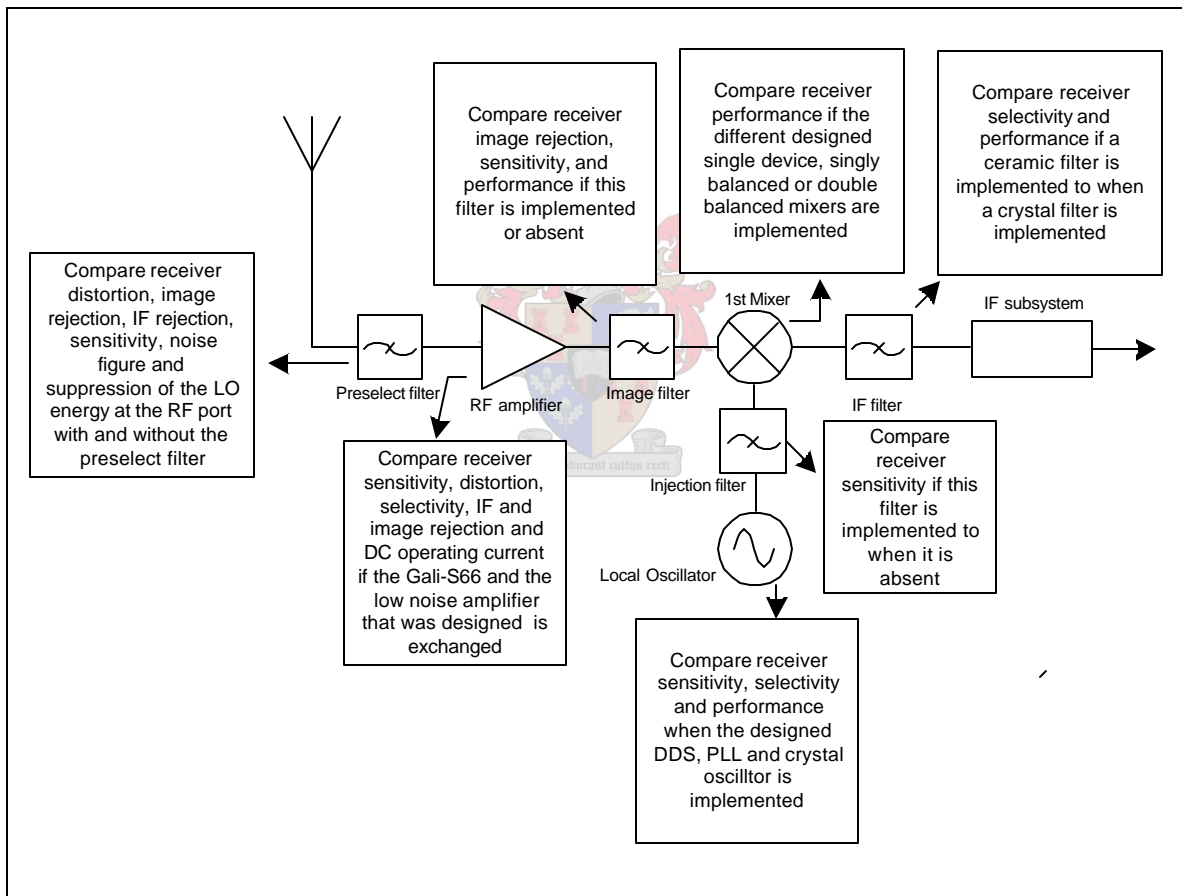


Figure 5-1 Summary of the proposed receiver measurements and comparisons.

A summary of the different receiver component options, which will be interchanged, is given in *Table 5-1*. These well-defined components, that were designed, enable comparison between the different receiver characteristics and the characteristics of these components. These results will be used in section 5.4 to verify the results attained using **ReceiverCALC^{1.1}**.



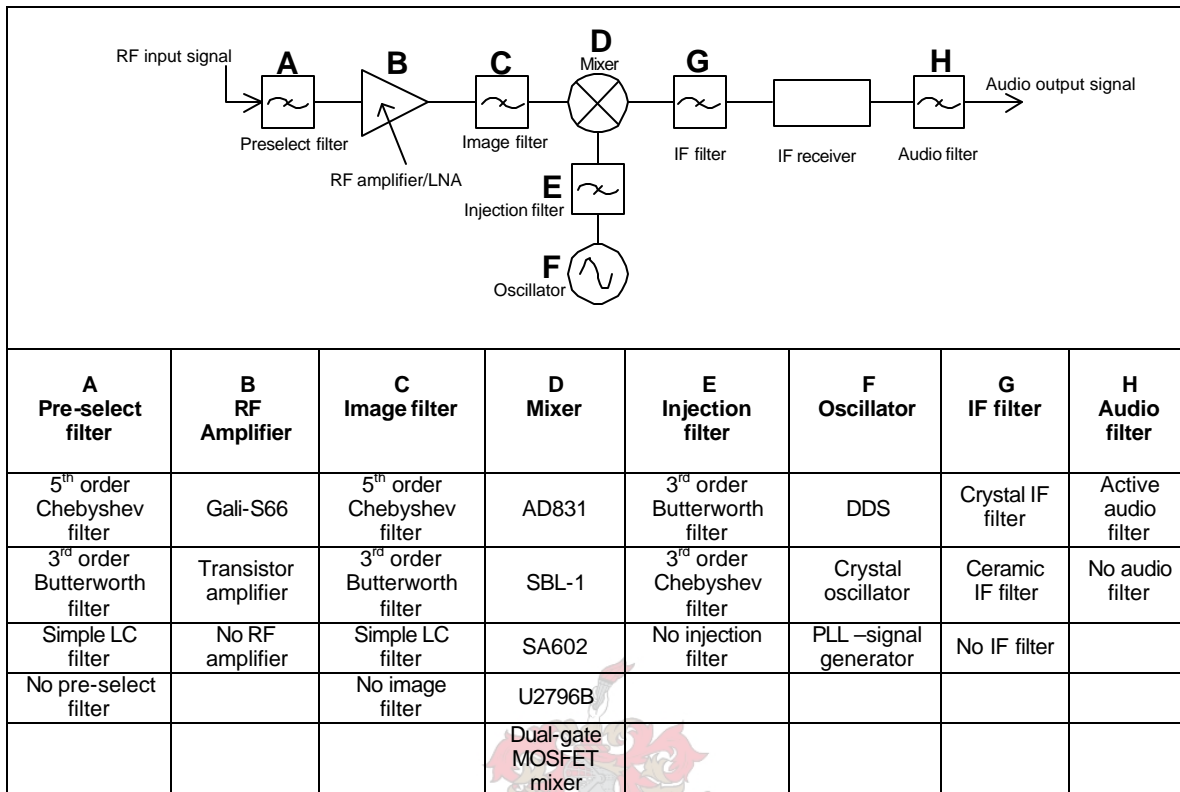


Table 5-1 Summary of the different receiver component options.

5.2 Measurement of radio specifications

The various measurement methods of the receiver characteristics that were discussed and defined in section 2.1.1 are described in this section. Measurement results are also given. Documents describing the technical characteristics and measurement methods of receivers from the European Telecommunications Standards Institute (ETSI) [ETSI EN 300 086-1 V1.2.1, March 2001], the Communications Division of the Ministry of Commerce, New Zealand [RFS26, Issue 2, ISBN:0-478-00470-0, October 1993], the Telecommunications Authority Hong Kong (HTKA) [HKTA1002 Issue 04, September 2002], as well as the Info-Communications Development Authority of Singapore (IDA) [IDA TS101, Issue 1 Rev 4, December 1999] were used. Their specification limitations on receiver characteristics are summarized and compared to the receiver specifications given in Table 5-2 [5-7] [59].

Radio characteristics	ETSI [6]	New Zealand [7]	HTKA [5]	IDA [59]	Specifications [Table 1-1]
Sensitivity	< 6dBmV for 20dB SINAD (< -100dBm for 50Ω load)	< -107dBm for 20dB SINAD	< 6dBmV for a 20dB SINAD (< -100dBm for 50Ω load)	< 0.5mV for a 12dB SINAD (< -113dBm for 50Ω load)	< 0.5mV for a 20dB SINAD (< -113dBm for 50Ω load)
Co-channel rejection ratio	0 –12dB	< 12dB	*NS	*NS	*NS
Adjacent channel rejection ratio	> 60dB	> 70dB	> 60dB	> 60dB	> 70dB
Spurious response rejection ratio	> 70dB	> 70dB	> 70dB	> 70dB	> 70dB
Desensitization	> 84dB	> 84dB	> 78dB	*NS	*NS
Spurious radiations	< -57 dBm	< -47 dBm	< 20nW (< -47 dBm)	< 20nW (< -47 dBm)	*NS

*NS - Not specified

Table 5-2 Receiver characteristic specifications limits.

5.2.1. Sensitivity

5.2.1. a Measurement procedure

To measure the sensitivity of a receiver, a test signal at the receiver frequency with a known test modulation is applied to the input of the receiver. The European Telecommunications Standards Institute [ETSI EN 300 086-1 V1.2.1, March 2001], the Communications Division of the Ministry of Commerce, New Zealand [RFS26, Issue 2, ISBN:0-478-00470-0, October 1993], and the Telecommunications Authority Hong Kong [HKTA1002 Issue 04, September 2002] all agree that a normal test modulation frequency is 1kHz and the frequency deviation is 60% of the maximum permissible deviation [6] [7] [5].

This application requires a channel spacing of 12.5kHz and therefore the maximum permissible frequency deviation according to the above stated documents is ±2.5kHz. Thus, a signal with a modulation of 1kHz and a frequency deviation of ±1.5kHz, which is 60% of ±2.5kHz is applied to the input of the receiver. The test signal input power is reduced until a SINAD ratio of 20dB is reached. The input power level at this point is the value of the maximum sensitivity. The measurements were only done under normal circumstances for the purposes of this project [6] [7] [5].



The HP8920A RF communication test set from Hewlett Packard, shown in *Figure 5-2*, was used to do this measurement. This test set includes a frequency generator that will generate the signal at the nominal test frequency and an audio analyzer that can measure the SINAD of the audio output of the receiver. This set-up is shown below in *Figure 5-3*. The audio filters of the HP8920A RF communication test set was set as wide as possible during measurements.



Figure 5-2 The HP8920A RF communication test set of Hewlett Packard.

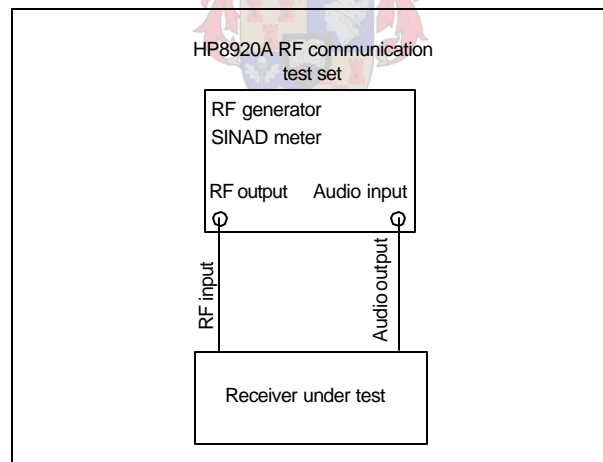


Figure 5-3 Set-up for measuring the receiver sensitivity.

5.2.1. b Measurements

Receiver systems were assembled, by combining the different well-defined components, summarized and shown in *Table 5-1*. The importance and function of every component and the restriction that it places on the receiver system's sensitivity performance were now measured. This was done by assembling various combinations of the components and measuring the sensitivity as defined in 5.2.1. a. The results of these measurements follow in *Table 5-3*.

No	A Pre-select filter	B RF amplifier	C Image filter	D Mixer	E Injection filter	F Local oscillator	G IF filter	H Audio filter	Measured Sensitivity	
									$\pm 1.5 \text{ kHz}$	$\pm 2.5 \text{ kHz}$
1	5 th order chebyshev	Transistor amplifier	No filter	U2796B	No filter	PLL	Crystal filter	Active filter	-108	-114
2	5 th order chebyshev	Transistor amplifier	3 rd order butterworth	U2796B	No filter	PLL	Crystal filter	Active filter	-107	-113
3	5 th order chebyshev	Transistor amplifier	3 rd order butterworth	U2796B	3 rd order butterworth	PLL	Crystal filter	Active filter	-107	-113
4	5 th order chebyshev	Transistor amplifier	3 rd order butterworth	U2796B	3 rd order butterworth	PLL	Crystal filter	No filter	-28	-39
5	No filter	Transistor amplifier	3 rd order butterworth	U2796B	3 rd order butterworth	PLL	Crystal filter	Active filter	-110	-116
6	No filter	Transistor amplifier	5 th order chebyshev	U2796B	3 rd order butterworth	PLL	Crystal filter	Active filter	-111	-117
7	3 rd order butterworth	Transistor amplifier	5 th order chebyshev	U2796B	3 rd order butterworth	PLL	Crystal filter	Active filter	-107	-113
8	3 rd order butterworth	Transistor amplifier	5 th order chebyshev	AD831	3 rd order butterworth	PLL	Crystal filter	Active filter	-102	-115
9	No filter	Transistor amplifier	5 th order chebyshev	AD831	3 rd order butterworth	PLL	Crystal filter	Active filter	-108	-120
10	No filter	Transistor amplifier	No filter	AD831	3 rd order butterworth	PLL	Crystal filter	Active filter	-109	-120
11	5 th order chebyshev	Transistor amplifier	No filter	AD831	3 rd order butterworth	PLL	Crystal filter	Active filter	-102	-114
12	No filter	Gali-S66	5 th order chebyshev	AD831	3 rd order butterworth	PLL	Crystal filter	Active filter	-114	-121
13	3 rd order butterworth	Gali-S66	5 th order chebyshev	AD831	3 rd order butterworth	PLL	Crystal filter	Active filter	-107	-115
14	Simple LC filter	Gali-S66	5 th order chebyshev	AD831	3 rd order butterworth	PLL	Crystal filter	Active filter	-105	-113
15	No filter	Gali-S66	5 th order chebyshev	U2796B	3 rd order butterworth	PLL	Crystal filter	Active filter	-114	-119
16	No filter	Gali-S66	5 th order chebyshev	SA602	3 rd order butterworth	PLL	Crystal filter	Active filter	-116	-120
17	No filter	Gali-S66	5 th order chebyshev	Dual gate Mosfet mixer	3 rd order butterworth	PLL	Crystal filter	Active filter	-108	-103
18	No filter	Gali-S66	5 th order chebyshev	SA602	3 rd order Chebyshev and 9dB attenuator	DDS	Crystal filter	Active filter	-100	-101
19	No filter	Gali-S66	5 th order chebyshev	SA602	3 rd order butterworth and 9dB attenuator	DDS	Crystal filter	Active filter	-113	-117
20	No filter	Gali-S66	No filter	SA602	No filter	PLL	Crystal filter	Active filter	-116	-120
21	No filter	Gali-S66	3 rd order butterworth	SA602	No filter	PLL	Crystal filter	Active filter	-117	-122
22	3 rd order butterworth	Gali-S66	5 th order chebyshev	SA602	No filter	PLL	Crystal filter	Active filter	-116	-120
23	3 rd order butterworth	Gali-S66	5 th order chebyshev	SA602	No filter	PLL	Crystal filter	No filter	-20	-21

24	3 rd order butterworth	Gali-S66	5 th order chebyshev	SA602	No filter	PLL	No filter	Active filter	-116	-119
25	3 rd order butterworth	Gali-S66	5 th order chebyshev	SBL-1	No filter	PLL	Crystal filter	Active filter	-112	-116
26	No filter	Gali-S66	3 rd order butterworth	SBL-1	No filter	PLL	Crystal filter	Active filter	-114	-119
27	No filter	Gali-S66	No filter	SBL-1	No filter	PLL	Crystal filter	Active filter	-113	-118
28	3 rd order butterworth	Gali-S66	No filter	SBL-1	No filter	PLL	Crystal filter	Active filter	-107	-103
29	No filter	Transistor amplifier	3 rd order butterworth	SBL-1	No filter	PLL	Crystal filter	Active filter	-109	-112
30	No filter	Gali-S66	5 th order chebyshev	U2796B	3 rd order Chebyshev	PLL	Crystal filter	Active filter	-116	-121
31	No filter	Gali-S66	5 th order chebyshev	U2796B	3 rd order Chebyshev	DDS	Crystal filter	Active filter	-105	-110
32	3 rd order butterworth	Gali-S66	5 th order chebyshev	U2796B	3 rd order Chebyshev	DDS	Crystal filter	Active filter	-102	-107
33	3 rd order butterworth	Gali-S66	5 th order chebyshev	SA602	3 rd order Chebyshev	DDS	Crystal filter	Active filter	-107	-113
34	3 rd order butterworth	Gali-S66	5 th order chebyshev	SA602	3 rd order Chebyshev and 6dB attenuator	Crystal oscillator	Crystal filter	Active filter	-117	-121
35	No filter	Gali-S66	5 th order chebyshev	SA602	3 rd order Chebyshev and 6dB attenuator	Crystal oscillator	Crystal filter	Active filter	-118	-122
36	No filter	Gali-S66	5 th order chebyshev	SA602	3 rd order Chebyshev and 6dB attenuator	Crystal oscillator	Ceramic filter	Active filter	-117	-121
38	No filter	Gali-S66	5 th order chebyshev	SA602	No filter	Crystal oscillator	Crystal filter	Active filter	-116	-121
39	No filter	Gali-S66	5 th order chebyshev	U2796B	3 rd order Chebyshev and 6dB attenuator	Crystal oscillator	Crystal filter	Active filter	-117	-118
40	No filter	Gali-S66	5 th order chebyshev	U2796B	No filter	Crystal oscillator	Crystal filter	Active filter	-118	-119
41	No filter	Gali-S66	5 th order chebyshev	Dual gate MOSFET	3 rd order Chebyshev and 6dB attenuator	Crystal oscillator	Crystal filter	Active filter	-89	-100
42	No filter	Gali-S66	5 th order chebyshev	Dual gate MOSFET	3 rd order Chebyshev	Crystal oscillator	Crystal filter	Active filter	-96	-100
43	No filter	Gali-S66	5 th order chebyshev	AD831	3 rd order Chebyshev	Crystal oscillator	Crystal filter	Active filter	-114	-122
44	No filter	Gali-S66	5 th order chebyshev	AD831	3 rd order Chebyshev	DDS	Crystal filter	Active filter	-116	-121
45	No filter	Gali-S66	5 th order chebyshev	AD831	No filter	DDS	Crystal filter	Active filter	-100	-110
46	No filter	Gali-S66	5 th order chebyshev	AD831	3 rd order butterworth	DDS	Crystal filter	Active filter	-115	-121

Table 5-3 Sensitivity measurement results for different receiver component combinations.

5.2.1. c Conclusion

The original sensitivity specification of -113dBm was met by a number of the combinations and was even exceeded by some. The influence of the different components on receiver sensitivity can clearly be seen. Of particular interest is the degrading influence of an attenuator before the first RF amplifier. It is interesting to note that none of the combinations in which the transistor amplifier is implemented meet the -113dBm sensitivity specification. The influence of every component on receiver sensitivity is discussed in 5.3. The different combinations and their sensitivity, measured with a deviation of $\pm 1.5\text{kHz}$, are compared in *Figure 5-4*. (See *Table 5-3*)

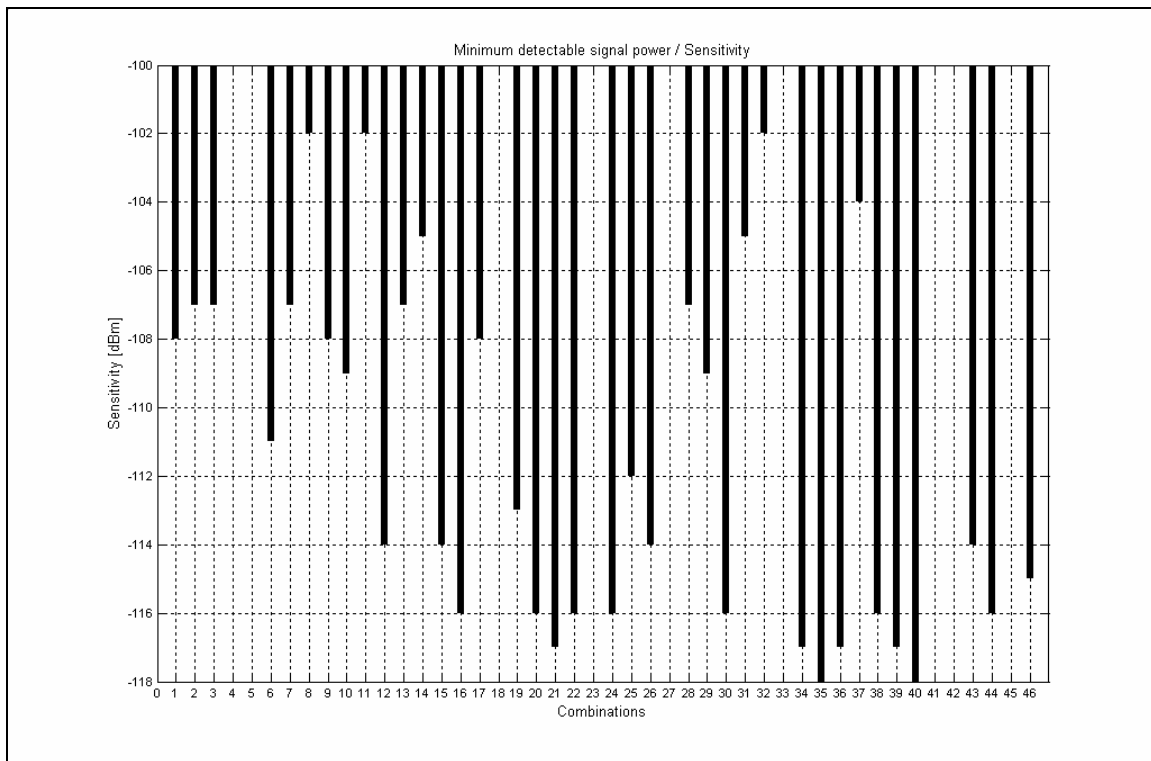


Figure 5-4 Sensitivity measurements summarized for every measured combination.

The sensitivity of the measurements with a deviation of $\pm 1.5\text{kHz}$ (60% of the maximum permissible frequency deviation) is less than the sensitivity of the measurements with the maximum permissible frequency deviation ($\pm 2.5\text{kHz}$). This is expected because more power is applied to the input of the receiver if a signal with a greater frequency deviation is used.



5.2.2. Adjacent channel rejection / Selectivity

5.2.2. a Measurement procedure

To measure the adjacent channel rejection of a receiver, two signal generators are used, as well as a SINAD meter at the receiver output. These signals, one at the adjacent channel above the desired frequency and one at the desired frequency, are connected to the receiver input through a combiner. The desired signal is modulated with a frequency of $1kHz$ and 60% of the maximum permissible frequency deviation. With the unwanted signal generator switched off, the amplitude of the desired signal generator is adjusted until a $20dB$ SINAD is achieved. The unwanted signal generator is switched on and modulated with 60% of the maximum permissible frequency deviation at $400Hz$. The amplitude level of this unwanted signal generator is increased until the SINAD reading at the output of the receiver is reduced to $14dB$. This $6dB$ reduction in the SINAD ratio of the output sinusoidal signal indicates that the signal quality has been halved [33] [5-7] [59].

The adjacent channel selectivity is the ratio in dB of the level of the unwanted test signal, to the level of the wanted test signal at the receiver input [5-7] [59].

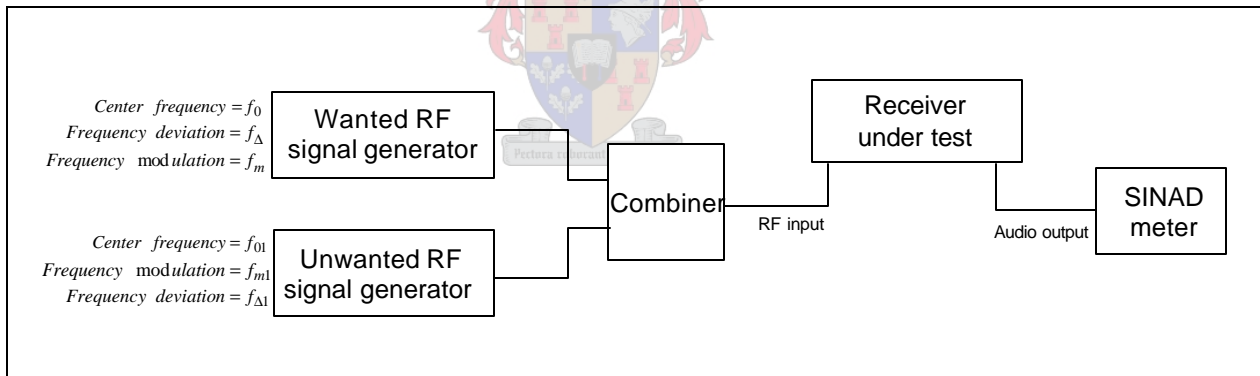


Figure 5-5 Measurement set-up for measuring the desensitization, adjacent channel, co-channel and spurious response - rejection ratio of the receiver.

This measurement should be repeated with the unwanted test signal frequency at the adjacent channel below the desired frequency. The two ratios can be documented as the upper and lower adjacent channel rejection or the smallest of the two measured ratios can be documented as the adjacent channel rejection [5-7] [59].

As previously stated, this application requires a channel spacing of $12.5kHz$ and therefore has a maximum permissible frequency deviation of $\pm 2.5kHz$. This was tested under normal circumstances only.



5.2.2. b Measurements

The role that every component plays in the receiver system's adjacent channel selectivity performance was now measured. This was done by assembling various combinations of the components and measuring the adjacent channel selectivity as defined in the 5.2.2. a. A receiver system was formed, by combining the different well-defined components already built, as summarized and shown in *Table 5-1*. The measured adjacent channel selectivity for every receiver combination is given in *Table 5-4*. The lowest value of the upper and lower adjacent channel selectivity ratio that was measured was taken as the adjacent channel selectivity of the specific receiver system. This is specified in *Table 1-1* and *Table 5-2* and should be greater than 70dB . The results that meet the specifications are accentuated.

No	A Pre-select filter	B RF amplifier	C Image filter	D Mixer	E Injection filter	F Local oscillator	G IF filter	H Audio filter	Selectivity
1	5 th order chebyshev	Transistor amplifier	No filter	U2796B	No filter	PLL	Crystal filter	Active filter	66
2	5 th order chebyshev	Transistor amplifier	3 rd order butterworth	U2796B	No filter	PLL	Crystal filter	Active filter	66
3	5 th order chebyshev	Transistor amplifier	3 rd order butterworth	U2796B	3 rd order butterworth	PLL	Crystal filter	Active filter	61
5	No filter	Transistor amplifier	3 rd order butterworth	U2796B	3 rd order butterworth	PLL	Crystal filter	Active filter	60
6	No filter	Transistor amplifier	5 th order chebyshev	U2796B	3 rd order butterworth	PLL	Crystal filter	Active filter	64
7	3 rd order butterworth	Transistor amplifier	5 th order chebyshev	U2796B	3 rd order butterworth	PLL	Crystal filter	Active filter	62
8	3 rd order butterworth	Transistor amplifier	5 th order chebyshev	AD831	3 rd order butterworth	PLL	Crystal filter	Active filter	57
9	No filter	Transistor amplifier	5 th order chebyshev	AD831	3 rd order butterworth	PLL	Crystal filter	Active filter	57
10	No filter	Transistor amplifier	No filter	AD831	3 rd order butterworth	PLL	Crystal filter	Active filter	57
11	5 th order chebyshev	Transistor amplifier	No filter	AD831	3 rd order butterworth	PLL	Crystal filter	Active filter	57
12	No filter	Gali-S66	5 th order chebyshev	AD831	3 rd order butterworth	PLL	Crystal filter	Active filter	60
13	3 rd order butterworth	Gali-S66	5 th order chebyshev	AD831	3 rd order butterworth	PLL	Crystal filter	Active filter	57
14	Simple LC filter	Gali-S66	5 th order chebyshev	AD831	3 rd order butterworth	PLL	Crystal filter	Active filter	56
15	No filter	Gali-S66	5 th order chebyshev	U2796B	3 rd order butterworth	PLL	Crystal filter	Active filter	58
16	No filter	Gali-S66	5 th order chebyshev	SA602	3 rd order butterworth	PLL	Crystal filter	Active filter	53



17	No filter	Gali-S66	5 th order chebyshev	Dual gate Mosfet mixer	3 rd order butterworth	PLL	Crystal filter	Active filter	41
18	No filter	Gali-S66	5 th order chebyshev	SA602	3 rd order Chebyshev and 9dB attenuator	DDS	Crystal filter	Active filter	59
19	No filter	Gali-S66	5 th order chebyshev	SA602	3 rd order butterworth and 9dB attenuator	DDS	Crystal filter	Active filter	56
20	No filter	Gali-S66	No filter	SA602	No filter	PLL	Crystal filter	Active filter	61
21	No filter	Gali-S66	3 rd order butterworth	SA602	No filter	PLL	Crystal filter	Active filter	60
22	3 rd order butterworth	Gali-S66	5 th order chebyshev	SA602	No filter	PLL	Crystal filter	Active filter	61
24	3 rd order butterworth	Gali-S66	5 th order chebyshev	SA602	No filter	PLL	No filter	Active filter	5
25	3 rd order butterworth	Gali-S66	5 th order chebyshev	SBL-1	No filter	PLL	Crystal filter	Active filter	70
26	No filter	Gali-S66	3 rd order butterworth	SBL-1	No filter	PLL	Crystal filter	Active filter	70
27	No filter	Gali-S66	No filter	SBL-1	No filter	PLL	Crystal filter	Active filter	67
28	3 rd order butterworth	Gali-S66	No filter	SBL-1	No filter	PLL	Crystal filter	Active filter	70
29	No filter	Transistor amplifier	3 rd order butterworth	SBL-1	No filter	PLL	Crystal filter	Active filter	67
30	No filter	Gali-S66	5 th order chebyshev	U2796B	3 rd order Chebyshev	PLL	Crystal filter	Active filter	64
31	No filter	Gali-S66	5 th order chebyshev	U2796B	3 rd order Chebyshev	DDS	Crystal filter	Active filter	59
32	3 rd order butterworth	Gali-S66	5 th order chebyshev	U2796B	3 rd order Chebyshev	DDS	Crystal filter	Active filter	59
33	3 rd order butterworth	Gali-S66	5 th order chebyshev	SA602	3 rd order Chebyshev	DDS	Crystal filter	Active filter	73
34	3 rd order butterworth	Gali-S66	5 th order chebyshev	SA602	3 rd order Chebyshev and 6dB attenuator	Crystal oscillator	Crystal filter	Active filter	65
35	No filter	Gali-S66	5 th order chebyshev	SA602	3 rd order Chebyshev and 6dB attenuator	Crystal oscillator	Crystal filter	Active filter	65
36	No filter	Gali-S66	5 th order chebyshev	SA602	3 rd order Chebyshev and 6dB attenuator	Crystal oscillator	Ceramic filter	Active filter	4
37	No filter	Gali-S66	5 th order chebyshev	SA602	3 rd order butterworth and 6dB attenuator	Crystal oscillator	Crystal filter	Active filter	61
38	No filter	Gali-S66	5 th order chebyshev	SA602	No filter	Crystal oscillator	Crystal filter	Active filter	65



39	No filter	Gali-S66	5 th order chebyshev	U2796B	3 rd order Chebyshev and 6dB attenuator	Crystal oscillator	Crystal filter	Active filter	67
40	No filter	Gali-S66	5 th order chebyshev	U2796B	No filter	Crystal oscillator	Crystal filter	Active filter	53
42	No filter	Gali-S66	5 th order chebyshev	Dual gate MOSFET	3 rd order Chebyshev	Crystal oscillator	Crystal filter	Active filter	73
43	No filter	Gali-S66	5 th order chebyshev	AD831	3 rd order Chebyshev	Crystal oscillator	Crystal filter	Active filter	70
44	No filter	Gali-S66	5 th order chebyshev	AD831	3 rd order Chebyshev	DDS	Crystal filter	Active filter	58
45	No filter	Gali-S66	5 th order chebyshev	AD831	No filter	DDS	Crystal filter	Active filter	70
46	No filter	Gali-S66	5 th order chebyshev	AD831	3 rd order butterworth	DDS	Crystal filter	Active filter	63

Table 5-4 Adjacent channel rejection for different receiver component combinations.

5.2.2. c Conclusion

The selectivity results of the different combinations are clearly influenced the most by the specifications of the IF filter. The influence of every receiver component on the selectivity is discussed in the section 5.3.

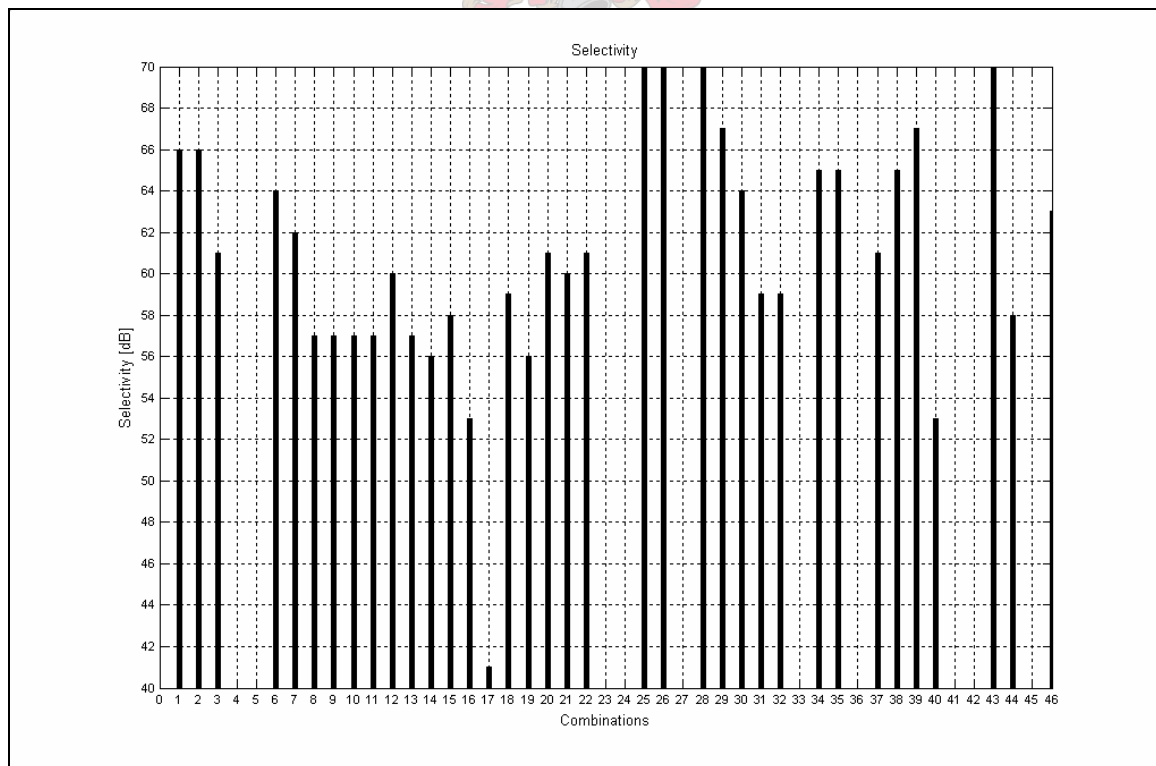


Figure 5-6 Selectivity results summarized for the different combinations.

5.2.3. Spurious response rejection

5.2.3. a Measurement procedure

The measurement set-up to measure the spurious response rejection ratio of the receiver is shown in *Figure 5-5*. A wanted signal modulated with $1kHz$ ($f_{\Delta} = \pm 1.5kHz$) and an unwanted test signal modulated with $400Hz$ are inserted into the receiver.

With the unwanted signal generator first switched off, the amplitude of the desired test signal at the receiver frequency, f_0 , is set on the level which will give a $20dB$ SINAD reading at the output of the receiver.

Next, the frequency of all the spurious responses is recorded by varying the frequency of the unwanted test signal over the frequency range from $100kHz$ to $2GHz$, with incremental steps of $5kHz$, as specified by the European Telecommunications Standards Institute [ETSI EN 300 086-1 V1.2.1, March 2001]. The unwanted test signal has a deviation of $\pm 5kHz$ and a signal level of $86dBmV$ ($-21dBm$ into a 50Ω load) [5-7].

After all the spurious response frequencies are recorded, the unwanted test signal deviation should be changed to 60% of the maximum permissible frequency deviation ($f_{\Delta 1} = \pm 1.5kHz$). The center frequency of the unwanted RF signal generator is set at each frequency where a spurious response occurred. For every frequency, the input level of the unwanted signal will be increased until a $6dB$ reduction in SINAD level of the output signal occurs [5-7].

The specific spurious response rejection ratio is expressed as the ratio in dB between the level of the unwanted and wanted test signal at the input of the receiver. This is specified in *Table 1-1* and *Table 5-2* and should be greater than $70dB$ [7] [59].



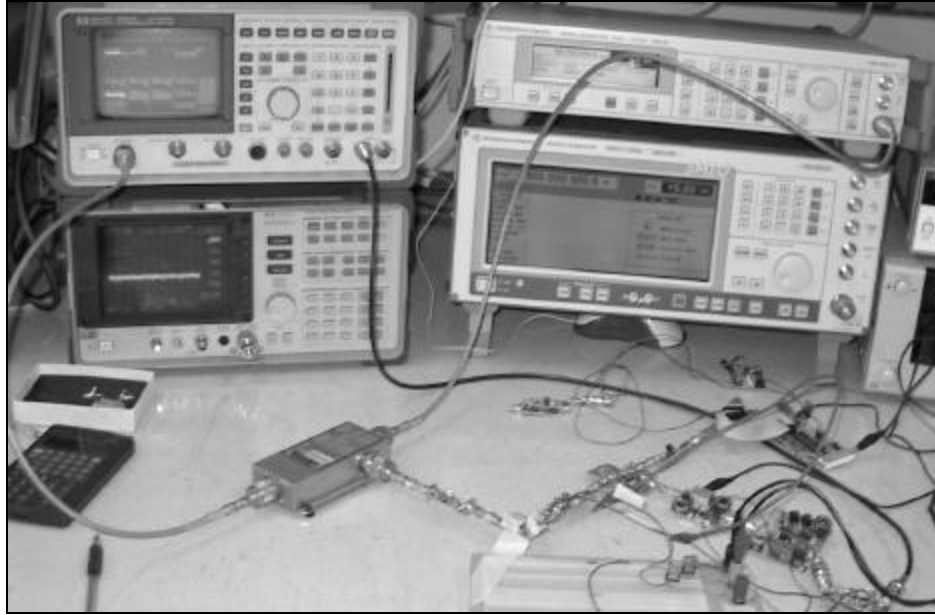


Figure 5-7 Image rejection ratio measurements in progress.

5.2.3. b Measurements

The image rejection ratio and the IF rejection ratio are specifically specified in *Table 1-1*. Therefore, these spurious responses are measured for every combination in this section. A general spurious response measurement was not done. Because of its length and complexity, it would have been difficult to do this measurement for all the combinations.

i. Image rejection

As summarized and shown in *Table 5-1*, a receiver system was formed, by combining the different well-defined components already built and measured in the previous chapter. The measured image for every receiver combination is given in *Table 5-5* beneath. The image rejection should be greater than $70dB$ and the results that meet this specification are accentuated.

Several of the measured receiver combinations meet the image rejection ratio specification. This rejection ratio is dependent mostly on the front-end and its filters. The effect of every component on this ratio will be discussed in detail in section 5.3.



No	A Pre-select filter	B RF amplifier	C Image filter	D Mixer	E Injection filter	F Local oscillator	G IF filter	H Audio filter	Image rejection [dB]
1	5 th order chebyshev	Transistor amplifier	No filter	U2796B	No filter	PLL	Crystal filter	Active filter	75
2	5 th order chebyshev	Transistor amplifier	3 rd order butterworth	U2796B	No filter	PLL	Crystal filter	Active filter	97
3	5 th order chebyshev	Transistor amplifier	3 rd order butterworth	U2796B	3 rd order butterworth	PLL	Crystal filter	Active filter	89
5	No filter	Transistor amplifier	3 rd order butterworth	U2796B	3 rd order butterworth	PLL	Crystal filter	Active filter	32
6	No filter	Transistor amplifier	5 th order chebyshev	U2796B	3 rd order butterworth	PLL	Crystal filter	Active filter	72
7	3 rd order butterworth	Transistor amplifier	5 th order chebyshev	U2796B	3 rd order butterworth	PLL	Crystal filter	Active filter	98
8	3 rd order butterworth	Transistor amplifier	5 th order chebyshev	AD831	3 rd order butterworth	PLL	Crystal filter	Active filter	>92
9	No filter	Transistor amplifier	5 th order chebyshev	AD831	3 rd order butterworth	PLL	Crystal filter	Active filter	63
10	No filter	Transistor amplifier	No filter	AD831	3 rd order butterworth	PLL	Crystal filter	Active filter	2
11	5 th order chebyshev	Transistor amplifier	No filter	AD831	3 rd order butterworth	PLL	Crystal filter	Active filter	71
12	No filter	Gali-S66	5 th order chebyshev	AD831	3 rd order butterworth	PLL	Crystal filter	Active filter	50
13	3 rd order butterworth	Gali-S66	5 th order chebyshev	AD831	3 rd order butterworth	PLL	Crystal filter	Active filter	82
14	Simple LC filter	Gali-S66	5 th order chebyshev	AD831	3 rd order butterworth	PLL	Crystal filter	Active filter	64
15	No filter	Gali-S66	5 th order chebyshev	U2796B	3 rd order butterworth	PLL	Crystal filter	Active filter	57
16	No filter	Gali-S66	5 th order chebyshev	SA602	3 rd order butterworth	PLL	Crystal filter	Active filter	82
17	No filter	Gali-S66	5 th order chebyshev	Dual gate Mosfet mixer	3 rd order butterworth	PLL	Crystal filter	Active filter	38
18	No filter	Gali-S66	5 th order chebyshev	SA602	3 rd order Chebyshev and 9dB attenuator	DDS	Crystal filter	Active filter	83
19	No filter	Gali-S66	5 th order chebyshev	SA602	3 rd order butterworth and 9dB attenuator	DDS	Crystal filter	Active filter	84
20	No filter	Gali-S66	No filter	SA602	No filter	PLL	Crystal filter	Active filter	20
21	No filter	Gali-S66	3 rd order butterworth	SA602	No filter	PLL	Crystal filter	Active filter	28
22	3 rd order butterworth	Gali-S66	5 th order chebyshev	SA602	No filter	PLL	Crystal filter	Active filter	94
24	3 rd order butterworth	Gali-S66	5 th order chebyshev	SA602	No filter	PLL	No filter	Active filter	94
25	3 rd order butterworth	Gali-S66	5 th order chebyshev	SBL-1	No filter	PLL	Crystal filter	Active filter	85
26	No filter	Gali-S66	3 rd order butterworth	SBL-1	No filter	PLL	Crystal filter	Active filter	26



27	No filter	Gali-S66	No filter	SBL-1	No filter	PLL	Crystal filter	Active filter	No
28	3 rd order butterworth	Gali-S66	No filter	SBL-1	No filter	PLL	Crystal filter	Active filter	22
29	No filter	Transistor amplifier	3 rd order butterworth	SBL-1	No filter	PLL	Crystal filter	Active filter	36
30	No filter	Gali-S66	5 th order chebyshev	U2796B	3 rd order Chebyshev	PLL	Crystal filter	Active filter	58
31	No filter	Gali-S66	5 th order chebyshev	U2796B	3 rd order Chebyshev	DDS	Crystal filter	Active filter	62
32	3 rd order butterworth	Gali-S66	5 th order chebyshev	U2796B	3 rd order Chebyshev	DDS	Crystal filter	Active filter	84
33	3 rd order butterworth	Gali-S66	5 th order chebyshev	SA602	3 rd order Chebyshev	DDS	Crystal filter	Active filter	92
34	3 rd order butterworth	Gali-S66	5 th order chebyshev	SA602	3 rd order Chebyshev and 6dB attenuator	Crystal oscillator	Crystal filter	Active filter	104
35	No filter	Gali-S66	5 th order chebyshev	SA602	3 rd order Chebyshev and 6dB attenuator	Crystal oscillator	Crystal filter	Active filter	84
36	No filter	Gali-S66	5 th order chebyshev	SA602	3 rd order Chebyshev and 6dB attenuator	Crystal oscillator	Ceramic filter	Active filter	86
37	No filter	Gali-S66	5 th order chebyshev	SA602	3 rd order butterworth and 6dB attenuator	Crystal oscillator	Crystal filter	Active filter	84
38	No filter	Gali-S66	5 th order chebyshev	SA602	No filter	Crystal oscillator	Crystal filter	Active filter	83
39	No filter	Gali-S66	5 th order chebyshev	U2796B	3 rd order Chebyshev and 6dB attenuator	Crystal oscillator	Crystal filter	Active filter	64
40	No filter	Gali-S66	5 th order chebyshev	U2796B	No filter	Crystal oscillator	Crystal filter	Active filter	60
42	No filter	Gali-S66	5 th order chebyshev	Dual gate MOSFET	3 rd order Chebyshev	Crystal oscillator	Crystal filter	Active filter	54
43	No filter	Gali-S66	5 th order chebyshev	AD831	3 rd order Chebyshev	Crystal oscillator	Crystal filter	Active filter	55
44	No filter	Gali-S66	5 th order chebyshev	AD831	3 rd order Chebyshev	DDS	Crystal filter	Active filter	52
45	No filter	Gali-S66	5 th order chebyshev	AD831	No filter	DDS	Crystal filter	Active filter	54
46	No filter	Gali-S66	5 th order chebyshev	AD831	3 rd order butterworth	DDS	Crystal filter	Active filter	51

Table 5-5 The image rejection of the receiver for different receiver component combinations.



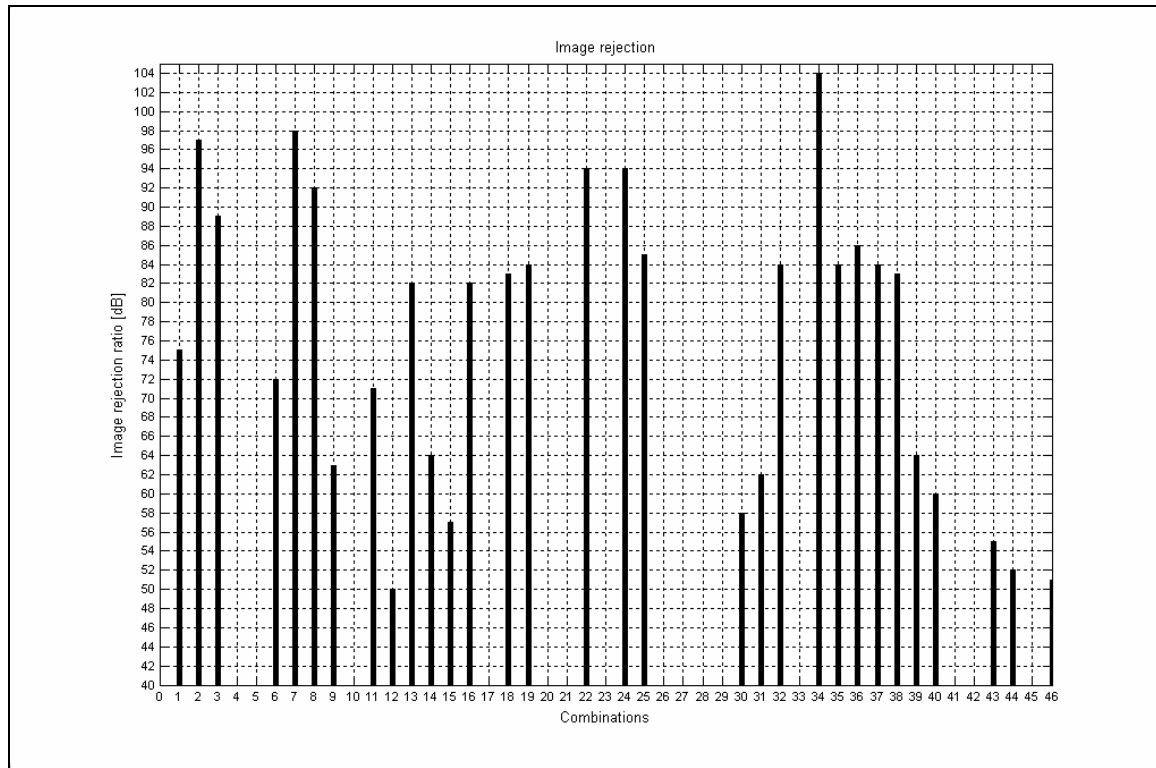


Figure 5-8 Image rejection ratio results summarized for the different combinations

ii. IF rejection

The measured IF rejection ratio for every receiver combination is given in *Table 5-6*. This is specified to be greater than 70dB and the results that meet this specification are accentuated.

Most of the measured receiver combinations have a very good IF rejection ratio that meets the specifications. This rejection ratio is the most sensitive to the front-end filters. The effect of every component on this ratio will be discussed in detail in section 5.3.

No	A Pre-select filter	B RF amplifier	C Image filter	D Mixer	E Injection filter	F Local oscillator	G IF filter	H Audio filter	IF rejection [dB]
1	5 th order chebyshev	Transistor amplifier	No filter	U2796B	No filter	PLL	Crystal filter	Active filter	98
2	5 th order chebyshev	Transistor amplifier	3 rd order butterworth	U2796B	No filter	PLL	Crystal filter	Active filter	97
3	5 th order chebyshev	Transistor amplifier	3 rd order butterworth	U2796B	3 rd order butterworth	PLL	Crystal filter	Active filter	90

5	No filter	Transistor amplifier	3 rd order butterworth	U2796B	3 rd order butterworth	PLL	Crystal filter	Active filter	89
6	No filter	Transistor amplifier	5 th order chebyshev	U2796B	3 rd order butterworth	PLL	Crystal filter	Active filter	94
7	3 rd order butterworth	Transistor amplifier	5 th order chebyshev	U2796B	3 rd order butterworth	PLL	Crystal filter	Active filter	98
8	3 rd order butterworth	Transistor amplifier	5 th order chebyshev	AD831	3 rd order butterworth	PLL	Crystal filter	Active filter	>92
9	No filter	Transistor amplifier	5 th order chebyshev	AD831	3 rd order butterworth	PLL	Crystal filter	Active filter	>93
10	No filter	Transistor amplifier	No filter	AD831	3 rd order butterworth	PLL	Crystal filter	Active filter	37
11	5 th order chebyshev	Transistor amplifier	No filter	AD831	3 rd order butterworth	PLL	Crystal filter	Active filter	94
12	No filter	Gali-S66	5 th order chebyshev	AD831	3 rd order butterworth	PLL	Crystal filter	Active filter	89
13	3 rd order butterworth	Gali-S66	5 th order chebyshev	AD831	3 rd order butterworth	PLL	Crystal filter	Active filter	98
14	Simple LC filter	Gali-S66	5 th order chebyshev	AD831	3 rd order butterworth	PLL	Crystal filter	Active filter	77
15	No filter	Gali-S66	5 th order chebyshev	U2796B	3 rd order butterworth	PLL	Crystal filter	Active filter	77
16	No filter	Gali-S66	5 th order chebyshev	SA602	3 rd order butterworth	PLL	Crystal filter	Active filter	63
17	No filter	Gali-S66	5 th order chebyshev	Dual gate Mosfet mixer	3 rd order butterworth	PLL	Crystal filter	Active filter	19
18	No filter	Gali-S66	5 th order chebyshev	SA602	3 rd order Chebyshev and 9dB attenuator	DDS	Crystal filter	Active filter	88
19	No filter	Gali-S66	5 th order chebyshev	SA602	3 rd order butterworth and 9dB attenuator	DDS	Crystal filter	Active filter	66
20	No filter	Gali-S66	No filter	SA602	No filter	PLL	Crystal filter	Active filter	21
21	No filter	Gali-S66	3 rd order butterworth	SA602	No filter	PLL	Crystal filter	Active filter	73
22	3 rd order butterworth	Gali-S66	5 th order chebyshev	SA602	No filter	PLL	Crystal filter	Active filter	95
24	3 rd order butterworth	Gali-S66	5 th order chebyshev	SA602	No filter	PLL	No filter	Active filter	94
25	3 rd order butterworth	Gali-S66	5 th order chebyshev	SBL-1	No filter	PLL	Crystal filter	Active filter	96
26	No filter	Gali-S66	3 rd order butterworth	SBL-1	No filter	PLL	Crystal filter	Active filter	63
27	No filter	Gali-S66	No filter	SBL-1	No filter	PLL	Crystal filter	Active filter	28
28	3 rd order butterworth	Gali-S66	No filter	SBL-1	No filter	PLL	Crystal filter	Active filter	98
29	No filter	Transistor amplifier	3 rd order butterworth	SBL-1	No filter	PLL	Crystal filter	Active filter	81
30	No filter	Gali-S66	5 th order chebyshev	U2796B	3 rd order Chebyshev	PLL	Crystal filter	Active filter	80
31	No filter	Gali-S66	5 th order chebyshev	U2796B	3 rd order Chebyshev	DDS	Crystal filter	Active filter	82



32	3 rd order butterworth	Gali-S66	5 th order chebyshev	U2796B	3 rd order Chebyshev	DDS	Crystal filter	Active filter	90
33	3 rd order butterworth	Gali-S66	5 th order chebyshev	SA602	3 rd order Chebyshev	DDS	Crystal filter	Active filter	93
34	3 rd order butterworth	Gali-S66	5 th order chebyshev	SA602	3 rd order Chebyshev and 6dB attenuator	Crystal oscillator	Crystal filter	Active filter	104
35	No filter	Gali-S66	5 th order chebyshev	SA602	3 rd order Chebyshev and 6dB attenuator	Crystal oscillator	Crystal filter	Active filter	82
36	No filter	Gali-S66	5 th order chebyshev	SA602	3 rd order Chebyshev and 6dB attenuator	Crystal oscillator	Ceramic filter	Active filter	86
37	No filter	Gali-S66	5 th order chebyshev	SA602	3 rd order butterworth and 6dB attenuator	Crystal oscillator	Crystal filter	Active filter	63
38	No filter	Gali-S66	5 th order chebyshev	SA602	No filter	Crystal oscillator	Crystal filter	Active filter	84
39	No filter	Gali-S66	5 th order chebyshev	U2796B	3 rd order Chebyshev and 6dB attenuator	Crystal oscillator	Crystal filter	Active filter	84
40	No filter	Gali-S66	5 th order chebyshev	U2796B	No filter	Crystal oscillator	Crystal filter	Active filter	81
42	No filter	Gali-S66	5 th order chebyshev	Dual gate MOSFET	3 rd order Chebyshev	Crystal oscillator	Crystal filter	Active filter	67
43	No filter	Gali-S66	5 th order chebyshev	AD831	3 rd order Chebyshev	Crystal oscillator	Crystal filter	Active filter	83
44	No filter	Gali-S66	5 th order chebyshev	AD831	3 rd order Chebyshev	DDS	Crystal filter	Active filter	86
45	No filter	Gali-S66	5 th order chebyshev	AD831	No filter	DDS	Crystal filter	Active filter	90
46	No filter	Gali-S66	5 th order chebyshev	AD831	3 rd order butterworth	DDS	Crystal filter	Active filter	89

Table 5-6 The IF rejection of the receiver for different receiver component combinations



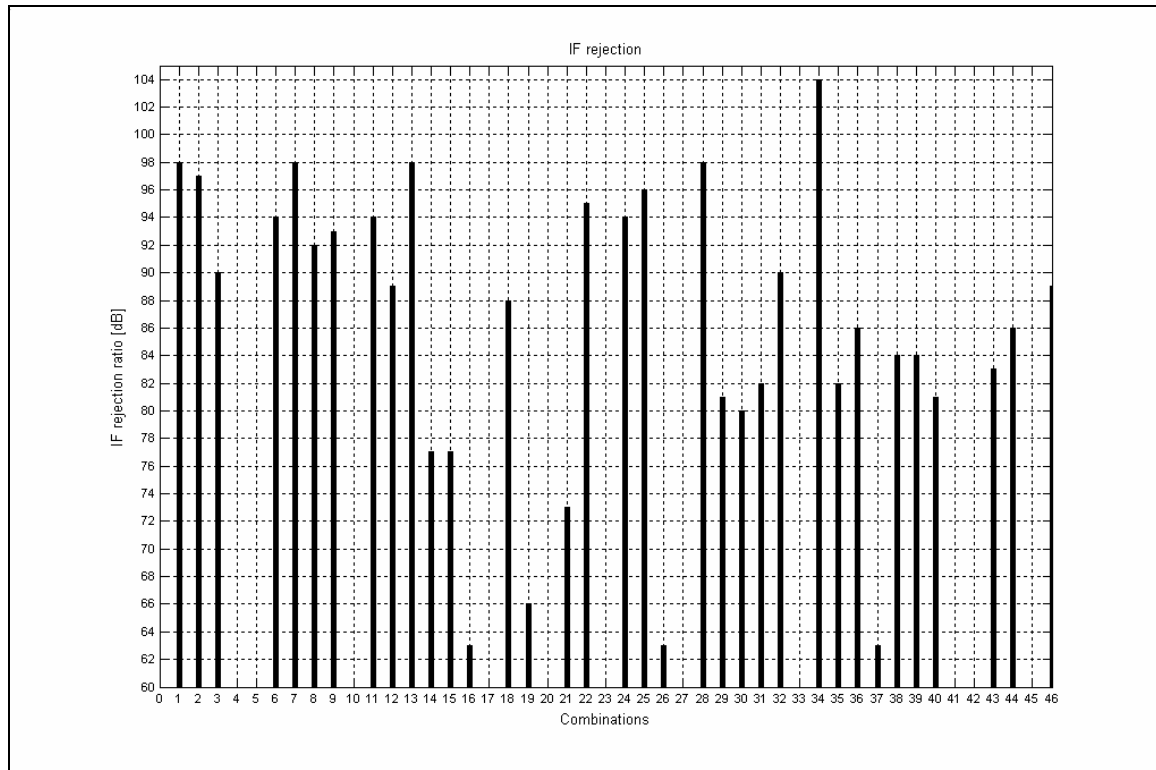


Figure 5-9 IF rejection results summarized for the different combinations

5.2.3. c Conclusion

The measured spurious response rejection ratios of the receiver depends mostly on the front-end section. The matching and the filters in this section as well as the isolation of the mixer influence the measured spurious response rejection ratios of the receiver. The rejection ratios that were measured, were all greater than the desired 70dB . The detailed explanation of the influence of different components in the receiver system on the receiver characteristics can be found in 5.3.

5.2.4. Desensitization

5.2.4. a Measurement procedure

Blocking or desensitization is a reduction in the output power or SINAD ratio at the output of the receiver due to an unwanted signal at another frequency. The measurement of this characteristic is done using two signal generators as shown in *Figure 5-5*. The desired frequency generator has a modulation frequency of $f_m = 1\text{kHz}$ and a deviation of $f_\Delta = \pm 1.5\text{kHz}$, while the unwanted signal in this measurement has no modulation [6-7].

Firstly, the desired frequency generator's amplitude is adjusted for a 20dB SINAD at the receiver output, while the unwanted signal generator is switched off. Next, with the unwanted signal



generator switched on, the amplitude of the unwanted signal generator is adjusted until a reduction of 6dB in the SINAD ratio of the output signal takes place (6dB reduction in the SINAD level occurs at output power reduction of 3dB). The frequency of the unwanted signal should be between a 1MHz and 10MHz offset from the desired signal frequency. Practical offsets is chosen as $\pm 1\text{MHz}$, $\pm 2\text{MHz}$, $\pm 5\text{MHz}$ and $\pm 10\text{MHz}$. The ratio in dB between the amplitude of the unwanted signal and the desired signal at the input of the receiver, when the SINAD falls to 14dB is the desensitization. The desensitization for every offset level is documented [5] [6].

5.2.4. b Measurements

The desensitization was measured of four receiver component combinations. According to Table 5-2 the desensitization ratio should be more than $78-84\text{dB}$. This specification was met by some of the combinations.

i. Combination 1

A Pre-select filter	B RF amplifier	C Image filter	D Mixer	E Injection filter	F Local oscillator	G IF filter	H Audio filter
3 rd order butterworth	Gali-S66	5 th order chebyshev	SA602	No filter	PLL	Crystal filter	Active filter

Table 5-7 Receiver combination 1 for measuring the receiver desensitization.

Offset from f_0	+1MHz	-1MHz	+2MHz	-2MHz	+5MHz	-5MHz	+10MHz	-10MHz
Desensitization [dB]	83	79	86	86	92	91	92	93

Table 5-8 Receiver desensitization ratios for combination 1.

ii. Combination 2

A Pre-select filter	B RF amplifier	C Image filter	D Mixer	E Injection filter	F Local oscillator	G IF filter	H Audio filter
No filter	Gali-S66	5 th order chebyshev	SA602	No filter	PLL	Crystal filter	Active filter

Table 5-9 Receiver combination 2 for measuring the receiver desensitization.

Offset from f_0	+1MHz	-1MHz	+2MHz	-2MHz	+5MHz	-5MHz	+10MHz	-10MHz
Desensitization [dB]	83	78	86	86	92	91	91	92

Table 5-10 Receiver desensitization for combination 2



iii. Combination 3

A Pre-select filter	B RF amplifier	C Image filter	D Mixer	E Injection filter	F Local oscillator	G IF filter	H Audio filter
No filter	Gali-S66	No filter	SA602	No filter	PLL	Crystal filter	Active filter

Table 5-11 Receiver combination 3 for measuring the receiver desensitization

Offset from f_0	+1MHz	-1MHz	+2MHz	-2MHz	+5MHz	-5MHz	+10MHz	-10MHz
Desensitization [dB]	83	77	86	85	91	91	91	91

Table 5-12 Receiver desensitization ratios for combination 3

iv. Combination 4

A Pre-select filter	B RF amplifier	C Image filter	D Mixer	E Injection filter	F Local oscillator	G IF filter	H Audio filter
No filter	Transistor amplifier	No filter	SA602	No filter	PLL	Crystal filter	Active filter

Table 5-13 Receiver combination 4 for measuring the receiver desensitization

Offset from f_0	+1MHz	-1MHz	+2MHz	-2MHz	+5MHz	-5MHz	+10MHz	-10MHz
Desensitization [dB]	71	72	75	75	85	84	93	89

Table 5-14 Receiver desensitization ratios for combination 4

5.2.5. Spurious radiation

5.2.5. a Measurement procedure

The spurious signal coupled to the antenna connector of the receiver will be radiated from the receiver by the antenna. These spurious signals at any frequency should be measured. This is done by connecting the receiver to a spectrum analyzer or a receiver via an 50Ω attenuator as shown below in *Figure 5-10*. The measuring receiver or spectrum analyzer is swept over a frequency range of $9kHz$ to $4GHz$, and the level at each frequency where a spurious component is detected, is documented as the spurious power level delivered into the 50Ω load [5-7] [59].



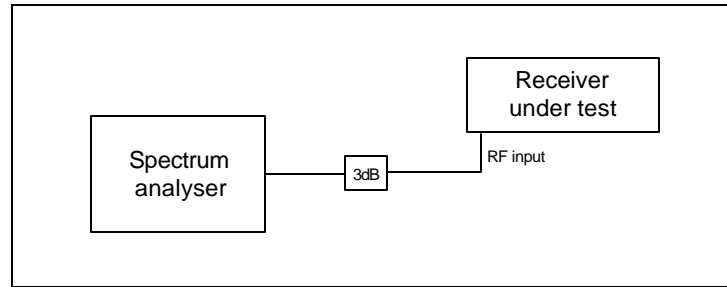


Figure 5-10 Measurement set-up for measuring the spurious radiations of the receiver

5.2.5. b Measurements

i. Combination 1

A Pre-select filter	B RF amplifier	C Image filter	D Mixer	E Injection filter	F Local oscillator	G IF filter	H Audio filter
3 rd order butterworth	Gali-S66	5 th order chebyshev	U2796B	3 rd order Chebyshev	DDS	Crystal filter	Active filter

Table 5-15 Receiver combination 1 for measuring the spurious radiations

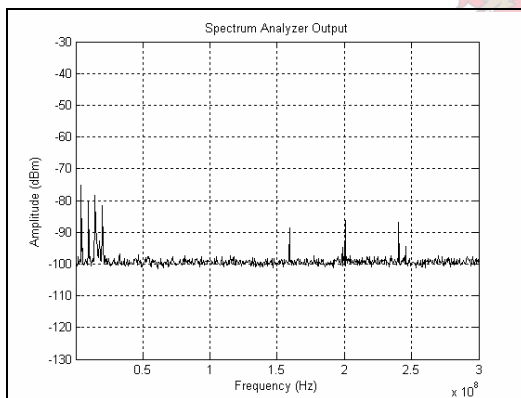


Figure 5-11 Spurious radiations detected over the frequency span from 1kHz to 300MHz

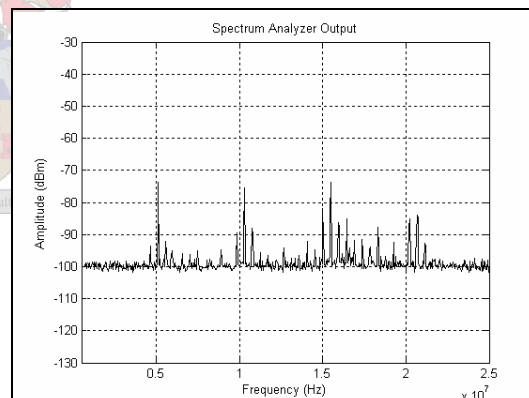


Figure 5-12 Spurious radiations detected over the frequency span from 500kHz to 25MHz

All the spurious signals on the antenna connector are smaller than -70dBm , which exceed the specifications in *Table 5-2* (the specified average is less than -47dBm).

The 6MHz signal that is radiated as illustrated in *Figure 5-12* is the clock of the ATmega8L that leaks through as well as the 12MHz signal that is probably the harmonic of this clock. The 20MHz signal that leaks through from the crystal oscillator on the DDS board can also be seen clearly. Both of these signals are square waves, which explain the harmonics in the lower frequency spectrum.



The harmonics of the 39.3MHz DDS signal at 157.2MHz , 196.5MHz and 235.8MHz can be seen in Figure 5-11.

ii. Combination 2

A	B	C	D	E	F	G	H
Pre-select filter	RF amplifier	Image filter	Mixer	Injection filter	Local oscillator	IF filter	Audio filter
3 rd order butterworth	Gali-S66	5 th order chebyshev	SA602	3 rd order Chebyshev	DDS	Crystal filter	Active filter

Table 5-16 Receiver combination 2 for measuring the spurious radiations

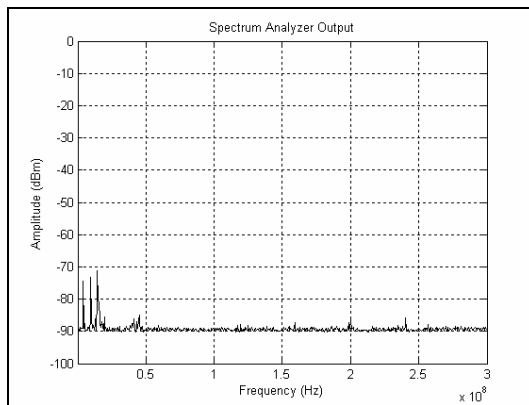


Figure 5-13 Spurious radiations detected over the frequency span from 1kHz to 300MHz

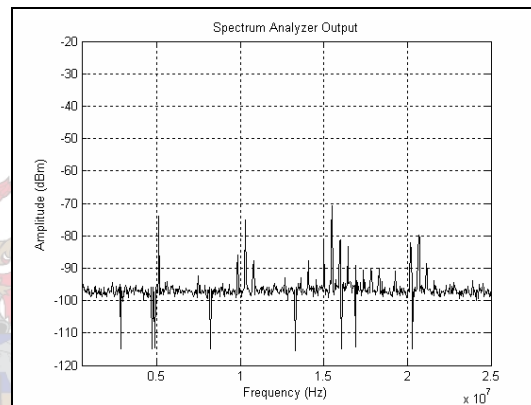


Figure 5-14 Spurious radiations detected over the frequency span from 500kHz to 25MHz

As with combination 1, the spurious responses on the antenna connector are all smaller than -70dBm .

Figure 5-14 shows the radiated 6MHz clock of the ATmega8L that leaks through, the 20MHz signal that leaks through from the crystal oscillator on the DDS board and the square wave harmonics of both. Figure 5-13 shows that the harmonics of the 39.3MHz DDS signal does not leak, as it did for combination 1.

The only difference between combination 1 and 2 is the mixer. In combination 1 the singly balanced U2796B is used, while the SA602 balanced mixer is used in combination 2. The LO-to-RF isolation of the SA602 was measured in section 4.1.2. b as $>103\text{dB}$, while the LO-to-RF isolation of the U2796B singly balanced mixer, described in 4.1.2. a, was $>41\text{dB}$. This explains the difference in the radiated spectrum. However, it is unimportant because both combinations will couple almost no spurious signals to the antenna connector.

iii. Combination 3

A Pre-select filter	B RF amplifier	C Image filter	D Mixer	E Injection filter	F Local oscillator	G IF filter	H Audio filter
3 rd order butterworth	Gali-S66	5 th order chebyshev	SA602	No filter	PLL	Crystal filter	Active filter

Table 5-17 Receiver combination 3 for measuring the spurious radiations

The isolation of the SA602 is excellent and no spurious radiations larger than -96dBm are detected over the whole frequency range between 1kHz and 2GHz .

iv. Combination 4

A Pre-select filter	B RF amplifier	C Image filter	D Mixer	E Injection filter	F Local oscillator	G IF filter	H Audio filter
3 rd order butterworth	Gali-S66	5 th order chebyshev	SBL-1	No filter	PLL	Crystal filter	Active filter

Table 5-18 Receiver combination 4 for measuring the spurious radiations

Only the LO signal at 39.3MHz leaks through and is coupled to the antenna connector from combination 4 as can be seen in Figure 5-15. This radiated response is very small and exceeds the specifications given in Table 5-2. No other spurious radiations were detected over the frequency range between 1kHz and 2GHz .

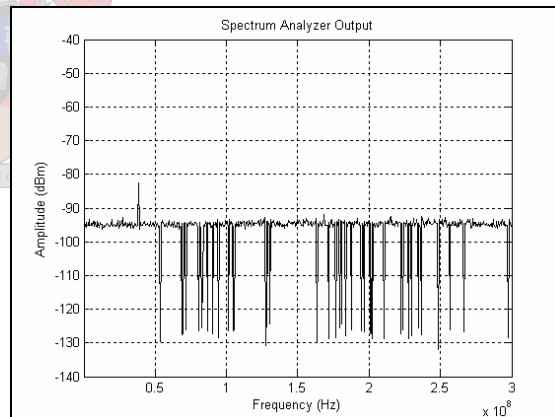


Figure 5-15 Spurious radiations detected over the frequency span from 1kHz to 300MHz

5.2.5. c Conclusion

The spurious response radiation of the receiver measures the effectivity of the receiver system in isolating the signals that are generated in the system from the antenna connector. The spurious radiations from all the combinations measured were very small and well within the specifications.

5.2.6. Co-channel rejection

5.2.6. a Measurement procedure

The measurement of the co-channel rejection of a receiver is similar to the measurement of the adjacent channel selectivity. Signals at the operating frequency are input into the receiver through a combining network. The amplitude of the desired signal is set to the required sensitivity level and the signal power of the unwanted signal generator is increased until the SINAD reading at the output of the receiver is reduced from 20dB to 14dB. The measurement set-up can be seen in *Figure 5-5*. The co-channel rejection is the difference in dB between the level of the unwanted test signal at this point and the level of the wanted test signal at the receiver input [6].

The modulation of the wanted and unwanted signals is $1kHz$ and $400Hz$ respectively, and the deviation is 60% of the maximum permissible frequency deviation [6].

This is repeated with the unwanted test signal at frequency offsets of $\pm 1.5kHz$ and $\pm 3kHz$. The lowest value of these five ratios is then recorded as the co-channel rejection ratio [6].

Thus, two signals at the receiver frequency, the desired one with a modulation frequency of $1kHz$ and the unwanted one with a modulation frequency of $400Hz$, and both with a frequency deviation of $\pm 1.5kHz$ are applied to the input of the receiver, through the combiner. The unwanted signal generator is switched off at first, while the input level of the wanted signal generator is adjusted to achieve an output signal with a $20dB$ SINAD. After this level is reached, the unwanted signal generator is switched on, and the signal level is increased until the SINAD ratio drops to $14dB$.

5.2.6. b Measurements

i. Combination 1

A Pre-select filter	B RF amplifier	C Image filter	D Mixer	E Injection filter	F Local oscillator	G IF filter	H Audio filter
3 rd order butterworth	Gali-S66	5 th order chebyshev	SA602	No filter	PLL	Crystal filter	Active filter

Table 5-19 Receiver combination 1 for measuring the co-channel rejection

Frequency [MHz]	f_o	$f_o + 1.5kHz$	$f_o - 1.5kHz$	$f_o + 3kHz$	$f_o - 3kHz$
Co channel rejection [dB]	5	7	7	3	3

Table 5-20 The co-channel rejection ratios of receiver combination 1



ii. Combination 2

A Pre-select filter	B RF amplifier	C Image filter	D Mixer	E Injection filter	F Local oscillator	G IF filter	H Audio filter
No filter	Gali-S66	5 th order chebyshev	SA602	No filter	PLL	Crystal filter	Active filter

Table 5-21 Receiver combination 2 for measuring the co-channel rejection

Frequency [MHz]	f_o	$f_o + 1.5kHz$	$f_o - 1.5kHz$	$f_o + 3kHz$	$f_o - 3kHz$
Co channel rejection [dB]	7	7	7	4	4

Table 5-22 The co-channel rejection ratios of receiver combination 2

iii. Combination 3

A Pre-select filter	B RF amplifier	C Image filter	D Mixer	E Injection filter	F Local oscillator	G IF filter	H Audio filter
3 rd order butterworth	Gali-S66	5 th order chebyshev	U2796B	No filter	PLL	Crystal filter	Active filter

Table 5-23 Receiver combination 3 for measuring the co-channel rejection

Frequency [MHz]	f_o	$f_o + 1.5kHz$	$f_o - 1.5kHz$	$f_o + 3kHz$	$f_o - 3kHz$
Co channel rejection [dB]	6	9	8	6	5

Table 5-24 The co-channel rejection ratios of receiver combination 3

5.2.7. Conclusion

The various measurement methods of the receiver characteristics were described in this section. Measurement results indicated that specifications were met by some of the measured combinations. These results will be interpreted in the next section.



5.3 Influence of the receiver components on receiver characteristics

The influence of the receiver components designed in chapter 4, on receiver performance as measured in 5.2, is discussed in this section.

5.3.1. Influence of the front-end amplifier on receiver performance

A comparison between the designed transistor amplifier and the Gali-S66 amplifier indicates that the Gali-S66 amplifier generally improves system performance. This is seen when comparing combinations 8 & 13, 9 & 12 and 26 & 29 in *Table 5-3*, *Table 5-4*, *Table 5-5* and *Table 5-6*. The sensitivity improves with $4-6\text{dB}$ and because the selectivity is dependent on the sensitivity, the selectivity is consequently improved. The sensitivity gets better when the Gali-S66 amplifier is used, even though its noise figure is slightly higher than the noise figure of the designed transistor amplifier, because of its higher gain. The IF and image rejection is marginally better if the transistor amplifier is used, because of the matching networks on the transistor amplifier that act as filters and reject signals that are not at 50MHz .

5.3.2. Influence of the front-end filters on receiver performance

One of the main reasons for employing a pre-select filter is the prevention of the saturation of the RF amplifier by strong interfering signals. This desensitization of the receiver is measured in section 5.2.4. b. However, for the measured combinations there are no differences in the desensitization ratio whether the pre-select and image filters are employed or not. This is caused by the high intercept points of the amplifiers and mixers involved.

The main function of the image reject filter is the rejection of the spurious response at the image signal. The pre-select filter also influences the spurious response rejection, but at the cost of a drop in sensitivity. The influence of the front-end filters on the receiver spurious response, selectivity and sensitivity performance is evaluated next by comparing combinations in *Table 5-3*, *Table 5-4*, *Table 5-5* and *Table 5-6*.

Firstly, the receiver performance is evaluated with and without the 3rd order Butterworth filter used as pre-select filter. The 5th order Chebyshev filter is employed as image reject filter. The introduction of the pre-select filter worsens the receiver sensitivity by $1-7\text{dB}$. This can be seen when comparing combinations 8 & 9, 12 & 13, 31 & 32 and 34 & 35. The deteriorated sensitivity is caused by the increase in the receiver noise figure when an attenuator is placed before the RF amplifier. Better spurious response rejection is however, expected and an improved image and IF rejection of $12-30\text{dB}$ is seen. The IF and image rejection improvement differ, because the matching networks and rejection of the other components also play a part in the spurious



response rejection of the system. The selectivity remains unchanged as was expected, because it is dependent mostly on the IF filter.

Next, the 3rd order Butterworth filter is used as image reject filter instead of the 5th order Chebyshev filter. The performance is compared with and without the 5th Chebyshev filter as pre-select filter by comparing combination 3 & 5. The sensitivity again decreases when using the pre-select filter, as expected. The selectivity and IF rejection stays constant, while the combination without the 5th order Chebyshev filter as pre-select filter has a much lower image rejection ratio of only 32dB compared to the 89dB of the combination that includes the pre-select filter. This can be explained by considering *Figure 4-77*. The image rejection of the 5th order Chebyshev filter is 65dB while the image rejection of the 3rd order Butterworth filter is a mere 33dB. The IF rejection is acceptable, because both filters attenuate 10.7MHz by around 60dB.

In combination 5 & 6, no pre-select filter is used, and the image reject filter is changed from the 3rd order Butterworth filter to 5th order Chebyshev filter. All the performance characteristics remains unchanged, except for the image rejection ratio, which is very low for the 3rd order Butterworth filter as described in the previous paragraph. Thus, the 5th order Chebyshev filter is a much more effective image reject filter.

In combination 3 and 7, the 3rd order Butterworth and 5th order Chebyshev filter are interchanged. The sensitivity remains unchanged, because the insertion loss of the filters is similar. The selectivity is not influenced, but the IF and image rejection are both better if the 5th order Chebyshev filter is used as the image reject filter.

The simple LC filter is compared to the 3rd order Butterworth filter as pre-select filter by comparing combination 13 & 14. The measured insertion loss of the 3rd order Butterworth filter is 0.5dB, while the insertion loss of the simple LC filter is 1.2dB. This small insertion loss difference causes the sensitivity to drop with 2dB, which demonstrates the effect of attenuators inserted before the RF amplifier. The IF and image rejection are less when using the simple LC filter, because the selectivity of this filter is not as good as the selectivity of the 3rd order Butterworth filter (as can be seen in *Figure 4-77*).

The receiver has almost no spurious response rejection when no pre-select or image reject filter is used. This can be seen by comparing combination 9 & 10, 20 & 21, 10 & 11, 26 & 27 and 27&28. In all this cases the image and IF rejection is very poor when no front-end filters are used and gets better when a front-end filter is employed. The selectivity stays the same for each case



while the sensitivity worsens when a filter is introduced. This is because of the degradation of the noise figure.

When only one front-end filter is used, as in combination 9 & 11 and 26 & 28, it seems as if better results are attained if it is employed after the RF amplifier, instead of introducing the attenuator before the amplifier. The receiver selectivity remains unchanged in both instances while the sensitivity is $6-7\text{dB}$ better with the filter after the front-end amplifier. The spurious response rejection tends to be marginally better with the filter employed before the RF amplifier.

The measured results can be summarized as follows:

- The selectivity of the system is seldom affected by the front-end filters, because system selectivity depends mostly on the selectivity of the IF filter.
- The front-end filter has the greatest influence on the spurious response rejection.
- The introduction of a front-end filter increases the IF and image rejection, while decreasing the sensitivity.
- The 5th order Chebyshev filter is a better image reject filter than the 3rd order Butterworth filter, because of its higher selectivity.
- The 3rd order Butterworth filter is the best pre-select filter, because it has the lowest insertion loss.
- The receiver has almost no spurious response rejection when no pre-select or image reject filters are used.

5.3.3. Influence of the mixer on receiver performance

The main function of the mixer in the system is to translate the frequency. Even though all the mixers that were designed do this, their other characteristics have an influence on receiver performance. For example, the receiver sensitivity will be affected by the noise figure and conversion gain or loss of the mixer. The sensitivity will furthermore be influenced by the rejection of AM noise from the LO. The isolation of the mixer will also play a significant role in the reduction of spurious radiation as well as spurious response rejection. The influence of the different mixers on receiver performance that were measured in 5.2 are compared in this section.

Firstly, the influence of different types of mixers on the receiver's spurious response rejection, sensitivity and selectivity are compared. This is done by comparing the active mixers: U2796B, SA602, Dual-gate MOSFET and AD831 mixers. Thus, combination 12, 15, 16 and 17 in *Table 5-3*, *Table 5-4*, *Table 5-5* and *Table 5-6* respectively, are compared.



The sensitivity of the combination with the single device dual-gate MOSFET mixer is -108dBm which is the lowest of these four combinations. This can be expected, because it has a very high conversion loss, the highest noise figure and the lowest average AM noise rejection.

The sensitivity of both the singly balanced U2796B mixer and the doubly balanced AD831 is -114dBm . This is an interesting result, because, even though the noise figures of these two mixers are similar the AD831 has 9dB more gain, which should decrease the noise figure and improve sensitivity. This mixer is also doubly balanced, which should result in better LO AM noise rejection than when the singly balanced mixer is used. The similar sensitivity can be explained by looking at the measured results in *Table 4-10*.

Here it can be seen that the LO AM noise rejection of the U2796B is marginally better than that of the AD831 which will improve the sensitivity. The effect of the difference in the gain is also less significant here than earlier in the receiver chain.

The best sensitivity of -116dBm is achieved by the combination that uses the SA602 mixer. This mixer has the highest average LO AM noise rejection (44dB more than that of the AD831), which explains the better sensitivity result of this mixer even though it has a 1dB higher noise figure and 7dB lower gain than that of the AD831.

Similar results are obtained when a comparison is made amongst combinations 35, 39, 42 and 43, with the SA602 again performing the best. The U2796B performs better in this instance than the AD831, which can again only be contributed to the fact that it has a better LO AM noise rejection, which plays a more significant role when using the crystal oscillator. A comparison between combination 7 & 8 shows that the receiver sensitivity improves when the U2796B is used rather than the AD831. Here the influence of the higher gain on the receiver noise figure and consequently the sensitivity is reduced even more by the introduced pre-select filter. Thus, it can be derived that the better LO AM noise rejection of the U2796B plays a very significant role.

The image rejection of combinations with the SA602 is the highest, which could be expected, because the gain at the image frequency of this mixer is low, due to the matching networks. On the other hand, the selectivity of the combinations that use the SA602 is usually poorer. This is because the input 1dB compression point of this mixer is the lowest of all the mixers, and thus, distortion will set in at lower input power levels. The selectivity of the combinations that use this mixer is still acceptable.



The active mixer which supports the best overall receiver performance is the SA602, with the AD831 and U2796B also performing well. The SA602 draws a mere 1.2mA, while the AD831 uses 96mA and the U2796B uses 2.3mA. Thus, the SA602 and U2796B are the best choices for portable applications.

Next, the receiver performance with the SA602 active doubly balanced mixer is compared to the receiver performance with the SBL-1 passive doubly balanced mixer. The noise figure of the SBL-1 is better than that of the SA602, while the SBL-1 has a $-5dB$ conversion loss compared to the $9dB$ conversion gain of the SA602. The sensitivity of the combination that uses the SA602 is $4dB$ better, while the selectivity of this combination is less, because of the lower 1 dB compression point of the SA602. The selectivity of the combination, using the SA602 is still acceptable and will be further improved when the IF filter is used on a board with a better isolation as previously discussed. The spurious response rejection of these combinations is similar due to their comparable RF-IF isolation.

The SA602 and U2796B mixers are now compared by comparing combination 32 & 33, where the DDS is used as the local oscillator. Here the SA602 performs at least $3dB$ better for every characteristic measured. When comparing the spurious radiations of these combinations in section 5.2.5, the SA602 has the best spurious radiation performance, which can be contributed to its high LO-RF isolation.

Thus, the best overall receiver characteristics were measured when using the SA602 mixer.

5.3.4. Influence of the injection filter on receiver performance

The injection filter attenuates the LO harmonics and wideband noise, and thus, improves the receiver sensitivity. This is deduced by comparing the receiver sensitivity for combinations 44 & 45 & 46 that all use the DDS as local oscillator. The best sensitivity is achieved by using the 3^d order Chebyshev filter and is worsened by $1dB$ when using the 3^d order Butterworth filter. The sensitivity is $6dB$ poorer when no injection filter is used, which indicates this filter's importance when the DDS is used as local oscillator.

The importance of this filter is decreased when the crystal oscillator is used, which has less harmonic content than the DDS. By comparing combination 35 & 38, it can be seen that for this instance the sensitivity is only decreased by $2dB$, when not using the injection filter.

When comparing the receiver sensitivity when the 3^d order Butterworth or Chebyshev filter is used as injection filter, the Chebyshev filter improves the sensitivity with $2-3dB$, irrespective of



whether the DDS or PLL is used as local oscillator. This can be seen by evaluating combinations 18 & 19 and 15 & 30.

This shows that the use of an injection filter improves receiver sensitivity and that the best injection filter to use is the 3rd order Chebyshev filter.

5.3.5. Influence of the local oscillator on receiver performance

The phase noise of the local oscillator will influence the adjacent channel selectivity performance of the receiver, while the wideband noise of the local oscillator will influence the receiver's sensitivity.

The higher wideband noise of the DDS worsens the selectivity as was expected. This can be seen by comparing combinations 16 & 19, 30 & 31 & 39 and 33 & 34. On the contrary, less phase noise of the DDS improves the selectivity (see combinations 16 & 19).

When comparing the selectivity of combinations 30 & 39, it can be seen that the crystal oscillator improves the selectivity as expected, because it has less phase noise.

By comparing combinations 43 & 44 it can be seen that the DDS, which has a poorer phase noise, worsens the selectivity. In combinations 46 & 12, the DDS has the best phase noise and consequently improves the selectivity of combination 46.

5.3.6. Influence of the IF filter on receiver performance

The IF filter with the narrowest bandwidth sets the overall system noise bandwidth and provides the adjacent channel rejection. This can be seen by comparing receiver selectivity with and without the IF filter, by evaluating combination 22 & 24. When the IF filter is absent, there is almost no adjacent channel selectivity. The sensitivity, on the other hand, remains unchanged regardless of the IF filter's presence. This is because the filter is almost last in the receiver chain and consequently its influence on the noise figure will be minimal. When the filter is absent, the Murata Cerafil filters that are used in the IF receiver will set the noise bandwidth. The consequent noise bandwidth remains relatively narrow, which explains the unaffected sensitivity. The spurious response rejection is not at all influenced by this filter, as was expected.

When comparing the influence of the ceramic IF filter to the influence of the crystal IF filter on the system performance, much better selectivity is found when using the crystal filter compared to almost no improvement when using the ceramic filter, because of the lower selectivity of this filter. This can be seen by evaluating combination 35 & 36. The sensitivity in this instance is slightly



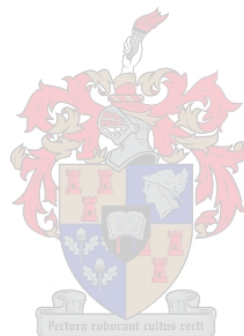
poorer, when the ceramic filter instead of the crystal filter is used, even though it is almost at the end of the receiver chain. This is caused by the $6dB$ conversion loss of the ceramic filter compared to the $2dB$ conversion loss of the crystal filter.

The crystal filter should be employed for best receiver selectivity and sensitivity results.

5.3.7. Influence of the audio filter on receiver performance

The audio bandwidth should be limited by an audio filter to attenuate interference and IF noise that originates after the first IF filter and thus, to enhance the signal-to-noise ratio.

The very important effect of the audio filter on the receiver system performance can be seen by comparing combinations 3 & 4 and 22 & 23. The receiver sensitivity increases by $79-96dB$ without the audio filter. Thus, it can be concluded that the use of an audio filter is essential.



5.4 Discussion and comparison of results

In this section, the receiver's performance values for some of the combinations were predicted with **ReceiverCALC[™] 1.1** and compared to the receiver performance measured in section 5.2. This was done by entering the measured characteristics of every receiver component (as discussed in chapter 4) into **ReceiverCALC[™] 1.1**. All the different combinations were saved on the Appendix CD, and can be opened with **ReceiverCALC[™] 1.1**.

A summary of the expected and measured performances is given in *Table 5-25*. All the values that meet the specifications are accentuated, while the anticipated values that compare well with the measured values, are marked with blue. Two expected sensitivity values are given. The first prediction takes the contribution of the image and the wideband LO noise to the noise figure into account. The second value uses only the cascaded noise figure to predict the sensitivity.

Thus, the approximation that is made when the image and LO wideband noise is not taken into account, can clearly be seen. For example the values in combinations 1-3, 6 & 7, predicted with **ReceiverCALC[™] 1.1** when the image and LO wideband noise is taken into account, compares well to the measured values. In contrast, the predicted values that are attained with **ReceiverCALC[™] 1.1** when using only the cascaded noise figure, give the false impression that the specifications will be met, which is not the case for these combinations. The inclusion of the image and LO wideband noise contribution to the noise figure, does not make a notable difference in all the instances, but is very important for some.

Most of the sensitivity predictions in *Table 5-25* compared well to the measured values. It can therefore be concluded that **ReceiverCALC[™] 1.1** is a useful radio receiver design tool.



Combination	Sensitivity for a deviation of $\pm 1.5kHz$ [dBm]			Selectivity [dB]	
	Expected		Measured	Expected	Measured
	[1]*	[2]*			
1	-107.6	-113.4	-108	46.7	66
2	-108.1	-113.2	-107	46.7	66
3	-110.2	-113.2	-107	46.7	61
6	-111.1	-114.5	-111	46.7	64
7	-110.6	-114	-107	46.7	62
8	-114	-114.2	-102	46.7	57
9	-114.5	-114.7	-108	46.7	57
10	-110	-114.9	-109	46.7	57
11	-111.2	-113.4	-102	46.7	57
12	-114.5	-114.6	-114	46.7	60
13	-114	-114.1	-107	46.7	57
14	-113	-113.3	-105	46.7	56
15	-113.2	-114.5	-114	46.7	58
16	-114.5	-114.5	-116	46.7	53
17	-81.04	-107.6	-108	46.7	41
18	-114.5	-114.5	-100	46.7	59
19	-114.5	-114.5	-113	46.7	56
20	-112.6	-114.5	-116	46.7	61
21	-114.5	-114.6	-117	46.7	60
22	-114	-114	-116	46.7	61
24	-114	-114	-116	Poor	5
25	-85.79	-113.8	-112	46.7	70
26	-87.28	-114.4	-114	46.7	70
28	-87	-114	-107	46.7	70
29	-81.99	-114.2	-109	46.7	67
30	-113.8	-114.5	-116	46.7	64
31	-114.1	-114.5	-105	46.7	59
32	-113.6	-114	-102	46.7	59
34	-114.1	-114	-117	46.7	65
35	-114.5	-114.5	-118	46.7	65
36	-114.4	-114.4	-117	Poor	4
38	-114.5	-114.5	-116	46.7	65
39	-114.2	-114.5	-117	46.7	67
40	-113.3	-114.5	-118	46.7	53
43	-114.5	-114.6	-114	46.7	70
44	-114.5	-114.6	-116	46.7	58
46	-114.5	-114.6	-115	46.7	63

Table 5-25 Comparison between expected and measured receiver performance

[1]* Take image as well as wideband LO noise contribution to the noise figure into account

[2]* Only cascaded noise figure is used to predict sensitivity



5.5 Conclusion

In this chapter, the correct measurement methods to measure receiver characteristics were discussed. The performance of the receiver was measured while interchanging the different well-defined receiver components discussed in the chapter 4. The measurement results confirmed the predicted influence of every component on the receiver characteristics.

The selectivity results of the different combinations were mostly influenced by the specifications of the IF filter, while the spurious response rejection ratio of the receiver was mostly dependent on the front-end section. The measured rejection ratios were all greater than the desired 70dB .

The spurious radiations from all the combinations measured were very small and well within the specifications.

A comparison between the designed transistor amplifier and the Gali-S66 amplifier indicated that the Gali-S66 amplifier generally improves system performance. The introduction of a front-end filter increased the IF and image rejection, while decreasing the sensitivity. The front-end filters had the greatest influence on the spurious response rejection. The receiver had almost no spurious response rejection when no pre-select or image reject filter was used.

The injection filter attenuated LO harmonics and wideband noise, and thus improved the receiver sensitivity. The local oscillator phase noise influenced the adjacent channel selectivity performance of the receiver, while the wideband noise of the local oscillator influenced the receiver's sensitivity.

The IF filter with the narrowest bandwidth provided the adjacent channel rejection. The receiver sensitivity dropped between $79-96\text{dB}$ without the audio filter. Thus, the use of an audio filter is essential.

A summary of the measured characteristics is given in *Table 5-26*. These characteristics compare well to those predicted with **ReceiverCALC^{1.1}**.



Combination	Sensitivity for a deviation of $\pm 1.5kHz$	Selectivity	Image rejection	IF rejection
1	-108	66	75	98
2	-107	66	97	97
3	-107	61	89	90
6	-111	64	72	94
7	-107	62	98	98
8	-102	57	92	92
9	-108	57	63	93
10	-109	57	2	37
11	-102	57	71	94
12	-114	60	50	89
13	-107	57	82	98
14	-105	56	64	77
15	-114	58	57	77
16	-116	53	82	63
17	-108	41	38	19
18	-100	59	83	88
19	-113	56	84	66
20	-116	61	20	21
21	-117	60	28	73
22	-116	61	94	95
24	-116	5	94	94
25	-112	70	85	96
26	-114	70	26	63
28	-107	70	22	98
29	-109	67	36	81
30	-116	64	58	80
31	-105	59	62	82
32	-102	59	84	90
34	-117	65	104	104
35	-118	65	84	82
36	-117	4	86	86
38	-116	65	83	84
39	-117	67	64	84
40	-118	53	60	81
43	-114	70	55	83
44	-116	58	52	86
46	-115	63	51	89

Table 5-26 Summary of the sensitivity, selectivity and spurious response rejection ratios of the measured combinations

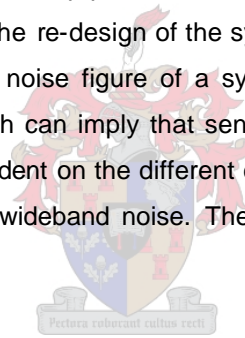


6 Conclusion and recommendations

6.1 Conclusion

Basic receiver topologies and theory were discussed. The receiver characteristics, namely sensitivity, selectivity, audio frequency response, image rejection, IF rejection, dynamic range, audio frequency output power, distortion and spurious responses were defined and receiver measurement procedures were discussed and completed. The characteristics of the different receiver components that influence receiver system characteristics were described and summarized. Important functions and design restrictions of the different receiver components were compared.

A study of the noise theory was done to help predict the noise figure of a system more accurately. This is extremely important to avoid the re-design of the system to improve sensitivity, especially for high performance receivers. The noise figure of a system is sometimes predicted by using only the cascaded noise figure, which can imply that sensitivity specifications are not met. The real noise figure of a system is dependent on the different component gains and noise figures, the image noise and the local oscillator wideband noise. The calculation of this real noise figure is explained thoroughly.



A software analysis tool called **ReceiverCALC^{1.1}** was developed to calculate the signal-to-noise ratio and characteristics of the receiver prior to the design process. This will enable designers to determine if specifications are met, and to use different components to improve performance before the design process commences. This program predicts the sensitivity, selectivity and dynamic range of receivers with defined component properties and can plot power diagrams and spurious response charts. **ReceiverCALC^{1.1}** is also a very helpful tool, when components become obsolete and need to be replaced. The receiver's system performance can be predicted accurately with this program.

A modular design approach was used to design the receiver. The receiver has been divided into components that were each designed, built and matched to 50Ω, and then measured and characterized separately. This modular design approach enables future designers to easily upgrade, increase bandwidth or replace components when components become obsolete.



Mixer theory was discussed and mixer terminology and measurement methods were defined. A few different mixers were designed, measured and characterized in detail. Different local oscillators were developed. A DDS was considered as a replacement for the existing radio's synthesized PLL local oscillator. A crystal oscillator was built, characterized and its performance was compared to that of the DDS and PLL. Phase noise theory was considered in detail, as well as its effect on the receiver system. Two front-end amplifiers were designed. The noise factor is dominated by the first component in the receiver. The effect on the system sensitivity using a low noise amplifier with a poor input impedance match was compared to the effect of an amplifier with a higher noise figure and an improved input impedance match. A ceramic and crystal IF filter was designed, built, characterized and compared. The selectivity of this filter's influence on the system's selectivity and performance was considered. An IF receiver system was developed and the necessary system input level to achieve a certain 20dB SINAD output, was defined. The distortion and characteristics of this system were evaluated. An audio filter and amplifier were designed and tested and various receiver filters were developed. Digital components were investigated, compared and used with analogue techniques. The energy consumption of the components was considered throughout the design process.

The receiver system was measured and the performance was evaluated when interchanging the different developed receiver components. The influence of every component on the receiver characteristics was confirmed with theory.

The measured receiver characteristics were compared to the predictions of **ReceiverCALC^{1.1}**. Conclusions were made concerning the usability of this software product.

6.2 Recommendations for future research

The preliminary development was done for a radio transceiver that will improve an existing narrowband system. This existing narrowband system operates between 48MHz and 50MHz and has certain limitations.

The foundation was laid for future research possibilities. This may include the following:

- Emphasis was placed on the receiver section and its mixer and local oscillator components. Consequently the transmitter section still needs to be designed to complete the transceiver system.
- Components can be replaced in the existing system, to achieve a broadband receiver system. Special development work can be done on the design of a broadband or tuneable front-end filter to improve the bandwidth of the system.



- The DDS can be implemented in the receiver as well as in the transmitter section of the transceiver. Thus, the modulation techniques of the DDS signal should be investigated.
- Research can also be done on the effect of the low power consumption constraint on receiver and transmitter performances and on the performance of separate components.
- **ReceiverCALC^{1.1}** can be improved, by adding a function to calculate the transducer gain that is used in the calculations, from the measured s-parameters.
- The foundation of the receiver system was laid, but improvements to any components in the system can easily be done due to the flexibility of the modular design approach. Thus, any component can be researched and improved if desired for example the crystal IF filter may be improved by laying it out on a strip line PCB.
- More digital components can be investigated and the effect of their characteristics on the system's performance be evaluated.

The measurement procedures and receiver characteristic predictions were researched and documented in detail for future development. Improvements to the existing system can be done with ease, due to the modular design approach used and with the help of the developed software tool, **ReceiverCALC^{1.1}**.



Acknowledgements

I would like to thank the following persons, who helped me during the completion of my thesis,

Professor Johann de Swardt for his guidance and expertise, patience and understanding

Everybody in E212 over the last few years, for their support and friendship, especially Wynand de Wit, Quintin Engelbrecht, Jacques Malan and Robert Kellerman



Brian Woods, for proof-reading my thesis

Wessel Croukamp and Ulrich Buttner for helping with all the technical bits and pieces

Janine Kulenkampff for proof-reading my thesis, and for all her support and encouragement

Annie, Marique, Twinita, Madeleine, Adri, Estelle, Jo, Celeste and Anneli for all their encouragement, prayers and support

My parents, Pieter and Linda Oosthuizen, for proof-reading my thesis, their help, priceless encouragement and love

My husband, Robert, for all his invaluable support, patience, encouragement and love: I love you so much

Jesus Christ, my Lord and Saviour, for life, everything and everybody He gave me: You are everything.



Bibliography

- [1] Peter Vizmuller, RF design guide: systems, circuits, and equations, Artech house, Inc, 1995.
- [2] Brad Brannon, Basics of designing a digital radio receiver, Analog Devices, Inc.
- [3] Donald A Hitto, Circuit design and technological limitations of silicon RFICs for wireless applications, Doctor of Philosophy in electrical engineering and computer science, Massachusetts institute of technology, June 2002.
- [4] Craig Michael Teusher, Low power receiver design for portable RF applications: Design and implementation of an adaptive multi-user detector for an indoor, wideband, CDMA application, Doctor of philosophy in engineering, University of California, 1998.
- [5] OFTA, Telecommunications authority Hong Kong, Performance specification for angle modulated radio transmitters and receivers for use as base, mobile and portable equipment in the land mobile radio service, Draft, HKTA1002 Issue 04, September 2002.
- [6] European telecommunications standards institute, Part 1: Technical characteristics and methods of measurement, European Standard (Telecommunication series), ETSI EN 300 086-1 V1.2.1, March 2001.
- [7] Ministry of Commence New Zealand , Communications division, Specification for radio apparatus, VHF and UHF land mobile service, Using angle modulation with 12.5kHz carrier frequency separation and a maximum deviation of $\pm 2.5\text{kHz}$, RFS26, Issue 2, ISBN:0-478-00470-0, October 1993.
- [8] The ARRL handbook for radio amateurs, seventy-seventh edition, ARRL, 2000.
- [9] David M Pozar, Microwave and RF design of wireless systems, John Wiley & Sons, Inc, 2001.
- [10] Kalle Kivekäs, Design and characterization of down-conversion mixers and the on-chip calibration techniques for monolithic direct conversion radio receivers, Report 34, Doctor of science degree, Helsinki University of Technology, October 2002.
- [11] Dough De Maw, Practical RF design manual, Prentice Hall, Inc, Englewood Cliffs, 1982.
- [12] Robert G. Swartz, Active Mixer ICs Challenge the Passive Status Quo, 15 September 2003.
- [13] Bert C Henderson, Mixers:Part1-Characteristics and performance, WJ Tech Notes vol.8#2, Watkins-Johnson company, April 1981.
- [14] Notes on IF rejection, 69.5.23.180/ars/pages/lab_text/notes_if.html
- [15] Mike Curtin and Paul O'Brien, Phase-locked loops for high-frequency receivers and transmitters-Part 2, Volume 33, Number 5, and May 1999.
- [16] Dr. Poman P.M., Microwave engineering: Microwave mixers, www.ece.uvic.ca/~whofer/elec454/Lecture%2018.pdf
- [17] Modern amplifier terms defined, Mini-circuits, 1999.
- [18] U2796B, 2 GHz singly balanced mixer datasheets, Atmel, 10 October 2000.



- [19] Understanding mixers, Mini circuits, 1999.
- [20] Stephen J Erst, Receiving systems design, Artech house, Inc., 1984.
- [21] Application note, Co-sitting of MPT1411 and MPT1329 equipment, Wood & Douglas, June 1997, www.woodanddouglas.co.uk/products/download/70000004.pdf.
- [22] Mixers, www.synergymwave.com/Articles/PDF/Mixers.pdf
- [23] RF terms, www.virtualtechnologiesltd.com/FAQs/rf%20terms.htm
- [24] Jeremy Everard, Fundamentals of RF circuit design with low noise oscillators, John Wiley & Sons, Ltd., 2001.
- [25] WH Hayward, Introduction to radio frequency design, Prentice-Hall, Inc., 1982.
- [26] David M Pozar, Microwave engineering, Second edition, John Wiley & Sons, Inc., 1998.
- [27] David B. Ruthledge, The electronics of radio, Cambridge University press, 1999.
- [28] Ian Hickman, Newnes Practical RF handbook, Newnes, An imprint Butterworth-Heinemann Ltd, 1993.
- [30] Aldert van der Ziel, Noise, Prentice-Hall, Inc., 1954.
- [31] RE Ziemer and WH Tranter, Principles of communications – Systems, Modulation, and Noise, Fourth edition, John Wiley & Sons, Inc., 1995.
- [32] Rulon Van Dyke, Relating cascaded noise figures to real world performance, RF time and frequency, www.rfdesign.com , January 2003.
- [33] Eric Drucker, Model PLL dynamics and phase-noise performance, Model PLL dynamics, Part2, Microwaves & RF, February 2000.
- [34] Ali Hajimiri, Phase noise in oscillators, smirc.stanford.edu/papers/Orals98s-ali.pdf
- [35] Stephen A Maas, The RF and microwave circuit design cookbook, Artech house, 1998.
- [36] Thomas H Lee and Ali Hajimiri, Oscillator phase noise: A tutorial, IEEE journal of solid-state circuits, Vol.35, No.3, March 2000.
- [37] Voltage controlled oscillators, Institute of micro electronic systems, CMOS RFIC design
- [38] Ryan P Scott, Carsten Lang rock and Brian H Kolner, High dynamic range laser amplitude and phase noise measurements techniques, IEEE journal on selected topics in quantum electronics, Vol.7, No.4, July/Augustus 2001.
- [39] Iulian Rosu, Phase noise in oscillators, www.qjs.net/va3iul/
- [40] Mike Curtin and Paul O'Brien, Phase locked loops fir high frequency receivers and transmitters –part 2, Analog dialogue 33-5, Analog Devices.
- [41] Alper Demir, Amit Mehrotra, and Jaijeet Roychowdhury, Phase noise in oscillators: A unifying theory and numerical methods for characterization, IEEE transactions on circuits and systems-I: Fundamental theory and applications, Vol.47, No.5, May 2000.
- [42] Todd Charles Weigandt, Low phase noise, low timing jitter design techniques for delay cell based VCOs and frequency synthesizers, Doctors degree, University of California, Berkley, 1998.
- [43] A technical tutorial on digital signal synthesis, Analog Devices, Inc., 1999.



- [44] Ralph S Carson, Radio communication concepts: Analog, John Wiley & Sons, January 1990.
- [45] Paul H Young, Electronic communication techniques, Third edition, Macmillan publishing company, 1994.
- [46] Chris Kelly, The advantages of DDS in function generators, Dataweek, 8 October 2003, www.dataweek.co.za
- [47] Optimizing VCO/PLL evaluations & PLL synthesizer designs, Mini Circuits.
- [48] Donald A. Neamen, Electronic circuit analysis and design, The McGraw-Hill companies, Inc., 1996.
- [49] Software for easy circuit design with Smith Chart, *Smith 184* Version 1.82, ©1995-1998 by Berne institute of technology, Switzerland.
- [50] Software high frequency design suite, *Microwave Office* Version 5.51, © Applied wave research, Inc, 2002, www.appwave.com/products/mwoffice/
- [51] Edgar Carmargo, Design of fet frequency multipliers and harmonic oscillators, Artech house 1998.
- [52] Peter Parker, An experimental HF direct conversion receiver, Amateur radio, October 2001. www.wia.org.au/armag/articles/Experimental_HF_dcr.pdf
- [53] A complete design-to-deploy, model driven architecture software package, Borland *Delphi* Professional Studio, Version 6.0, © Borland Software Corporation, 1983-2001, www.borland.com
- [54] Software language and technical computing environment, *Matlab*, Version 6.0.88, Release 12, ©The MathWorks, Inc., 1984-2000, www.mathworks.com
- [55] Complete board-level design system for windows, Design Explorer 99, Version 6.0.4, © Protel International Limited, 1995-1999.
- [56] WW Mumford & EH Schelbe, Noise performance factors in communication systems, Horizon house, 1968.
- [57] Liam Devlin, Mixers, www.plextek.com/papers/mixers2.pdf
- [58] Bert C Henderson, Mixers: Part2 –Theory and technology, WJ Communications, Inc., www.wj.com
- [59] Info-communications development authority of Singapore, Type approval specification for frequency modulated VHF/UHF radio base and mobile stations equipment for use in the land mobile radio service, IDA TS101, Issue 1 Rev 4, December 1999.
- [60] Paul Horowitz & Winfield Hill, The art of electronics, Second edition, Cambridge university press, Great Britain, 1995.
- [61] James W. Nilsson & Susan A. Riedel, Electric circuits, fifth edition, Addison-Wesley publishing company, Inc., United States of America, 1996.
- [62] Micheal Perrot, High speed communication circuits and systems, Lecture 3, S-parameters and impedance transformers, Massachusetts institute of technology, 2003.

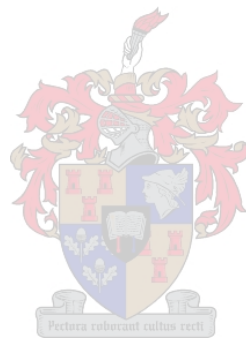


[63] Alvin K. Wrong, Reviewing key areas when designing with the SA605, Application note A1994, Philips semiconductors, 3 November 1997.

[64] Alvin K. Wrong, Evaluating the SA605 SO and SSOP demo-board, Application note AN1995, Philips semiconductors, 29 October 1997.

[65] SA602 Doubly balanced mixer and oscillator, data sheet, Philips semiconductors, 7 November 1997.

[66] R M Marston, Audio IC Users' Handbook, Newnes, A division of Reed Educational and professional publishing Ltd., 1997.



Appendix A – LNA amplifier design

The detailed design of the LNA, which is discussed in section 4.2.2. follows. This design consist three parts namely

- Designing the biasing network
- Determine the stability
- Design matching networks

1. Design of the biasing network

A common emitter circuit with a voltage divider biasing circuit, two coupling capacitors and two RF chokes is chosen to switch the transistor on. This circuit can be seen in *Figure A.1 (a)* beneath. The function of the coupling capacitors is to provide DC isolation between the amplifier and the high frequency network. The RF chokes is inductors with a large value that will have high impedance at high frequencies. This will provide isolation between the biasing network and small high frequency signal, to ensure that this energy is not wasted in the biasing network.

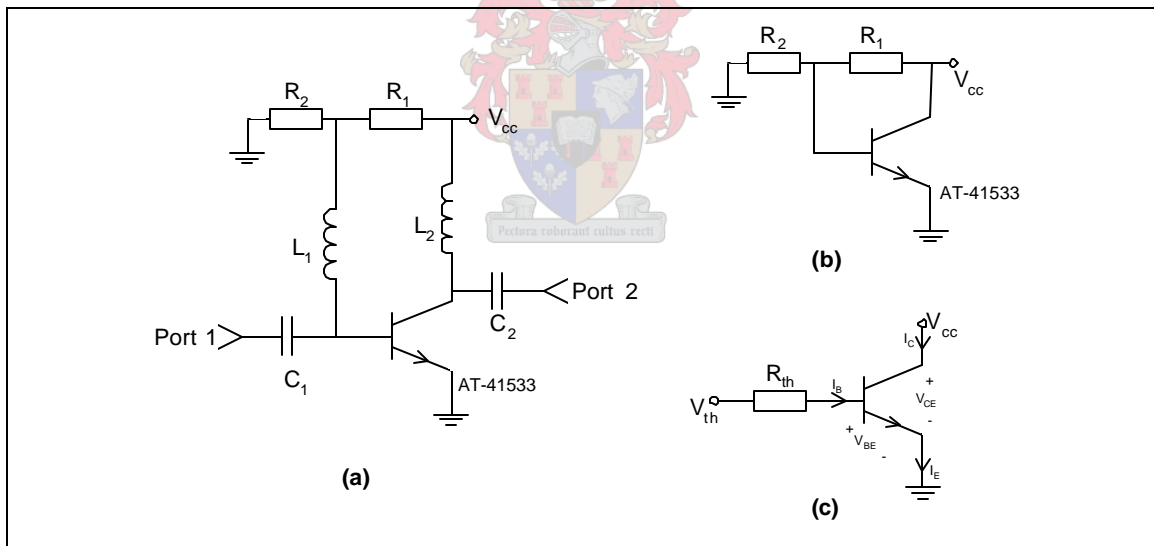


Figure A.1 (a) The biasing circuit (b) The equivalent biasing circuit at DC (c) The Thevenin equivalent circuit

The equivalent biasing network at DC is shown in *Figure A.1 (b)*. It is assumed that the coupling capacitors will act as open circuits and the inductors as short circuits at DC. The Thevenin equivalent of this DC equivalent circuit can be seen in *Figure A.1 (c)*. The Thevenin equivalent voltage and resistance can be calculated by using the following formulas:

$$V_{TH} = \frac{R_2}{R_1 + R_2} V_{cc} \quad (A.1)$$

$$R_{TH} = \frac{R_1 R_2}{R_1 + R_2} \quad (A.2)$$

Firstly, it was decided to choose $V_{cc} = 5V$ and $I_c = 5mA$. At low frequencies, the small signal current gain h_{fe} is essentially equal to \mathbf{b} [48]. Thus $\mathbf{b} \approx h_{fe} = 150$ is found on the datasheets of the AT-41533 transistor.

I_B can now be calculated by using I_c and \mathbf{b} as follows [48]

$$I_c = \mathbf{b} I_B \Rightarrow I_B = \frac{I_c}{\mathbf{b}} = \frac{5mA}{150} = 33.3mA \quad (A.3)$$

The following formula can be derived from *Figuur A.1 (c)*

$$I_B = \frac{V_{TH} - V_{BE}}{R_{TH}} \quad (A.4)$$

V_{BE} is chosen as $0.7V$. By substituting $V_{cc} = 5V$; $I_B = 33.3mA$ and $V_{BE} = 0.7V$ into equation (A.1), (A.2) and (A.4), the following three formulas can be found:

$$\frac{V_{TH} - 0.7}{R_{TH}} = 33.3mA \quad (A.5)$$

$$V_{TH} = \frac{5R_2}{R_1 + R_2} \quad (A.6)$$

$$R_{TH} = \frac{R_1 R_2}{R_1 + R_2} \quad (A.7)$$

By substituting these three formulas into each other and choosing $R_1 = 10k\Omega$; R_2 is calculated as $1.765k\Omega$.

This resistor values was now used to determine if any of the absolute maximum ratings of the transistor would be exceeded. All the voltages and currents were determined to be well within the specified maximum ratings.

Next, the values of the RF chokes and coupling capacitors are determined. The value of s_{11} is estimated from the datasheets as $s_{11} = 0.84 \sqrt{-20} = 0.789 - 0.287i$. The input impedance can be calculated from s_{11} by substituting it into

$$z_{11} = \frac{50(1 + s_{11})}{1 - s_{11}} = 116.28 - 226.24i \quad (\text{A.8})$$

The imaginary part of the input impedance is negative and thus capacitive. Thus, if large resistors are used that functions correctly at 50MHz, the inductors are almost unnecessary. Just to be certain, the reactance of the RF choke is chosen to be much greater than the reactance of the transistor's input impedance. Thus

$$\omega L_1 = -226.24\Omega \quad (\text{A.9})$$

It was decided to choose $L_1 = L_2 = 200\text{nH} \Rightarrow X_L = \omega L = 62.83\Omega \gg -226.24\Omega$

The values of the coupling capacitors are determined next. These capacitors should be similar to a short circuit at 50MHz. Thus to ensure a reactance as smaller than 5Ω at 50MHz the capacitor should be chosen to be

$$\frac{1}{\omega C} < 5\Omega$$

$$\Rightarrow C > \frac{1}{2\pi \cdot 50 \cdot 10^6 \cdot 5} = 636\text{pF} \quad (\text{A.10})$$

Thus, if the value of the capacitor is greater than 636pF the capacitor should function similar to a short circuit at 50MHz, if it functions correctly. The capacitor values is chosen as

$C_1 = C_2 = 820\text{pF} \Rightarrow X_c = \frac{1}{\omega C} = 3.8\Omega$. The calculated bias circuit is shown below in *Figure A.2*.

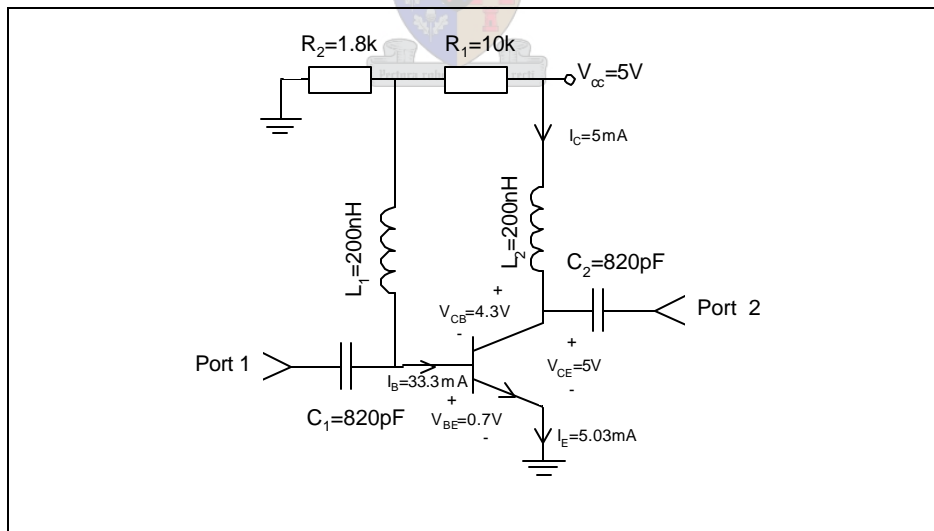


Figure A.2 The bias circuit

This circuit was build and measured. The transistor switches on and draws current. The bias circuit was determined to be successful.

2. Determine stability

To determine if the amplifier is unconditionally stable for all frequencies, the scattering parameters of the preliminary amplifier were measured on the network analyzer. This was done for $300\text{kHz} < f < 1\text{GHz}$ and with an input signal of -30dBm . The measured s-parameters were drawn into *Microwave office* [50] and stability circles were plotted to determine if the circuit is unconditionally stable over all frequencies.

If the circuit is unconditionally stable, all the stability circles should lie outside the Smith chart. Stability circles that lie inside the Smith chart implies an unstable amplifier that will oscillate. This is a result of positive feedback or too much gain. A resistor was added over the output of the amplifier to dissipate energy and as a result lower the gain. This was simulated, in *Microwave office* [50] and appeared to stabilize the amplifier.

The new s-parameters of the amplifier were measured on the network analyzer, with the resistor added over the output of the amplifier, to determine if this stabilized the amplifier as simulated. The measured values were drawn into *Microwave office* [50] and stability circles were plotted as shown in *Figure A.3*.

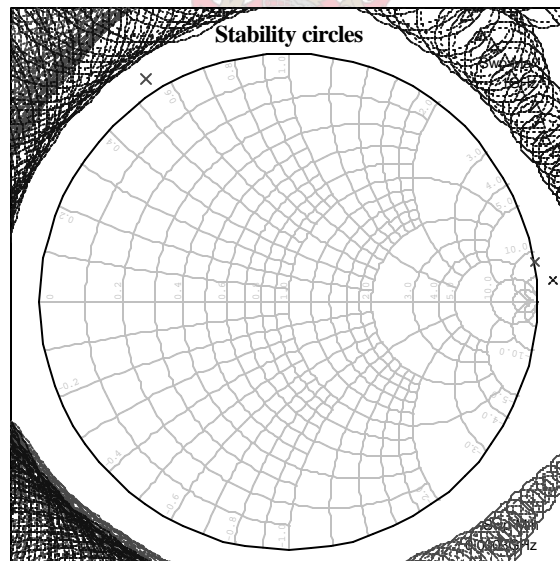


Figure A.3 The stability circles calculated from the s-parameters that was measured after a 1200 resistor was added over the output of the amplifier.

All the stability circles lie outside the Smith chart, which implies that the amplifier is unconditionally stable over the entire measured frequency band (300kHz-1GHz).

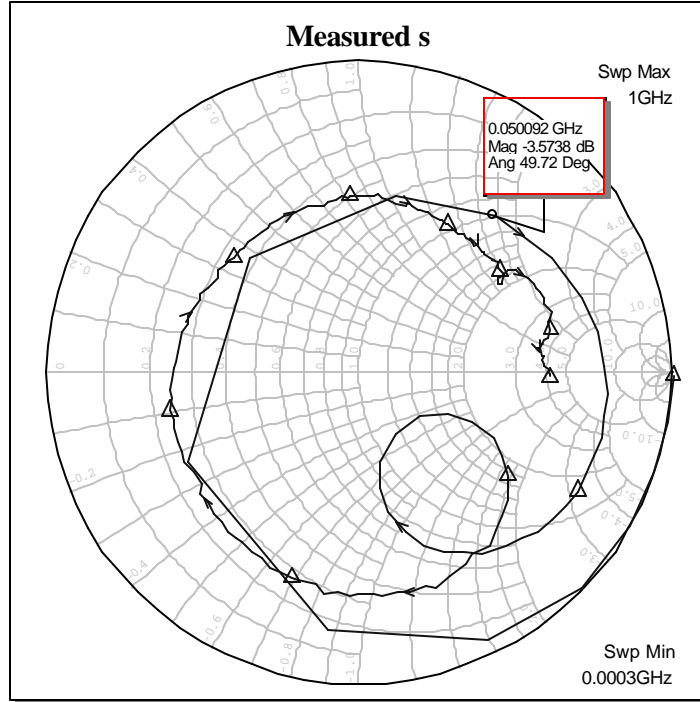


Figure A.5 Measurement of s_{11} on the network analyzer

An output-matching network can now be designed by utilizing the measured s-parameters. This network was designed for maximum gain, by matching the output section to Γ_L^* where Γ_L is calculated using equations

$$\Gamma_s = \frac{B_1 \pm \sqrt{B_1^2 - 4|C_1|^2}}{2C_1} \quad \text{and} \quad \Gamma_L = \frac{B_2 \pm \sqrt{B_2^2 - 4|C_2|^2}}{2C_2} \quad (\text{A.10})$$

where

$$B_1 = 1 + |s_{11}|^2 - |s_{22}|^2 - |\Delta|^2 \quad \text{and} \quad B_2 = 1 + |s_{22}|^2 - |s_{11}|^2 - |\Delta|^2$$

$$C_1 = s_{11} - \Delta s_{22}^* \quad \text{and} \quad C_2 = s_{22} - \Delta s_{11}^*$$

For maximum power transfer, from and to the transistor, the input and output impedance matching networks should be designed to match $\Gamma_{in} = \Gamma_s^*$ and $\Gamma_{out} = \Gamma_L^*$. Δ is defined as the determinant of the scattering matrix, $\Delta = s_{11}s_{22} - s_{12}s_{21}$.

With the help of *Matlab* [54], Γ_L was determined as $\Gamma_L = 1.8943 - 1.3225i$ or $0.3549 - 0.2478i$. $\Gamma_L = 0.3549 - 0.2478i$ lies inside the Smith chart, and an output-matching network was now designed for $\Gamma_L^* = 0.3549 + 0.2478i$ with the help of *Smith 184*[49] and is shown in *Figure A.6*.

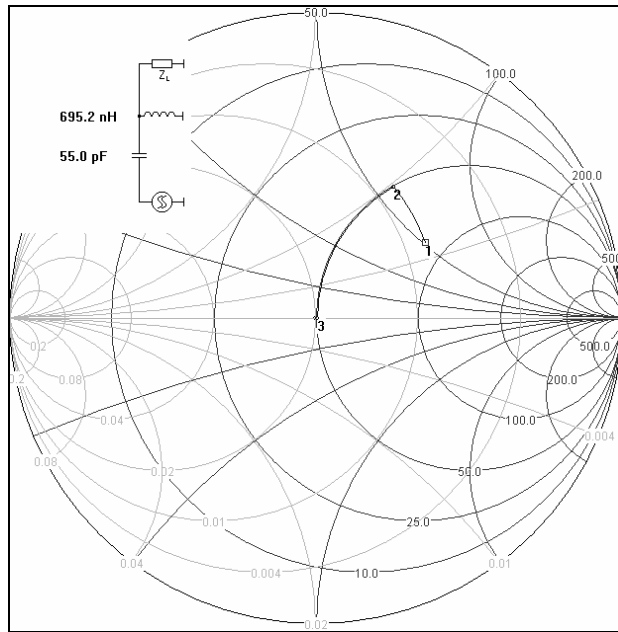


Figure A.6 Output impedance match design with the help of Smith 184[49]

This output matching section was added to the amplifier and this was measured on the network analyzer and plotted in *Microwave office* [50]. The measured s_{22} is shown in below in *Figure A.4*.

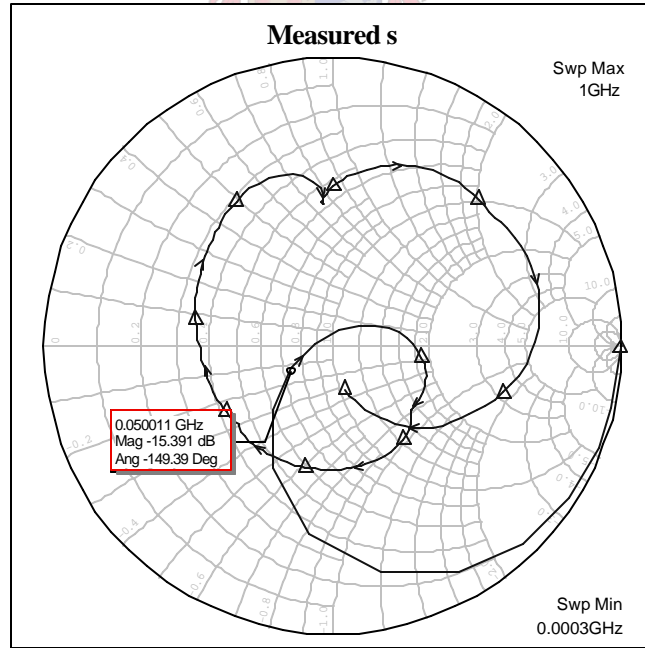


Figure A.7 s_{22} as measured on the network analyzer

Two back-to-back diodes at the transistor input pin is sometimes added as a safety measure. The disadvantage of these diodes is that they will generate IM distortion when high input levels are present, even if the RF amp is powered down. They were not included in this design [6 p55].

The final measured s-parameters were used to draw the stability circles in *Microwave office* [50]. This stability circles is shown in *Figure A.8* and implies that the amplifier is unconditionally stable over the measured frequency band.

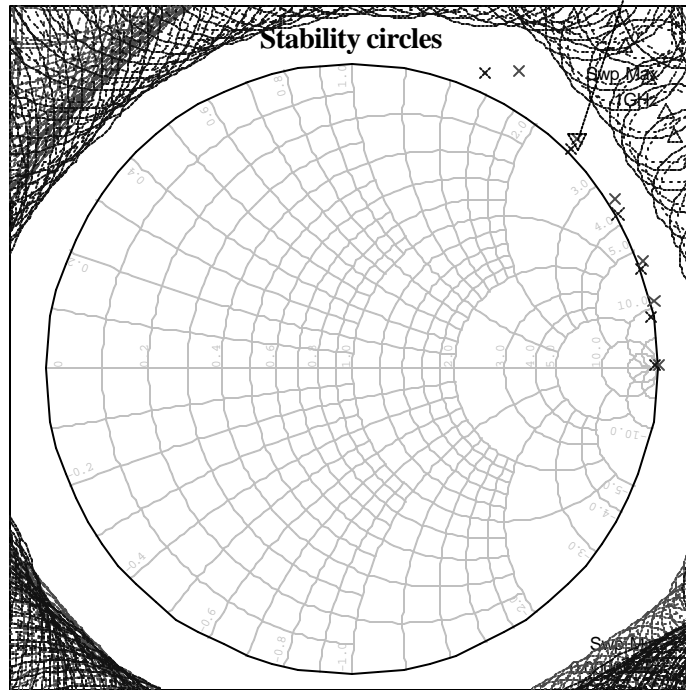


Figure A.8 Stability circles drawn from final measured s-parameters

Appendix B – DDS design

The design of the DDS that is discussed in section 4.3.2. a, follows.

1. Hardware design

The AD9851 is a DDS IC with a six-time reference clock enable function, a built in 10 bit analog to digital converter and a tuning resolution of approximately 0.04Hz. Reference clock rates of up to 180MHz can be accommodated. It produces a sine wave that can be used directly as a frequency source.

The circuit diagram of this frequency source component is shown in *Figure B.1* In this diagram C_1 - C_5 are all supply bypassing capacitors. JP_3 is a screw mount terminal, where the power supply is connected to the component, while JP_1 is the header that connects the AD9851 to the microcontroller, which will control the output frequency.

U_3 is the reference clock oscillator. For the purposes of this design, a reference clock oscillator from STC frequency technology, the STCO31-SMD7X5 metal lid surface mount crystal clock oscillator at 20MHz was chosen. Thus, with the 6X reference clock enabled a system reference clock of 120MHz was used.

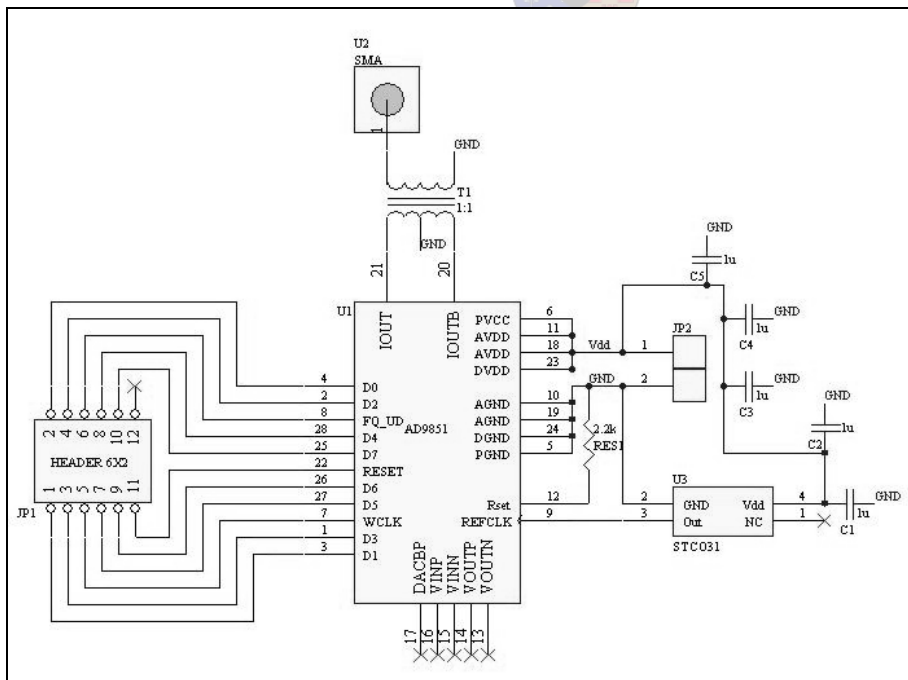


Figure B.1 Circuit diagram of the AD9851 direct digital synthesizer component that was designed

The output pins of the digital to analog converter, requires a current to voltage transformation. The T1-6T transformer from Mini-circuits was used to do this current to voltage transformation.

The value of I_{out} can be set with $RES1$ and the relationship given in the datasheets as

$$I_{out} = 39.93 / RES1 \quad (B.1)$$

$RES1$ was chosen as $2.2k\Omega$, therefore I_{out} can be expected to be $18mA$. $I_{outMAX} = 30mA$ should not be exceeded.

2. Programming the DDS

The AD9851 is essentially a digitally controlled oscillator, which will generate an output frequency dependent on the contents of its 40-bit register. The contents of this 40-bit register and thus the output frequency of the AD9851 were chosen in this application to be controlled by the low-power ATmega8L microcontroller from the ATMEL AVR family of microcontrollers.

The ATmega8L was chosen for its low power consumption, which is a major consideration in portable devices. An active supply current of $\pm 9mA$ is predicted by the datasheets, when operating at a frequency of $6MHz$ and with a supply voltage of $5V$. The active supply current during operation was measured to be $7.7mA$.

The 40-bit register on the AD9851 can be loaded by the ATmega8L microcontroller in serial or parallel mode. This is done by loading a 40-bit control word that contains 5-bit phase modulation information, an enable bit that will enable the $6\times$ reference clock multiplier as well as a serial mode enable bit and a power down bit. After this, the 32-bit frequency control word is loaded from the least to the most significant bit. The relationship between the frequency control word and the frequency of the output signal is

$$f_{out} = \frac{(CW \times SysCLK)}{2^{32}} \quad (B.2)$$

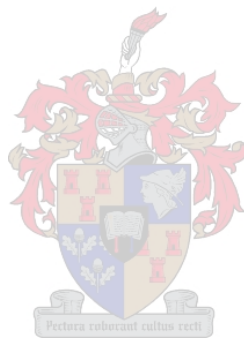
Where f_{out} is the frequency of the output signal in $[MHz]$, CW is the decimal value of the frequency control word and $SysCLK$ is the reference clock or $6\times$ the reference clock if the $6\times$ reference clock multiplier is enabled.

It was decided to program the microcontroller to tune the direct digital synthesizer, and thus the local oscillator frequency, to vary from $39.25MHz$ to $39.35MHz$, in steps of $12.5kHz$. Thus the

receiver will be able to receive 9 channels, separated by $12.5kHz$, between the receive frequencies $49.95MHz$ and $50.05MHz$.

The user is able to tune the radio from one channel to the next one or previous one, by pushing one of two buttons. This generates external interrupt on the microcontroller and causes it to write a new 40-bit register on the AD9851.

The ATmega8L was programmed using CodeVisionAVR. CodeVisionAVR is a development environment, C compiler and an in system programmer for the ATMEL AVR family of microcontrollers. The C program that was programmed unto the microcontroller can be found on the appendix CD.



Appendix C – IF receiver design

The IF receiver design, that is discussed in section 4.6.1, follows. The circuit diagram of this component is shown in *Figure C.1*.

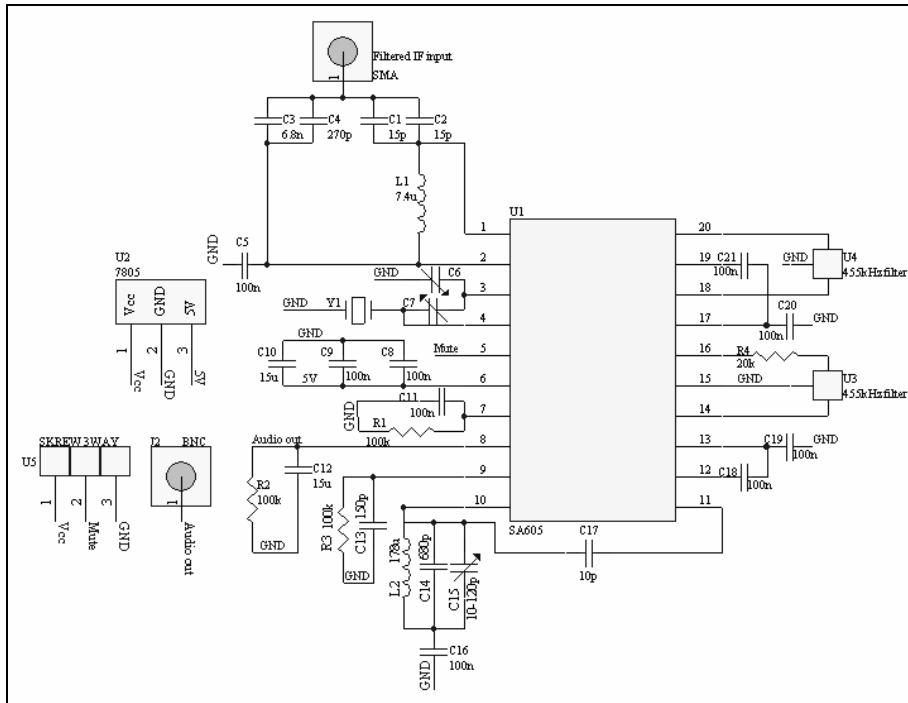


Figure C.1 Circuit diagram of the SA605 IF receiver system that was designed

L_1 , C_1 , C_2 , C_3 and C_4 are part of a tapped capacitor impedance matched output network that was designed, for an input frequency of 10.7MHz. The calculated values are given in the circuit diagram. C_5 is an AC short for pin 2.

The first IF frequency of the super heterodyne receiver is 10.7MHz, while the second IF frequency is 455kHz. Thus a LO signal of 10.245MHz is needed. The SA605 has an on board transistor for the local oscillator, but external components need to be added to enable oscillation at the LO frequency. Different oscillators can be realized of which the Colpitts oscillator configuration was chosen. A 10.245MHz crystal resonator was used namely Y_1 as well as two variable capacitors, C_6 and C_7 [63].

The 455kHz output of the mixer is filtered, with U_4 , loaded into the IF amplifier and filtered again using U_3 before it is loaded into the IF limiting amplifiers. This filtering is done by the CFULA455KF4A-B0 ceramic filter, from the Murata's Cerafil range for communications

equipment. According to the datasheets, this filter has a center frequency of $455kHz \pm 1.5kHz$, a $6dB$ pass band of $\pm 7.5kHz$, a minimum stop band attenuation of $27dB$, a maximum loss of $6dB$ and an input and output impedance of $1.5k\Omega$. The output of the mixer is internally loaded with a $1.5k\Omega$ resistor, and the input resistance of the IF amplifier and limiter is $1.5k\Omega$. Thus matching to these filters is not necessary [63] [64].

The SA605 includes a received signal strength indicator (RSSI) pin, which will reveal if any instability is present (pin 7). This reading should be less than $250mV$ if the device is biased and no signal is fed into the device. This RSSI output is a current to voltage converter and an $91k\Omega$ external resistor is needed to get the desired response. Therefore, R_1 is chosen as $100k\Omega$ which is close to this value [63] [64].

A reading higher than $250mV$ on the RSSI output pin indicates a regeneration problem, due to poor lay out or too much gain in the IF component. Too much IF gain may cause instability. Thus, it is usually necessary to introduce external loss by using a resistor as shown with R_4 . To achieve a certain insertion loss, the value of the resistor necessary can be calculated with the following formula [63]

$$X_{dB} = 20 \log \frac{\sqrt{(960 + R_{ext}) R_{flt}}}{960 + R_{ext} + R_{flt}} - Filterloss \quad [dB] \quad (C.1)$$

where X_{dB} is the intercomponent loss wanted, $R_{ext} = R_4$ is the external added resistor, $R_{flt} = 1.5k\Omega$ is the filter's input impedance and the filter loss is given as $6dB$. A RSSI output below $250mV$ was achieved by introducing a $18dB$ loss between the components, which corresponds to an external resistor value of $20k\Omega$ [63].

C_{21} and C_{20} is the decoupling capacitors for the IF amplifier, while C_{18} and C_{19} is the decoupling capacitors for the IF limiter amplifier [64].

Pin 9 is the audio output pin, while the muted audio output on pin 8 is the same as the audio output pin, except for the fact that the audio output on this pin can be turned off by grounding pin 5. This pin was used for the output, thus pin 5 needs to be connected to 5V externally. R_2 and R_3 convert the audio output current to a voltage [63] [64].

The quad tank components, L_2 , C_{14} and C_{15} , are calculated with the equation [64]

$$f = \frac{1}{2p\sqrt{LC}} \quad (C.2)$$

where $f = 455\text{kHz}$, L is chosen as 178mH and then the total capacitance C , is calculated to be 700pF . To make this tunable, a 680pF capacitor is used in parallel with a $0\text{--}120\text{pF}$ variable capacitor [64].

C_{16} is used to AC ground the quad tank and C_{17} provides a 90° phase shift for the quadrature detector [63].

C_8 , C_9 and C_{10} are all supply bypassing capacitors

